HIGHWAY RESEARCH RECORD

Number 112

Concrete Pavement Design

7 Reports

Presented at the
44th ANNUAL MEETING
January 11-15, 1965

SUBJECT CLASSIFICATION
25 Pavement Design

HIGHWAY RESEARCH BOARD
of the
Division of Engineering and Industrial Research
National Academy of Sciences—National Research Council
Washington, D. C.
1966

Department of Design

W. B. Drake, Chairman
Assistant State Highway Engineer
Kentucky Department of Highways, Lexington

HIGHWAY RESEARCH BOARD STAFF

F. N. Wray, Engineer of Design
R. C. Edgerton, Assistant Engineer of Design

PAVEMENT DIVISION

Milton E. Harr, Chairman
Professor of Soil Mechanics, School of Civil Engineering
Purdue University, Lafayette, Indiana

COMMITTEE ON RIGID PAVEMENT DESIGN
(As of December 31, 1964)

F. H. Scrivner, Chairman
Pavement Research Engineer
Texas Transportation Institute, Texas A & M University
College Station

W. Ronald Hudson, Secretary
Department of Civil Engineering
University of Texas, Austin

Henry Aaron, Chief Engineer, Reinforced Concrete Pavement Division, Wire Reinforcement Institute, Washington, D. C.
Phillip P. Brown, Consultant, Soils, Mechanics and Paving, Bureau of Yards and Docks, Department of the Navy, Washington, D. C.
Harry D. Cashell, Deputy Chief, Structural Research Division, U. S. Bureau of Public Roads, Washington, D. C.
B. E. Colley, Manager, Paving Development Section, Portland Cement Association, Skokie, Illinois
E. A. Finney, Director, Research Laboratory Division, Michigan State Highway Department, Lansing
Phil Fordyce, Supervising Engineer, Pavement Engineering, Portland Cement Association, Chicago, Illinois
W. S. Housel, University of Michigan, Ann Arbor
F. N. Hveem, Sacramento, California
W. H. Jacobs, Executive Secretary, Rail Steel Bar Association, Chicago, Illinois
C. D. Jensen, Director of Research and Testing, Pennsylvania Department of Highways, Harrisburg
Wallace J. Liddle, Engineer of Materials and Research, Utah State Department of Highways, Salt Lake City
Phillip L. Melville, Civil Engineering Branch, Engineering Division, Military Construction, Office, Chief of Engineers, Department of the Army, Washington, D. C.
Ernest T. Perkins, Executive Director, East Hudson Parkway Authority, Pleasantville, New York

Thomas B. Pringle, Chief, Civil Engineering Branch, Engineering Division, Military Construction, Office of Chief of Engineers, Department of the Army, Washington, D. C.

M. D. Shelby, Research Engineer, Texas Highway Department, Austin

W. T. Spencer, Assistant Chief, Division of Materials and Tests, Indiana State Highway Commission, Indianapolis

Otto A. Strassenmeyer, Associate Highway Engineer—Research and Development, Connecticut State Highway Department, Wethersfield

William Van Breemen, Research Engineer, Engineering Research, New Jersey State Highway Department, Trenton

K. B. Woods, Head, School of Civil Engineering and Director, Joint Highway Research Project, Purdue University, Lafayette, Indiana

Foreword

Why is so much literature printed relating to the structural design of pavements? Why are so many kinds of pavement built? One might think that highway engineers and the many other professional people who share in supplying durable, trafficable surfaces over which vehicles may easily travel are only seeking to exhibit their originality. Pavement design is one of the oldest subjects of study confronting engineers since the invention of the wheel.

Of course, engineers, including paving engineers, are constantly acquiring and investigating new ideas—otherwise they could hardly be called engineers. This Record presents seven short technical reports describing new research on subjects in the general category of rigid pavement design.

In a laboratory test track at the University of Illinois, a pozzolanic material consisting of fly ash mixed with lime was used in various proportions with cement and stabilized aggregates for bituminous covered pavements. The strengths and behaviors of various thicknesses of pozzolanic pavement test sections, under both static and dynamic wheel loadings, are presented in the first paper.

Critical mechanical properties of lightweight aggregate concrete and their effects on pavements were the subject of some studies reported as a cooperative research project at the University of Texas. Field experiment to verify the finding of this research is recommended in the second paper.

An addition to the much-discussed subject of pavement joints is the short paper that gives the results of Iowa's recent study of variously spaced, undoweled joints in plain concrete pavements. Like several other states, Iowa has found that the omission of dowels at joints results in faulting, or unevenness of slabs, and a consequent increase in pavement roughness as the slabs become severely loaded under heavy truck traffic.

An experiment in Connecticut to investigate the merits of a self-expanding cement as a method to induce prestressing in concrete pavement slabs is described in one of these papers. The report explains the background, design concepts, and the principal features of the construction, as well as the instrumentation and testing. The chief value of the project seems to have been to single out certain causes of the unexpected results and to indicate improvement in plans for a future experiment.

A second-phase research report included in the Record gives Maryland's experience with two continuously-reinforced concrete pavements constructed in 1959. It presents the results of observations and well-instrumented tests made over a period of 4½ years. Crack opening in the concrete has increased slightly and the maximum steel strains at the cracks have decreased. The rates of change are greater in pavement sections containing a smaller percentage of steel.

The next paper reports on Oregon's two recently constructed continuously-reinforced pavements. Although these projects are on the Interstate Highway System, they are considered to be experimental in design because they will be observed and studied as to their performance in comparison with selected sections of conventionally designed pavement.

The last paper discusses friction as a restraint to movements of concrete pavement slabs. Differences in design concepts relating to the advantages and disadvantages of high-friction valves are compared for different engineers in India, the United States and Europe. The investigator, at the Indian Institute of Technology, reports on his findings from tests for friction on different types of subgrade and subbases.

Contents

Behavior of Pozzolanic Pavements Under Load

ERNEST J. BARENBERG, Assistant Professor, Department of Civil Engineering, University of Illinois

Cured and hardened pozzolanic materials are strong and resistant to flexing, thus distributing the load over a large area by slab action. This report presents the results of a study of the behavior of pozzolanic pavements under static and dynamic loads. Load-deflection characteristics and the ultimate load-carrying capacity of the slabs under static loads are discussed in terms of elastic and ultimate theory. The behavior of pozzolanic test pavements under repeated loads is compared with fatigue data from flexure specimens, and criteria for predicting the fatigue life of the pavements are discussed.

•POZZOLANIC MATERIALS are rapidly assuming a role of economic significance in many areas of the country. The availability of suitable quality fly ash in these areas enables the lime-fly ash aggregate to be used competitively with other stabilized materials as a quality paving material. The outstanding performance of many miles of pozzolanic pavements now in service is a testimony to the durability of the material.

Since pozzolanic materials require an asphaltic wearing surface for best performance, there is a tendency to classify pozzolanic pavements as flexible pavements, and to base the thickness design on the same factors which influence the thickness design of unbound granular materials. These materials, however, develop considerable flexural rigidity, and thus a pozzolonic pavement behaves more nearly like a rigid pavement than a flexible one. A research program was undertaken to demonstrate the slab-type behavior of pozzolanic pavements under static and dynamic loads. Significant findings from this program are reported herein.

The research program on the behavior of pozzolanic pavements was a part of a larger program on pozzolanic materials conducted at the University of Illinois, but only the results pertinent to the behavior of pozzolanic pavements are discussed in this paper. The results from other phases of the program have either been reported (1, 2) or will be presented in technical publications in the near future.

TEST PROGRAM

Research on pozzolanic materials and pavements was divided into two parts: a laboratory investigation to evaluate the physical properties of the material, and a pavement behavior and evaluation phase. The laboratory program was conducted before initiating the pavement behavior phase to guide the research staff in the selection of the pavement characteristics to be studied. Pavement behavior observation and evaluation were carried out at the University of Illinois pavement test track, and consisted of both static and dynamic tests on the pavement. The test track facilities and its capabilities are discussed by Ahlberg and Barenberg (1).

In the laboratory phase of the program, fundamental studies were carried out to determine the physical properties of the pozzolanic material including strength, change in strength with time, modulus of elasticity, Poisson's ratio, fatigue properties and resistance to alternate cycles of freezing and thawing and wetting and drying.

Paper sponsored by Committee on Rigid Pavement Design.

TABLE 1

SCHEDULE OF POZZOLANIC PAVEMENTS TESTED

Test Pavement	Thickness	Flexural Strength[a] (psi)	Type Load
	(a) Test Set I		
1	4.0	98	Static-interior
2	4.0	104	Static-interior
3	4.0	275	Static-interior
4	4.0	280	Static-interior
5	4.0	287	Static-edge
6	4.0	290	Static-edge
7	4.0	79	Static-interior
8	4.0	86	Static-interior
	(b) Test Set II		
1	4.3	185	Dynamic-interior
2	3.8	185	Dynamic-interior
4	4.8	185	Dynamic-interior
5	4.3	185	Dynamic-interior
	(c) Test Set III		
1	4.3	75	Dynamic-interior
2	4.8	75	Dynamic-interior
3	5.3	75	Dynamic-interior
4	5.8	75	Dynamic-interior
5	4.8	75	Dynamic-interior
6	5.3	75	Dynamic-interior
	(d) Test Set IV		
1	4.0	76	Dynamic-edge
2	4.0	170	Dynamic-edge
3	4.0	230	Dynamic-edge
4	5.5	230	Dynamic-edge
5	5.5	170	Dynamic-edge
6	5.5	76	Dynamic-edge

[a]At initial loading.

TABLE 2

PHYSICAL CHARACTERISTICS OF SUBGRADE MATERIAL

Characteristic	AASHO Designation	Value
AASHO class.		A-6 (8)
Opt. moist. cont.	T99-57	13.0
Max. dry dens.	T99-57	120
L. L., %	T89-54	25
P. L., %	T90-54	14
P. I., %	T91-54	11
Grain-size distr, % passing sieve:	T88-57	
No. 4		98
No. 10		96
No. 40		92
No. 100		85
No. 200		79
0.02 mm		61
0.05 mm		39
0.002 mm		27

In the pavement behavior and evaluation phase of the program, 8 pavement sections were tested to failure under static loads positioned at the interior and near the edge of the pavement. In addition, 34 pavement sections were tested under dynamic loads; 18 were standard flexible pavements with crushed stone bases and various surfaces and 16 were pozzolanic pavements. The thickness, strength, and position of the loads were altered for the different test pavements.

Only the test results from the pozzolanic pavements are presented in this paper. A summary of these pavements is given in Table 1. Test pavements 3 and 6 of test set II were made of crushed stone base and so were omitted from the table.

Materials and Construction Procedures

The properties of the materials used in the pavement behavior and evaluation phase of the program as reported by Ahlberg and Barenberg (1) are repeated here for reference.

Subgrade. — One hundred and fifty tons of selected subgrade material was taken from borrow pit No. 1 for the AASHO Road Test near Ottawa, Ill. Routine classification tests were made in the laboratory on samples of the subgrade material, which was a yellow-brown soil with an AASHO classification of A-6. The physical characteristics of the subgrade soil are summarized in Table 2. Additional information on soil from the same source is available in publications (5, 6) relating to the AASHO Road Test.

Before placing the subgrade soil, a granular filter was placed on the bottom of the test track pit. The filter material was a graded aggregate ranging from 3/4-in. to minus No. 200 sieve. The granular filter was compacted with a pneumatic tamper.

After the granular filter had been placed and compacted, the subgrade was placed over the filter material. Before placing the soil in the test track pit, vertical sheet metal separators were placed along both the interior and external walls of the test track pit so that the subgrade soil and the material for the vertical granular filter could be kept separate. The soil and the filter material were maintained at approximately the same level during placing. The filter material and

TABLE 3

COMPACTED PROPERTIES OF THE SUBGRADE

Property	Test Set			
	I	II	III	IV
Compacted density, pcf	91.9	117.6	116.6	115.1
Percent of standard	76.7	98.0	97.2	95.9
Moisture content, %	15.7	13.1	12.8	13.6
Modulus of subgrade reaction, psi/in.	50.0	150.0	163.0	60.0

TABLE 4

GRADATION OF GRAVEL FOR POZZOLANIC BASE

Sieve Size	Grain Size Distr.[a] (%)
3/4-in.[b]	100
3/8-in.	87
No. 4	73
No. 10	52
No. 40	23
No. 200	8
0.02 mm	4
0.05 mm	2
0.002 mm	1

[a]AASHO designation, T88-57.
[b]Material larger than 3/4 in. discarded.

TABLE 5

PROPERTIES OF FLY ASH FOR POZZOLANIC BASE

Property	Value (%)
Major constituent (approx.):	
Silicon dioxide	41
Aluminum oxide	25
Ferric oxide	21
Calcium oxide	4
Sulfur trioxide	1
Loss on ignition	7.2
Grain-size distr., passing sieve:	
No. 10	100
No. 40	98
No. 200	87
No. 325	79

the subgrade soil were first compacted around the vertical separators by hand. The vertical separators were removed before final compaction.

The subgrade soil was placed in the track and pulverized with a rotary hoe. Water was added to the soil during pulverization to bring the soil to the desired moisture content. The material was compacted in layers with 3-in. compacted thickness. Several methods of compaction were investigated to determine which would give the most uniform results. After considerable experimentation, it was found that, of the methods tried, pneumatic tampers gave the most uniform densities. Three to five passes of the tampers were required to bring the soil to the desired density. Alternate passes of the tamper were made in transverse directions to minimize directional densification of the subgrade.

During the process of subgrade placement, continuous testing was performed to control the moisture content and compacted density. After the soil was placed and brought to grade, plate-bearing tests were conducted on the subgrade. Results are given in Table 3. In-place CBR tests were performed on most subgrades with the CBR values for the subgrade soil of test sets II and III between 15 and 20, and for test sets I and IV between 2 and 5. For test sets I and IV the subgrade soil was intentionally placed wet of optimum to obtain the desired low CBR and plate-bearing values.

At the completion of each test set, the subgrade material was removed to a depth of 1 ft or more, pulverized, and replaced in the manner previously described before placing the base courses for the next test set.

A special soil planer was developed to bring the subgrade to the desired elevation. The planer trimmed the subgrade to a tolerance of ± 0.03 in., and the compacted base materials to within ± 0.1 in.

Pozzolanic Bases. — The pozzolanic material used in this study was composed of 82 percent gravel, 14 percent fly ash, and 4 percent lime. The gravel used for the pozzolanic bases came from a stockpile of subbase material used in the AASHO Road Test, and was the same material as was used for the cement-treated and bituminous-treated bases in the special base study of the AASHO Test (5). The grain-size distribution of the gravel is given in

TABLE 6

PROPERTIES OF LIME FOR POZZOLANIC BASE

Property	Value (%)
Major constituents (approx.):	
Calcium carbonate	4
Calcium hydroxide	59
Magnesium hydroxide	2
Magnesium oxide	33
Grain-size distr., passing sieve:	
No. 30	100
No. 100	97
No. 200	90
No. 325	85

TABLE 7

GENERAL CHARACTERISTICS OF POZZOLANIC BASE MATERIAL

Characteristic	AASHO Designation	Value
Composition, % by wt:		
Lime		4
Fly ash		14
Gravel		82
Max. dry den.	T99-49	135.4
Opt. moist. cont.	T99-49	7.8

Table 4. Properties of the fly ash used in the pozzolanic base are given in Table 5. Properties of the monohydrated dolomitic lime used are given in Table 6.

The general characteristics of the pozzolanic base material are given in Table 7. Figure 1 shows the general relationship between strength and age for the pozzolanic material cured under ambient conditions in the laboratory. There was a continuous strength gain of the material over an extended period of time, with the rate of gain varying somewhat for the different test sets because of differences in the ambient conditions. The trends shown in the figure are average values. Specimens cured in moist sand at approximately 70 F for 28 days attained a compressive strength of 710 psi, and those cured for 7 days in a sealed container at 130 F attained a compressive strength of 1,360 psi.

Flexural strength of the material was determined using 3- by 3- by 12-in. specimens loaded at the one-third points in accordance with the procedures outlined in ASTM Standard Test D-1360. Compressive strength specimens were the standard 4-in. diameter by 4.6-in. high proctor specimens. The modulus of elasticity was evaluated by measuring the maximum strains at the top and bottom of the flexure specimens using SR-4 strain gages bonded to the specimens. The modulus of elasticity was calculated from the curvature in the specimens as determined from the maximum strains at the top and bottom of the specimen. Poisson's ratio was determined in the usual manner, using transverse strain measurements on the compressive specimens, and was in the range of 0.08 to 0.15. A value of 0.10 was selected as an average value for routine calculations. The coefficient of thermal expansion for the material was approximately 6×10^{-6}.

The hardened pozzolanic material exhibited no weight loss during the freezing and thawing or wetting and drying durability tests. Fatigue characteristics of the pozzolanic material have been studied and the results reported (2). Because of the strength gain in characteristics of the pozzolanic material during the repeated load applications, the fatigue life of the material is highly sensitive to the age at initial loading and the rate of load applications. Thus the general fatigue characteristics can be used only as a general guide for evaluating the material's fatigue life.

The pozzolanic base materials were proportioned and mixed at approximately the optimum water content for maximum density in a 1½-cu ft pug mill mixer. The pozzolanic base was placed in the test track, leveled, and compacted with pneumatic tampers in the manner described for the compaction of the subgrade material. After compaction, the material was trimmed to the desired elevation with the planer.

Experimental Test Pavements

The test track was divided radially into 6 segments for pavement testing, each segment making a separate test pavement with either a transition section or a construction joint placed between each test pavement. A test set is composed of 6 test pavements placed and tested simultaneously in the test track. Test pavements in the various sets are given in Table 1.

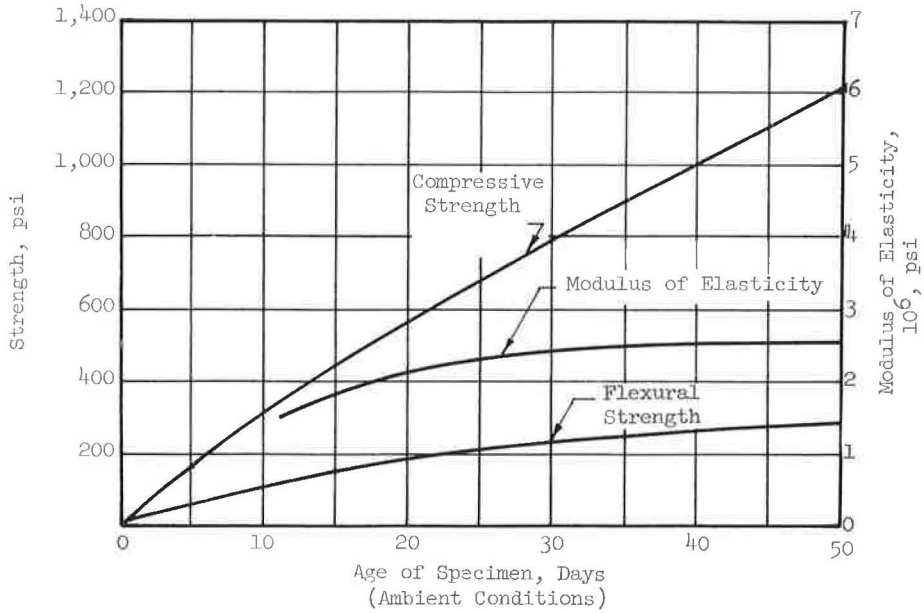

Figure 1. Strength-age relationships for pozzolanic base material.

TABLE 8

ULTIMATE CAPACITY OF STATICALLY LOADED PAVEMENTS, TEST SET I

Characteristic	Load No.							
	1	2	3	4	5	6	7	8
Load placement	Int.[a]	Int.	Int.	Int.	Edge	Edge	Int.	Int.
Age at loading, days	8	9	21	22	24	25	5	6
Flex. strength at loading, psi	98	104	275	280	290	293	79	86
Ultimate load, lb	8, 750	6, 000	17, 750	16, 250	5, 750	5, 750	8, 250	10, 000
Deflection at ultimate load, in.	0. 164	0. 105	0. 214	0. 219	0. 070	0. 080	0. 227	0. 151

[a]Int. = interior load placement.

Static Load Tests

Static tests were conducted on the pavements in test set I. The pavements were tested at different ages to study the effect of the strength of pozzolanic materials on the load deflection and ultimate load-carrying capacity of the pavements. Positions of the test loads and the age at testing are shown in Figure 2. A summary of the results from control tests on the pozzolanic material is given in Table 8. The eight test pavements were made possible because a portion of the pavement tested in the first stage was removed and replaced with a new pavement section (Fig. 2). Six pavements were tested under loads placed at an interior point on the pavement, and 2 were tested with the loading plate tangent to the edge of the pavement.

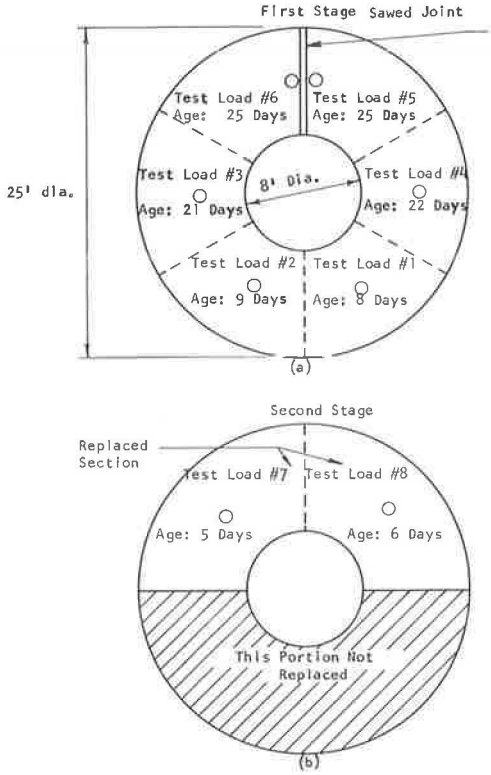

Figure 2. Plan view showing location of static test loads and age at testing.

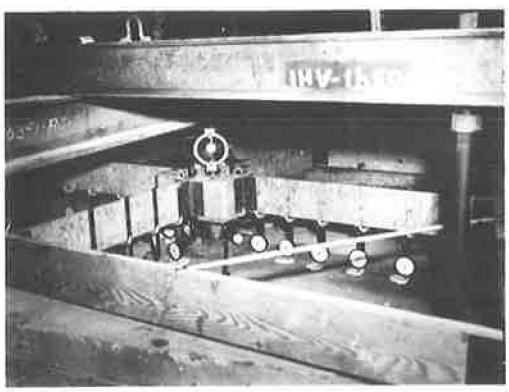

Figure 4. Closeup showing the position of the dial indicators with base of loading jack and proving ring in left center.

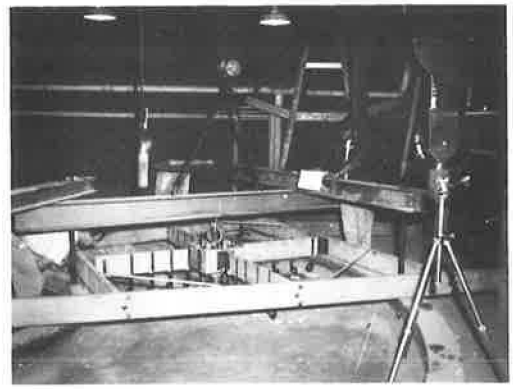

Figure 3. Overall view of reaction frame and dial indicator support frame for static load tests showing test in progress.

Static loads were applied to the test pavements by means of a hydraulic jack and a reaction frame. The loads were applied in increments which were made progressively smaller as the ultimate capacity of the pavements was approached. All loads were applied through a 7-in. diameter plate set on a quick setting mortar for easy leveling. The 7-in. plate was used because it covers approximately the same area as the tires used on the loading frame.

The deflection of the loading plate was measured by four dial indicators resting on an 18-in. diameter plate inserted between the 7-in. loading plate and the loading jack. The deflection of the pavement surface away from the loaded area was also measured with dial indicators resting on smoothed hydrocal pads cast on the pavement surface. All dial indicators were supported from a special frame supported outside the pavement test area. The reaction frame, dial indicator support frame, and the dial indicators in place are shown in Figures 3 and 4. The location of the dial indicators for the interior and edge loads are shown in Figures 5 and 6, respectively.

Load deflection curves for loads placed at the interior points on the pavement surface are shown in Figure 7. Deflection profiles for selected loads are shown in Figures 8 through 13. Theoretical deflections given by Westergaard's equations (3) are also shown in the figures. Similar curves for the edge loading condition are shown in Figures 14, 15, 16, 17 and 18. A resumé of the ultimate loads for the pavements and the strength of the pozzolanic material at the time of testing is given in Table 8.

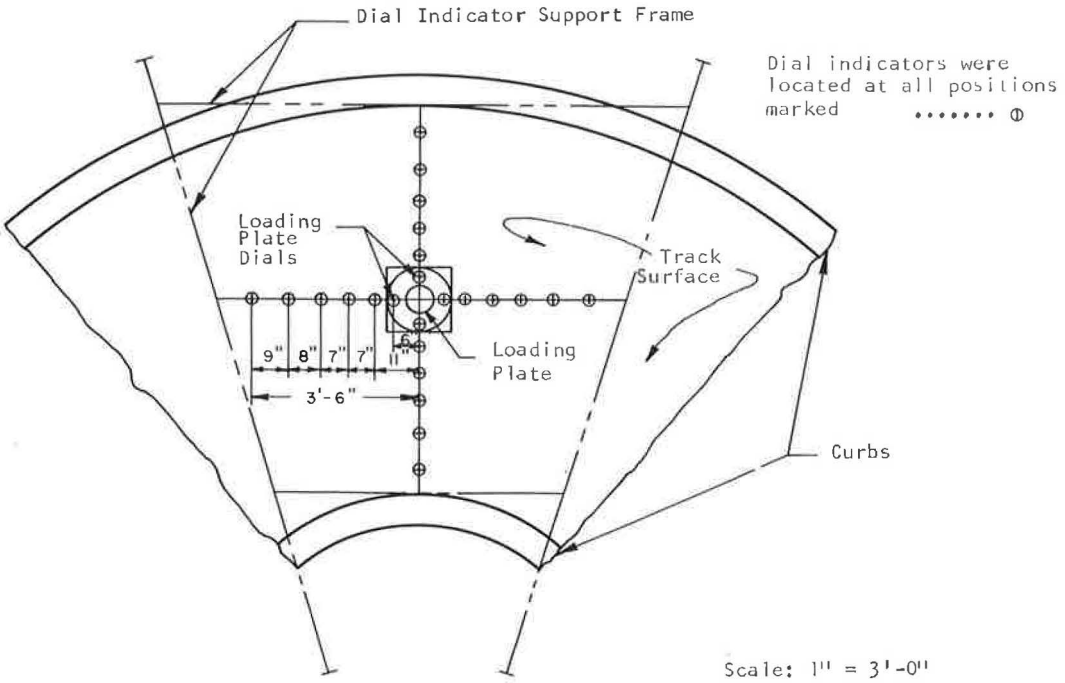

Figure 5. Plan view showing location of dial indicators for measuring surface deflection under static loads at interior point on pavement.

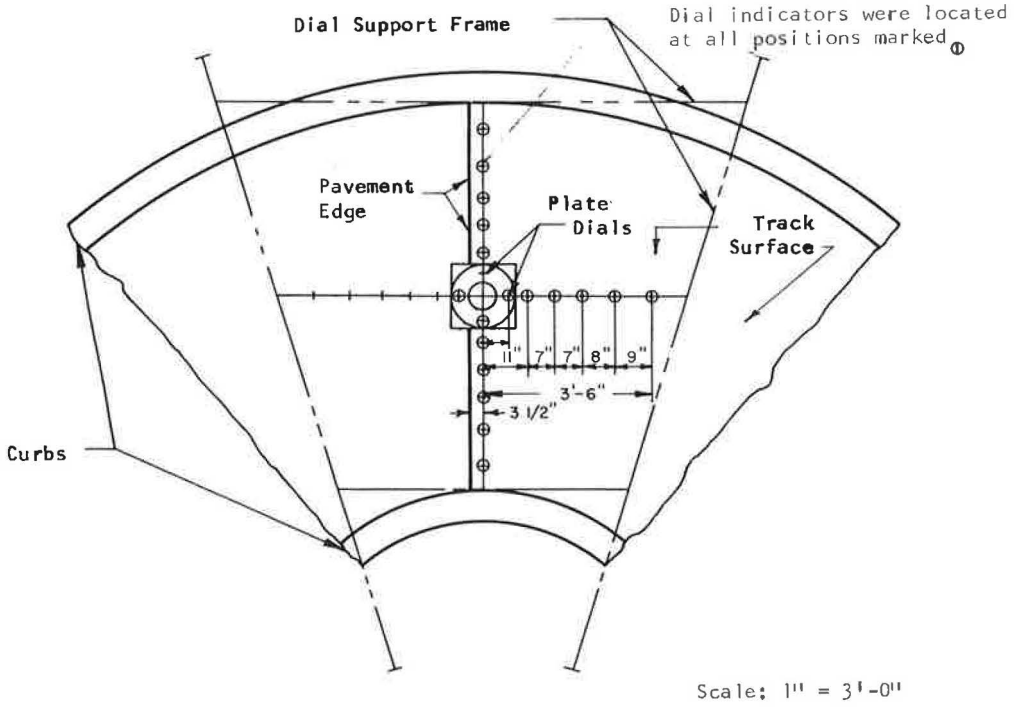

Figure 6. Plan view showing location of dial indicators for measuring surface deflection under static loads applied near edge of pavement.

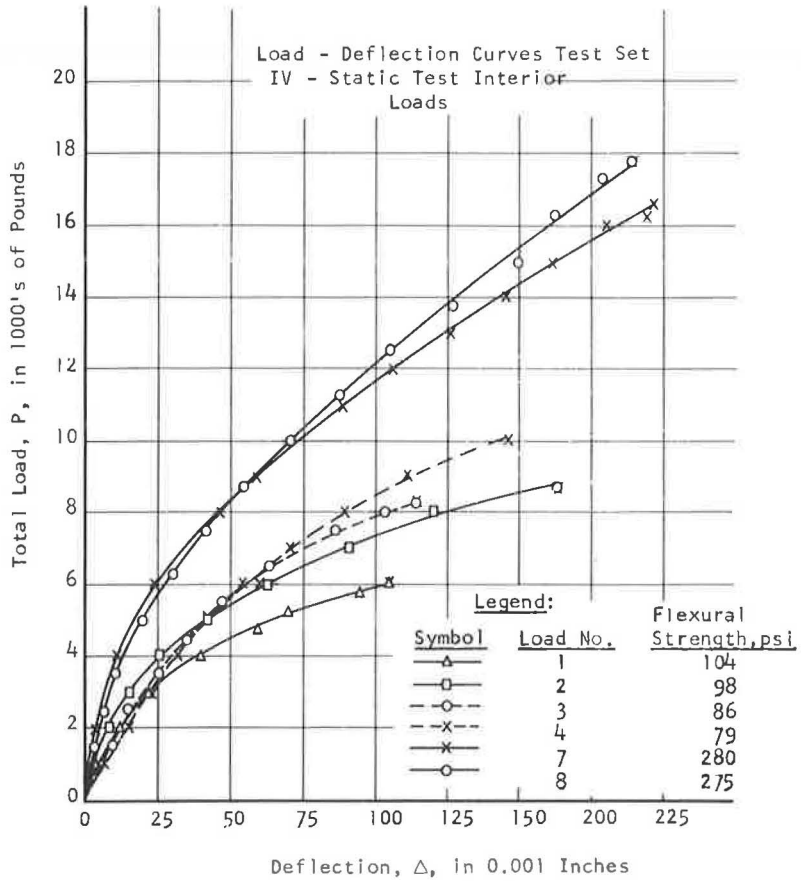

Figure 7. Load deflection curves for pozzolanic pavements under static loads at interior point.

Test pavements under interior loading failed by punching a cone from the pavement. After the pavements had failed, a section approximately 2½ ft sq was sawed from the pavement and removed, thus exposing the punched-out cone. The removed sections and the cones are shown in Figures 19 and 20. The crack patterns on the bottom surface of the cones are particularly significant.

Pavements tested under edge loads failed by developing semicircular cracks at an interior point (Figs. 21 and 22). The initial crack always appeared first along a radial line perpendicular to the pavement edge. The crack farthest from the pavement edge in Figure 21 appeared first, with the crack nearer the edge developing as additional loads were applied.

Dynamic Load Tests

The test pavements of test sets II, III and IV were tested under dynamic loads in the pavement test track. A general layout of the test track and supporting area is shown in Figure 23, and the loading frame used in the dynamic testing is shown in Figure 24. The loading frame revolves at a rate of approximately 25 rpm, and with each revolution 2 wheel loads up to approximately 3, 200 lb each are applied to the pavement. The loading frame oscillates radially as it revolves allowing the loads to be applied over a wheelpath ranging from the width of the tire up to a width of approximately 30 in. (1). Test sets II and III were tested under interior loading conditions. A thickened transition section was used between the different pavement sections to provide continuity

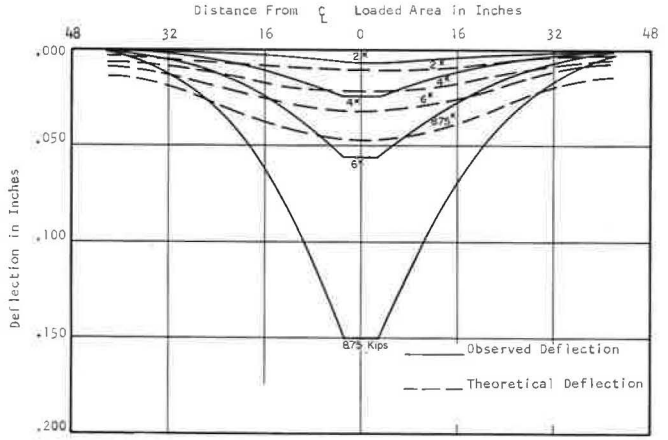

Figure 8. Load No. 1: surface deflection of pozzolanic base under static load at interior point.

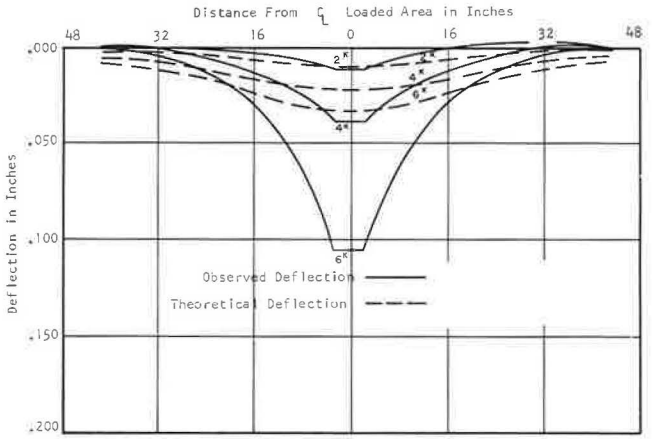

Figure 9. Load No. 2: surface deflection of pozzolanic base under static load at interior point.

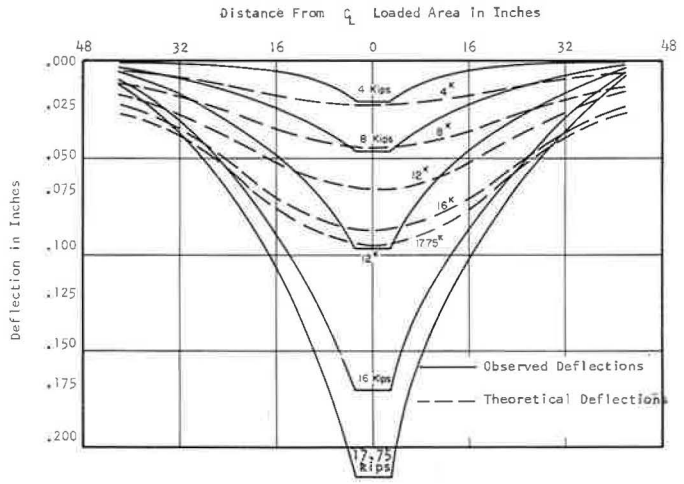

Figure 10. Load No. 3: surface deflection of pozzolanic base under static load at interior point.

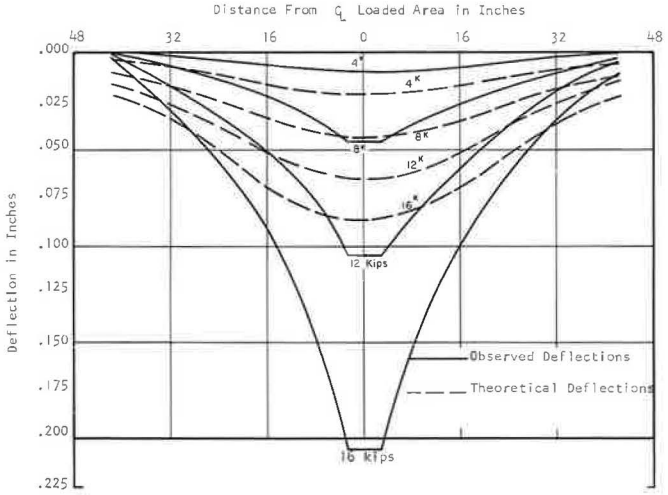

Figure 11. Load No. 4: surface deflection of pozzolanic base under static load at interior point.

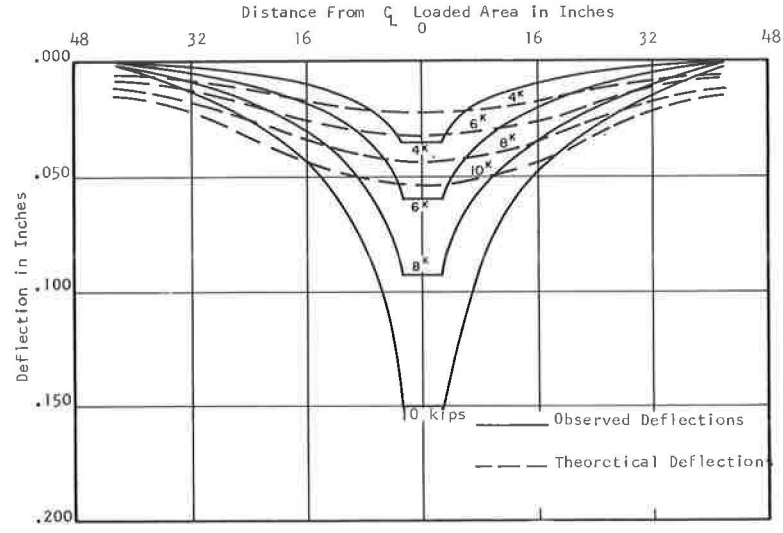

Figure 12. Load No. 7: surface deflection of pozzolanic base under static load at interior point.

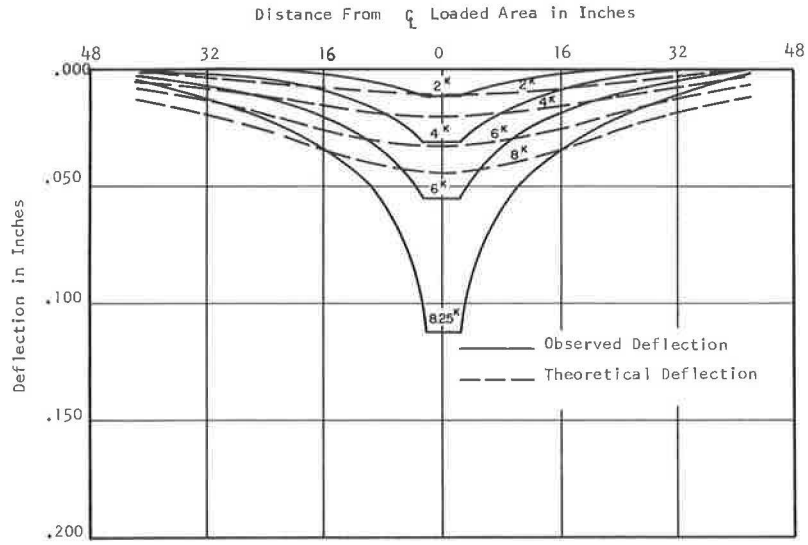

Figure 13. Load No. 8: surface deflection of pozzolanic base under static load at interior point.

of pavement action between test pavements. Test set IV was constructed to test the behavior of pavements under edge loading conditions. Construction joints, which provided no load transfer between pavements, were placed between the pavements thus simulating the most severe edge loading condition anticipated from a transverse crack across a pavement.

Initial loading was applied to the test pavements of test set II after accelerated curing equal to approximately 28 days under ambient conditions. At the time of initial loading, the pozzolanic-stabilized material had a modulus of rupture of 185 psi. A summary of the properties of the pozzolanic material and the gain in strength during loading is given in Table 9. More than a million applications of the 1, 850-lb wheel load were applied to the test pavements of test set I during the 120-day period. After

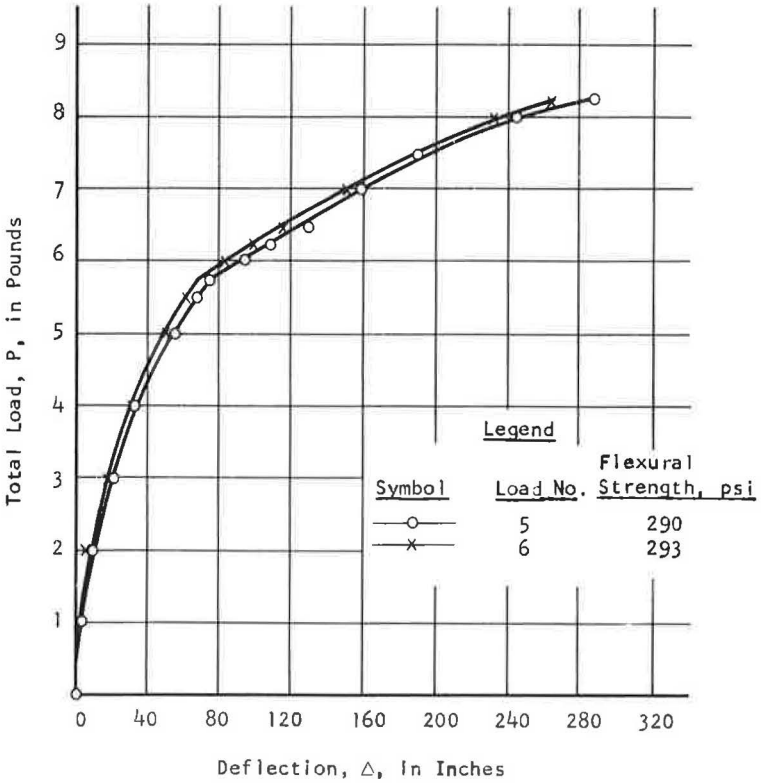

Figure 14. Load Deflection curves for static loads 5 and 6, applied near edge of pavement.

the million loads had been applied without evident distress in the pavements, the load was increased to 3,180 lb/wheel and an additional 300,000 load applications applied. Again, there was no sign of pavement distress, and since the strength of the material was increasing continuously further testing was terminated. Flexural strength of the pozzolanic material at the termination of the test was well in excess of 350 psi.

Pavements in test set III were loaded initially with the 3,180-lb wheel load 5 days after placement of the pozzolanic-stabilized material. Again, the pavements were tested under interior loading conditions with the thickened transition section between pavements. The thickness of the test pavements is given in Table 1, and a summary of the strength and strength gain properties for the pozzolanic material for test set III is given in Table 10.

Slightly more than 500,000 load applications were applied to test pavements of test set III in a 14-day period. During this time the modulus of rupture of the pozzolanic material increased from approximately 75 psi to 192 psi. Test pavements 1 and 5 failed during the first day of loading operation with a well developed crack pattern readily apparent after approximately 15,000 load applications. There is some indication that the initial failure of test pavements occurred after approximately 5,000 load applications but the cracks on the surface were not readily apparent at that time. A map of the crack pattern from the surface of test pavement 1 is shown in Figure 25. A section taken across the wheelpath of test pavement 1 after failure is shown in Figure 26.

Test pavement 5 of test set III deteriorated so rapidly, and to such an extent, that the crack development and the failure pattern could not be studied. After complete failure of test pavement 5, the pozzolanic material was removed with honeycombing and segregation of the aggregate observed near the bottom of the test pavement.

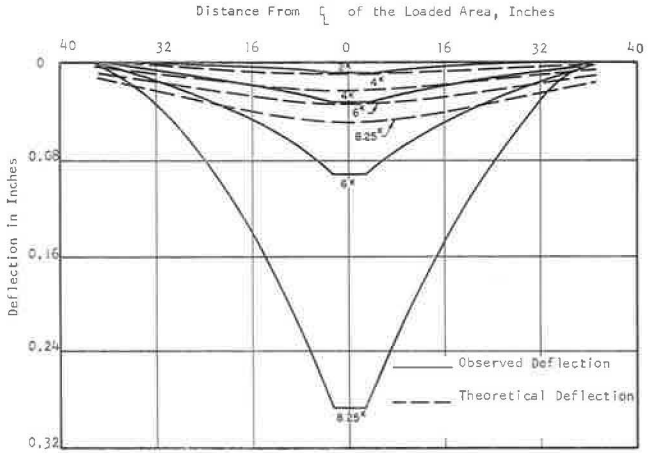

Figure 15. Load No. 5: surface deflection of pozzolanic pavement parallel to edge of pavement under static loads applied near edge.

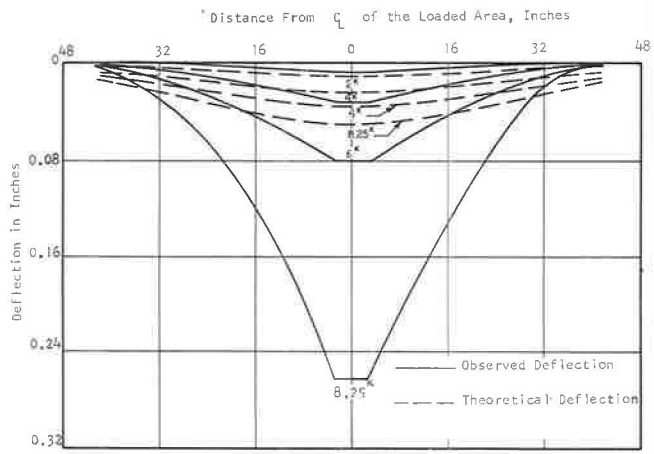

Figure 16. Load No. 6: surface deflection of pozzolanic pavement parallel to edge of pavement under static loads applied near edge.

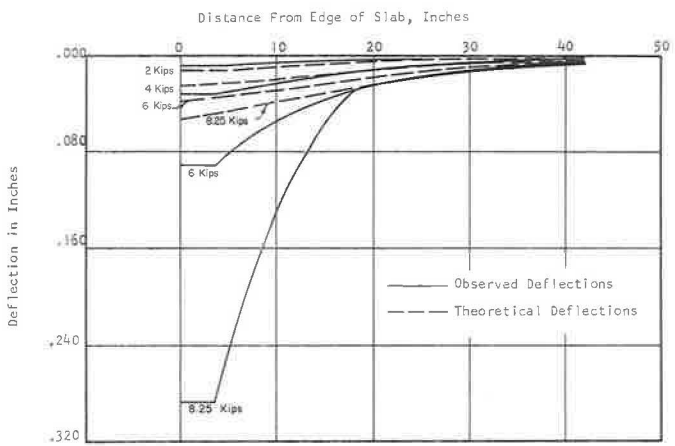

Figure 17. Load No. 5: surface deflection of pozzolanic pavement along line perpendicular to edge of pavement, under static load applied near edge.

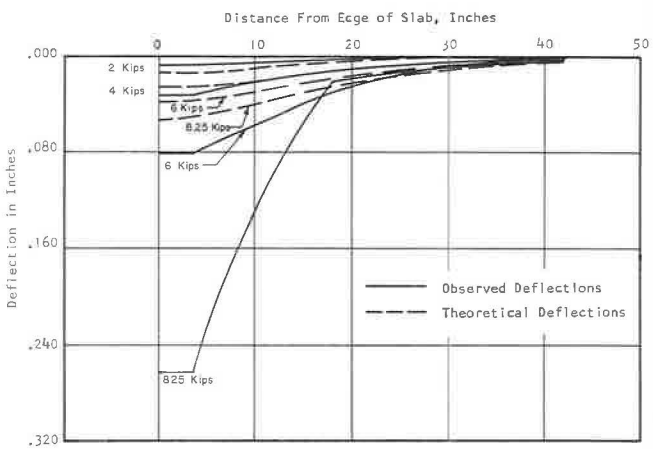

Figure 18. Load No. 6: surface deflection of pozzolanic pavement along line perpendicular to edge of pavement, under static load applied near edge.

Application of the loads on pavements 2, 3, 4 and 6 was terminated after the 500,000 applications as it was evidenct that no further pavement distress was occurring, and the strength of the pozzolanic material had increased to such an extent that pavement damage due to repeated load applications was unlikely.

Test set IV was designed to evaluate pozzolanic pavements under edge load conditions with dynamic loads. Two pavement thicknesses of 4.0 and 5.5 in. were tested with one test pavement of each thickness placed on each of 3 different days so that the effect of both thickness and strength on the ability of the pavement to withstand repeated load applications could be evaluated. Pavement thickness, age at the start of testing, properties of the subgrade, and properties of the pozzolanic stabilized material for test set IV are given in Table 11. Edge conditions for the test pavement were obtained by forming construction joints at the intersection of the test pavement sections. These construction joints were filled with an asphaltic patching mixture before testing.

Test pavement 1 showed excessive deflection with the first load application, and after approximately 10 load applications a network of cracks was clearly visible on the pavement surface. After approximately 40 load applications, the pavement had disintegrated to the extent shown in Figure 27.

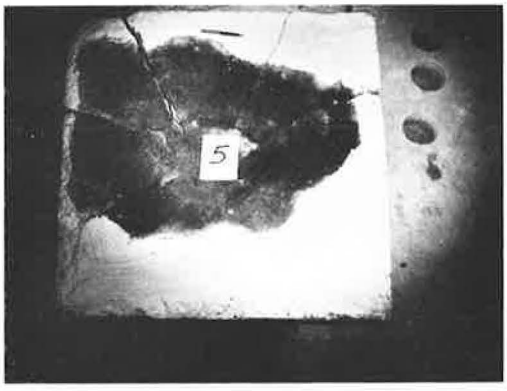

Figure 19. Bottom face of inverted section of pavement after failure under static load.

Visible cracks appeared on the surface of test pavement 6 after approximately 80 load applications. The cracks expanded with additional load applications and additional cracks developed. After approximately 140 load applications, cracks were also visible in test pavement 2. After approximately 175 load applications, the crack patterns in test pavements 2 and 6 had developed to the extent shown in Figures 28 and 29. Complete structural failure followed the initial cracking of both test pavements 2 and 6. Test pavement 2 had failed completely after approximately 600 load applications and test pavement 6 after approximately 1,700 load applications, all of which were applied during the first day of loading. After failure, test pavements 1, 2 and 6 were replaced with a high early strength concrete pavement so that additional load applications could be applied to the remaining test pavements.

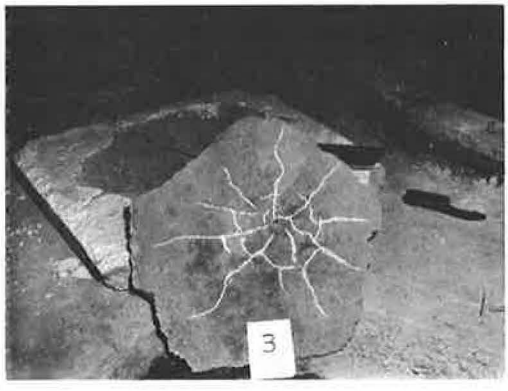

Figure 20. Bottom surface of typical cones punched out of pavement in static load tests.

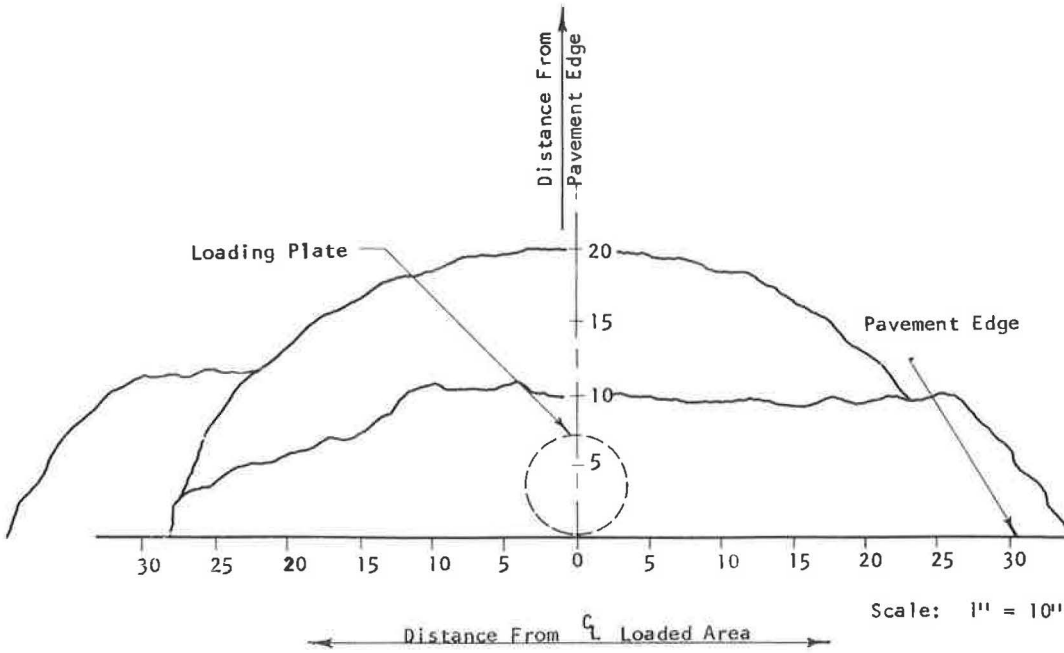

Figure 21. Load No. 5: crack pattern on surface of pavement at end of static load test.

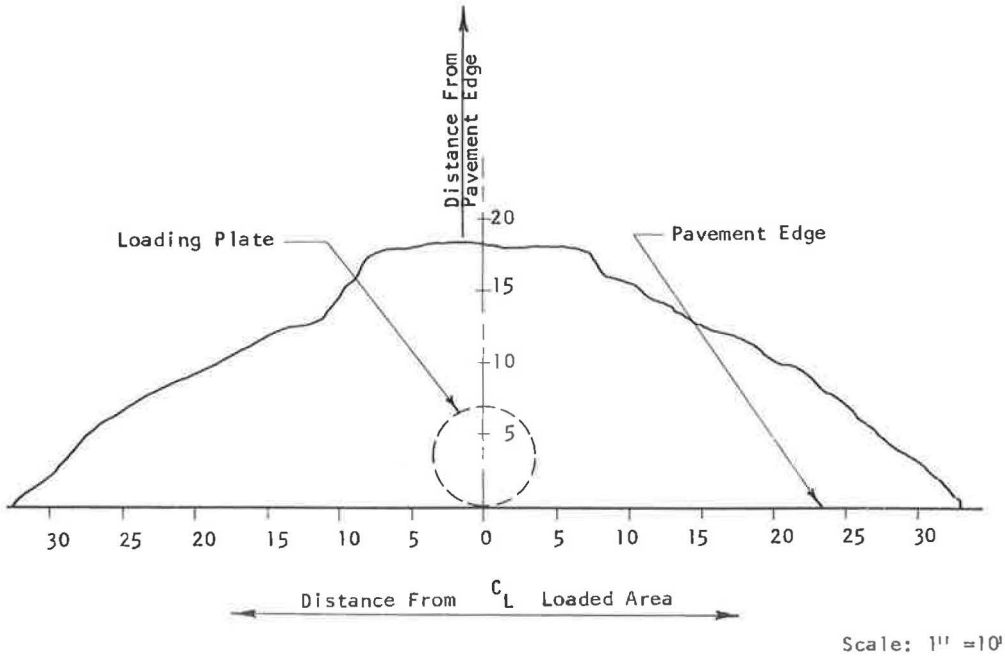

Figure 22. Load No. 6: crack pattern on surface of pavement at end of static load test.

TABLE 9

SUMMARY OF DATA ON POZZOLANIC MATERIAL FOR PAVEMENT OF TEST SET II

Strength Property	Age[a] (days)					
	0	4	12	28	50	120
Flexural, psi	185	196	219	254	257	352
Compressive, psi	1,110	1,140	1,080		1,520	1,680
Modulus of elasticity, $\times 10^6$, psi[b]		2.3	2.5	2.3	2.4	2.5

[a]After initial loading.
[b]The modulus of elasticity was determined from strain measurements on flexure specimens.

TABLE 10

SUMMARY OF DATA ON POZZOLANIC STABILIZED MATERIAL FOR TEST PAVEMENT OF TEST SET III

Strength Property	Age[a] (days)		
	0	5	14
Flexural, psi	75	160	192
Compressive, psi	420	890	1,180
Modulus of elasticity, $\times 10^6$, psi	1.3	1.9	—

[a]After initial loading.

TABLE 11

SUMMARY OF DATA ON POZZOLANIC MATERIAL FOR TEST PAVEMENT OF TEST SET IV

Strength Property	Age[a] (days)					
	5	9	16	16	9	5
Flexural, psi	76	170	230	230	170	76
Compressive, psi	300	580	800	800	580	300

[a]After initial loading.

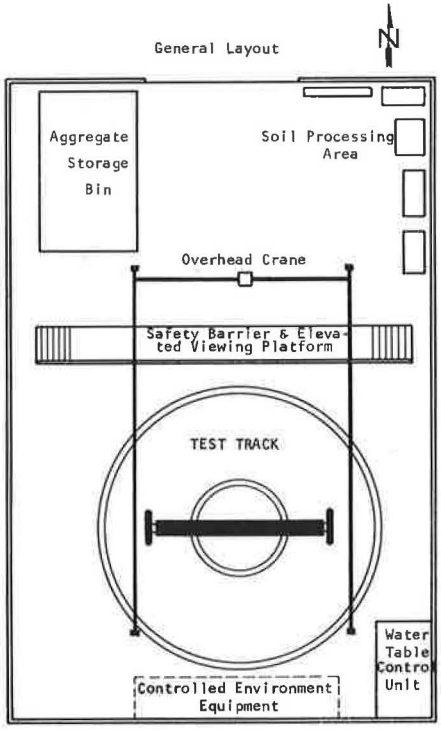

Figure 23. University of Illinois pavement test track.

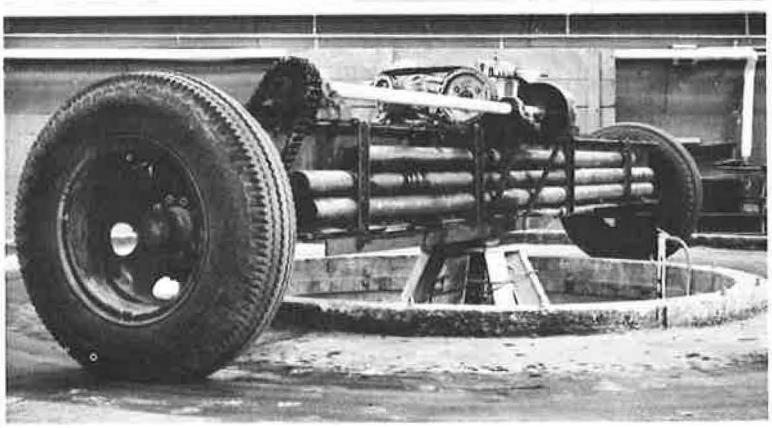

Figure 24. Loading frame used in test track for dynamic load tests.

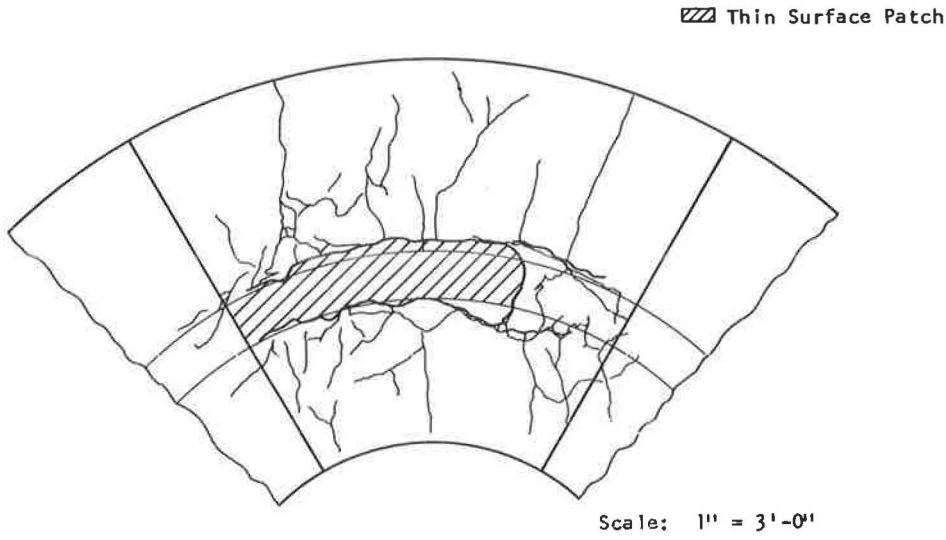

Figure 25. Surface crack pattern of test pavement 1, test set III, after approximately 15,000 load applications.

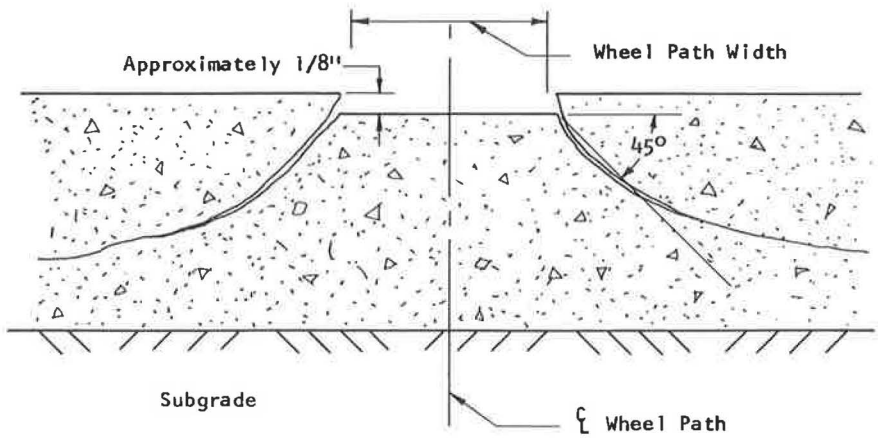

Figure 26. Test pavement 1, test set III: section through wheelpath in area of failure after approximately 15,000 load applications.

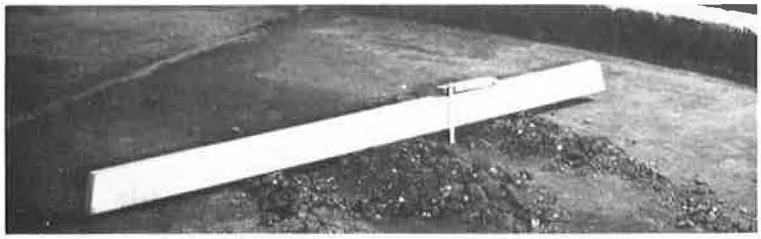

Figure 27. Test pavement 1 of test set IV after 40 applications of load, showing severe rutting and complete disintegration of material caused by excessive load applied before adequate curing.

Figure 28. Crack patterns observed on test pavement 2 of test set IV after 175 load applications with white paint applied to outline location of cracks.

Figure 29. Crack patterns observed on test pavement 6 after 175 load applications, with white paint applied to outline location of cracks.

Testing resumed on the remaining test pavements approximately 36 hr after the initial loading, and slightly more than 500, 000 applications of the 3, 180-lb wheel load were applied to test pavements 3, 4 and 5 without any evidence of pavement distress. At this time, the loading was discontinuous because the apparent gain in strength of the material had made pavement failure under repeated load applications unlikely.

RESULTS

Pozzolanic stabilized materials take on additional set with time and become hard and resistant to flexing. Pavements made of these materials, after a reasonable set, distribute the load over an extended area of subgrade in the same manner as plain

concrete pavements, and thus should be classified as rigid pavements. The extent of the load distribution is evident in the results from the static load tests.

Elastic theories of pavement behavior such as Westergaard's (3) equations accurately predicted the deflection profile and the maximum deflection of the pozzolanic pavements under static loads, provided the load was significantly less than the ultimate load carrying of the slab. As the load was increased above approximately one-half the ultimate load-carrying capacity of the slab, the pavement deflection increased more than indicated by the elastic theory with each load increment. These elastic theories of pavement behavior were, however, completely invalid for predicting the ultimate load-carrying capacity of the slab, as the latter was many times greater than that indicated by the elastic theories and the modulus of rupture for the material.

Meyerhof (4) developed equations for estimating the ultimate load-carrying capacity of plain concrete slabs based on the Rankine failure criterion for the material. Since the physical properties of hardened pozzolanic materials are similar to those of plain concrete, Meyerhof's equations should also apply to the pozzolanic material.

According to Meyerhof, the failure of nonreinforced slabs made from a material much stronger in compression than in tension should proceed in the following manner. When a central concentrated load, much less than ultimate, is applied over a small circular area on a slab in full contact with the base, the stresses and deflection of the slab can be computed using elastic theories for infinite slabs on an elastic subgrade. As the load increases, the bending stresses below the load become equal to the flexural strength of the material and the slab begins to yield, leading to radial tensile cracks in the bottom of the slab (Fig. 30a). With increasing load the radial cracks increase in length until the circumferential, flexural stresses along the arc with radius b become equal to the flexural strength of the material, at which time a circumferential crack appears on the slab surface and the slab collapses completely. The initial yield moment along a unit section of the slab can be calculated from elastic theory, with the yield moment of the slab given by

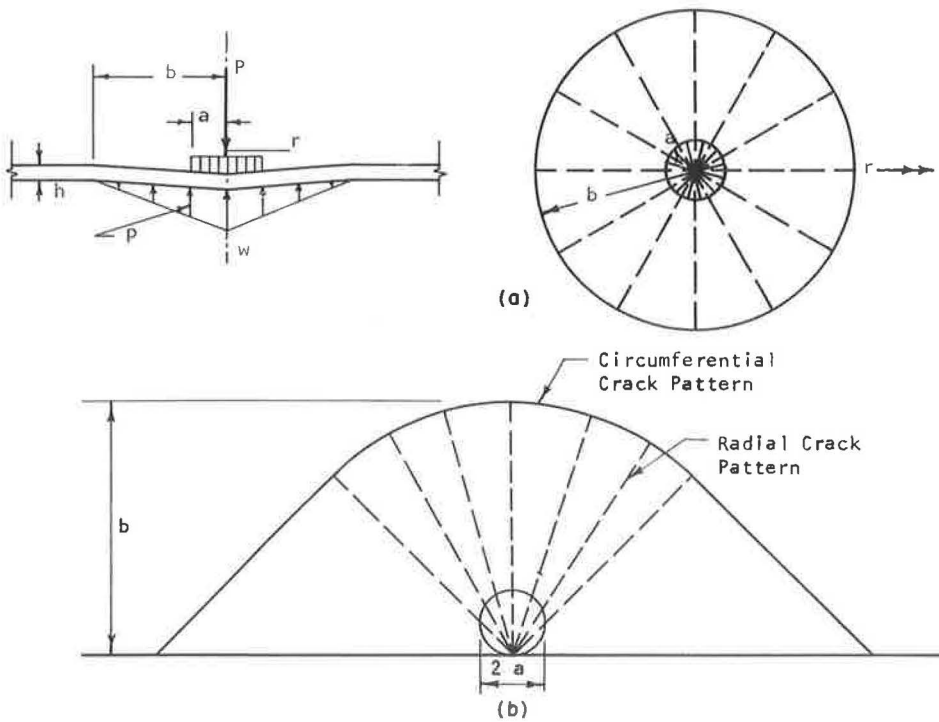

Figure 30. Failure pattern of rigid slab under (a) interior loading and (b) edge loading, as predicted by Meyerhof (4).

$$M_y = \frac{f_b h^2}{6} \tag{1}$$

where

M_y = yield moment per unit length of slab,
h = slab thickness, and
f_b = modulus of rupture of the material.

Using the dense liquid subgrade assumed by Westergaard, the radius of relative stiffness for the pavement is given by

$$L = \sqrt[4]{\frac{E h^3}{12(1 - \mu^2)k}} \tag{2}$$

where

E = modulus of elasticity of the slab,
k = modulus of subgrade reaction, and
μ = Poisson's ratio.

With this nomenclature, Meyerhof showed that the ultimate load-carrying capacity of the slab under interior loads is given by

$$P_o = \frac{4\pi M_o}{\left(1 - \frac{a}{3L}\right)} \quad \left(\text{for } \frac{a}{L} > 0.2\right) \tag{3}$$

where

M_o = yield moment for the slab, and
a = radius of the circular loaded area.

For a concentrated load applied over a circular area placed tangent to the edge of the slab, the yield load can again be estimated from elastic theory. As the load increases beyond that causing yield stresses in the bottom of the slab, radial tension cracks develop and widen until a circumferential crack (Fig. 30b) forms on the surface leading to the complete collapse of the slab. The collapse load for plain concrete slabs under edge loads is given by

$$P_o = \frac{(\pi + 4) M_o}{\left(1 - \frac{2a}{3L}\right)} \quad \left(\text{for } \frac{a}{L} > 0.2\right) \tag{4}$$

The limit of $a/L > 0.2$ in Eqs. 3 and 4 is based on the assumption that the circumferential crack is at a distance of $3L$ from the loaded area. Since the crack usually forms at a distance of $2L$ or less from the load, this ratio can be reduced somewhat.

Since, for nonreinforced slabs, $M_o = M_y = (f_b h^2)/6$, Eqs. 3 and 4 can be rewritten in the following forms:

For interior loads:

$$P_o = \frac{2\pi f_b h^2}{3\left(1 - \frac{a}{3L}\right)} \tag{5}$$

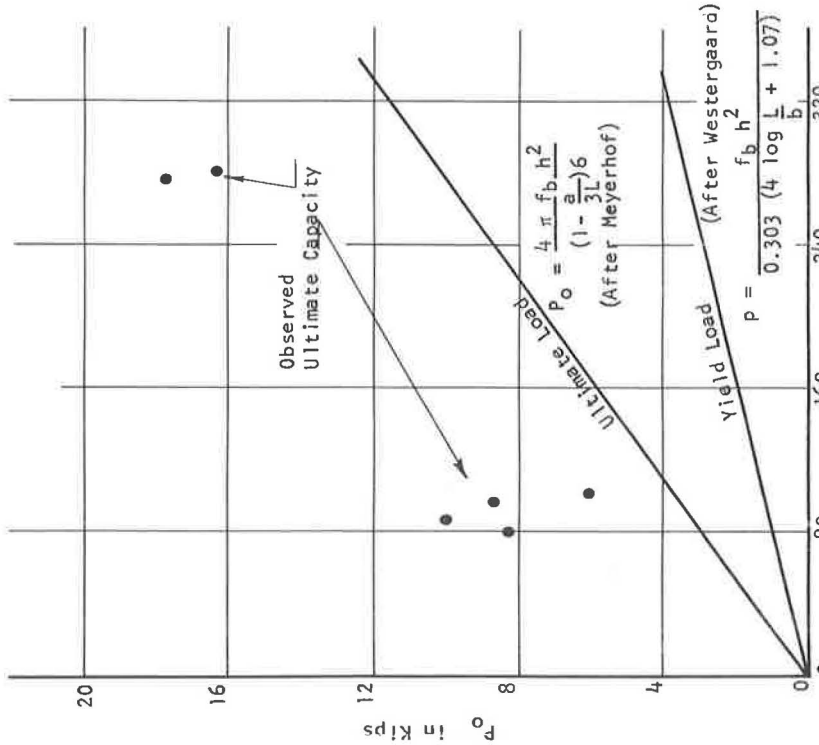

Figure 31. Comparison of theoretical failure loads and observed ultimate loads for 4 in. pozzolanic pavement under interior loading.

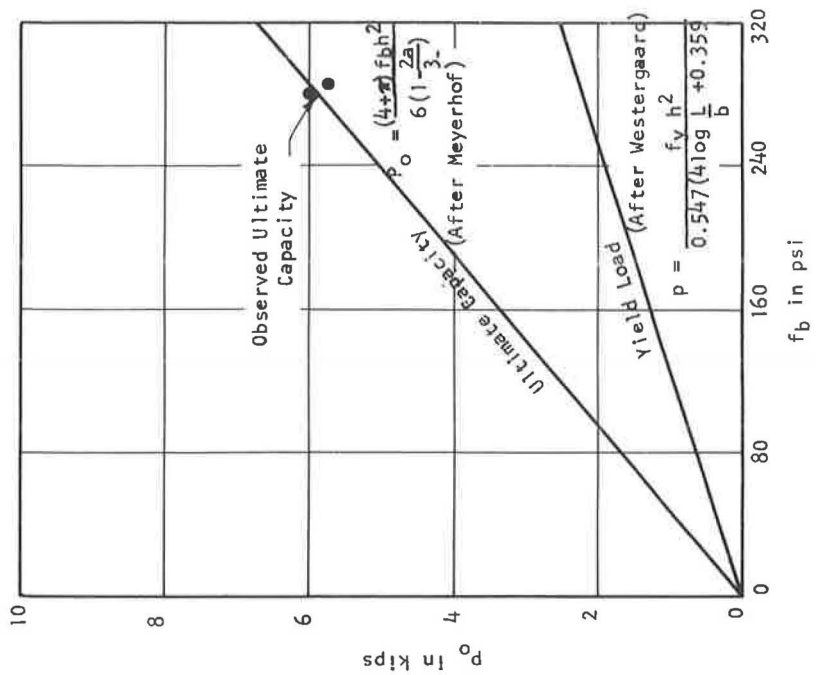

Figure 32. Comparison of theoretical failure loads and observed ultimate loads for 4 in. pozzolanic pavement under edge loading.

For edge loads:

$$P_o = \frac{(4 + \pi) f_b h^2}{6\left(1 - \frac{2a}{3L}\right)} \quad (6)$$

Comparison of the theoretical ultimate loads given by Eq. 5 and the results from the interior load test are shown in Figure 31. Comparison of the ultimate load given by Eq. 4 and the results from the edge load tests are shown in Figure 32. The yield loads determined from Westergaard's equations are also shown on the appropriate figures.

The theoretical collapse load given by Meyerhof's theory is approximately 2.5 to 3 times the yield load for the slabs. Since the elastic theory was valid for all loads of less than one-half of ultimate, the deflection predicted by the elastic theory could be assumed valid for loads up to the yield load for the pavement.

Failure under the interior loads was a pop-through type failure and the anticipated circumferential crack on the pavement surface did not develop. However, the ultimate load at failure for all interior loads was greater than predicted by Meyerhof's theory. A possible explanation for this behavior is the arching action which develops in large slabs made of a material much stronger in compression than in tension. As yielding occurs in the areas of high tensile stress, there is a concomitant shift in the neutral axis of the slab. This shifting of the neutral axis causes the arching action (Fig. 33),

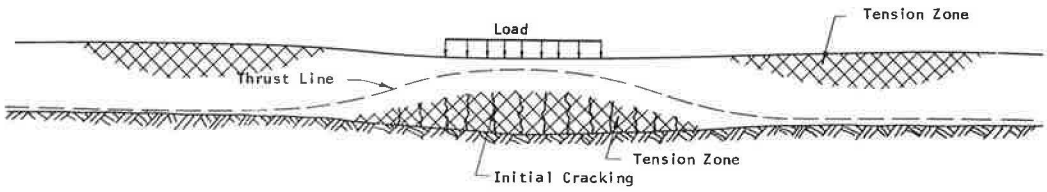

Figure 33. Schematic of stress pattern and arching phenomenon in slabs loaded at interior point.

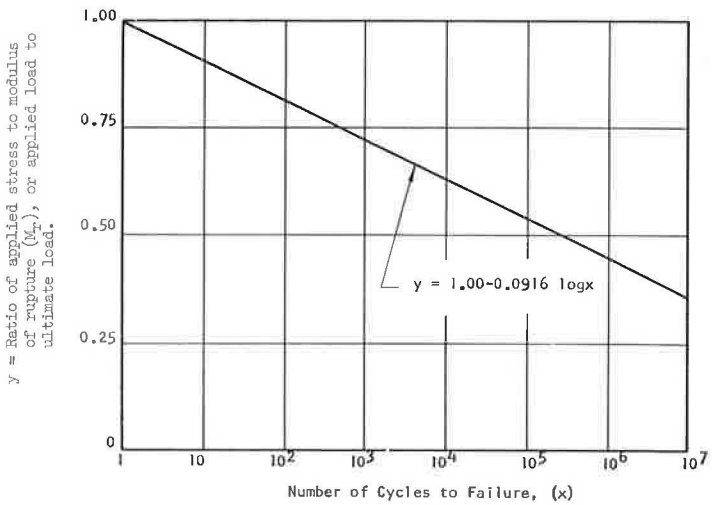

Figure 34. Fatigue behavior of lime-fly ash-aggregate-mixture (2).

which in turn prevents the circumferential crack from developing as expected. Radial cracks developed in the bottom of the slab as expected (Fig. 20).

Arching action does not develop near the edge of the pavement and, as a result, the failure mechanism under the edge loads was more nearly as anticipated. The observed collapse load under the edge loading is in good agreement with the values given by Meyerhof's equations.

Test sets II, III and IV were tested under repeated dynamic loads and thus should be analyzed in terms of the fatigue properties of the material. Fatigue properties of the pozzolanic material used in the test pavements were reported by Ahlberg and McVinnie (2), and the results are summarized in Figure 34.

The classical method for evaluating the fatigue properties of materials is to determine the number of load applications to failure based on a ratio of the stress in the slab to the modulus of rupture of the material. However, the results of the fatigue tests can also be interpreted in terms of the ultimate strength criterion. Since the modulus of rupture for the fatigue specimens is calculated from the ultimate load applied to the specimen and based on the linear theory, there is a linear relationship between the modulus of rupture and the ultimate load the specimens can carry. Therefore, since the number of load applications to failure determined from the ratio of the applied to the ultimate collapse load is the same as for the ratio of the theoretical to the failure stress, the load ratio criterion can also be used to evaluate the fatigue life of the pavements. A comparison of the expected number of load applications to failure, using the ratio of theoretical stress to yield stress and the ratio of applied load to ultimate load for test sets II, III and IV, is given in Table 12.

Neither the stress ratio criterion nor the load ratio criterion accurately predicted the number of load applications to failure for the interior loads of test sets II and III, although the load ratio criterion gave a better indication of the potential load carrying capacity than the stress ratio criterion. With both criteria the actual performance of

TABLE 12

SUMMARY OF RESULTS FROM DYNAMIC TESTING PROGRAM

Pavement No.	Pavement Thickness (in.)	M_r at Init. Loading (psi)	Applied Load	Theoret. Stress by Elastic Theory (psi)[a]	Ult. Load-Carrying Cap. (lb)[b]	Ratio of Theoret. Stress to M_r	Ratio of Applied Load to Ult. Load	Expected Load Applications to Failure[c]		Loads Applied to 1st Observed Failure[d]
								Using Theoret. Stress to M_r Ratio	Using Applied to Load Ratio	
Test Set II										
1	4.3	185	1,850	122	8,200	0.66	0.23	5,100	1×10^8+	1×10^8+[e]
3	3.8	185	1,850	150	6,000	0.81	0.31	120	7×10^7-	1×10^8+
4	4.8	185	1,850	101	9,500	0.55	0.20	81,000	1×10^8+	1×10^8+
5	4.3	185	1,850	122	8,200	0.66	0.23	5,100	1×10^8+	1×10^8+
Test Set II										
1	4.3	260	3,180	210	11,500	0.81	0.28	120	1×10^8	3×10^5[e]
3	3.8	260	3,180	258	8,400	0.99	0.28	1	1×10^7	3×10^5+
4	4.8	260	3,180	174	13,300	0.67	0.24	4,000	1×10^8+	3×10^5+
5	4.3	260	3,180	210	11,500	0.81	0.28	120	1×10^8	3×10^5+
Test Set III										
1	4.3	75	3,180	198	3,120	>>1	1.02	<<1	1	1.5×10^4
2	4.8	75	3,180	168	3,880	>>1	0.82	<<1	90	5×10^5+
3	5.3	75	3,180	143	4,680	>>1	0.68	<<1	3,100	5×10^5+
4	5.8	75	3,180	122	5,620	>>1	0.56	<<1	63,000	5×10^5+
5	4.8	75	3,180	168	3,880	>>1	0.82	<<1	90	1.5×10^4
6	5.3	75	3,180	143	4,680	>>1	0.68	<<1	3,100	5×10^5+
Test Set IV										
1	4.0	76	3,180	360	1,630	>>1	1.95	<<1	<1	<10
2	4.0	170	3,180	385	3,650	>>1	0.87	<<1	20	175
3	4.0	230	3,180	395	4,880	>1	0.65	<1	7,000	5×10^5+
4	5.5	230	3,180	230	9,050	1.00	0.35	1.0	1×10^7	5×10^5+
5	5.5	170	3,180	227	6,230	>1	0.51	<1	3×10^5	5×10^5+
6	5.5	76	3,180	213	3,030	>>1	1.05	<<1	≃1	80

[a]Data derived from reference 3.
[b]Data derived from reference 4.
[c]Data derived from Figure 34.
[d]Values with + sign showed no sign of failure at termination of the loading program.
[e]Pavements loaded with 1 million applications of the 1, 850-lb. load followed by 300, 000 applications of the 3, 180-lb. load.

TABLE 13

EFFECT OF STRENGTH GAIN WITH AGE ON THE NUMBER OF LOADS
(Test Pavement 3, Test Set IV)

Characteristic	Age[a] (days)				
	0	1 1/2	3	10	16[b]
Flexural strength, psi	230	247	260	310	340
Ult. load-carrying capacity	4,880	5,250	5,520	6,600	7,240
Applied load	3,180	3,180	3,180	3,180	3,180
Load ratio	0.65	0.61	0.58	0.48	0.44
No. of loads to failure based on load ratio at age indicated	7×10^3	1.6×10^4	3×10^4	4×10^5	8×10^5
Cumulative loads applied through day indicated	1.7×10^3	8×10^3	3×10^4	2×10^5	5×10^5

[a]After initial loading.
[b]Testing stopped at 500,000 load applications on this day.

the pavements far exceeded the expected performance. There are several possible reasons for this phenomenon.

As shown in Figure 31, the actual load-carrying capacity of the pavements under interior loads is somewhat greater than predicted by the ultimate theory, thus giving an actual load ratio less than that assumed from theoretical calculations. This decreased load ratio would lead to a higher number of load applications than indicated in the table for failure, bringing the observed load applications into better agreement with the theoretical number.

Under transient loads the supporting capacity of the subgrade is greater than indicated from static load tests. The increased subgrade support would increase the load-carrying capacity of the pavements and also give a smaller load ratio and a greater number of expected load applications to failure.

The increase in strength of the pozzolanic material during the load applications has a demonstrated effect on the number of load applications to failure (2). The potential influence of this gain in strength is demonstrated in Table 13 for test pavement 3 of test set IV. During the early part of the test the load applications accumulated faster than the increase in the required number of loads to failure, and the two were of the same order of magnitude during the third day of loading. After the third day, however, the required number of load applications to failure increased faster than the load applications could be accumulated. Since the pavement did not fail on the third day when the applied loads were equal to the number theoretically required for failure, it appeared likely that the pavement would not fail under the repeated load, and testing was terminated.

A study of the fatigue life for the pavements in test set IV indicates that the load ratio criterion is reasonably valid for predicting the expected life for the pavement of the test pavements under the edge loading. Of the pavements which did not fail, only test pavement 3 could have reasonably been expected to fail under repeated load applications when the load ratio criterion is applied. As demonstrated previously, this pavement did not fail, primarily because the gain in strength for the material was such that the pavement strength increased at a faster rate than the cumulative damage was done to the pavement. Hence, using the fatigue behavior of the material and the load ratio criterion, the failure of test pavements 5 and 6 was accurately predicted. There appears to be a consistent tendency for this procedure to give answers on the conservative side, even when using the load ratio criterion.

SUMMARY AND CONCLUSIONS

Pozzolanic materials gain strength at a relatively slow rate, but continue to gain in strength indefinitely but at a decreasing rate. Although the 7- and 28-day strengths are relatively low compared to concrete, after an extended period of time the strength of a high quality pozzolanic material may approach that of average quality concrete.

Even partially cured and hardened pozzolanic materials are stiff and resistant to flexural deformation. Measured values of the modulus of elasticity in flexure are between 1.5×10^6 and 2.5×10^6 after curing approximately 7 days under ambient conditions. With a modulus of this magnitude it can be expected that pozzolanic pavements will distribute the load over large areas of subgrade, thus producing low subgrade stresses.

Results from the pavement behavior studies clearly show that pozzolanic pavements act as slabs and distribute the load extensively, especially if the applied load is small compared with the ultimate capacity of the pavement. The load deflection characteristics of pozzolanic pavements can be predicted with reasonable accuracy with elastic theories of pavement behavior provided the calculated maximum stress in the pavement using the elastic theory is less than the modulus of rupture of the material.

The ultimate load-carrying capacity of the pavement is from two and one-half to three times the load which produces a theoretical maximum stress equal to the modulus of rupture of the material. The ultimate load-carrying capacity can be estimated by Meyerhof's theory for the collapse load.

Predicted fatigue life of pozzolanic pavements based on the yield load for the pavements is completely unrealistic. Predicted fatigue life based on a ratio of the applied to the ultimate load gives somewhat better results provided the gain in strength during the load applications is taken into account. Even with the load ratio criterion, however, the predicted life is conservative.

Based on the results from the repeated load applications on test pavements, it appears that the pozzolanic pavements which do not fail during the first several days of loading will probably not fail due to repeated load applications acting alone.

Finally, the load-carrying capacity of pozzolanic pavements can be improved either by increasing pavement thickness or by increasing the strength of the material. The simplest method for increasing the strength of the pozzolanic material is to allow additional curing time before loading. Since the rate of strength gain of pozzolanic materials is susceptible to the surrounding climatic conditions, the length of time for curing will also depend on the existing climatic factors of temperature and moisture. Sufficient curing time should be allowed before loading so that the pavement can carry the maximum anticipated load applied near the edge of the pavement without exceeding the ultimate load-carrying capacity of the pavement, with a reasonable factor of safety included.

ACKNOWLEDGMENTS

This research was carried out as a cooperative program between the University of Illinois Engineering Experiment Station and individual organizations from private industry. The author wishes to thank all those who contributed to the program.

REFERENCES

1. Ahlberg, H. L. and Barenberg, E. J. The University of Illinois Pavement Test Track — A Tool for Evaluating Highway Pavements. Highway Research Record No. 13, p. 1, 1963.
2. Ahlberg, H. L. and McVinnie, W. W. Fatigue Behavior of a Lime-Fly Ash-Aggregate Mixture. Highway Research Board Bull. 335, p. 1, 1962.
3. Westergaard, H. M. Stresses in Concrete Pavements Computed by Theoretical Analysis. Public Roads, Vol. 7, No. 2, 1926.
4. Meyerhof, G. G. Load-Carrying Capacity of Concrete Pavements. Journal, ASCE, Vol. 88, No. SM3,p. 89, June 1962.
5. The AASHO Road Test Report 2, Materials and Construction. Highway Research Board Spec. Rept. 61B, 1962.
6. The AASHO Road Test Report 5, Pavement Research. Highway Research Board Spec. Rept. 61E, 1962.

Critical Mechanical Properties of Structural Lightweight Concrete and Their Effects on Pavement Design

WILLIAM B. LEDBETTER, Assistant Professor of Civil Engineering, Texas A and M University;
ERVIN S. PERRY, Assistant Professor of Civil Engineering,
JAMES T. HOUSTON, Teaching Assistant in Civil Engineering, and
J. NEILS THOMPSON, Professor of Civil Engineering, University of Texas

This study examines the critical mechanical properties of structural lightweight concrete which might affect the performance of concrete pavements. The properties resulting from unrestrained and restrained volume change are presented, with particular attention given to compressive, direct tensile, and indirect tensile (split cylinder) strengths at various ages of the concrete.

The critical properties determined in this study indicate that concrete pavements can be designed with lightweight concrete, and that expected performance from the effects of warping stresses and pavements deflection will be better than that of pavements made with regular weight concrete. However, the effects of restrained volume change of lightweight concrete on pavement performance can be detrimental if improper curing, or curing for too short a time, occurs. The need for further research on the effects of curing on lightweight concrete pavement performance is emphasized.

•THIS STUDY had as its objectives: (a) to explore the properties of volume changes of a structural lightweight concrete due to temperature changes and moisture changes during curing (1, 2); (b) to explore trends of relationships between compressive, split cylinder, and flexural strengths; (c) to report further information on the direct tensile properties (3); (d) to present relationships between direct tensile, compressive, and split cylinder strengths, and to show how these are affected by different curing conditions; (e) to explore properties of the static modulus of elasticity in both tension and compression; and (f) to determine the effects of all lightweight structural concrete properties (4) investigated in this study on the design and performance of concrete pavement structures constructed with structural lightweight concrete.

VARIABLES

Material Variables

The foregoing objectives were accomplished for concrete made with one structural lightweight coarse aggregate and for concrete made with one regular-weight coarse aggregate. Only regular-weight fine aggregate was used. A structural, lightweight, semicoated, expanded shale (5) with a nominal maximum size of ¾ in. was used as a coarse aggregate in all tests of lightweight concrete. Cement factors of 4 sk/cu yd and 5 sk/cu yd were used with air contents of 2 percent (no air entrainment) and 6 percent (using an air entrainment additive).

Paper sponsored by Committee on Rigid Pavement Design.

Curing Variables

The three curing conditions employed were termed bag cured, oven cured, and air cured. Bag curing consisted of moist curing the specimens in sealed polyethylene plastic bags at 75 F, with a relative humidity of approximately 100 percent. The oven-cured specimens were cured at approximately 110 F and low humidity. The temperature in the oven probably varied ±5 F. The air-cured specimens were cured at approximately 50 percent relative humidity and 75 F generally prevailing in the laboratory. Concrete properties were determined at ages of ½, 2, 7, and 28 days in conjunction with the foregoing variables.

CONSTANTS

To isolate the relationships between test parameters, the following variables were held constant throughout this study: (a) mixing time and sequence, (b) cement type, (c) batch size, (d) air-entrainment type, (e) consistency, (f) test procedure (specimen size, rate of loading, etc.), and (g) fine aggregate type (regular weight only).

Materials, mixing techniques, and testing procedures have previously been discussed (1, 2).

DIRECT TENSILE TEST

General

Concrete tensile strength has long been of significance to design engineers. This property has been very difficult, if not impossible, to determine accurately and reliably. Many methods have been developed and tried, but none has experimentally evaluated this important property with any high degree of certainty (6). The main reasons for this difficulty lie in the nature of the material. Concrete, being relatively weak in tension, is significantly influenced by small eccentricities in applied tensile loads, stress concentrations, variations in paste-aggregate ratios throughout the specimen, etc.

In 1955 a method was reported by Todd (7) which offered a technique to determine tensile strength, tensile stress-strain relationship, and the effects of restrained volume changes on tensile strength and stress-strain characteristics of structural concrete. This idea has been amplified and developed at the University of Texas. Several studies have been made on the use of this method and the applications of the information obtained to structural problems(8, 9, 10).The method has been further modified and used extensively in this study.

Test Specimen

The test specimen consists of a thick-walled steel tube on which electrical SR-4 strain gages are mounted; these gages are protected by a brass sleeve around the tube, and the tube is encased in a specimen of concrete. Figure 1 shows an overall view of the steel tube and the brass sleeve. The tube surface has deformations which aid in bonding the concrete to the steel. The brass sleeve, in addition to moisture-proofing the gages, serves to reduce the cross-sectional area of the concrete, and thereby to insure concrete failure at the point where the gages are mounted.

An overall view of the completed tube assembly is shown in Figure 2. Petrosene wax is sloped around the ends of the sleeves in a gradual taper to reduce stress concentrations in the concrete surrounding the steel specimen. Figure 3 shows the complete specimen encased in the concrete and loaded to concrete failure, with the failure crack painted to indicate its position. A schematic drawing of the entire assembly is shown in Figure 4. The "0" rings in the sleeve prevent moisture in the concrete from entering the cavity around the gages.

Two etched-foil type 90-deg rosette SR-4 strain gages are mounted on the steel tube, with one grid of each parallel to the longitudinal axis of the tube and the other grid perpendicular to the axis. A close-up view of the strain gages is shown in Figure 5. These two gages (a total of four grids) are wired together to form a full wheatstone

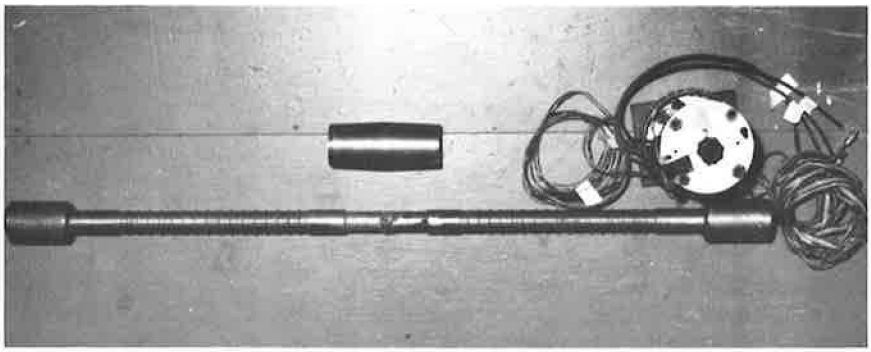

Figure 1. Disassembled steel tube and brass sleeve.

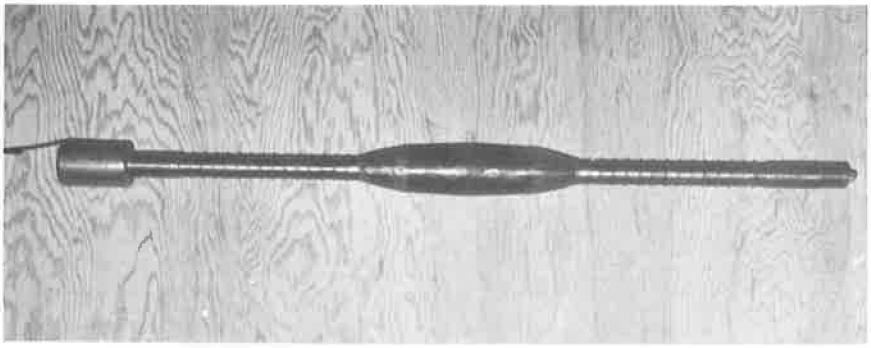

Figure 2. Assembled steel tube and brass sleeve.

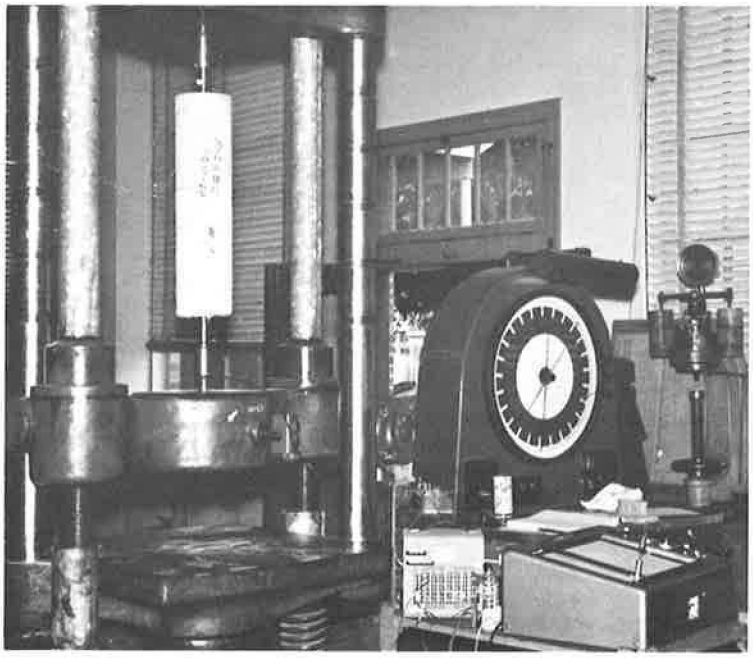

Figure 3. Overall view of direct tensile test concrete specimen loaded to failure.

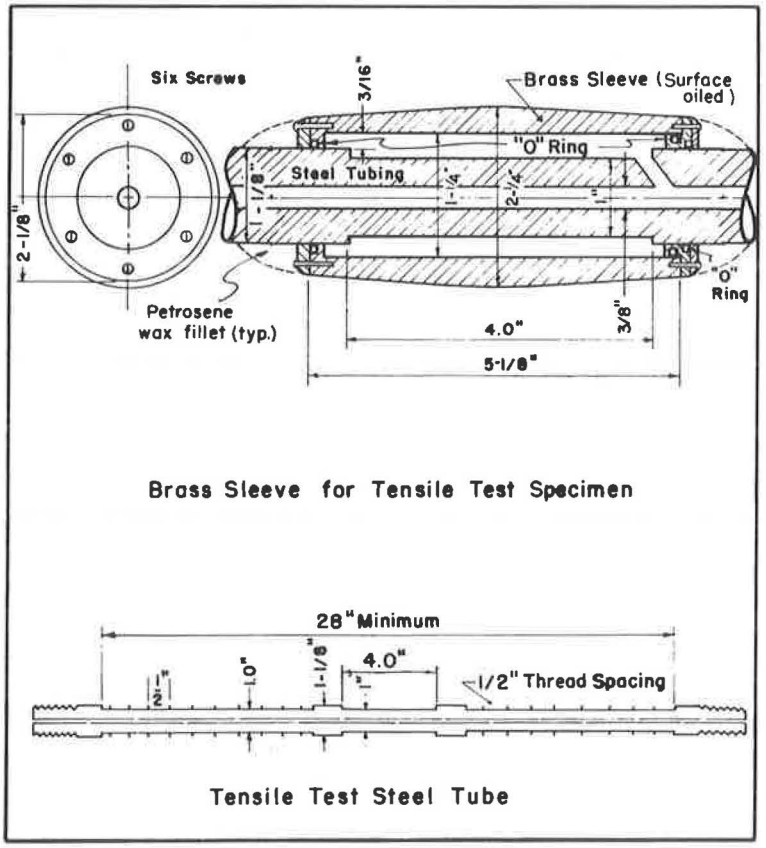

Figure 4. Concrete direct tensile test specimen.

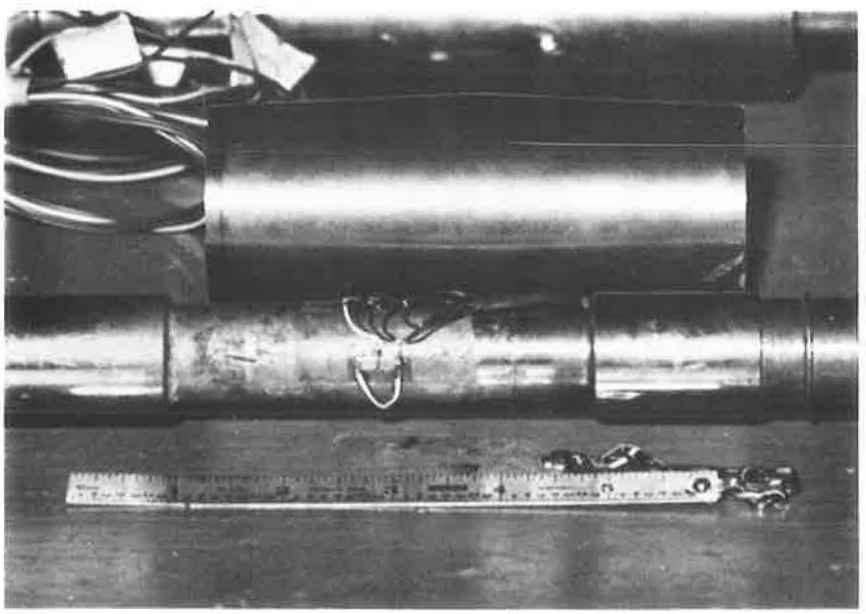

Figure 5. Closeup of direct tension steel tube showing 90-deg rosette etched foil SR-4 strain gage.

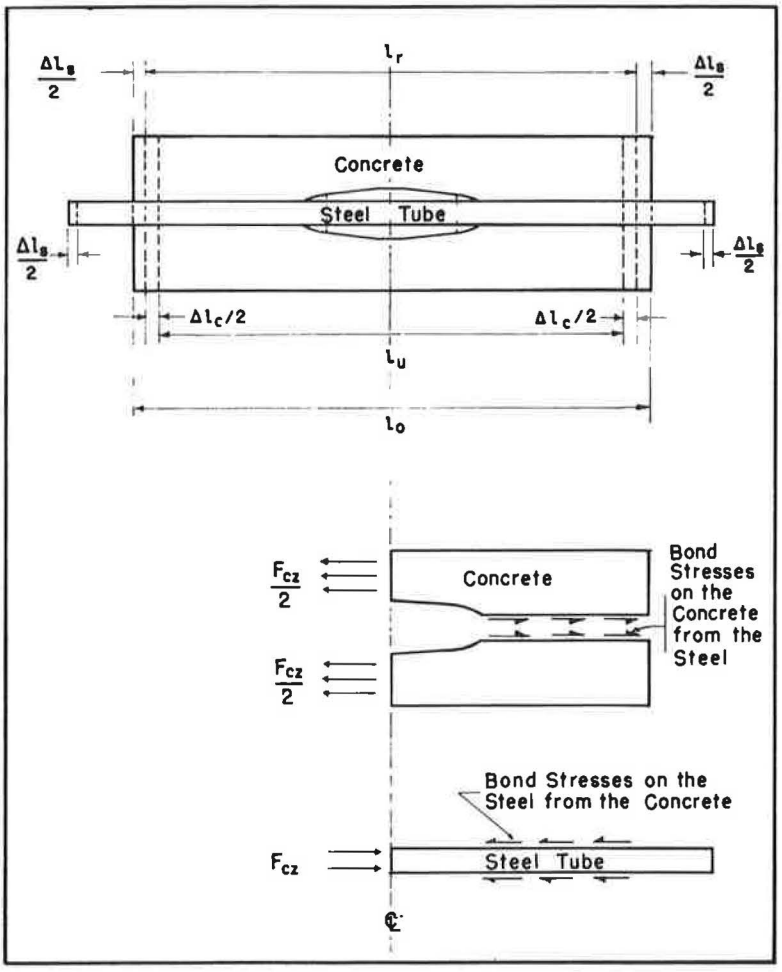

Figure 6. Direct tensile test specimen showing simplification of forces resulting from restrained hydration shrinkage in the concrete.

bridge circuit. The lead wires are carried from the gages along the inside of the tube to the end of the specimen and then to a switch unit.

Restrained Shrinkage Measurement

With the strain-gage arrangement on the steel specimen, the strains occurring on the tube surface can be accurately measured from the time the concrete is molded around the steel specimen. As the concrete hardens from a viscous pseudofluid into a pseudocrystalline solid, extremely complicated chemical reactions and changes of state occur, which cause volume changes to occur in the concrete mass. The steel, being relatively stable dimensionally, partially restrains this volume change in the concrete, thereby causing strains to occur in the steel and the concrete.

A simplified schematic of the effects of a restrained concrete shrinkage is shown in Figure 6. Due to the occurrence of shrinkage phenomenon in the concrete, the concrete of original length ℓ_o would, if unrestrained, shrink to an unrestrained length ℓ_u. But, because of the presence of the steel, only partial shrinkage can take place to a restrained length ℓ_r somewhere between ℓ_o and ℓ_u. Ideally, this results in a net tensile strain in the concrete, ϵ_{cz}, due to restrained concrete volume changes of

$$\epsilon_{cz} = \frac{\ell_r - \ell_u}{\ell_o} = \frac{\Delta\ell_c}{\ell_o}$$

and, ideally, a net compressive strain in the steel ϵ_{sz} of:

$$\epsilon_{sz} = \frac{\ell_o - \ell_r}{\ell_o} = \frac{\Delta\ell_s}{\ell_o}$$

if it is assumed that no slippage occurs between the steel and the concrete. During this volume change period, there are no external forces on the specimen; therefore, since equilibrium exists at the centerline of the specimen, the total tensile force in the concrete must equal the total compressive force in the steel from the restrained shrinkage. Or,

$$F_{cz} = -F_{sz} \tag{1}$$

where

F_{cz} = total force in concrete due to restrained volume changes, lb; and
F_{sz} = force in steel due to restrained volume changes, lb.

It follows, therefore, if the true steel strain the steel ϵ_{sz} is measured, that the force in the concrete, and hence the stress in the concrete, can be computed by:

$$\sigma_{cz} = \frac{F_{cz}}{A_c} = \frac{-F_{sz}}{A_c} = \frac{-\epsilon_{sz} E_s A_s}{A_c} \tag{2}$$

where

σ_{cz} = concrete stress due to restrained volume changes, psi; and
A_c = concrete cross-sectional area, sq in.

Therefore, by measuring the strain in the steel at the centerline of the specimen at given time intervals, or continuously from the time the concrete is poured, a concrete stress vs concrete age can be accurately determined throughout the hydration period.

An important point in the foregoing analysis is that no assumption was made concerning the relationship between the true steel strain due to restrained volume changes ϵ_{sz} and the concrete strain due to restrained volume changes ϵ_{cz} at the centerline during this restrained shrinkage process. Obviously, since the forces in the steel and the concrete are equal as given in Eq. 1,

$$\epsilon_{sz} \neq \epsilon_{cz}$$

at the centerline unless the relationship between A_s / A_c and E_s / E_c is such that the strains could be equal without violating Eq. 1. This presents no difficulties since the steel and concrete are unbonded at the centerline of the specimen and slip at the interface can take place easily.

Direct Tensile Load Test

During the tensile load test, a uniaxial tensile load is applied to the ends of the steel tube. The composite specimen of steel and concrete combines to carry the applied external load. Using a slide-wire potentiometer bridge circuit attached to the load dial on the testing machine, the change in resistance corresponding to the change in the applied load was fed into the Y-axis of a Mosely Autograph X-Y plotter. The signal from

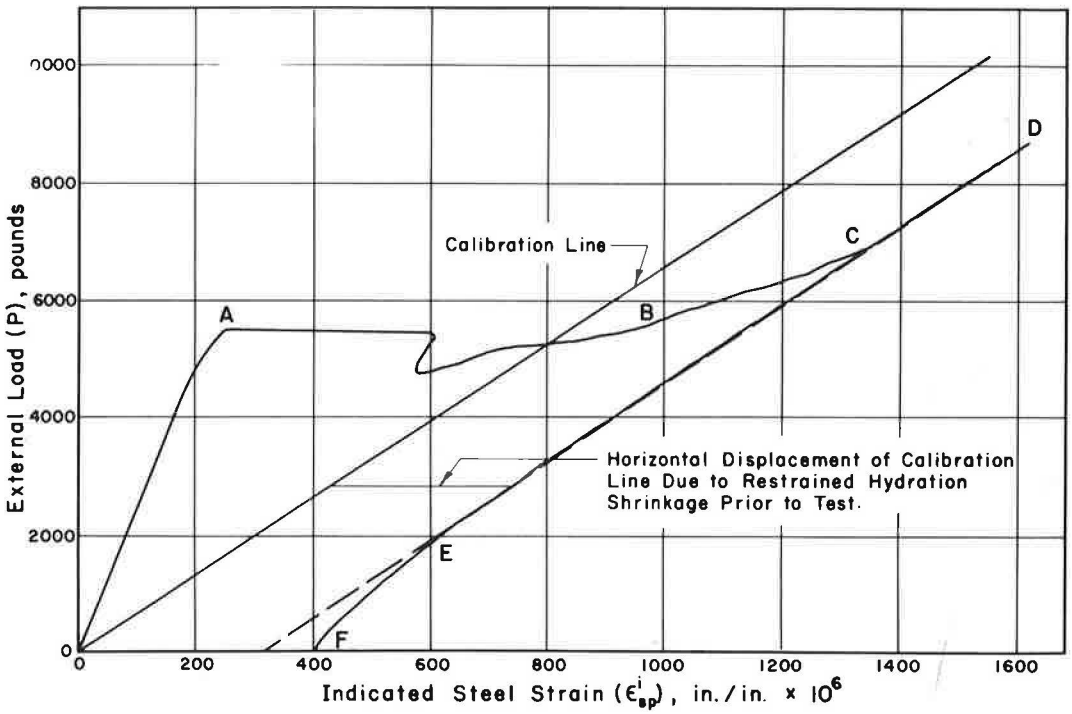

Figure 7. External load-indicated steel strain test trace for direct tensile test of concrete.

the full external bridge strain-gage circuit in the specimen was fed into the X-axis of this same plotter. After suitable load and strain calibration, external applied load vs indicated steel strain was accurately traced on a sheet of graph paper by this plotter. A reproduction of a test trace of external load vs indicated steel strain is shown in Figure 7.

The load is carried by the composite action of concrete and steel from point 0 to point A. At point A the concrete has reached its full tensile capacity and on application of the additional load, the concrete fails in tension. As this occurs, the load being carried by the concrete is suddenly shifted to the steel with a corresponding sudden increase in indicated steel strain.

To determine the net load being carried by the concrete, it is necessary to plot on the graph the results of the load vs indicated steel-strain calibration line of the bare specimen (without the concrete) which is determined by running a separate load test with the bare specimen. Then the external load carried by the concrete P_c is simply the vertical distance between the 0A curve and the steel calibration line.

$$P_c = P - P_s$$

and

$$\sigma_{cp} = \frac{P_c}{A_c} \tag{3}$$

where

P = total external load, lb;
P_s = external load in steel, lb; and
σ_{cp} = concrete stress due to external load, psi.

Often the initial concrete crack does not extend throughout the cross-section of the concrete and, after initial cracking at point A, the reduced concrete section may carry some small additional load before completely failing as is shown between points B and C in the figure. The drop in the applied load between point A and B is due to the fact that the machine is not straining fast enough to counteract fully the rapid changes in strain at concrete failure, thus causing the applied load to drop off momentarily. There is also a slight time lag in plotting time due to the relatively slow dynamic response capability of the X-Y plotter. From points C to D the steel at the centerline of the specimen is carrying the entire external load, and the line is parallel to the steel calibration line. The test trace from C to D is horizontally separated from the steel calibration line by an amount equal to the initial compressive strain, ϵ_{sz}, in the steel. As unloading occurs, the test trace unloads to a point E, parallel to the steel calibration line, then deviates from this parallel line as the concrete crack does not close completely because of broken particles of concrete that become displaced on the fracture face.

During an early portion of the curve up to point A, the external load is carried by both the steel and the concrete at the centerline of the specimen. Assuming there is sufficient bond at both ends of the concrete specimen to insure that no slippage is occurring under load, for compatibility to exist at this centerline,

$$\epsilon_{sp} = \epsilon_{cp} \tag{4}$$

where

ϵ_{sp} = steel strain due to an external load; and
ϵ_{cp} = concrete strain due to an external load.

This strain condition is quite different from that existing from strain volume changes before testing, and thus

$$P_c \neq P_s \tag{5}$$

which is reversed from the conditions existing before loading.

Eq. 4 was verified experimentally by placing two concrete embedment gages inside the concrete adjacent to the steel specimen gages on opposite sides of the cylinder to measure ϵ_{cp} directly. An extremely close agreement was obtained.

This, the true concrete strain, ϵ_{cp}, from the external applied load can be determined from the test trace.

Using Eqs. 3 and 4, the concrete stress-strain curve from applied external loads can be calculated and plotted. From this curve the modulus of elasticity of the concrete in tension E_{ct} can be calculated. Referring to Eq. 2 and assuming the E_{ct} during testing is the same as the E_{ct} just before testing, ϵ_{cz} can be determined by

$$\epsilon_{cz} = \frac{\sigma_{cz}}{E_{ct}} \tag{6}$$

Therefore, combining Eqs. 2 and 3, the total corrected tensile stress σ_{ct} in the concrete can be calculated from

$$\sigma_{ct} = \sigma_{cz} + \sigma_{cp} \tag{7}$$

And, combining Eqs. 4 and 6, the total corrected tensile strain in the concrete ϵ_{ct} can be calculated from

$$\epsilon_{ct} = \epsilon_{cz} + \epsilon_{cp} \tag{8}$$

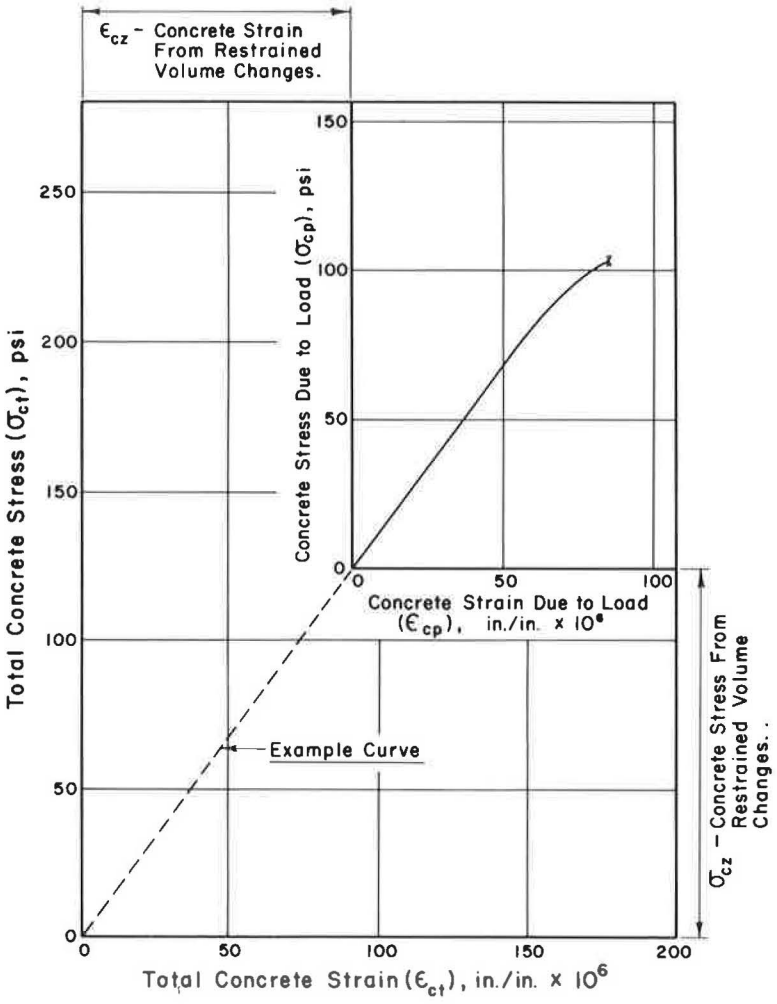

Figure 8. Structural lightweight concrete direct tensile stress-strain curve.

Figure 8 shows a sample concrete direct tensile stress-strain curve and the coordinate axes for the total stress-strain and the stress-strain from the external applied load. This figure is a graphical representation of Eqs. 7 and 8 and summarizes the information which may be obtained from the direct tensile test method.

TENSILE STRENGTH PROPERTIES

General

Tensile stress-strain properties, the effects of curing conditions on tensile strengths, and the various relationships between direct tensile, compressive, and split-cylinder strengths are presented in this section. Data used in plotting some of the curves are given in Table 1.

Effects of Environment on Tensile Stress-Strain Properties

Examples of the tensile stress-strain curves obtained in this investigation are shown in Figures 9 through 11. Each curve represents a single test. The dashed portion of each of the curves, whose ordinate is labeled σ_{cz}, represents the amount of restrained concrete volume-change stress present in the concrete before testing. The solid portion

TABLE 1

STRUCTURAL LIGHTWEIGHT CONCRETE DIRECT TENSILE TEST DATA TABULATION (AVERAGE VALUES)

Curing	Cement Factor (sk/cu yd)	Air (%)	Age (days)	f'_c (psi)	f_{sp} (psi)	f_t (psi)	σ_{cz} (psi)	f_{tu} (psi)	$\epsilon_{ct} \times 10^6$	$\epsilon_{cz} \times 10^6$
Bag	5.0	6.0	7	3,160	398	289	-21	310	177	-10
Air				2,860	326	183	20	163	93	11
Oven				2,860	336	249	89	160	148	40
Bag	5.0	6.0	28	4,920	505	375[a]	-24	399	—[a]	- 6
Air				3,500	468	331	61	270	184	25
Oven				3,260	326	237	143	94	146	74
Bag	4.0	6.0	7	2,170	296	180	-22	202	99	- 9
Air				1,979	249	130	53	77	87	28
Oven				1,600	214	119	87	32	88	54
Bag	4.0	6.0	28	2,620	280	178	- 3	182	84	- 1
Air				2,345	255	156	96	60	95	45
Oven				1,860	216	225	123	102	177	91
Bag	5.0[b]	1.0	7	4,780	456	221	7	214	84	2
Bag	5.0[b]	1.0	28	4,750	496	372	26	346	92	5
Bag	5.0	2.0	7	3,827	420	222	-11	233	102	- 4
Oven				3,093	330	245	136	109	129	63
Bag	5.0	2.0	28	5,475	455	223	-77	300	142	-24
Bag	4.0	2.0	7	2,601	329	190	0	190	113	0
Air				1,944	285	166	30	136	105	12
Oven				1,807	195	158	94	64	95	48
Air	4.0	2.0	28	2,210	368	207	102	105	78	20
Oven				1,740	210	142	136	6	54	41

[a]Bond, rather than tensile, failure occurred in this specimen.
[b]This mix is regular-weight concrete (SG).

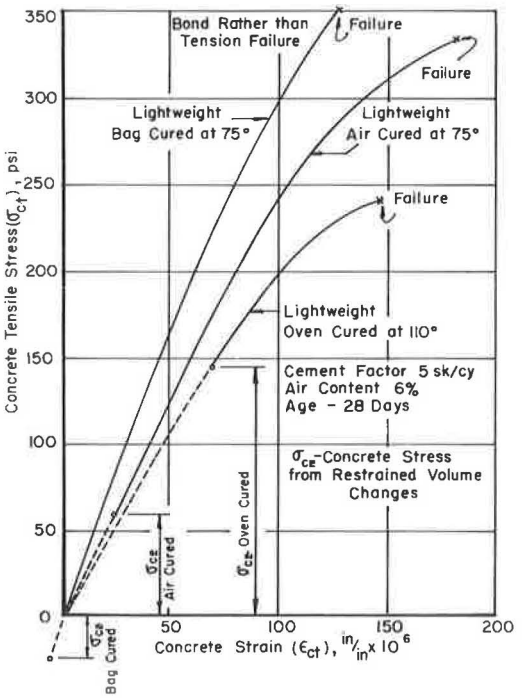

Figure 9. Stress-strain curves for three curing conditions for cement factor = 5 sk/cu yd, 6% air, and age of 28 days.

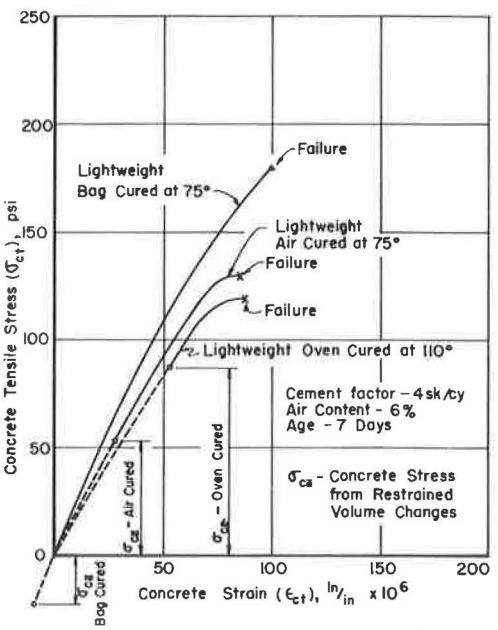

Figure 10. Stress-strain curves for three curing conditions for cement factor = 4 sk/cu yd, 6% air, and age of 7 days.

represents the stress-strain characteristics obtained from the direct tension test. The dashed portion of the curves does not represent the actual stress and strain behavior during the period before testing, but does represent the residual stress existing in the concrete at the beginning of the tension test. The corresponding residual strain was determined by the following procedure.

The strain at the beginning of the solid portion of the stress-strain curves was determined by projecting a straight line with a slope of E, determined from the loading phase of the tension test, back to zero stress. This represents the strain that would relieve the residual stress, using the modulus of elasticity existing at the time of test. The actual residual strain, which was affected by creep and changes in the modulus of elasticity with age, was obviously larger.

Since each curve represents only a single test, values of tensile strength, tensile strain, and modulus of elasticity in these curves may not be the generally expected values.

Observation of these stress-strain curves reveals several important factors which affect the tensile strength of concrete. In general, the bag-cured specimens exhibited the highest tensile strength and the highest modulus of elasticity. Air-cured specimens had the next highest tensile strength and oven-cured specimens had the lowest tensile strength.

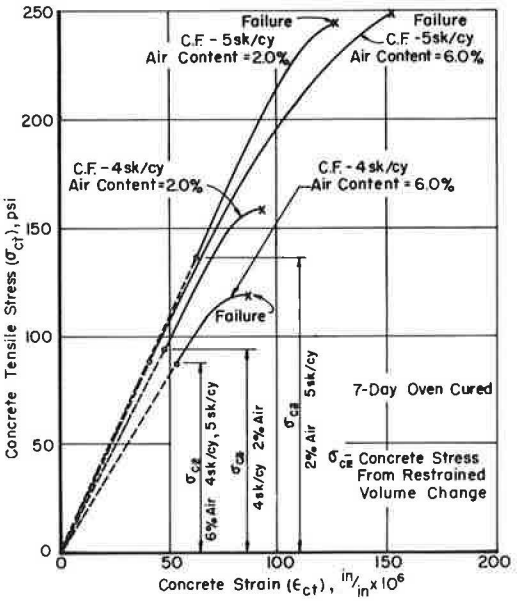

Figure 11. Stress-strain curves for 7-day oven-cured specimens with different cement factors and air contents.

The ultimate tensile strength at 28 days was generally larger than that at 7 days, regardless of environment. The slopes (modulus of elasticity) for the concrete with 5 sk/cu yd were steeper than for the concrete with 4 sk/cu yd.

The results for bag-cured specimens were approximately as expected. However, in regard to air-cured specimens, the tensile strength of the 5-sk, 6 percent air specimen was high, and the 5-sk, 2 percent air specimen was low. The 4-sk tests resulted in lower values than the 5-sk tests, and the higher air contents resulted in lower values of modulus of elasticity. Figures 9 and 10 also show that the residual stresses of the bag-cured specimens tended to be compressive, whereas the residual stresses of the air and oven-cured specimens tended to be tensile.

One other factor, (Fig. 9) was the failure of the bag-cured specimen in bond rather than tension. This probably suggests that bond strength was reduced as a result of an environment such as bag curing which reduces the tendency for shrinkage to occur. This aspect merits further investigation.

The restraint given to the concrete volume changes by the bar in the direct tensile test is quite similar to that of a reinforcing bar in concrete pavements. The percentage of reinforcement is different, however. Deep concrete which has no volume change except near the surface where environmental conditions vary has this same type of restraint. The difference between the ultimate tensile strength (f_t) and the restrained concrete stress (σ_{cz}) represents the usable tensile strength (f_{tu}). Figures 9, 10 and 11 show that the usable tensile strength was greatly affected by oven curing.

Effect of Curing Condition on Split Cylinder Strength

From the results presented thus far, bag curing provided a more favorable environment for hydration, resulting in higher tensile strengths. Figure 12 is a plot of air-cured and oven-cured split-cylinder strengths vs bag-cured split-cylinder strengths. Bag curing is used here as a base and the line of equality represents equal air-cured and oven-cured strengths with companion bag-cured strengths. A least squares fit of the first order to data points was made with a computer for the two curing conditions. The air-cured specimens exhibited only about 91 percent of the split-cylinder strengths

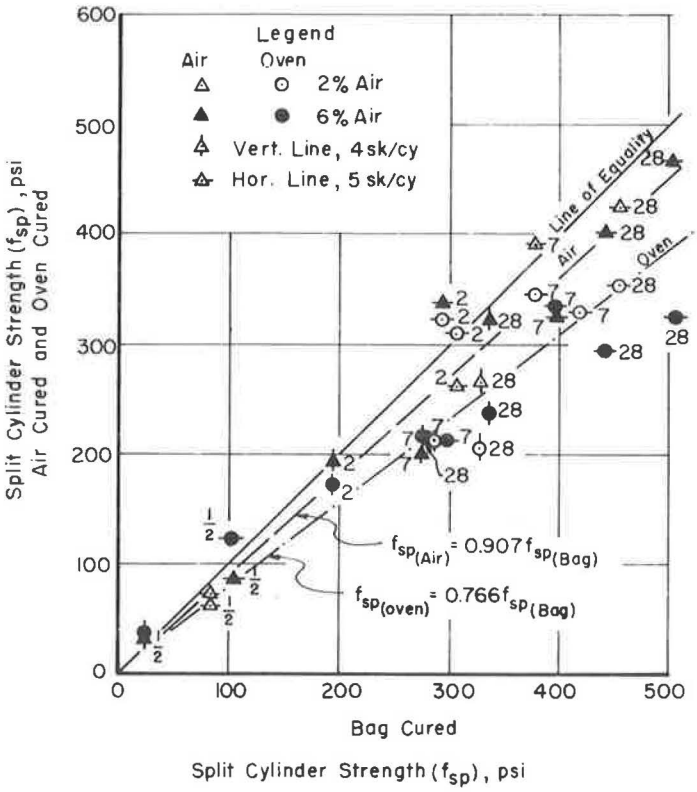

Figure 12. Effect of curing conditions on split cylinder strengths.

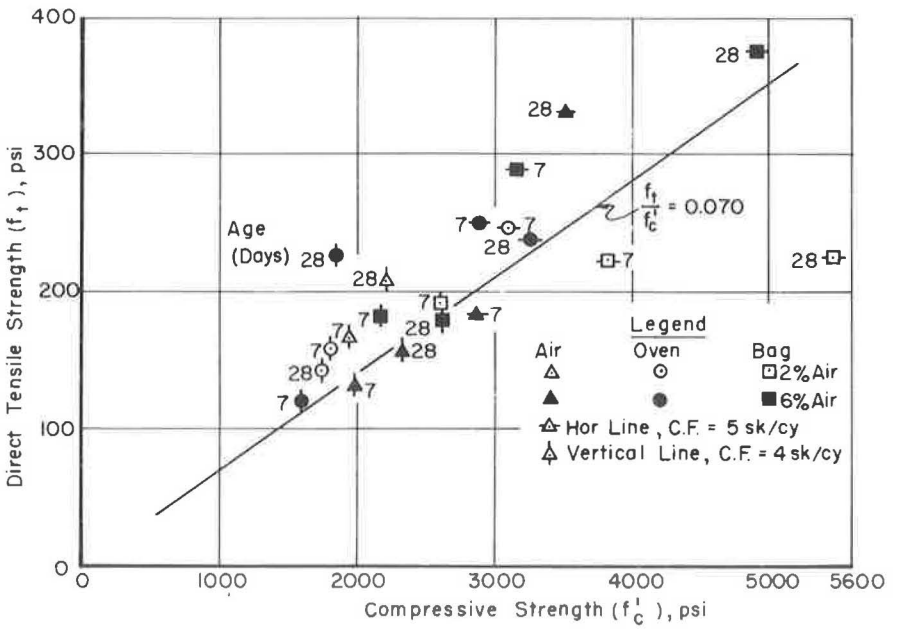

Figure 13. Relationship between direct tensile strength (f_t) and compressive strength (f'_c).

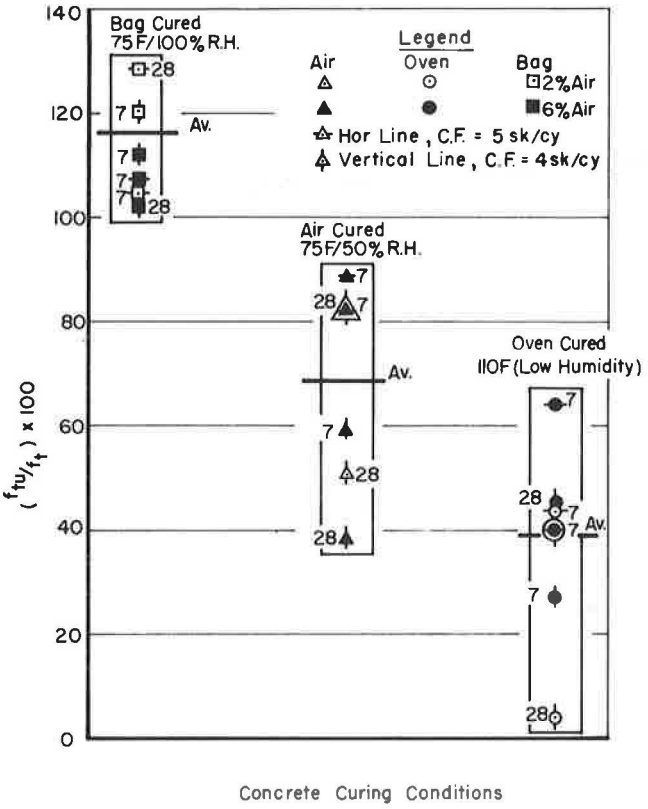

Figure 14. Percent of total available tensile strength for restrained structural lightweight concrete as a function of curing conditions.

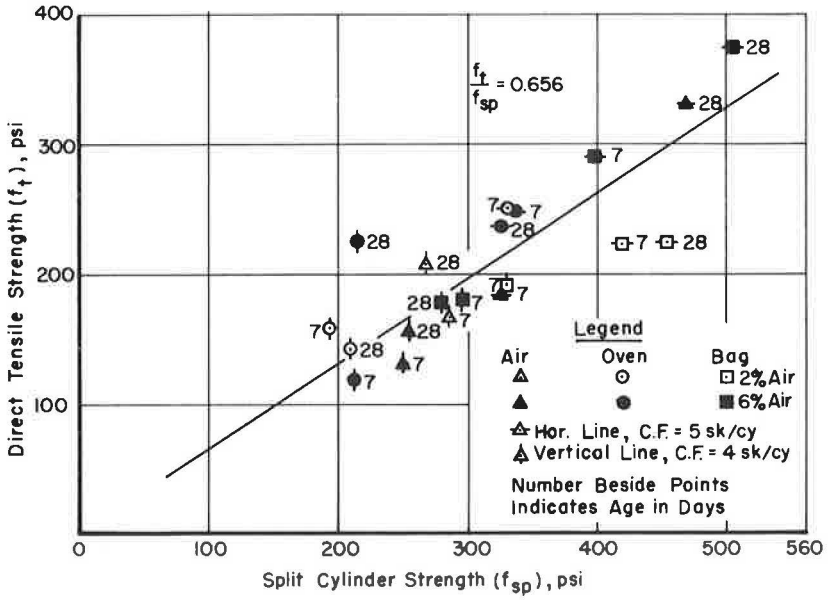

Figure 15. Relationship between direct tensile and split-cylinder strengths.

for the bag-cured specimens. The oven-cured strengths were only about 77 percent of the bag-cured strength.

Relationship Between Direct Tensile and Compressive Strengths

Figure 13 shows a plot of all of the compressive-strength and companion direct tensile-strength data collected in this investigation. Some of the plotted points were average values from two or more tests. Even though some scatter in the data exists, particularly for the bag-cured, 2 percent air-content specimens, a definite straightline relationship was determined between the direct tensile strength and compressive strength. The tensile strength was approximately 7. 0 percent of the compressive strength for all curing conditions and strengths investigated. A wide range of strengths is shown in Figure 13, which helps to validate the results.

As discussed earlier, improper curing procedures cause a significant loss in tensile capacity of structural lightweight concrete that is restrained from undergoing volume changes by reinforcement. To demonstrate this, in Figure 14 the percent of usable tensile strength is plotted against type of curing, from the results given in Table 1. The amount of loss in available or usable tensile strength between the bag-cured and either the air- or oven-cured specimens is significant. The following relationship between usable tensile strength (f_{tu}) and compressive strength was determined to exist for data collected:

$$f_{tu} = 0.08 f'_c - 64 \tag{9}$$

It should be emphasized that this is not a fixed relationship, because of the variable environmental conditions.

Relationship Between Direct Tensile and Split-Cylinder Strengths

The relationship between direct tensile strength and split-cylinder strength is shown in Figure 15. Here again, a very good straightline relationship exists. The split-cylinder should be more than the direct tensile strength, mainly because of the difference in the stress conditions of the two tests. With the aid of Figure 15, the direct tensile strength can be approximated from

$$f_t = 0.07 f'_c = 0.66 f_{sp} \tag{10}$$

In cases where the tensile strength of the concrete is used and where restraint to concrete volume change exists, the usable tensile strength should be a more accurate design value than tensile strength, flexural strength, or a percentage of the compressive strength. Figure 16 is a plot of usable tensile strength vs the split cylinder strength for all three environmental conditions. The general trend as determined from a computer analysis for the three environmental conditions indicates that there is no fixed relationship between usable tensile strength and split-cylinder strength. For comparison purposes, the relationship for all data, although not a firm relationship, was computed to be

$$f_{tu} = 1.03 f_{sp} - 168 \tag{11}$$

Thus, a high value of the usable tensile strength can not be assumed without proper curing and close control. The general trends for compressive strength (Eq. 9) and split cylinder (Eq. 10) are shown in Eq. 12:

$$f_{tu} = 0.08 f'_c - 64 = 1.03 f_{sp} - 168 \tag{12}$$

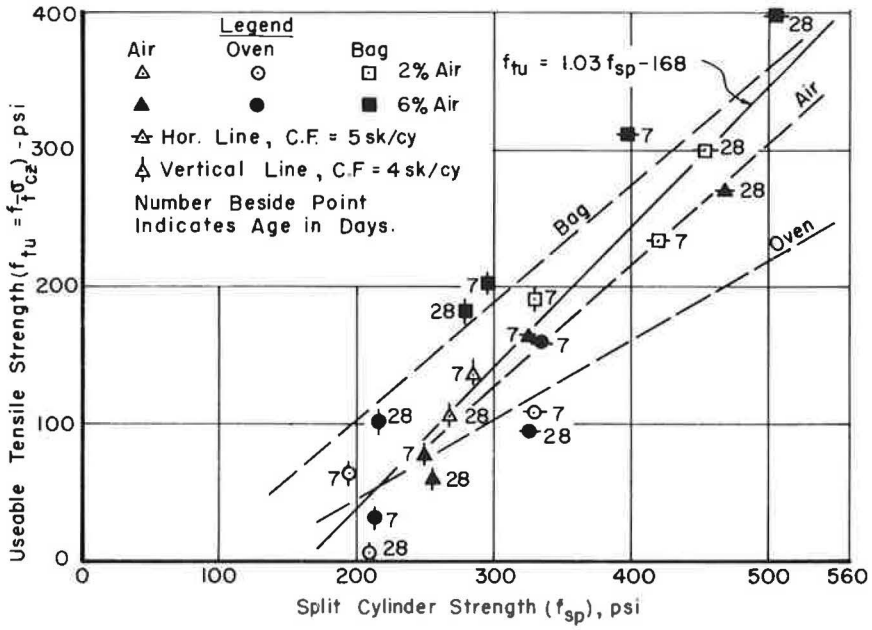

Figure 16. Relationships between usable tensile strength and split-cylinder strengths.

TABLE 2

COMPARISON OF COMPRESSIVE AND TENSILE MODULUS OF ELASTICITY

Curing	Cement Factor (sk/cu yd)	Percent	Age (days)	Modulus of Elasticity		Difference Based on Comp. (%)
				Compressive	Tensile	
Air	4	2	7	2.33	2.42	+ 3.9
Bag			28	2.81	2.74	- 2.5
Oven			7	1.80	2.00	+11.1
Air	4	6	7	2.59	1.86	-28.2
Air			28	2.21	2.12	- 4.1
Bag			7	2.43	2.25	- 7.4
Bag			28	2.60	2.70	+ 3.8
Oven			7	1.55	1.62	+ 4.5
Oven			28	1.83	1.33	-27.3
Bag			7	2.64	2.92	+10.6
Bag	5	2	28	3.09	2.52	-18.4
Oven			7	2.32	2.14	- 7.7
Air	5	6	7	2.62	2.38	- 9.2
Air			28	2.46	2.45	- 0.4
Bag			7	2.81	2.29	-18.5
Bag			28	3.29	3.36	+ 2.1
Oven			7	2.64	2.15	-18.6
Oven			28	2.55	1.93	-24.3
					Avg.	- 7.3

STATIC MODULUS OF ELASTICITY

A summary of all modulus of elasticity data is given in Table 2. Values given are secant modulii at 50 percent of the ultimate strength in compression or 50 percent of the ultimate tensile strength.

From these data it is apparent that the curing environment of structural lightweight concrete has some effect on the modulus of elasticity. The oven-cured specimens had noticeably lower values than those which were air or bag cured. This was especially true for the mixes made with a cement factor of 4 sk/cu yd.

A comparison of the values of modulus of elasticity obtained from tension and compression tests on companion specimens is given in Table 2. In general, the values in tension and compression may be considered as the same since the average difference was less than 10 percent. However, the tensile values of E tend to be slightly less than the compressive values.

According to Pauw (11), the modulus of elasticity of either regular-weight concrete or structural lightweight concrete may be approximated by

$$E = 33.6\, w^{3/2} \sqrt{f'_c} \qquad (13)$$

where

w = unit weight of concrete in pcf at time of test, and
f'_c = compressive strength of concrete in psi.

This formula was used to calculate the modulus of elasticity of various specimens for which the unit weights and compressive strengths were recorded in this investigation. The calculated values were compared with the measured values and were approximately 14 percent lower. The data were then plotted similar to Pauw (11) and fitted with a straight line through the origin, using a least-squares technique. This straight-line fit is shown in Figure 17.

From the data obtained in this investigation, the modulus of elasticity of structural lightweight concrete can be better approximated by

$$E = 37.6\, w^{3/2} \sqrt{f'_c} \qquad (14)$$

It should be recognized that in determining the slope mathematically, the line was forced to go through zero.

LIGHTWEIGHT CONCRETE DESIGN AND PAVEMENT PERFORMANCE

General

With the properties of structural lightweight concrete determined in this study, it is possible to analyze the design and performance of a concrete pavement structure built with this material. Inasmuch as only one lightweight aggregate was used, the results of this analysis are limited and generalizations involving all lightweight concrete cannot be made. However, test methods and procedures have been developed and analyzed to determine critical properties of structural concrete made with any material and to analyze their effects on pavement structure performance.

The following examines the various properties determined in this study in terms of a comparison of the effects of lightweight concrete properties and regular-weight concrete properties on pavement design and performance.

Concrete Pavement Design Formulations

The present-day design formulations include a design determination of (a) concrete thickness, (b) contraction joint spacing, (c) distributed steel requirements, and (d) continuous reinforcement.

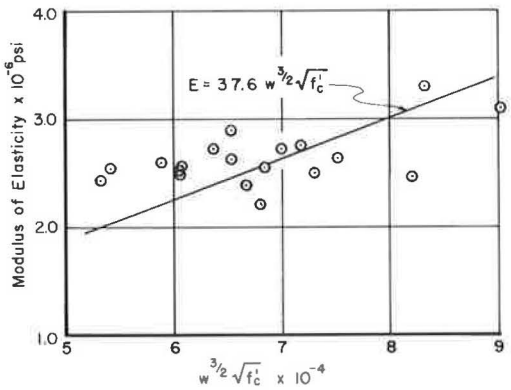

Figure 17. Relationship between secant modulus of elasticity and compressive strength and unit weight of concrete.

Concrete Thickness. — The design formulation of the thickness of concrete pavement was one of the major results of the AASHO Road Test (12). Combining the results of the road test with previous research studies and experience, AASHO published an Interim Guide for the design of rigid pavement structures (13), which was extended by the Texas Highway Department to cover the various types of concrete pavement constructed in Texas (14).

From this development, the following pavement-thickness design equation was developed:

$$\log \Sigma L = -8.8682 - 3.513 \log \left[\frac{J}{S_c D^2} \left(1 - \frac{2.61\, a}{Z^{0.25} D^{0.75}} \right) \right] + 0.9155 \frac{G}{\beta} \qquad (15)$$

where

ΣL = number of accumulated equivalent 18-kip single axle loads;
J = a coefficient dependent on load transfer characteristics for slab continuity;
S_c = modulus of rupture (flexural strength) of concrete at 28 days (psi);
D = nominal thickness of concrete pavement (in.);
$Z = \frac{E_c}{k}$;
E_c = modulus of elasticity for concrete (psi);
k = modulus of subgrade reaction (psi/in.);
a = radius of equivalent loaded area = 7.15 in. for road test 18-kip axles;
$G = \frac{4.5 - P_t}{3}$;
P_t = servicability at end of time, t; and
$\beta = 1 + \frac{(1.624)(10^7)}{(D+1)^{8.46}}$.

At first glance, Eq. 15 appears rather formidable and cumbersome to solve for the design pavement thickness (D). However, it was a simple matter to program the equation on the computer and solve for (ΣL) for all combinations of variables, and present the results in the form of a design nomograph (14). It is relatively easy to enter the nomograph with the design parameters and concrete properties involved and arrive at a design pavement thickness.

The comparisons of Eq. 15 for selected example parameters are shown in Figure 18 for continuously-reinforced concrete pavement (CPCR). Similar comparisons for jointed concrete pavement (CPJ) are given in Figure 19. In all cases the required thickness of structural lightweight concrete was less than the required thickness for regular-weight concrete. As the example strengths were the same for the two types of concrete, the difference in design thickness must be due to the lower modulus of elasticity for structural lightweight concrete. This agrees with the theoretical development of slabs on elastic foundations by Westergaard (15). The lower the modulus of elasticity, the lower the tensile stresses in the concrete, and hence the thinner the pavement must be to withstand the applied traffic load. Structural lightweight concrete, therefore, with its lower modulus of elasticity, offers an advantage over regular-weight concrete, in that less material is required to carry the load.

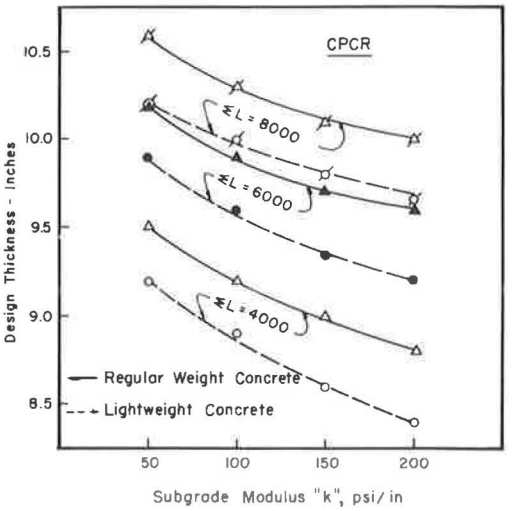

Figure 18. Design thickness for CPCR of regular and lightweight concrete as a function of load application and subgrade modulus.

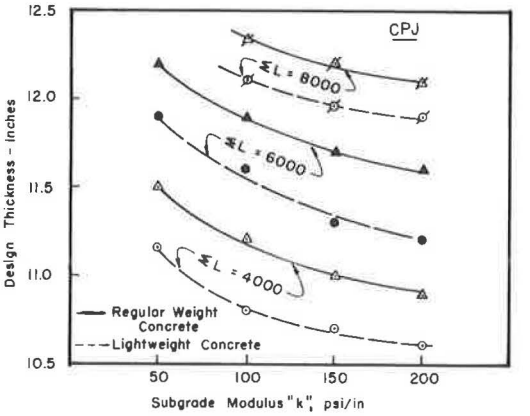

Figure 19. Design thickness for CPJ of regular and lightweight concrete as a function of load application and subgrade modulus.

Contraction Joint Spacing.— Jointed unreinforced concrete pavement requires transverse contraction joints spaced along the pavement length. Unfortunately, there are no design formulations to determine the required joint spacing (16),and, therefore, for the most part, past experience has been relied on to arrive at suitable designs.

The required joint spacing is strongly dependent on the volume changes of the concrete, which is a critical property and is subsequently discussed.

Distributed Steel.— The amount of distributed steel in jointed, reinforced concrete pavement is directly dependent on the weight of the slab, all other factors being equal. Inherent in this concept is the assumption that the concrete is sufficiently strong to support the load. If it is reasonable to assume that the friction factor between the pavement and the subgrade is practically the same for each type of concrete, the regular-weight concrete slab would require 30 percent more distributed steel per foot width of slab than structural lightweight concrete. Therefore, as with the required thickness, less material is required for structural lightweight concrete.

Of course, another important assumption inherent in using this concept for lightweight concrete is that the lightweight concrete volume changes are no greater than regular-weight concrete volume changes.

Continuous Reinforcement.— In the design of continuously-reinforced concrete pavement without transverse joints, enough steel is placed in the slab to force the concrete to develop numerous transverse, hairline cracks. The steel does not prevent cracking; on the contrary, it induces cracking. However, it keeps the cracks tightly closed. This type of pavement has been used extensively in Texas, as well as in many other states, with excellent results. The basic design equation of the steel percentage is given by McCullough and Ledbetter (17). This basic equation has been modified to include a term for the subbase friction factor, F, for inclusion in the AASHO Interim Guide (13).

Using this modified equation to compare the relative amounts of steel required for regular-weight and lightweight concrete pavement, the only difference between the two types of concrete which affects the formula is the modulus of elasticity. Solving the equations using typical example values for the two types of concrete results in slightly more steel being required for lightweight concrete (0.56 percent) than for regular-weight concrete (0.54 percent).

Concrete Pavement Performance

Comparisons have been made between regular-weight and lightweight concrete pavement structures based on existing pavement design formulations. As is the case with

almost all design procedures, the capability of a given product to meet design requirements does not always insure performance in service. Many material properties considered critical to the performance of the concrete pavement structure are not considered directly in the design.

Concrete Warping Stresses. — The effects of concrete volume changes with changes in temperature is an important consideration when evaluating a pavement material which will be subjected to rather severe temperature changes and differentials between the top and bottom of the slab. The theoretical warping stresses developed from temperature differentials was formulated by Bradbury (18).

$$\sigma_t = \frac{CE_c \epsilon T}{2} \tag{16}$$

where

σ_t = maximum stress (psi) in extreme fiber at edge of slab, in direction of slab length;
C = coefficient, directly proportional to slab length;
ϵ = coefficient of thermal expansion (in./in./OF), and
T = difference in temperature between the top and bottom of slab.

The value for the warping stress is directly proportional to the product of coefficient of thermal expansion, ϵ, and the modulus of elasticity E_c. Using typical properties for pavement slabs of the same length and thickness, regular-weight concrete would contain 114 percent more stress due to warping than structural lightweight concrete. This means that the distance between transverse contraction joints, which is reflected in the coefficient C, can be increased on pavements constructed with structural lightweight concrete, and thereby effect a savings in construction costs. This also means that structural lightweight concrete undergoes less volume change from changes in temperature and therefore is more dimensionally stable over long periods of time. This points to an expected increase in the performance capability of structural lightweight concrete in terms of warping stresses.

Volume Changes—Moisture.—Volume changes from changes in moisture content of the concrete constitute another important property seriously affecting pavement structure performance. The restrained concrete volume change stresses can be almost eliminated during the critical early life of the concrete by proper curing. However, before this factor can be fully appraised, additional research is needed on lightweight concretes made with other aggregates and with curing conditions more nearly approximating current field curing practices. The results of this study indicate that restrained lightweight concrete volume changes could be very serious and should be investigated further. Pavement structures constructed with lightweight concrete should be watched closely for any performance effects which may result from restrained volume changes.

CONCLUSIONS

The following conclusions appear valid for the parameters studied in this investigation.

1. The correlation of flexural strengths with either compressive strengths or split-cylinder strengths was poor, which further indicated the difficulty of using flexure as an index of strength and more particularly of tensile strength. A comparison of bag-cured lightweight concrete with the bag-cured regular weight concrete showed that their compressive, direct tensile, and split-cylinder strengths were practically identical; but the flexural strength of the lightweight concrete was often 20 to 25 percent lower than the flexural strength of the regular-weight concrete. The obvious conclusion is that flexural strength test is a poor indicator, often unduly restrictive and incorrect, of lightweight concrete strength and quality.

2. The split-cylinder strengths for the three different environments resulted in the air-environment specimens testing at approximately 91 percent of the bag environment

and the oven-environment specimens testing at approximately 77 percent of the bag environment. This test shows considerable promise as an indicator of concrete strength and quality.

3. This investigation has produced a procedure which not only accurately determines the tensile strength of concrete but also provides a measure of residual tensile stress developed by volume change. This procedure can also be used to establish the influence of different aggregates, mix designs, admixtures, environments, etc., on tensile strength and the development of residual stress from volume changes.

4. When the lightweight aggregate concrete used in this study was restrained by a reinforcing bar, it developed either compressive or tensile residual stresses depending on the curing environment. Residual compressive stresses as high as 80 psi were developed with a bag environment, whereas residual tensile stresses as high as 140 psi were developed in an oven environment. The intermediate environment in air resulted in residual tensile stresses as much as 100 psi.

5. For this lightweight aggregate concrete the (direct) tensile strength was related to the split cylinder strength and compressive strength as $f_t = 0.66 f_s = 0.07 f'_c$.

6. The usable tensile strength of this lightweight aggregate concrete was significantly reduced under unfavorable environmental conditions during the curing period. Further, neither the split-cylinder strength test nor the compression strength test indicated the usable tensile strength of the reinforced concrete.

7. Since the expanded shale used in this investigation is a low absorption aggregate, it is anticipated that aggregates with higher absorptions may result in even lower usable tensile strengths under restrained volume change and unfavorable environmental conditions.

8. For all practical purposes, the modulus of elasticity for both tension and compression for concrete made with this particular expanded shale coarse aggregate was the same except for several values which were affected by experimental inconsistencies in curing.

9. For the tests made in this investigation, the relationship of modulus of elasticity to unit weight and compressive strength was found to be $E = 37.6\, w^{3/2} f'^{1/2}_c$. This relationship is reasonably close to Pauw's (19) value of $E = 33.6\, w^{3/2} f'^{1/2}_c$.

10. Using the values obtained in this study for the properties investigated, the following design comparisons can be made for the various types of concrete pavements: (a) the required pavement thickness for lightweight concrete is around 0.3 in. less than regular-weight concrete of the same strength; (b) for jointed reinforced concrete pavement, regular-weight concrete requires 30 percent more distributed steel than lightweight concrete of the same joint spacing; and (c) for continuously-reinforced concrete pavement, lightweight concrete requires slightly more steel (0.56 percent) than regular-weight concrete (0.54 percent).

11. In evaluating the expected pavement performance the following comparisons can be made: (a) for given slab dimensions, concrete warping stresses due to temperature differentials between the top and bottom of the slab for regular-weight concrete will be 114 percent greater than for lightweight concrete; and (b) volume change of lightweight concrete, if unfavorably cured, can result in sizable residual stresses in the concrete; and if restrained, as they would be in a concrete pavement, these volume changes could be extremely detrimental to the performance of the pavement structure.

RECOMMENDATIONS

1. Since the technique developed in this investigation provides a measure of both the tensile strength and usable tensile strength which might occur under a restrained volume change condition, it is recommended that the effects of the following be investigated: (a) properties of aggregates—particularly absorption, (b) mix design, (c) limiting and practicable curing environment, (d) use of molecular films to reduce evaporation, and (e) percentages of steel.

2. The effects of curing environment on bond strength should be investigated for at least two lightweight aggregate types: one with a relatively high absorption capacity, and one with a relatively low absorption capacity.

3. Dynamic tensile properties should be investigated for a structural lightweight concrete.

4. Test sections of structural lightweight concrete pavement should be constructed and evaluated over a period of time to verify the laboratory conclusions reached in this study.

ACKNOWLEDGMENTS

The authors are grateful to the Texas Highway Department and the U. S. Bureau of Public Roads for their sponsorship of this research.

REFERENCES

1. Ledbetter, W. B., and Thompson, J. Neils. Relationship Between Critical Mechanical Properties and Age for Structural Lightweight Concrete. Univ. of Texas, Center for Highway Res., Feb. 1964.
2. Houston, J. T., and Thompson, J. Neils. Volume Changes in Unrestrained Structural Lightweight Concrete. Univ. of Texas, Center for Highway Res., to be publ.
3. Ledbetter, W. B., Perry, Ervin S., Houston, James T. and Thompson, J. Neils. Critical Mechanical Properties of Structural Lightweight Concrete and The Effects of These Properties on the Design of the Pavement Structure. Univ. of Texas, Center for Highway Res., to be publ.
4. Shideler, J. J. Lightweight Aggregate Concrete for Structural Use. Proc. Jour. of Amer. Concrete Inst., Vol. 54, Oct. 1957.
5. Shideler, J. J. Manufacture and Use of Lightweight Aggregate for Structural Concrete. PCA Dev. Dept. Bull. D40, Jan. 1961.
6. Troxell, G. E., and Davis, H. E. Composition and Properties of Concrete. New York, McGraw-Hill, 1956.
7. Todd, J. D. The Determination of Tensile Stress-Strain Curves for Concrete. Proc. Inst. of Civ. Eng. (England), Vol. 4, No. 2, Pt. 1, Paper No. 6012, Mar. 1955.
8. Hinson, A. J. Testing Mechanism for Concrete in Pure Tension. Univ. of Texas, Unpubl. rept. 1955.
9. Rane, V. S. Shrinkage Effect on Diagonal Tension Strength of Reinforced Concrete Beams. Univ. of Texas, Master's thesis, Jan. 1961.
10. Washa, George W., and Fluck, Paul G. Extent of Sustained Loading on Compressive Strength and Modulus of Elasticity of Concrete. Amer. Concrete Inst., May 1950.
11. Pauw, Adrain. Static Modulus of Elasticity of Concrete as Effected By Density. Proc. Jour. of Amer. Concrete Inst., Vol. 57, No. 6, Dec. 1960.
12. The AASHO Road Test Report 5, Pavement Research. Highway Research Board Spec. Rept. 61E, 1962.
13. AASHO Interim Guide for the Design of Rigid Pavement Structures. AASHO Committee on Design, Apr. 1962.
14. Hudson, W. R., and McCullough, B. F. An Extension of Rigid Pavement Design Methods. Texas Highway Dept. Departmental Research Rept., No. 64-1, 1964.
15. Westergaard, H. M. Stresses in Concrete Pavements Computed by Theoretical Analysis. Public Roads, Vol. 27, No. 2, Apr. 1926.
16. Yoder, E. J. Principles of Pavement Design. New York, John Wiley & Sons, 1959.
17. McCullough, B. F., and Ledbetter, W. B. LTS Design of Continuously Reinforced Concrete Pavement. Transactions of ASCE, Vol. 127, Pt. 4, 1962.
18. Bradbury, Royall D. Reinforced Concrete Pavements. Wire Reinforcement Inst.,Washington, D. C., 1938.

Spacing of Undoweled Joints in Plain Concrete Pavement

CLARENCE DEYOUNG, Assistant Materials Engineer, Iowa State Highway Commission

In 1955 the Iowa State Highway Commission constructed approximately 16 mi of experimental portland cement concrete pavement containing sections without contraction joints and sections in which the joints were sawed at 20, 50 or 80 ft. None of the joints were doweled. Approximately half of the joints were left unsealed.

After 8 yr of service the pavement test sections have an average slab length of from 19 to 37 ft. Faulting of at least 1/16 in. is evident at 70 percent of the joints spaced at 20 ft. The incidence of faulting is greater for the joints spaced at 50 and 80 ft. Measurements made in April 1964 revealed that more than 92 percent of the joints were open at least 1/16 in. more than their original sawed width of 1/8 in. The effect of joint sealing was not conclusive, but it appears that the seal may have been useful in keeping debris out of the joints spaced at 20 ft.

•HUNDREDS OF MILES of portland cement concrete pavement have been constructed in Iowa during the past 40 yr, and during that time there have been numerous changes in the thinking of design engineers regarding the use and design of joints. Ten years ago the Iowa State Highway Commission adopted a tentative policy of sawing undoweled contraction joints at 20-ft intervals, while omitting expansion joints except at bridge approaches. This policy has been continued to the present in the construction of almost all concrete pavement on primary highways in Iowa.

When 20-ft joint spacing was adopted, the Commission was aware of the good past performance of some Iowa pavements having joint spacing greater than 20 ft, as well as that of some pavements containing no contraction joints. This recognition led to further investigation of joint spacing. The formal investigation was confined largely to one 16-mi experimental project containing sections without contraction joints and sections in which the joint spacing was 20, 50 or 80 ft. Approximately half of the joints in each section were filled with an asphalt-rubber sealer; the others were left unsealed.

The objectives of the experimental joint construction were to examine the performance of a plain concrete pavement as it may be influenced by the distance between undoweled contraction joints and to compare the performance of sealed and unsealed joints.

The experimental pavement was constructed in 1955. This report contains observations and data obtained during the past 8 yr of pavement service.

PROJECT DESCRIPTION

Correct evaluation of the observations and measurements presented in this report requires preliminary consideration of the pavement materials, construction procedures, and the traffic to which the pavement has been subjected.

Location

The pavement containing the experimental joint spacing is located just west of Des Moines in central Iowa along approximately 16 mi of US 6. This section of US 6 is currently part of the connecting link between two completed portions of Interstate 80.

Paper sponsored by Committee on Rigid Pavement Design.

The area has a well-developed erosional topography with broad flat valleys and rolling-to-hilly upland divides. The general location of the project is shown in Figure 1.

Subgrade

A considerable amount of subgrade preparation was undertaken before paving, including the placing of from 3 to 12 in. of reclaimed road surfacing or select glacial clay. Reclaimed road surfacing was used to top off the subgrade, and did not constitute a subbase. The various subgrade materials are distributed throughout the project approximately as follows: reclaimed road surfacing, 24 percent; select glacial clay, A-6 (11) to A-7-6 (16), 63 percent; alluvial silty clay, A-7-6 (14-18), 7 percent; and loess silty clay, A-7-6 (11-14), 6 percent.

Reclaimed road surfacing as used in Iowa is generally a gravelly sandy loam falling in the A-4 (0) to A-4 (2) groups.

Pavement Design

The pavement is 24 ft wide with a 10-9 ½-10 in. cross-section. The only reinforcement is ½-in. by 3-ft tie bars, spaced at 30-in. centers, across the longitudinal joint. The only experimental features are the transverse joint spacing and joint sealing. The experimental sections are given in Table 1. All the sections have earth shoulders.

Materials

The aggregate used in the concrete pavement was washed sand and gravel in the ratio of 45 percent sand and 55 percent gravel. The cement was Type I, furnished by two manufacturers. The cement content of the mix was 6.4 sk/cu yd. Air entrainment in the range of 4 to 6 percent was obtained by means of an admixture.

Construction

The pavement was cured with wet burlap for at least 20 hr, after which a clear wax-base curing compound was applied. All contraction joints were sawed, with every fourth joint in the 20-ft sections and all joints in the 50- and 80-ft sections done during the first 24 hr. The remaining joints in the 20-ft sections were sawed within 72 hr. The saw cuts were ⅛ in. wide by 1 ½ in. deep.

Pavement construction began July 12, 1955, and was completed October 22, 1955. Table 1 gives the maximum and minimum temperatures for the days each section was paved.

Traffic

When the pavement was constructed in 1955, it was part of Iowa 90, and the traffic count was less than 2,000 veh/day. Later it was designated US 6 and became the connecting link between completed portions of Interstate 80. This resulted in a considerable increase in traffic, with an especially significant increase in tractor-truck combinations. The traffic data are as follows:

Year	Total Vehicles	Single-Unit Trucks	Tractor-Truck Combinations
1955	1,720	—	—
1959	2,250	352	244
1962	3,775	330	515
1964	4,870	430	664

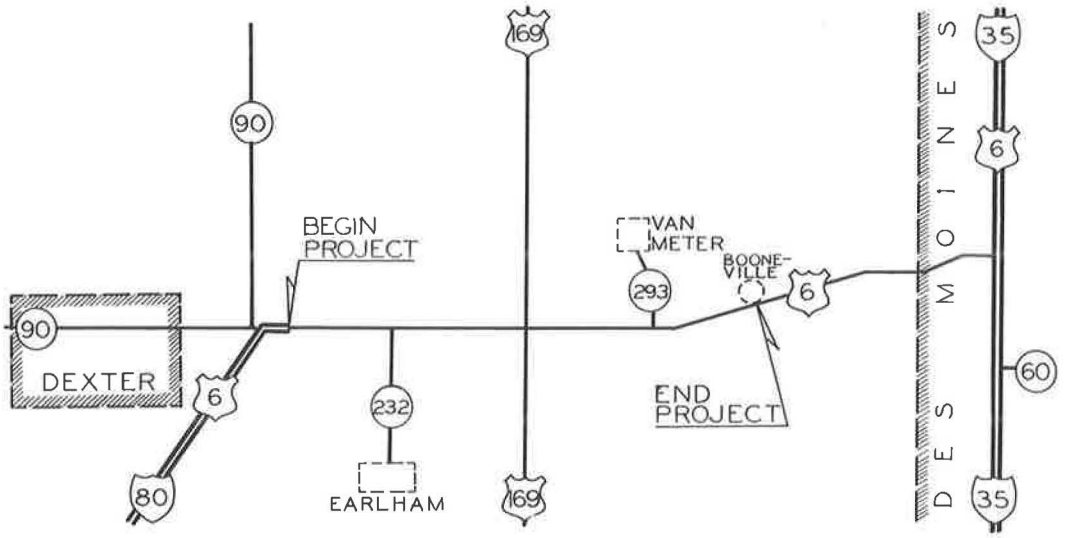

Figure 1. General location of experimental sections.

TABLE 1

EXPERIMENTAL JOINT SECTIONS

Sect. No.	Sect. Length (ft)	Joint Spacing (ft)	Joint Sealed or Open	Date Paved (1955)	Max. Temp. (° F)	Min. Temp. (° F)
1	3,200	None		7/15-27	99	64
2	2,700	None		8/17-19	98	66
3	7,434	None		10/3-10	80	37
4	2,636	None		10/10-11	80	53
5	1,137	None		7/12-13	93	66
6	4,040	20	S	7/29-30	103	76
7	1,345	20	S	8/16-17	97	66
8	5,400	20	S	10/15-19	70	30
9	3,664	20	O	8/2-8	95	62
10	1,370	20	O	8/15-16	93	61
11	5,300	20	O	10/11-15	80	30
12	4,047	50	S	8/9-11	86	58
13	3,512	50	S	8/27-31	99	52
14	1,335	50	S	8/15	93	61
15	4,673	50	S	9/22-28	78	46
16	558	50	O	8/12	85	58
17	1,350	50	O	8/13	85	57
18	5,300	50	O	10/19-22	72	36
19	2,161	80	S	8/26	99	72
20	1,270	80	S	10/1	69	41
21	682	80	S	9/20-22	80	54
22	4,601	80	S	9/8-13	99	43
23	5,922	80	O	8/20-25	97	60
24	1,526	80	O	10/1	69	41
25	5,275	80	O	9/13-20	96	56

OBSERVATIONS AND MEASUREMENTS

Annual Condition Survey

A condition survey of the pavement has been made each year beginning in November 1955. The locations of all cracks were recorded along with notes concerning the general condition of the joints and cracks. Blow-ups and evidence of pumping were also noted. Information from these surveys is given in Table 2.

Fault Measurements

When the condition survey was made in November 1963, all joints were measured to determine the amount of faulting. The measurements were made in both traffic lanes at about 3 ft from the edge of the pavement with the device shown in Figure 2. The measurements are summarized in Table 3.

Width of Crack and Joint Openings

In April 1964, measurements were made of the joint and crack openings in 13 of the 25 experimental sections. One measurement was made for each joint and crack at a point about 5 ft from the edge of the pavement. Pictures were taken of the joints and cracks, and the width of each opening was shown by the scale included in the picture. Figure 3 shows the equipment used in taking the pictures. Figure 4 is an example of the finished pictures. The data are presented in Table 4. A series of check measurements indicated that within the degree of the accuracy of the measurements no significant change in the joint openings occurred during the time required to take photographs of the joints.

Road Roughness

The Iowa State Highway Commission uses a BPR-type trailer for measuring the surface roughness of pavements. The roughness of the experimental pavement was measured shortly after completion of the pavement in 1955. It was determined with the same machine again in October 1963. Both sets of measurements are given in Table 5.

RESULTS

In planning this experiment it was assumed that the primary purpose of transverse joints in concrete pavements is to control the cracking which accompanies volumetric changes in concrete and which also results from combined warping and load stresses. It is recognized that the optimum distance between contraction joints depends on numerous factors, and is not the same for all pavements.

Slab Length

Figure 5 shows the changes in slab length which occurred in the experimental pavement. The numerical data for the curves are given in Table 2. The average slab length at the time of the last crack survey was from 19 to 37 ft. Therefore, the optimum joint spacing for this pavement lies within this range, provided the sole criterion is the duplication of the average slab length resulting from random cracking. The proper functioning of undoweled contraction joints, however, requires consideration of additional criteria.

Joint Faulting

Effective load transmission across a joint is highly desirable because it precludes formation of unprotected corners and because it prevents, or at least minimizes, differential movement of the slab ends. Such movement frequently results in permanently faulted joints and pumping of the underlying subbase or subgrade material.

Figure 6 summarizes the measurements of joint faulting. The curves show the percentage of joints at each spacing which have faulted by the indicated amount. Of the

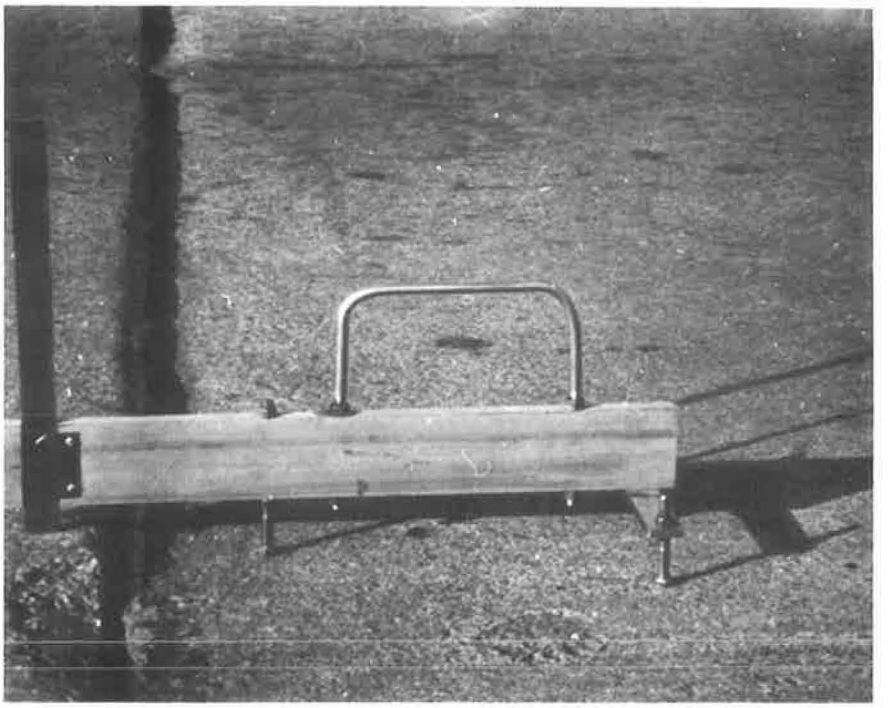

Figure 2. Measuring device for joint faulting.

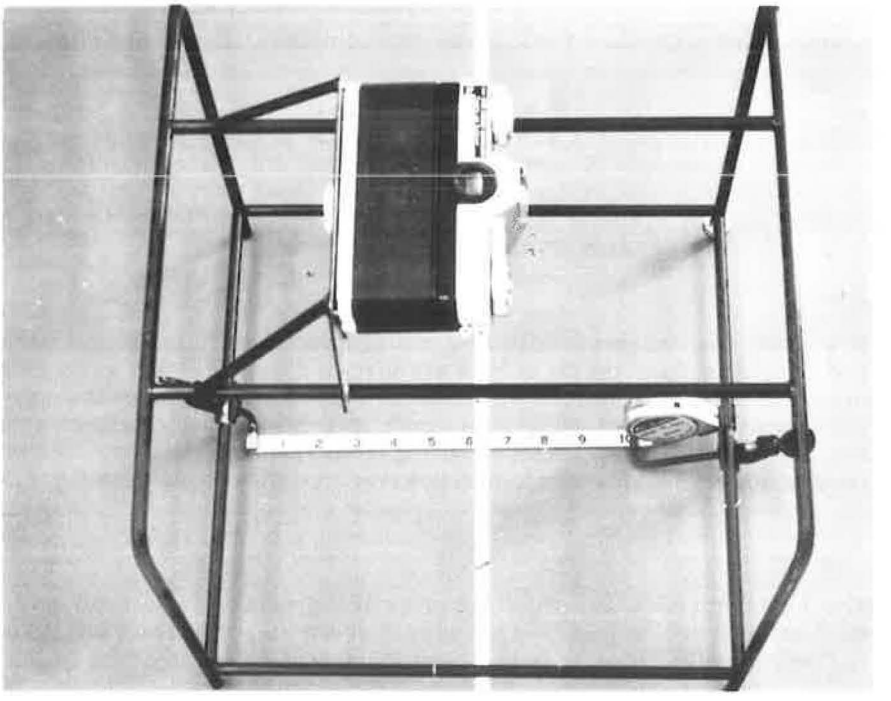

Figure 3. Equipment used to photograph joint and crack openings.

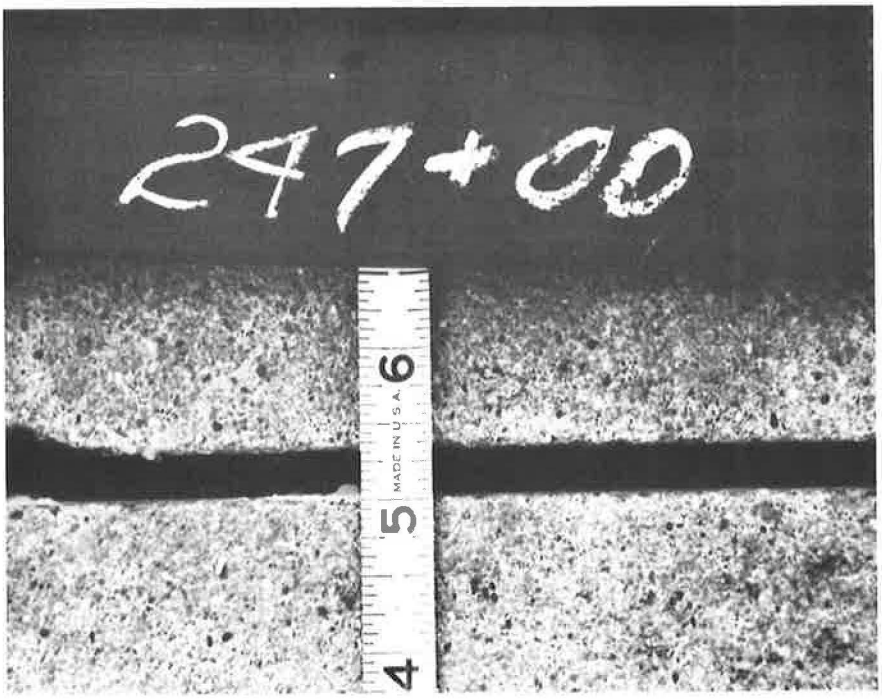

Figure 4. Example of type of photograph from which measurements of joint and crack openings were made.

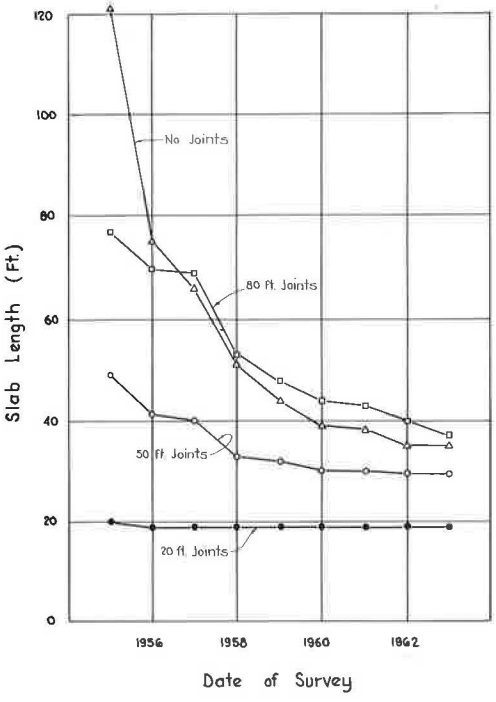

Figure 5. Change of slab length with time.

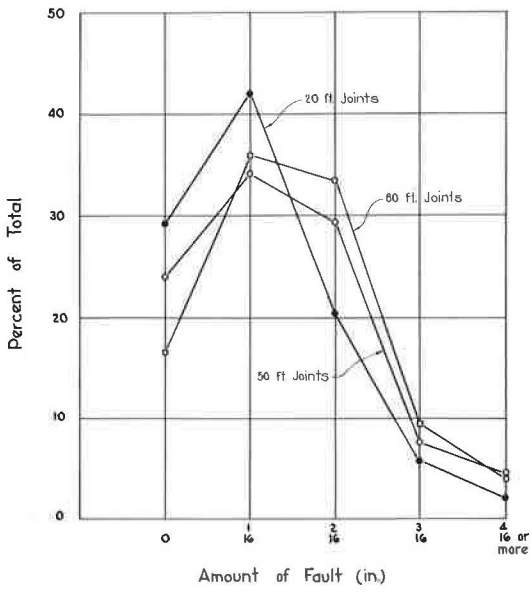

Figure 6. Relation of faulting to contraction joint spacing.

TABLE 2

SLAB LENGTH

Joint Spacing (ft)	No. of Sect.	Total Length (ft)	Avg. Length, Nov. or Dec. (ft)								
			1955	1956	1957	1958	1959	1960	1961	1962	1963
20	6	21,119	20	19	19	19	19	19	19	19	19
50	7	20,775	49	41	40	33	32	30	30	20	29
80	7	21,437	77	70	69	53	48	44	43	40	37
None	5	17,107	121	75	66	51	44	39	38	35	35

TABLE 3

JOINT FAULTING

Joint		Percent of Joints Faulted by:							
Spacing (ft)	Condition	None	1/16 In.	2/16 In.	3/16 In.	4/16 In.	5/16 In.	6/16 In.	7/16 In. or More
20	Sealed	24.3	40.1	25.4	7.5	2.0	0.5	0.2	0
20	Open	34.9	44.5	15.1	3.6	1.2	0.5	0.2	0.1
20	All	29.3	42.0	20.5	5.7	1.6	0.6	0.2	0.1
50	Sealed	25.2	36.0	26.0	7.3	3.6	1.4	0.2	0
50	Open	21.2	31.0	35.6	8.3	3.1	0.4	0.4	0
50	All	23.8	34.4	29.4	7.7	3.4	1.0	0.3	0
80	Sealed	14.7	45.5	35.8	2.5	0.5	0.5	0.5	0
80	Open	17.6	29.7	32.0	14.3	4.7	0.6	0	0.7
80	All	16.5	35.9	33.6	9.6	3.0	0.6	0.4	0.4

TABLE 4

JOINT AND CRACK OPENINGS

Crack or Joint Opening (1/16 in.)	Percent of Total						
	20-Ft Sections		50-Ft Sections		80-Ft Sections		No Joints
	Joints	Cracks	Joints	Cracks	Joints	Cracks	
1				52		65	7
2	8		4	26		33	33
3	37		31	18	9		11
4	30		22	4	19		30
5	9		16		12	2	
6	6		19		19		
7	3		6		19		7
8	2				17		4
9	2				5		
10	1						
11							
12	1		2				
13							
14	1						4
15							
16							4

TABLE 5

ROAD ROUGHNESS

Joint		Roughness, 1955 (in./mi)		Roughness, 1963 (in./mi)	
Spacing (ft)	Condition	E. B'd.	W. B'd.	E. B'd.	W. B'd.
None	—	105	98	112	104
20	Open	107	109	118	118
20	Sealed	91	93	104	108
50	Open	106	102	115	119
50	Sealed	111	113	113	117
80	Open	114	112	117	120
80	Sealed	100	95	102	103

joints spaced at 20 ft, 29.3 percent have not faulted, or have faulted less than 1/16 in. The corresponding figures for joints spaced at 50 and 80 ft are 23.8 and 16.5 percent. Thus it appears that the joints spaced at 20 ft have been least susceptible to faulting.

Pumping

This favorable view of 2-ft joints is somewhat distorted because most of the pumping observed throughout the project was in areas with 20-ft joint spacing. Pumping is evident at nine locations, of which seven are in 20-ft joint sections and two are in 50-ft joint sections. Pumping was first reported in 1961, approximately the time when heavy truck traffic began to increase substantially.

Width of Joint and Crack Openings

Load transmission across an undoweled joint in concrete pavement depends entirely on aggregate interlock. It has been estimated that aggregate interlock is effective across openings up to 0.037 in. wide (1). Measurements of joint openings in the experimental sections show that the percentage of joints open 3/16 in. or more are as follows: 20-ft joint spacing, 92 percent; 50-ft joint spacing, 96 percent; and 80-ft joint spacing, 100 percent.

Since the joints were sawed 1/8 in. wide, it appears reasonable to assume that by now aggregate interlock is effective at only a very few joints.

The measurements made in April 1964 are representative of joint and crack openings as they existed at that time. During the first few years many of the 50- and 80-ft joints were open 1/2 in. or more. Some of the first cracks in the no-joint sections also opened as much as 2 in.

Joint Sealing

Approximately one-half of the joints were sealed at the time of construction; the others were left open. No maintenance was performed on the joints during the study period and consequently many of the joint seals are now in poor condition.

It is assumed that the purposes of a joint seal are to prevent the passage of surface water through the joint and to prevent the intrusion of debris between the slab ends. The value of joint sealing might be indicated by comparing the width of openings of sealed and unsealed joints. Such a comparison is given in Table 6.

The value of this comparison depends on the theory that the joint openings vary in width from time to time according to the temperature and moisture content of the concrete, and that debris between the slabs may prevent a joint from closing. Table 6 compares the sealed and unsealed joints on the basis of those open 3/16 in. or less, since the initial sawed opening was 2/16 in. This may be misleading in the case of joints spaced at 50 and 80 ft because these joints would tend to open wider than the 20-ft joints and also remain open wider even without being jammed with debris.

Blow-Ups

Seven blow-ups have occurred of which five were in sections without contraction joints. The other two occurred in a section with unsealed contraction joints spaced at 20 ft and a section with a spacing of 80 ft.

CONCLUSIONS

The following conclusions apply in particular to the experimental pavement discussed in this report.

1. If the purpose is simply to control the formation of transverse cracks, a joint spacing of from 19 to 37 ft may be adequate.
2. From measurements of joint openings it appears doubtful that aggregate interlock is maintained even by joints spaced at 20 ft.
3. On a percentage basis, the incident of faulting is less for the joints spaced at 20 ft than for those spaced at 40 or 80 ft. The magnitude of faulting is also least for the 20-ft joints.

TABLE 6

COMPARISON OF SEALED AND OPEN JOINTS

Spacing (ft)	Percent Open 3/16 In. or Less[a]	
	Open	Sealed
20	25	63
50	35	35
80	9	9

[a]Percent of total measured.

4. Initial sealing of the joints spaced at 20 ft may have been effective in preventing the intrusion of debris.

ACKNOWLEDGMENTS

Appreciation is expressed to the U. S. Bureau of Public Roads for help in planning the experiment sections.

The author wishes to acknowledge the assistance of design and research personnel of the Iowa State Highway Commission and Stephen E. Roberts, Research Engineer, in the preparation of this report.

Annual condition surveys were conducted by the Des Moines Laboratory of the Iowa State Highway Commission.

REFERENCE

1. Kelley, E. F. Application of the Results of Research to the Structural Design of Concrete Pavements. Public Roads, Vol. 20, No. 5, July 1939.

An Experimental Self-Stressing Concrete Pavement: I. Construction Report

CHARLES E. DOUGAN, Division of Research & Development, Connecticut State Highway Department

An experimental reinforced concrete pavement, in which an expansive or self-stressing cement was used, was constructed in September 1963. The purpose of the experiment was to explore the feasibility of producing a thin prestressed concrete pavement in which the tension in the prestress strands results from pavement expansion. The 1, 500-ft experimental section contains three slabs 24 ft wide, 6 in. deep, and approximately 490 ft long. The control pavement is of standard 40-ft contraction joint design, 9 in. thick, laid in two 12-ft lane widths.

This report presents information on background, design features, construction processes and experiences, instrumentation and measurements taken during and immediately after construction, and it offers suggestions for the consideration of future experimenters.

Early difficulties with consistency control and, consequently, with concrete finishing were reduced through changes in composition. The expected amount of expansion, as projected on the basis of earlier experimentation, was not achieved in the experimental slabs.

•ABOUT 70 YEARS AGO it was established that the chemical interaction between the tricalcium aluminate in portland cement and calcium sulfate in an aqueous solution imparts expansive properties to concrete. Subsequent research revealed that the resultant salt (calcium sulfoaluminate, of molecular composition 3 $CaO.Al_2O_3.3CaSO_4.30\text{-}32H_2O$) had absorbed water molecules into its final crystalline structure. Approximately 20 years ago a French engineer, Lossier, produced an expansive clinker claimed to be a calcium sulfoaluminate and controlled by regulating the availability of water and the use of blast-furnace slag. Recently Alex Klein of the University of California (1, 2) developed a component for expansive cement which is a clinker proven by X-ray diffraction and petrographic examination to be essentially a true anhydrous calcium sulfoaluminate and free lime. This recent work offered encouragement for the use of expansive cement, under conditions of controlled growth action, to develop self-stressing qualities in resultant concrete.

In December 1962, the Connecticut State Highway Department and other interested parties decided at a meeting to explore the feasibility of constructing an experimental self-stressing concrete pavement in Connecticut. Represented by staff personnel, at the first and also later meetings, were the U. S. Bureau of Public Roads; Concrete Research and Development Corporation (CONRAD), Van Nuys, Calif.; Blakeslee Prestress, Division of C. W. Blakeslee and Sons, Inc., New Haven, Conn.; and the Connecticut State Highway Department.

On the basis of information presented, construction of an experimental section of this new type of pavement was recommended to Commissioner Ives and subsequently authorized. The U. S. Bureau of Public Roads concurred in the decision and offered its fullest cooperation.

Paper sponsored by Committee on Rigid Pavement Design.

TABLE 1

MOISTURE CONTENT AND DENSITY OF GRAVEL SUBBASE DETERMINED BY NUCLEAR PROBE

Station	Subbase and Subgrade	Dry Density (pcf)	Moisture (%)	Sample Depth (in.)	Type of Material
81+00	Subbase	127.5	2.8	0-12	
	Subgrade	102.0	14.7	12-20	Red, silty, sand
83+50	Subbase	116.0	2.6	0-16	
	Subgrade	83.5	22.2	16-24	Brown, silty, fine gravel
86+00	Subbase	117.0	3.4	0-24	
88+50	Subbase	125.0	2.4	0-24	
91+50	Subbase	126.0	4.0	0-24	
	Subgrade	90.0	15.5	24-28	Reddish brown clay
95+00	Subbase	118.0	3.5	0-24	
	Subgrade	83.0	17.5	24-28	Reddish brown clay

Later meetings led to an agreement for a pilot installation of self-stressing pavement at the prestressed concrete plant of C. W. Blakeslee and Sons, Inc., in Hamden, Conn., to obtain further information on this new type of construction before beginning the state project. The pilot installation, consisting of a single slab 185½ ft long, 13⅓ ft wide, and 6 in. deep, was placed on June 14, 1963 (3).

SITE DESCRIPTION

After completion of the pilot installation, the final plans for the experimental pavement were drawn to fit the selected project site, Route 2 in Glastonbury (State Project No. 53-100). The project, a four-lane divided highway with fully controlled access, was then under contract.

The experimental pavement was installed in the southbound roadway from station 81+40 to station 96+60 (4, 5). This roadway is a tangent section from station 81+40 to station 96+19.9 with a +1.5 percent grade. Station 96+19.9 is the P. C. of a superelevated horizontal curve to the right with the same grade.

At the northern end of the test section, station 81+40, the roadway is on fill approximately 10 ft in height, with a 6-in. gravel subbase. Starting approximately at station 82+00, there is a transition from 6 to 24 in. of gravel at station 82+50, as the roadway enters a cut which continues throughout the remainder of the test section. The cut starts at approximately station 83+50 in a sandy gravel, and runs into a reddish brown clay about station 85+00, which continues throughout the rest of the test section. Table 1 gives values of the dry density and moisture content for the gravel subbase and subgrade obtained with a nuclear probe.

DESIGN AND PREPARATION

Final design of the test section called for three self-stressing slabs: two end slabs 494 ft long and one middle slab 490 ft long. The slabs were to be placed 24 ft wide and 6 in. deep. Hereafter, the individual slabs will be referred to as I, II, and III. The approximate limiting stations of the slabs are 81+51 to 86+45, 86+55 to 91+45, and 91+55 to 96+49, respectively (Figs. 1 and 2).

Paving

To overcome anticipated problems with the keyway and the formation of a longitudinal joint, the experimental pavement was placed full width (24 ft) with no longitudinal joint rather than by the conventional lane-at-a-time method which was used on the remainder of the project.

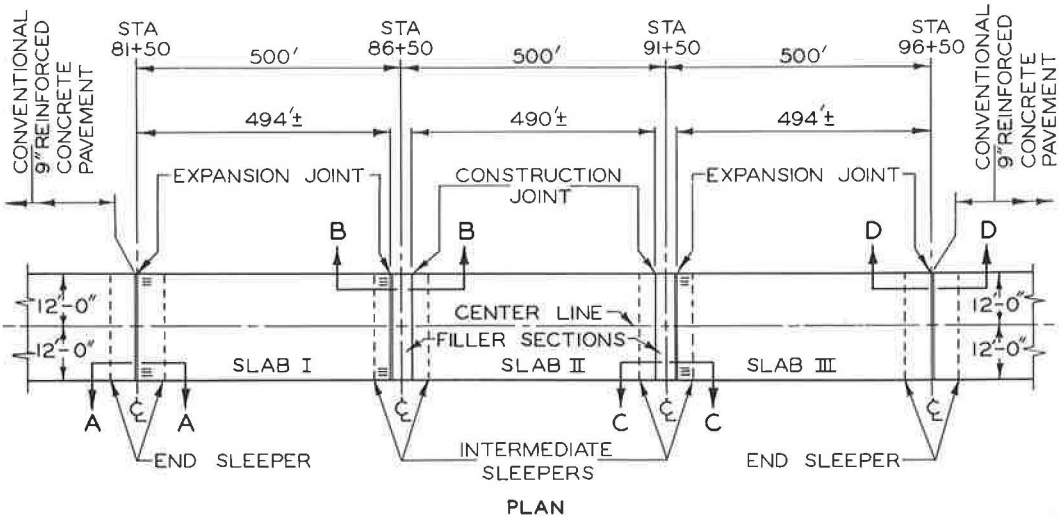

Figure 1. Self-stressing concrete pavement.

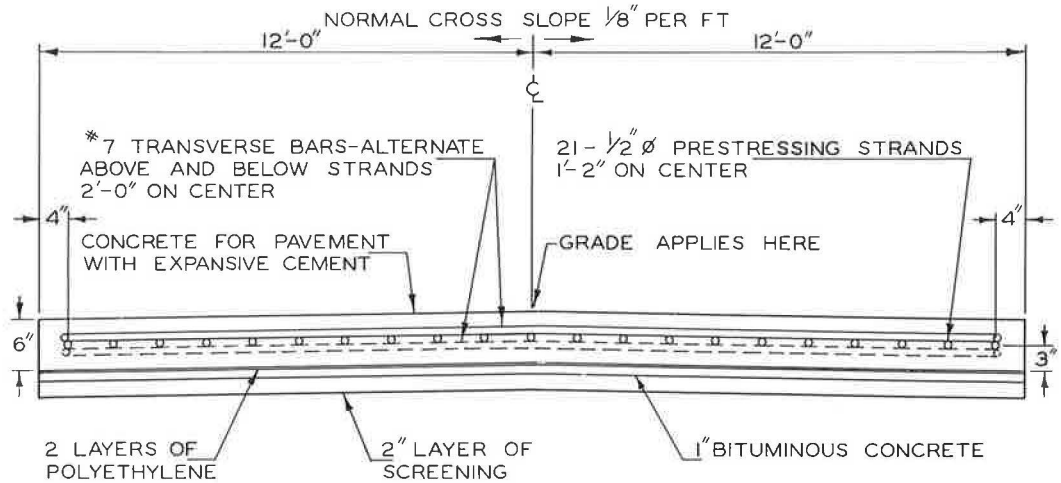

Figure 2. Typical cross-section of pavement.

Figure 3. Backfilling forms with 2-in. layer of trap rock screenings and 1-in. layer of dense-graded bituminous concrete.

Modification for Depth

The subbase was prepared to normal requirements for a 9-in. concrete pavement, using 9-in. forms. The forms were then backfilled with a 2-in. layer of trap rock screenings and a 1-in. layer of dense-graded bituminous concrete to give the required slab thickness of 6 in., as shown in Figure 3. The placement of two layers of polyethylene sheeting, each of 4-mil minimum thickness, was required on the surface of the bituminous concrete to permit slab growth with a minimum of subgrade friction.

Sleeper Slabs

A reinforced concrete sleeper slab was required at each end of the experimental slabs to support the ends of the pavement and to provide anchorage for devices to restrain the thin slab from curling. The sleeper slab was 20 ft long, 24 ft wide, with its surface set flush with the surface of the bituminous concrete. A steel beam (15WF55) was embedded in each sleeper slab, transverse to the roadway. The beams were placed at stations 81+45, 86+50, 91+50, and 96+55. Sleeper slabs at these locations are referred to as blocks A, B, C, and D, respectively (Figs. 4 and 5). Each beam was cut into two 12-ft sections and set to the crown of the finished roadway (Fig. 6). Before placing the beam, holes were cut into the web to permit anchoring the longitudinal steel to the web. The beam also served as a rigid header to jack against during the initial tensioning of the longitudinal reinforcement, and was burned off reasonably flush with the surface of the sleeper before the concrete for the filler section was placed.

Six hold-down devices (Fig. 7) were also set in the sleeper slabs to restrain the ends of the experimental slabs from curling without restraining the pavement growth. Figure 1 shows that the hold-downs were located only in slabs I and III. By extending No. 5 deformed steel bars through the bulkheads forming the termini of slab II, it was possible to tie the concrete filler, over the sleeper slab, to the experimental slab. This mass of concrete was considered sufficient to restrain the ends of slab II from curling. The hold-downs were omitted at the terminal end of slab III. To avoid curling, the longitudinal reinforcement was lowered ½ in. below the neutral axis of the slab. The downward component of the resultant longitudinal stress was judged sufficient to resist curling.

Referring again to Fig. 4, blocks B and C are a uniform 9 in. thick, while blocks A and D (Fig. 5) contain a 3-in. vertical step. The step was required to accommodate the conventional 9-in. reinforced concrete pavement on the terminal blocks. Against the vertical face of the 3-in. step, a 3- by 1½-in. block of foam glass was placed to allow for movement due to temperature changes.

In constructing blocks B, C, and D, the contractor merely removed the gravel subbase to the required depth and poured the blocks, using the faces of the excavation as forms (Fig. 8). For block A, he used the forms which he had already set. In each block, class A truck-mixed concrete with an extra bag of cement per cubic yard was used to develop high early strength in the concrete (see Appendix). The surface of the sleeper slabs was finished with a steel float, and the concrete cured with wet burlap. To minimize subgrade friction, the polyethylene sheeting was carried over the surface of the sleeper slab as shown in Figure 9.

Reinforcement

Longitudinal reinforcing for the pavement was ½-in. diameter, 7-wire strand prestressing cable (ASTM 416), spaced 14 in. on centers, with outside strands 4 in. from the edge of pavement. Each longitudinal cable was continuous for the full 1, 500-ft length of the experimental section. The cables were initially tensioned to a load of approximately 1, 000 lb. The tensioning was accomplished by jacking the individual cables in each slab and clamping the strands to hold them taut, as shown in Figure 10. Tensioning of the longitudinal cables was required to prevent catenary curvature between the transverse reinforcement, and thus to keep the longitudinal reinforcement at the neutral axis of the slab.

NOTE
FACE OF EXPANSIVE CEMENT CONCRETE AT BULKHEADS AT TIME OF INITIAL POUR TO BE AT STATIONS 81+51 - 86+45 - 86+55 - 91+45 - 91+55 AND 96+49

FOR NOTATIONS NOT SHOWN SEE FIGURE 5

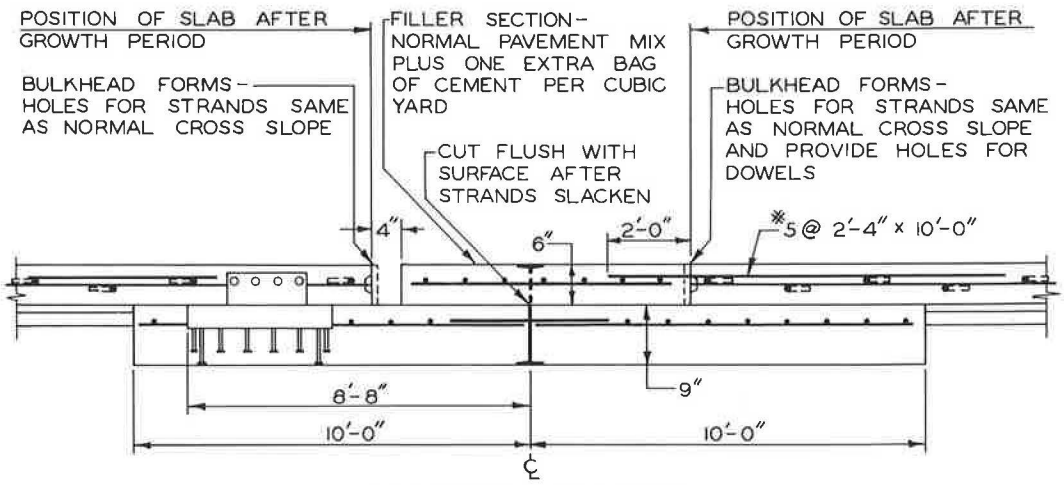

Figure 4. Intermediate sleeper slab.

NOTE
BULKHEAD FORMS -
SECTION A-A HOLES FOR STRANDS SAME AS NORMAL CROSS SLOPE
SECTION D-D HOLES FOR STRANDS 3/8" LOWER THAN NORMAL CROSS SLOPE

SECTION A-A & D-D

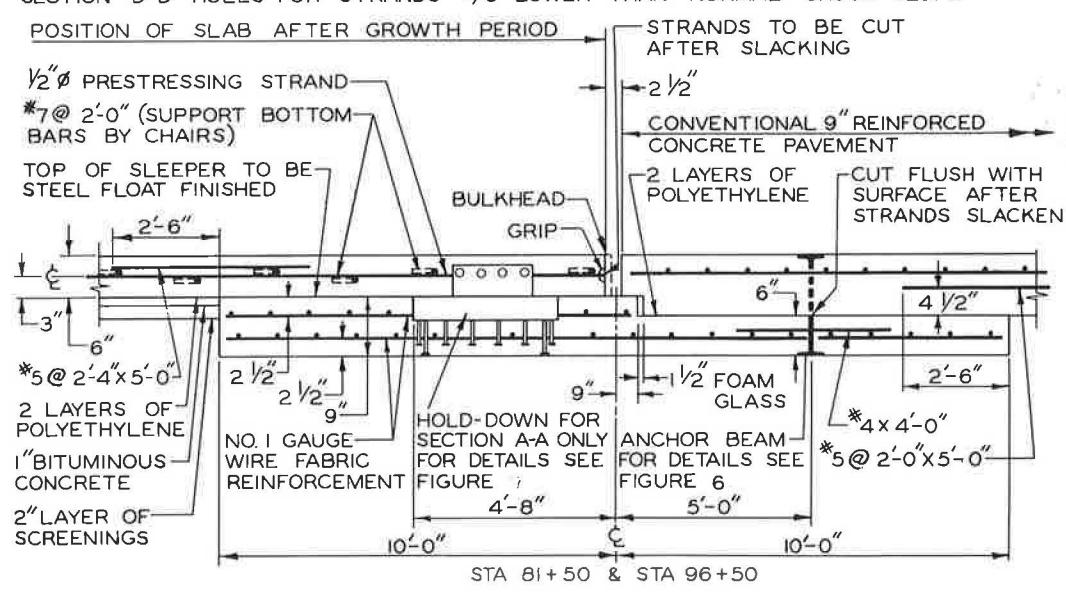

Figure 5. Terminal sleeper slab.

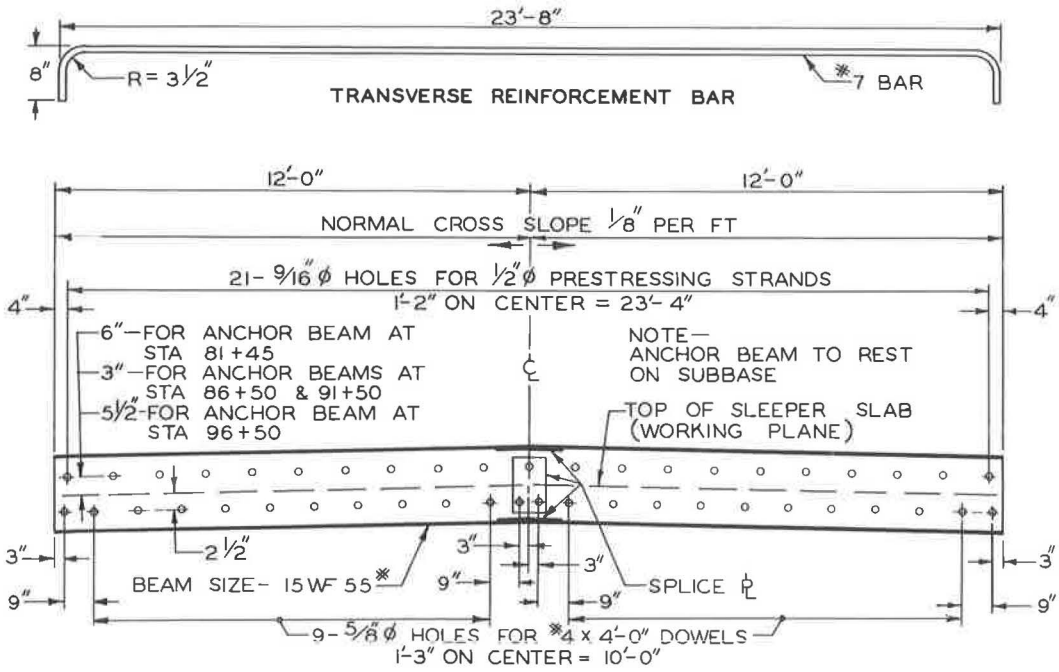

Figure 6. Anchor beam and transverse reinforcement bar.

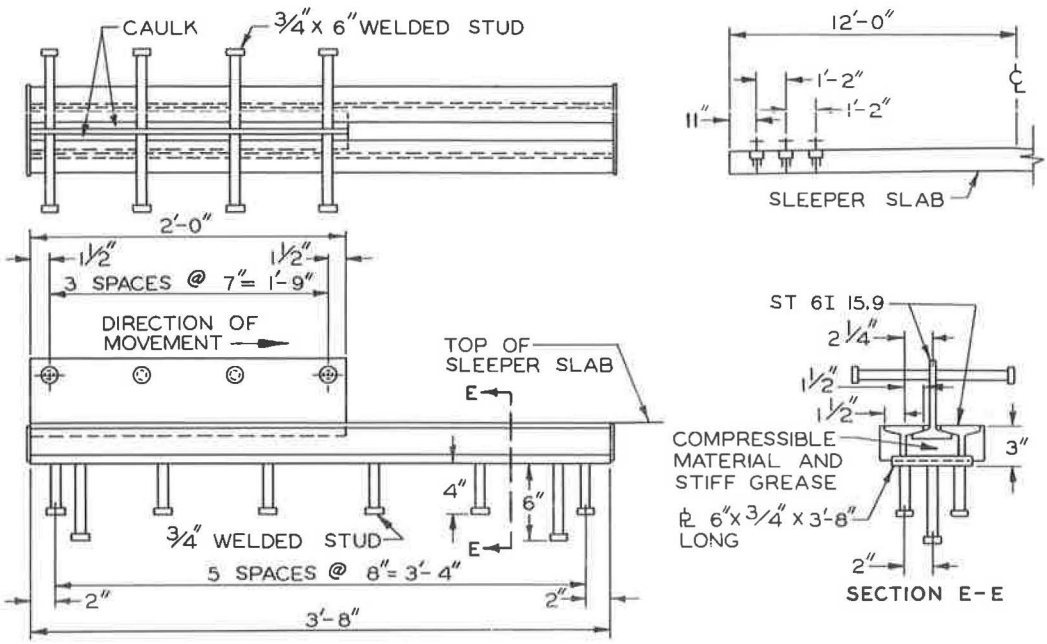

Figure 7. Hold-down device.

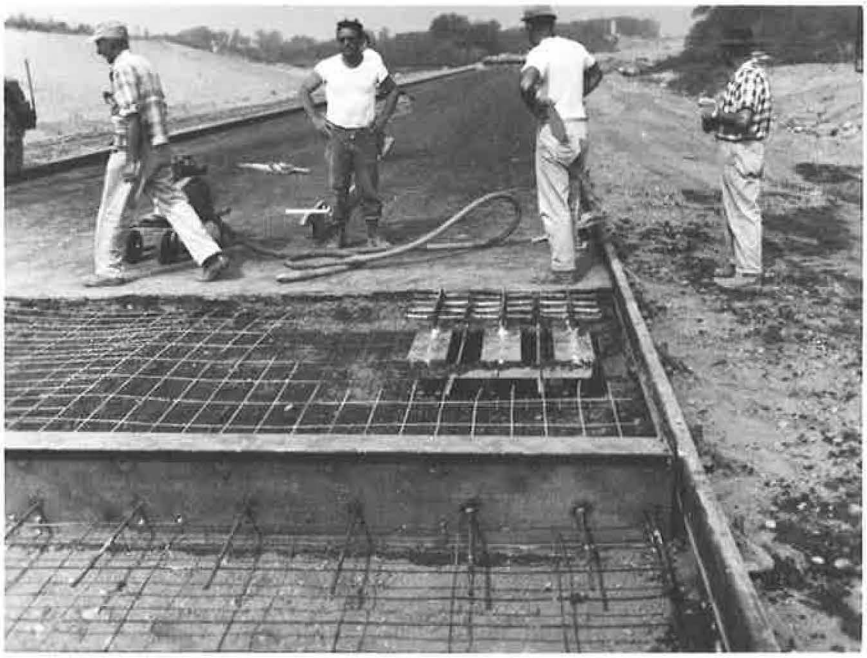

Figure 8. Pouring of blocks B, C, and D, using faces of excavation as forms.

Figure 9. Polyethylene sheeting being carried over surface of sleeper slab.

Figure 10. Tensioning of longitudinal prestressing reinforcement cables.

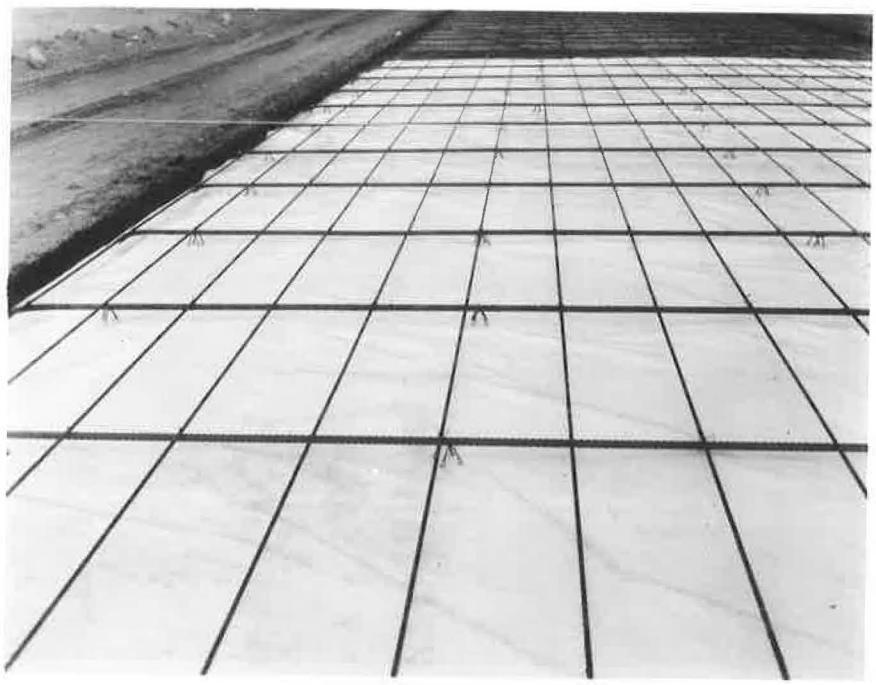

Figure 11. Transverse reinforcement by No. 7 deformed steel bars, tied to longitudinal bars; all steel supported by chairs.

Transverse reinforcement was provided by No. 7 deformed steel bars (ASTM A432 and ASTM A305) spaced 2 ft on centers, alternating above and below the longitudinal strands (Fig. 6). The ends of the deformed bars were bent 90 degrees to form hooks of 8 diameter length which were laid flat to clear the forms by 1½ in. All transverse steel was tied to the longitudinal steel and all steel was supported by chairs as shown in Figure 11.

Mix Design

The preliminary mix design proposed an 8½-bag mix which otherwise conformed to State Highway Department Specifications. A high cement content was deemed necessary to insure the desired growth of the pavement in the field. By using a retarding admixture, it was proposed that the concrete be placed at a slump of 1½ ± ½ in. with a water-cement ratio of 4.0 gal/sk. It was thought that any increase in the water-cement ratio would be detrimental to the pavement. An air-entraining admixture in an amount sufficient to give 4 to 6 percent entrained air was also required to insure durability of the concrete pavement.

To assure the moisture required for continued growth, fog spray was required for a minimum of 24 hr, followed by a cover of polyethylene sheeting for the remainder of the curing period.

PAVING

The paving operation started at the northern end of slab I on September 13, 1963. The concrete was delivered from a central mixing plant to the paving site in 8 cu yd agitator trucks, over a haul distance of approximately ½ mi. The concrete was placed directly from discharge chutes, using both sides of the forms.

As the first load of concrete was being placed, it was quite evident that the material would be difficult to work, as can be seen in Figure 12. The concrete was to be placed with a 1½ ± ½-in. slump, but the material from the first truck had no slump within 5 min after it had been placed. Even after prolonged vibration, it was impossible to consolidate the material thoroughly and raise enough mortar to finish the concrete. When the strike-off moved onto the forms it was unable to displace and distribute the concrete across the pavement. When the transverse screed pushed the forms out of line, finishing operations were stopped, the material was removed from the forms, and the paving operation was moved to slab II.

Slab II

When the paving operation was resumed, additional water had been added to the mix, but the workability remained poor. To complicate matters further, the strike-off broke down about 20 ft from the start and the transverse screed was used to strike off the concrete already deposited in the forms. The screed had little success as the material still remained 2 to 3 in. above the forms. It was impossible to finish the concrete even after water had been sprayed on the unfinished concrete. It was now evident that the retarding qualities of the retarding admixture were inadequate to delay the set of the concrete sufficiently.

Before it was possible to finish this section of pavement, the concrete above the reinforcement was removed. The concrete remaining in the forms was sprayed with water and a surface layer of fresh, high-slump concrete was placed and struck off. Segregation was very noticeable as the new material was being deposited, as shown in Figure 13. The fluidity of the material was demonstrated by the waves of aggregate and mortar that were pushed over the forms during the strike-off operation. Since this type of mix offered the greatest workability, it was accepted and slump tests were dropped from the field testing.

Although the concrete was very wet during placement, it became stiff within 10 min after placing, as evidenced by the large roll of stiff mortar carried by the transverse screed. It was decided that no concrete would be accepted at the paving site which had been in transit more than 15 min, and only two trucks were to be dispatched from the

Figure 12. Placement of first load of concrete, showing inadequate slump.

Figure 13. Placement of high-slump concrete, showing considerable segregation.

plant at a time. This slowed the paving operation considerably, but it enabled the finishers to work closely behind the machines.

Finishing the pavement was a difficult task. As the finishers attempted to float the surface of the pavement, coarse aggregate adjacent to the reinforcement was forced over the steel and through the surface of the pavement. Because of the trouble with the coarse aggregate and other surface irregularities, it was necessary to wet the surface of the pavement and finish most of the slab by hand. Final finishing of the slab was to be with a wet burlap drag, but the operation was not successful as the concrete was too stiff. The resultant surface texture of the pavement was, therefore, very rough and irregular in appearance, with pronounced waves in the direction of paving. The waves were attributed to the transverse reinforcement tied to the top of the longitudinal cables. In an attempt to remove the surface irregularities, the contractor used a circular floor finisher on the pavement. This machine was used with some success as it tended to plane the pavement's surface to a fairly uniform height, but the machine could not finish the entire slab because some of the material had been in place for several hours.

The required cure was applied by state maintenance forces as soon as possible after the concrete had been finished, using a Bean hydraulic sprayer with a spray gun fed by a high-pressure water line, as shown in Figure 14.

Because of the expected expansion of the concrete the contractor was required to remove any obstacles which might impede the growth; therefore, all form pins and collars at bulkheads were removed as soon as possible after the paving operation ceased. The unrestrained forms remained in place and were stripped the following day.

Table 2 gives data on weather conditions, entrained air, and temperatures of plastic concrete for the paving dates.

Slab I

On September 16, 1963, slab I was paved. Based on previous experience, changes in the mix design were made resulting in the finished surface of slab I being much smoother than the surface of slab II. The changes were (a) the maximum size aggregate was reduced from 2- to 1¼-in. crushed stone and (b) the amount of retarding admixture was raised from 25 to 42½ oz/cu yd as shown in the Appendix. To facilitate storage of the paving equipment, the direction of paving was reversed and the operation proceeded from block B to block A.

Throughout the day the concrete was very fluid as the discharge began and became stiffer as the discharge continued because of segregation in the trucks. However, visual inspection of cores removed from the test section indicated that the resultant concrete was fairly homogeneous. Although the revised mix design reduced difficulties in the machine-finishing operation, it was still necessary to hand finish portions of the slab because of the rapid set.

Approximately 225 ft south of the bulkhead at block A, the concrete adjacent to the median began to puff and crack before the completion of the day's paving. The distress appeared as hair cracks in the surface of the pavement. The edges of the cracked pavement then puffed up and exposed the material beneath the surface. The affected area is shown in Figure 15, the day after the completion of slab I. Unfortunately, the area was subjected to abuse before a complete photographic record could be obtained. A possible explanation for this failure is presented in an article in the Journal of the American Concrete Institute, which stresses the need for close control over extent of expansion and time interval during which it takes place. The article states:

> for unrestrained concrete, the expansion must not take place before the concrete gains sufficient tensile strength to be stressed in tension rather than disrupted by the expanding forces. For restrained applications, the concrete must be enough to withstand the compressive stresses developed. (6)

Conceivably, the distress described fits one or a combination of these cases. Also, the temperature of the plastic concrete in the distressed area was 84 F, which is considerably higher than any other recorded.

Figure 14. Curing of concrete, using hydraulic sprayer with spray gun fed by high-pressure water line.

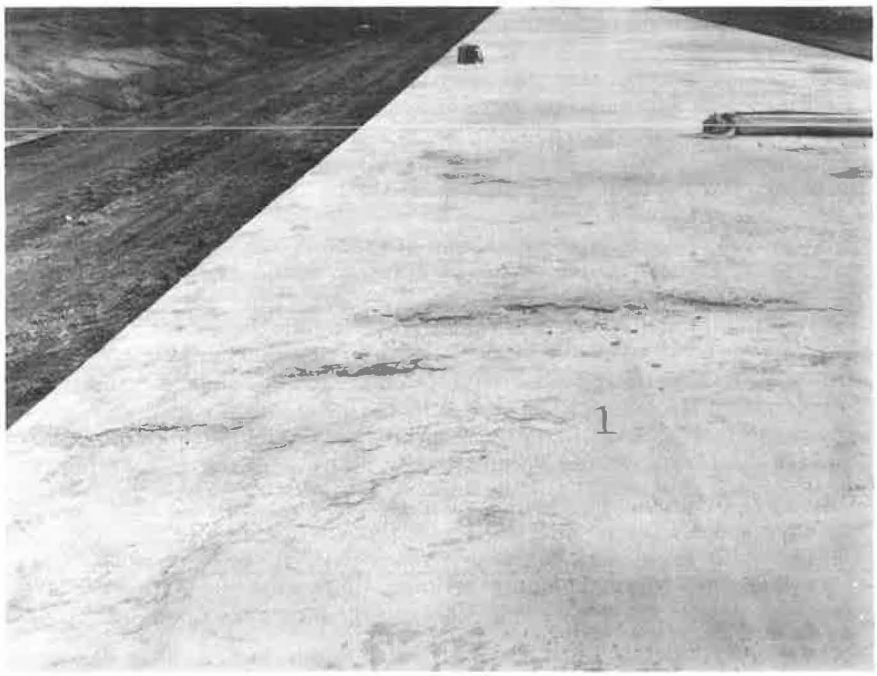

Figure 15. Surface cracks in slab I, day after completion.

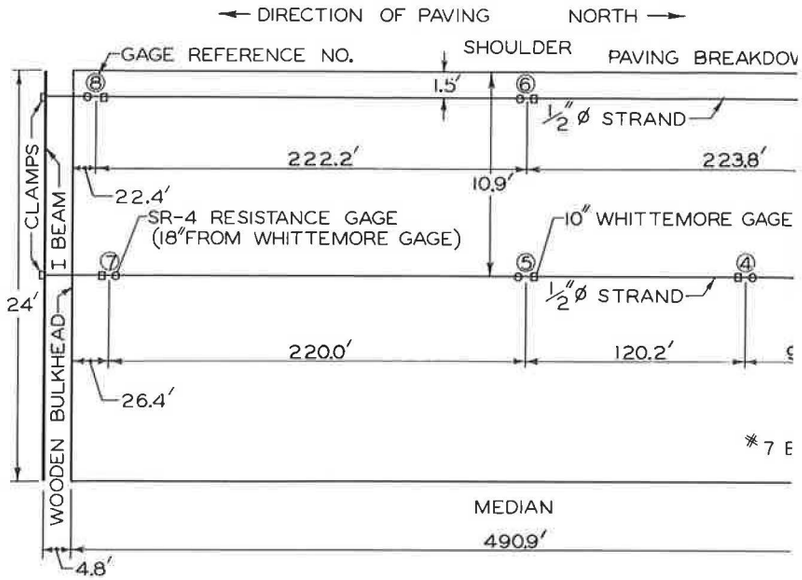

Figure 16. Approximate strain-gage locations slab II

Figure 17. Strain-measuring devices in place before conc

reference line corresponded to the face of the bulkhead adjacent to th
pansive cement concrete slabs. Two monuments were set at each sl
reference line could be established using a transit. Monuments were
work area to avert any possible damage to them, and were placed ir

TABLE 2

DATA ON TEMPERATURE AND AIR ENTRAINMENT FOR THE DATES OF PAVING

Date	Air Temp. (° F)	Concrete Temp. (° F)	Entrained Air (%)
9/13/63	50 - 68	72 - 75	5 - 5½
9/16/63	48 - 55	72 - 78[a]	4¾ - 5¼
9/17/63	49 - 65	72 - 76	4½ - 5

[a]Temperature of 84° F recorded in vicinity of station 83+75.

Slab III

Slab III was paved on September 17, 1963. Paving was started in a southerly direction proceeding from block C to block D. As previously mentioned, unlike slabs I and II, this slab was not wholly on a tangent. This necessitated the removal of the crown from the transverse screeds, which was done by lowering the crown by hand ¼ in. every 30 ft, starting at approximately station 94 + 00. Full superelevation was reached at about station 96 + 00. As the paving operation was halted during the changeover, it became necessary to wet the concrete already in the forms before placing any new material, and to increase the sand content of the concrete mix to aid in the finishing operation, as shown in the Appendix.

As the paving operation neared the point of full superelevation it became increasingly difficult to retain the high-slump concrete in the forms. The material flowed to the low side, displacing the longitudinal and transverse reinforcement. Subsequently, the water content of the mix was reduced which increased finishing difficulties, but the reinforcement remained in place.

About halfway through the paving operation, surface cracks developed adjacent to the median, at approximately station 91 + 90. When the distress was noticed, the area was immediately saturated with water via the hydraulic sprayer. No signs of distress were found during later inspections of the affected area. The expansive concrete probably healed itself when water was applied in an amount sufficient to sustain the hydration reaction of the expansive component.

In general, the paving operation proceeded smoothly as evidenced by the lack of difficulties in accomplishing the transition from the tangent section to full superelevation. Later in this report, slab III is reported as having the least amount of edge cracking. Consequently, it is believed that slab III reflects improved construction techniques over those used in slabs I and II.

Filler Blocks

Normal paving operations outside of the experimental area were started by the contractor after the completion of slab III. Gaps left in the test section over the concrete sleeper slabs were to be filled in as the contractor's operation approached their location. Gaps over the intermediate sleepers were filled with normal paving concrete plus one extra sack of cement per cubic yard, leaving a 4-in. joint adjacent to slabs I and III.

At the terminal blocks, normal paving concrete was used as the filler with a 2½-in. joint left at the ends of the experimental pavement. No. 5 deformed bars, 5 ft long, spaced 2 ft on centers, were originally required in the filler blocks over the terminal sleepers to augment the pavement's flexural strength and to act as a load transfer unit spanning the end of the sleeper block to the gravel subbase (Figs. 4 and 5). Due to an oversight, the steel was not put in the filler sections. Instead, a Harris load transfer unit and a unitube joint former were installed over the ends of the sleeper slabs at points of unequal subgrade support.

Joints left at the experimental sections will be filled with an extruded n
pression seal at a later date. For the present, the joints are filled with w
the joint edges and prevent the intrusion of large particles of incompressik
Final details on the design of the joint material will be reported later.

INSTRUMENTATION

The task of instrumenting the pavement was shared by the U. S. Bureau
Roads and the Division of Research and Development.

Strain Measurements

Strain measurements on transverse and longitudinal reinforcement were
the U. S. Bureau of Public Roads personnel. Two methods of measuremer
ployed: direct measurement with a Whittemore gage and electrical measu
resistance type, SR-4 strain gages. The approximate locations of the stra
devices are shown in Figure 16. Whittemore readings were obtained by pl
collars on the steel and then placing wooden boxes around the reinforcemer
readings were to be taken. The boxes were filled with sand and pinned to t
concrete to prevent the intrusion of concrete during the paving operation.
gages were glued to a wire taken from a prestressing cable. The wire was
to the reinforcement and the device sealed in a metal box. Wires leading f
gages to a Wheatstone bridge were taped to the transverse steel and run th
in the form to the shoulder. Figure 17 shows the strain-measuring device
before concreting. The white box at the left contains the Whittemore colla
black box to the right an SR-4 gage.

Although slab II was selected for the strain-measuring instrumentation
that slab I would be paved first, the contractor actually paved slab II first,
ize himself with this new material.

Before instrumenting the reinforcement, a sample of prestressing cable
the job site was loaded to obtain calibration data for the Whittemore and SR
the State Highway Materials Testing Laboratory at Portland, Conn. The Sl
read inconsistently with respect to the Whittemore gage. The SR-4 gages i
strains of approximately one-half the magnitude of the corresponding Whitt
readings.

Initial field readings were taken shortly after concreting. Subsequent re
taken throughout the growth period and continued for 5 days. These readin
that the elongation of the prestressing tendons practically ceased within 24
placement of the concrete. At the end of 100 hr the Whittemore readings ir
age unit tensile strains in the longitudinal strands of 0.00184, 0.00138, 0.(
0.00145 near the northern end, quarter point, midlength and the southern e
respectively. Conversion of these tensile strains in the strands to compres
in the concrete results in respective values of 91, 68, 28 and 72 psi. In ad
foregoing compressive stresses, subgrade friction also induced compressi
in the concrete as the slab expanded. The unit tensile strain at the midleng
transverse bar was 0.00115 at the end of 100 hr, which converts to 137-psi
stress in the concrete.

The direct readings taken with the Whittemore gage are considered mor
than readings taken with the measurement device utilizing SR-4 strain gage
the tensile strains in the prestressing strands determined with the strain-g
support the values obtained with the Whittemore gage. At the end of 100 hr
gage device indicated average unit tensile strains in the longitudinal prestr
of approximately 0.00200, 0.00145, 0.00100 and 0.00150 for the previously
locations. Corresponding compressive stresses in the concrete are 95, 72
74 psi.

Growth Measurements

Longitudinal expansion of the experimental slabs at the ends was measu
tablishing a reference line transverse to the roadway at the end of each slal

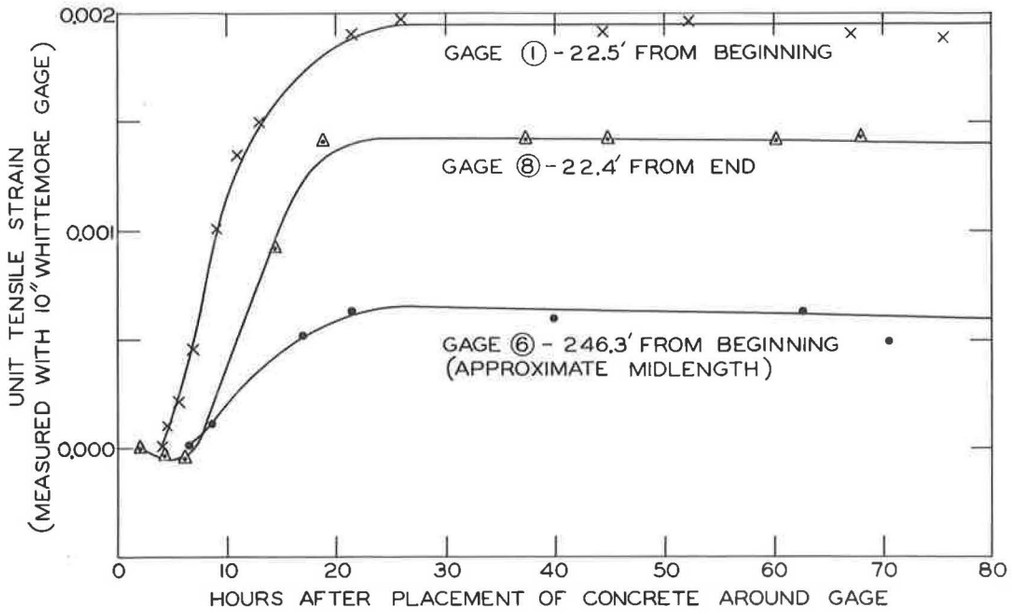

Figure 18. Strains measured in edge strand.

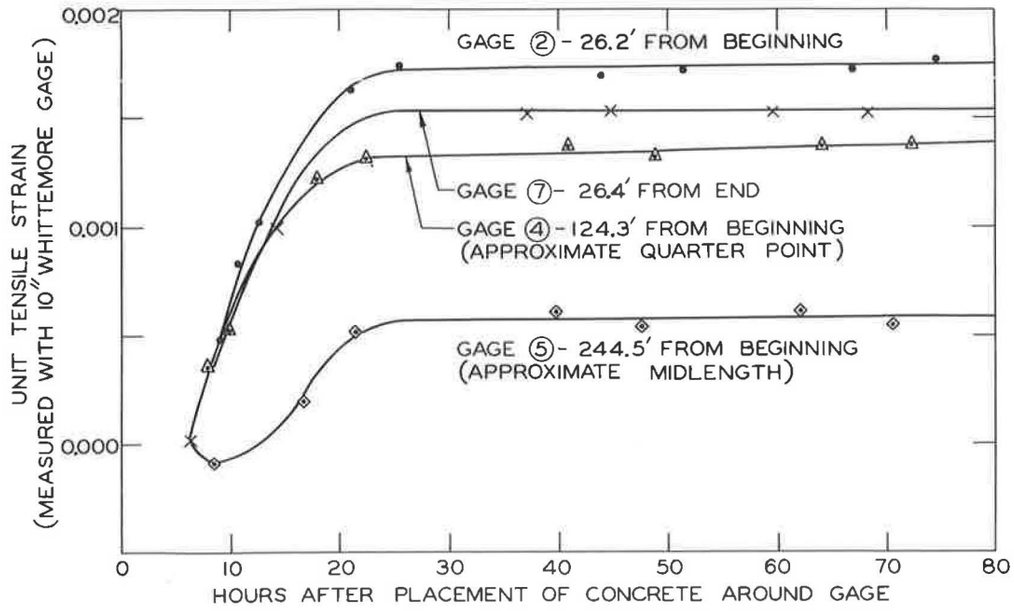

Figure 19. Strains measured in center strand.

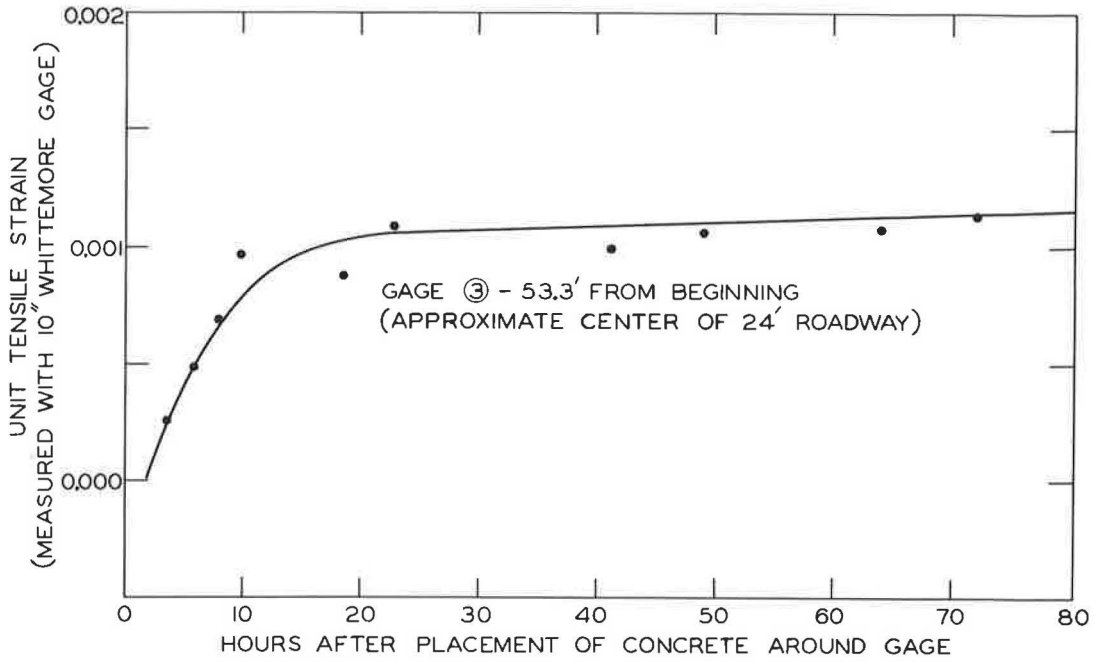

Figure 20. Strains measured on No. 7 transverse bar.

base material to be free from any frost action. Transverse growth measurements were also taken at the ends of the slabs to establish the amount of growth which occurred, and also to estimate the amount of self-stress in the pavement.

Supplementary growth measurements were taken at 50- and 100-ft intervals by placing brass plates in the surface of the concrete pavement in slabs I and III. The plates were placed 6 in. from the edge of pavement, 50 ft on centers adjacent to the shoulder and 100 ft on centers adjacent to the median. Growth measurements taken in this manner were expected to give additional data on the magnitude of the growth throughout the slabs and were to be used as a rough check on readings obtained by a transit.

Pavement Cross-Section

Cross-sections of the pavement were taken by a state survey party to determine if the ends of the slabs would curl. Elevations were taken at the ends of the slabs, 50 ft from the ends, and at the midpoints of the slabs, using reference monuments as bench marks. All foresights were as short as possible and all readings were to the nearest thousandth of a foot. Additional readings will be obtained during the winter and summer months as a check on any possible heaving or curling of the slabs.

Joint Movement

Further instrumentation of the experimental pavement was undertaken to obtain data on thermal expansion of the slabs caused by seasonal variations in temperature. For this purpose, brass plugs were placed in the pavement at all transverse joints in the experimental area. Two groups of plugs were installed at each location, adjacent to the median and the shoulder, with each group consisting of two sets of plugs placed 6 and 18 in. from the edge of pavement. One plug of each set was installed in the filler block and the other in the experimental pavement. Future readings at these locations will give data on the relative amount of movement occurring in slabs of this design. At present, data are insufficient to make any statements about movement at the joints.

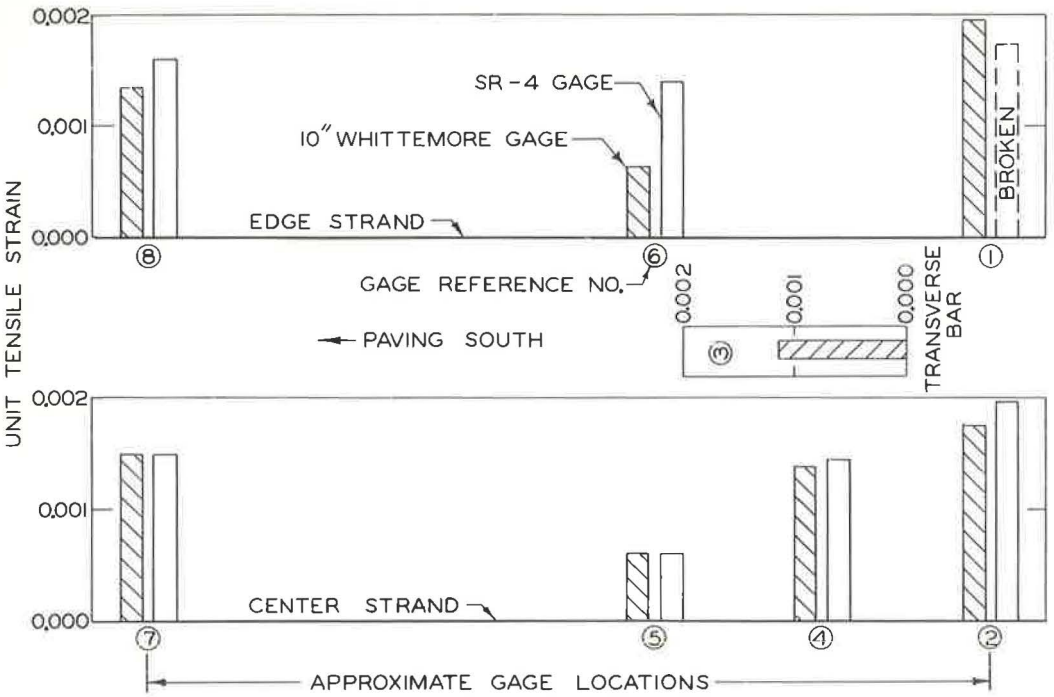

Figure 23. Strains in steel 4 days after placement of concrete.

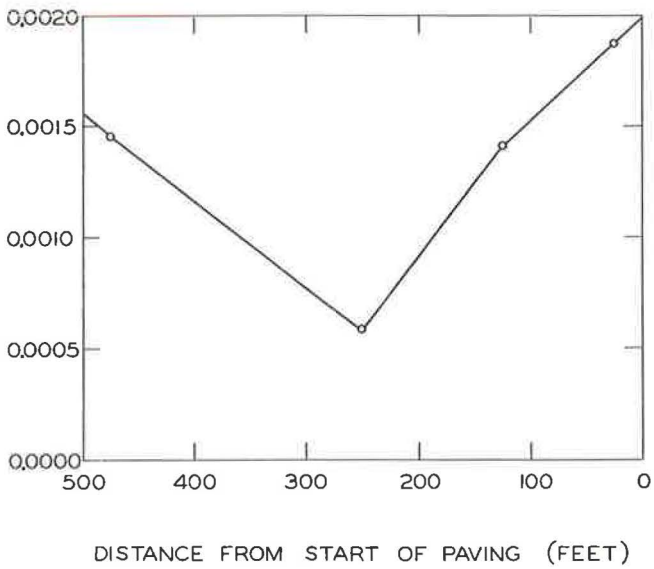

Figure 24. Average strain in the longitudinal strands after 4 days.

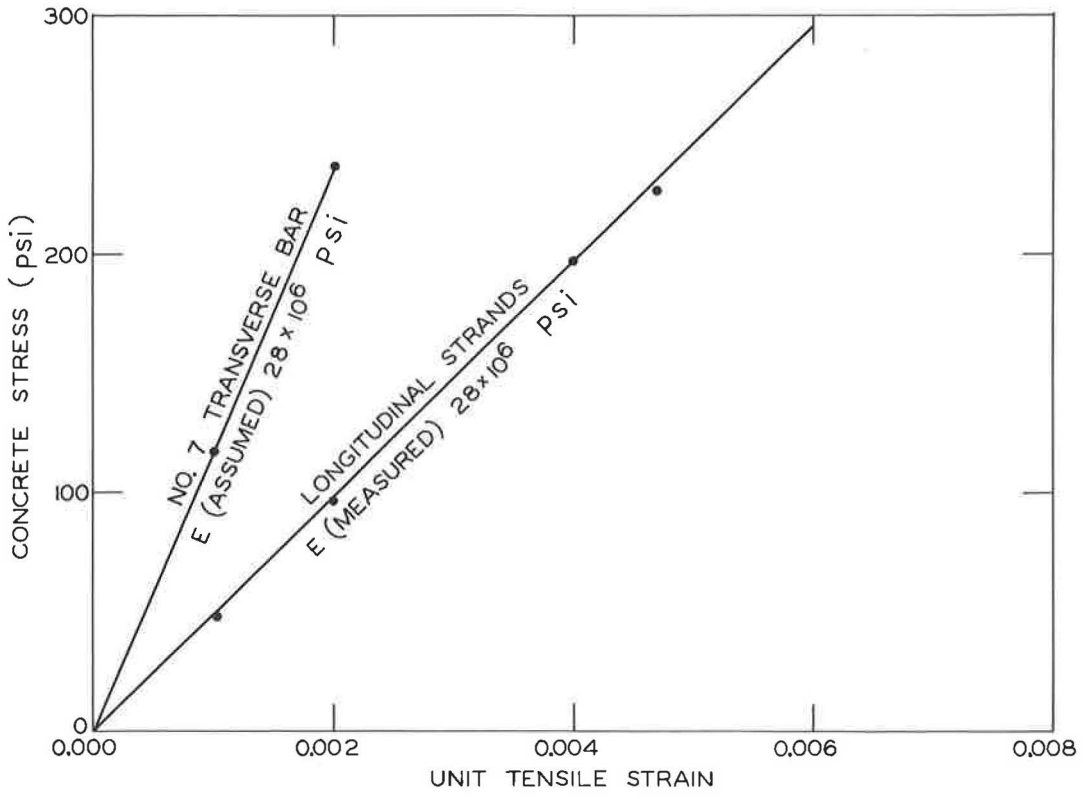

Figure 25. Relationship between tensile strain in prestressing steel and compressive stress in concrete induced by the steel forces.

Pavement Distress

Inspections of the finished pavement showed that the following two types of failures occurred.

1. The spot failure in the form of puffing and cracking was described previously (see Fig. 15).

2. Longitudinal surface cracks 7 to 10 in. long, which occurred about 3 in. from the edges of the slabs, are shown in Figure 29. This cracking is attributed to the heavy transverse reinforcement being close to the surface of the pavement. The crack spacing is about 4 ft, which corresponds to the spacing of the transverse reinforcement above the neutral axis of the slab. The major cause of this failure is now thought to be the restrained and unrestrained concrete within and beyond the 90-degree bent ends of the transverse bars because such cracks were not observed on the low side of the super-elevated portion of slab III where the bent ends of the transverse bars were flush with the the edge face of pavement.

As the paving operation progressed, there was a significant reduction in longitudinal cracking. The number of cracks located from the first to the last day of paving were 103, 62, and 50, respectively. Although slab III contained the least number of longitudinal cracks, this condition is accounted for, in part, by the fact that the hooked ends were flush with the edge of pavement as described previously.

A thin layer of a white deposit was observed on all exposed surfaces of the experimental slabs the day following placement of the concrete. This laitance, or exudation product, could be mistaken for white pigmented membrane-forming curing compound. Under the fog cure, the layer could be easily flaked off by hand; after drying it hardened to a chalk-like consistency and separated locally in the form of blisters as shown in Figure 30. Under traffic, the membrane-like coating was crushed into dust and worn away.

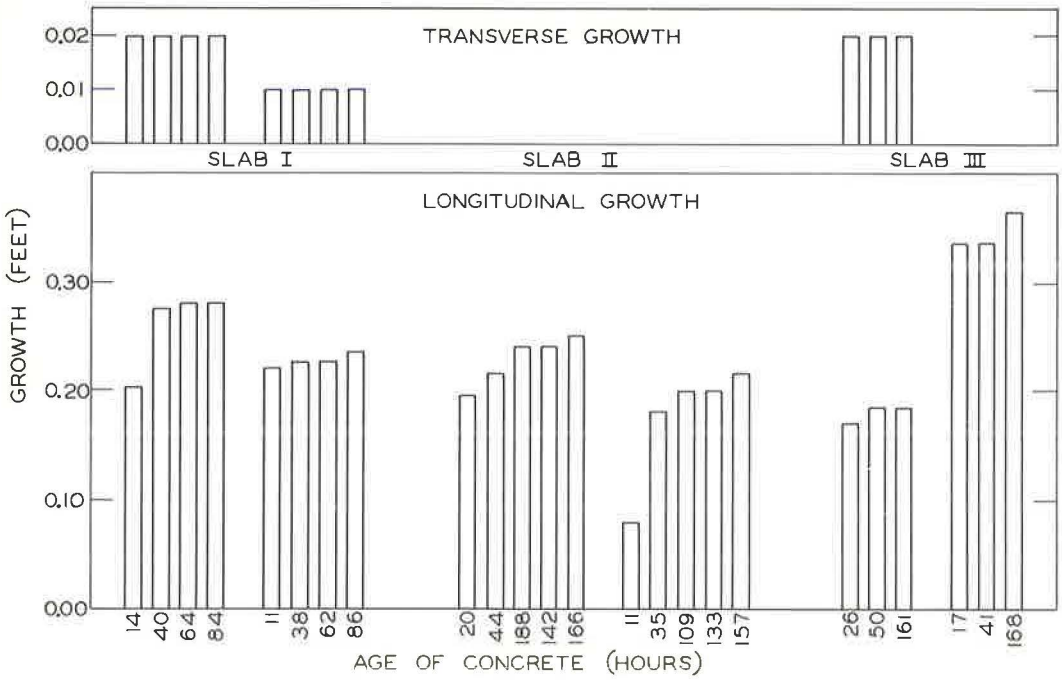

Figure 26. Incremental growth of pavement ends.

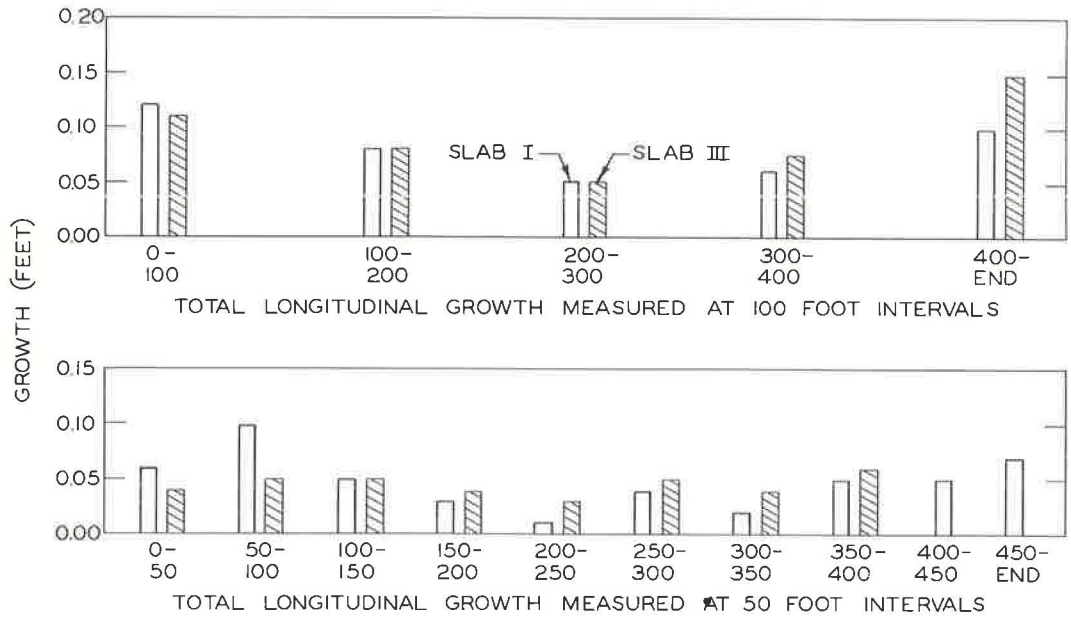

Figure 27. Longitudinal growth measurements.

A sample of the material obtained for laboratory analysis was inadvertently discarded; therefore its chemical composition was not determined. The theory is advanced that expansive forces within the concrete caused water containing one or more chemical

Figure 28. Slack cables protruding from ends of slabs.

substances, in particular, free lime, to be forced to the surface. There is no present indication that the quality of the concrete was affected in any manner.

Compressive Strength

Table 3 gives the compressive strength of 4-in. diameter cores taken from the experimental pavement. Although beams and cylinders are normally used to determine the modulus of rupture and the compressive strength of regular concrete pavement, they were eliminated in the experimental section. It was thought that because the new material has expansive properties, conventional methods of test would not yield reliable results. Cores were taken from each slab to obtain a truer measure of the compressive strength of the expansive cement concrete. The 7-day breaks averaged 4, 030 psi and the 28-day breaks averaged 4, 590 psi.

Visual inspection of the cores, as they were removed from the pavement, indicates that the experimental concrete was fairly homogeneous, despite the difficulties described earlier. Significant voids were found in only 2 of the 29 cores, adjacent to the reinforcement in the pavement.

Suggestions for Future Self-Stressing Pavements

The following suggested revisions in the design and construction of self-stressing pavement may benefit future projects.

1. Subbase.—A smooth, well-rolled gravel subbase, with a bituminous-treated surface, may be adequate to minimize subgrade friction.
2. Hold-down.—Thus far, the effect of curling has been negligible, which suggests that a less complicated apparatus could be used.
3. Reinforcement.—Transverse bars could be placed without the 90-degree bend. This change would eliminate the longitudinal cracking previously discussed.
4. Paving operation.—The time lapse between mixing and placing could be minimized by using a paver. This should make it possible to retain sufficient workability in a low-slump concrete to allow for successful finishing.

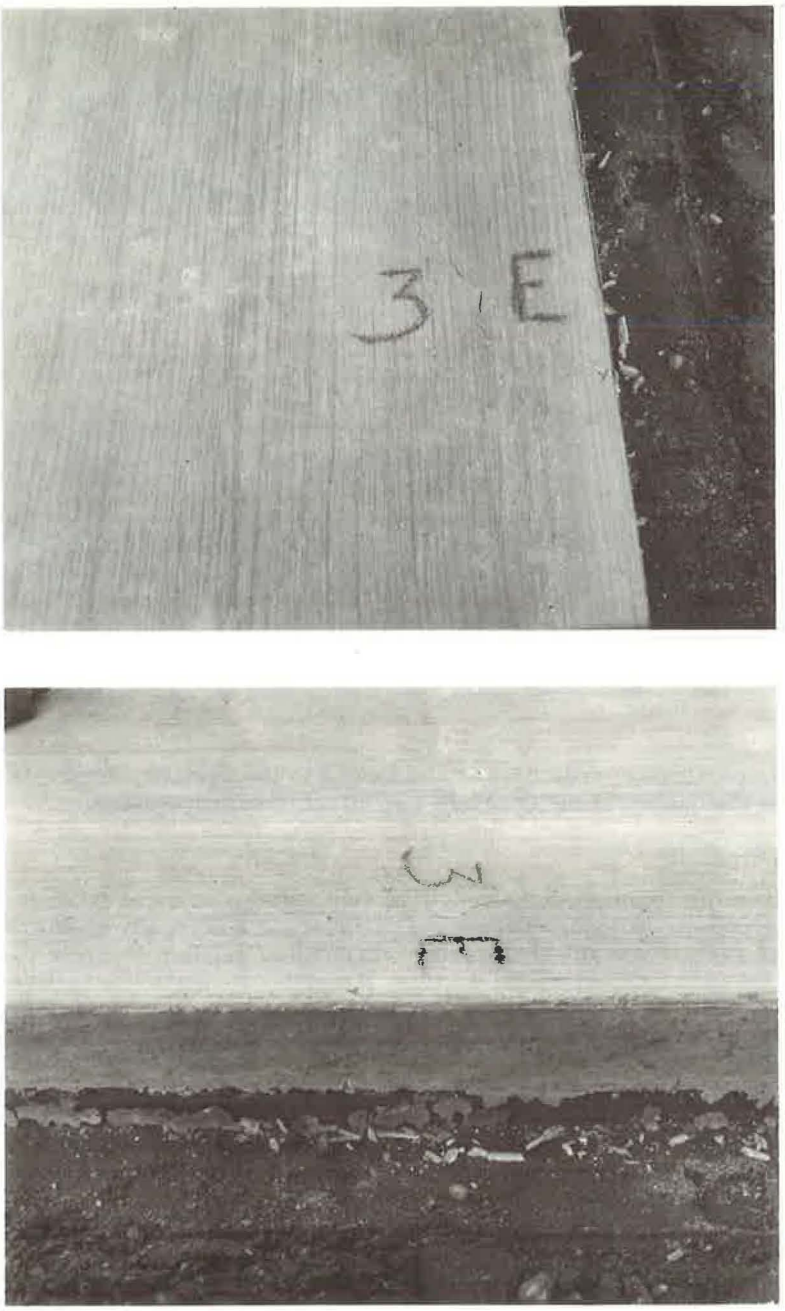

Figure 29. Longitudinal surface cracks occurring at edges of slabs.

5. Mix Design.—Although the retarding admixture probably affected the setting time of the portland cement fraction, the effect on the expansive component was not sufficient to prevent the rapid slump loss throughout construction. Present thinking is that the fineness of grind of the expansive component may be responsible for its excessive water affinity. With a coarser ground expansive component, the rapid slump loss may be eliminated or measurably reduced. Favorable consideration should be given to $1\frac{1}{4}$-in.

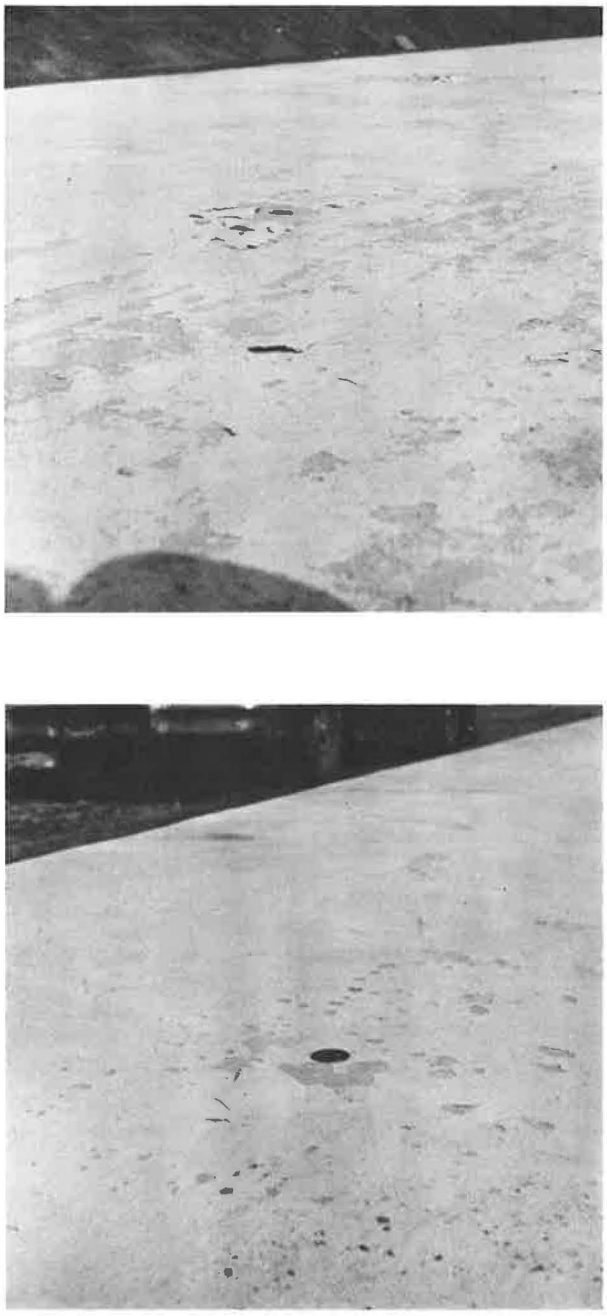

Figure 30. Blisters formed on exposed surface of experimental slab from dried exudation product.

maximum size aggregate because of the thin slab. Experience indicates that the smaller stone would facilitate the paving operation with no appreciable loss in strength to the resultant concrete.

CONCLUSION

The test section of concrete pavement was planned and built to evaluate the potential of expansive cement as applied to one specific type of highway structure. This was in

TABLE 3

COMPRESSIVE STRENGTHS OF EXPANSIVE CEMENT CONCRETE CORES[a]

	Slab I	Slab II	Slab III
	(a) 7-Day Breaks (psi)		
	4,490	3,800	4,490
	3,960	3,590	4,080
	4,190	4,140	4,060
	4,470	4,230	2,870
Avg.	4,276	3,940	3,875
	(b) 28-Day Breaks (psi)		
	4,490[b]	4,240[b]	4,440[b]
	4,080[b]	4,090[b]	6,010[b]
	4,940	4,970[c]	4,980
	5,080	4,840	2,890[c]
	4,620	5,220[d]	4,380
			4,150
			4,330
Avg.	4,642	4,672	4,454

[a]All compressive strengths are corrected to the required L/D of 2.

[b]Cores taken for 7-day breaks and held for 28 days in moist room at Portland Laboratory (all other values obtained from cores taken from pavement just before 28-day break).

[c]Void in core adjacent to steel in core.

[d]Portion of steel reinforcement remained in core when broken.

keeping with the expressed desire of Commissioner Howard S. Ives to remain constantly alert for new product developments and their use in the highway field.

The purpose of this report is to present a factual account of the work accomplished, including the difficulties which are normal by-products of such experimental undertakings. It is hoped that this account may benefit other experimenters.

REFERENCES

1. Klein, A., Karby, T., Polivka, M. Properties of an Expansive Cement for Chemical Prestressing. Journal of the American Concrete Institute, Vol. 58, No. 1, pp. 59-82, July 1961.
2. Lin, T. Y., and Klein, A. Chemical Prestressing of Concrete Using Expanding Cements, Journal of the American Concrete Institute, Vol. 60, No. 9, pp. 1187-1218, September 1963.
3. Pasko, T. J. The Experimental Prestressed Slab Constructed at the C. W. Blakeslee and Sons, Inc., Prestress Plant in Hamden, Connecticut. Unpubl., Aug. 1963.
4. Pasko, T. J. The Experimental Prestressed Pavement Constructed on Route 2 in Glastonbury, Conn. Unpubl., Nov. 1963.
5. Pasko, T. J. An Analysis of Strains Measured in the Prestressing Tendons of the Glastonbury Pavement. Unpubl., May 1964.
6. Admixtures for Concrete, Journal of the American Concrete Institute. ACI Committee 212, Vol. 60, No. 11, pp. 1503-1505.

Appendix

MIX DESIGN

The concrete was mixed for 3 min in a central mixing plant. The original mix used for paving on September 13, 1963 was composed as follows:

Cement, 800 lb;
Water, 34 gal;
2 in. stone, 1,010 lb;
¾ in. stone, 1,010 lb;
Sand, 950 lb;
Plastiment (4 oz/sk) 34 oz/cu yd;
Darex - ⅜ to ½ oz/sk or to give 5 percent ± 1 percent; and
Entrained air, w/c = 4 gal/sk.

The composition of the cement was as follows: 35 percent by weight of the cement was the expanding agent and 65 percent was portland cement. Ingredients were ground together and furnished in bulk to the job site. The stone was 50 percent 2 in., 50 percent ¾ in. by weight; absorption, 0.79 percent. The sand's fineness modulus was 2.80; its absorption, 0.93 percent.

Mix used for paving on September 16 and 17. No change in the sources of aggregates. Previous data on the raw materials still apply.

Cement, 800 lb;
1 ¼ in. stone, 1,310 lb;
½ in. stone, 705 lb;
Sand, 925 lb;
Plastiment, 42½ oz/cu yd; and
Darex 3 oz/sk = 25 oz/cu yd.

On September 17, additional sand was put in the mix to aid the finishers as the paving operation started into the banked curve in slab III. The aggregate weights then became the following:

1¼ in. stone, 1,210 lb;
½ in. stone, 610 lb; and
Sand, 1,085 lb.

For September 16 and 17, the water was not tabulated because of the trouble in placing the material. Water was added to the aggregates to give a workable mix as it was being placed.

Class A concrete mix. Material used in sleeper slabs was as follows:

Cement, 644 lb;
Water, 35 gal;
1¼ in. stone, 1,310 lb;
½ in. stone, 705 lb;
Sand, 1,180 lb; and
Darex, 3 oz/batch.

Concrete was truck-mixed at the job site for 3 min. Concrete was placed with an average slump of 2 in.

Maryland Investigation of Continuously-Reinforced Concrete Pavement: 1959-1964 Strain Observations

RICHARD H. NIXDORF and HENRY A. LEPPER, JR.
Civil Engineering Department, College of Engineering, University of Maryland

The Maryland experimental continuously-reinforced concrete highway pavement was constructed on the Baltimore-Harrisburg Expressway, Interstate 83, during the summer of 1959. The pavement and subbase thicknesses are constant; steel percentages of 0.5, 0.6, and 0.7 percent and bar size Nos. 4, 5, and 6 are the variables.

Strain and temperature measuring instruments were installed at six sites to investigate the behavior of the reinforcing steel in the vicinity of induced cracks. Instrumented bar mat panels containing different amounts and sizes of reinforcing steel were constructed in each of the sections.

Observations of steel strains, crack openings, and pavement temperatures have been made over a 4½-yr period. The instruments and gages, with a few exceptions, have given satisfactory readings since construction.

Reinforcement strains and crack openings vary with the daily range in pavement temperatures. Strain at the crack per degree temperature change is generally greater in winter than in summer. The highest steel strains at the crack and the largest crack openings occurred in the sections containing the smallest amount of reinforcing (0.5 percent). The magnitude of the reinforcing strain is not appreciably affected by the bar size and is controlled primarily by the percentage of reinforcement. The width of the crack opening, however, is governed by both the percentage of steel and bar diameter. Construction conditions also have an apparent influence on pavement stresses.

In all sections of experimental pavement, certain trends occur with age. The crack openings have shown a slight increase and the maximum steel strains at the crack have decreased as the pavement aged. The rates of increase or decrease are greater in sections with smaller percentages of steel.

•CONTINUOUSLY-REINFORCED concrete highway pavement is reinforced longitudinally by continuous steel over the entire length of the pavement, eliminating the need for joints. Restraint imposed by the weight of the slab and subgrade friction in the end portions prevents large movements due to expansion or contraction of the concrete within the central portion of the pavement. Since the central portion of the pavement is restrained, there are no changes in length due to expansion or contraction, and therefore, compressive or tensile stresses are induced in the pavement as temperature and moisture variations occur. The compressive stresses which develop are small in relation to the strength of the concrete and do not cause any structural damage to the pavement. The tensile stresses, however, develop to sufficient magnitude to cause transverse cracking of the concrete. The function of the reinforcement is to prevent these cracks from opening to an extent detrimental to the pavement. The longitudinal reinforcement must be of sufficient amount and strength to serve this purpose.

Paper sponsored by Committee on Rigid Pavement Design.

DESCRIPTION OF PROJECT

Objectives

The primary objectives of the Maryland continuously-reinforced concrete pavement field tests (3) were to make a thorough study of the behavior of the pavement with particular emphasis on the following:

1. The relative effects of different amounts (0.5, 0.6 and 0.7 percent) of longitudinal reinforcement of constant bar size; and
2. The relative effects of different bar sizes (Nos. 4, 5 and 6) with the amount of reinforcement constant at 0.5 percent.

Scope

This paper discusses data gathered with instrumentation embedded in the concrete in each of six test sections of continuously-reinforced pavement. The instrumentation consists of SR-4 strain gages attached to the bars, temperature coils, and Whittemore gage lines on the surface of the concrete pavement. Data were gathered on steel strains, crack openings, and pavement temperatures at and near induced cracks near the center of each continuously-reinforced length. In addition to the instrumented panels, information concerning crack spacing and crack openings was gathered (4).

Test Sites and Properties

During the summer of 1959, six continuously-reinforced sections of highway pavement were constructed as part of the Baltimore-Harrisburg Expressway I-83. These test sections are situated between Mt. Carmel and Middletown Road interchanges in the vicinity of Parkton, about 25 mi north of Baltimore. The continuously-reinforced lengths ranged from 1,800 ft for a single section to 9,800 ft consisting of 3 sections. Detailed descriptions of the field test sites have been given previously (3, 5).

The test sites, numbered one through six (Fig. 1) from south to north, in the southbound roadway, contain an instrumented panel near the center of each. The instrumented panel consists of two bar mats in the shoulder lane, in which eight reinforcing bars have been replaced by instrumented bars.

The continuously-reinforced pavement is 8 in. thick, placed on a 6-in. layer of selected subbase material of crushed local rock. The controlled variables in the experimental pavement are the size and the amount of the reinforcing steel.

Sites 1, 2, and 3 all contain, nominally, 0.5 percent steel with bar size Nos. 5, 4 and 6 in each of the three sites, respectively. There are no intermediate joints between sites 4, 5, and 6; the transition from one section to the next is accomplished by changing the bar mats and percentages of reinforcement. The reinforcement in sites 4, 5, and 6 is composed of No. 5 bars in 0.6, 0.5, and 0.7 percent, respectively.

The reinforcement is deformed bar hard-grade billet steel. The mats are made in 16-ft lengths. Each mat is approximately 6 ft wide. The longitudinal reinforcement is tied to seven No. 3 transverse bars per mat. The specified longitudinal overlap is 12 in. for the No. 4 bars, 13 in. for the No. 5 bars and 15 in. for the No. 6 bars. All reinforcement is located at middepth of the concrete. The following average values of reinforcement yield point were found: bar size No. 4, 71,300 psi; bar size No. 5, 61,500 psi; and bar size No. 6, 55,000 psi.

The instrumented panel near the center of the length of each test site included strain and temperature measuring devices (Fig. 2). The regular reinforcing bars in each mat were replaced by instrumented bars. The instruments which furnished data for this study were as follows: (a) temperature compensating gages; (b) strain gages on the reinforcing steel; (c) temperature measuring coils in the slab; and (d) Whittemore strain gage lines on the surface of the concrete.

The instruments are located within the length of one bar mat, in the shoulder lane near the middle of the length of each test section.

The temperature compensating gages are SR-4 strain gages, type AB-7, which are mounted on $1\frac{1}{2}$-in. long pieces of reinforcing steel and covered with waterproofing and

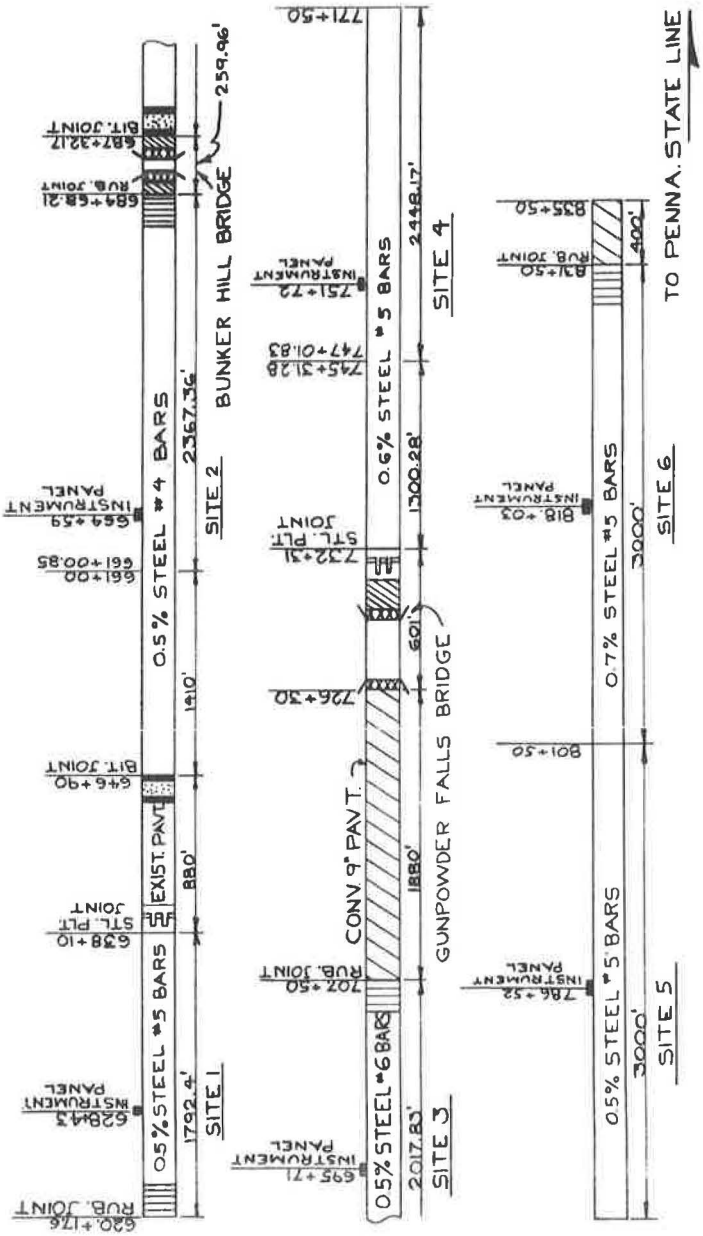

Figure 1. Experimental sections, Baltimore-Harrisburg Expressway.

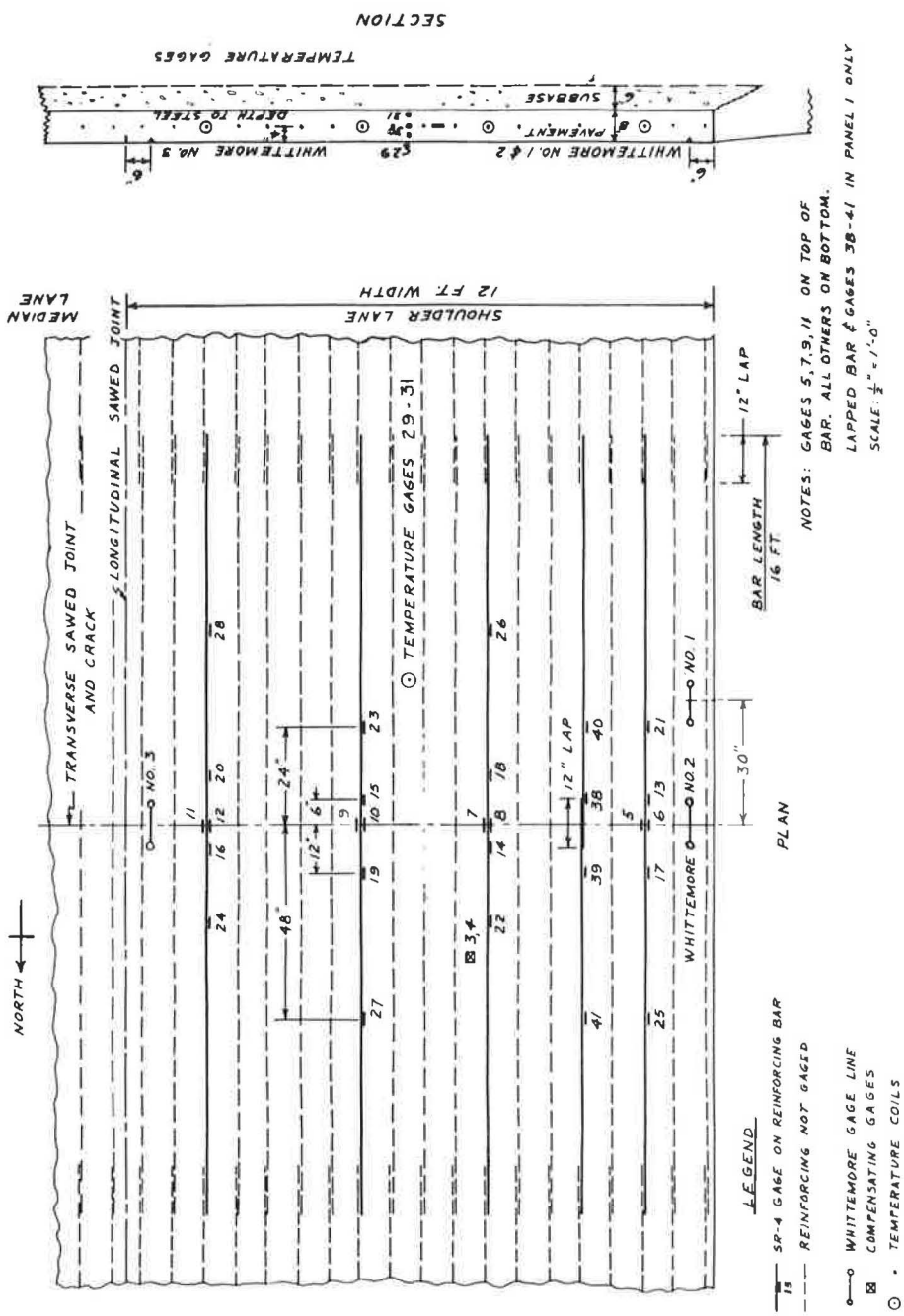

Figure 2. Arrangement of instruments in pavement.

protective tape. The temperature compensating gages are located at middepth in the pavement, 4 to 5 ft from the shoulder edge. The readings from these gages provide temperature compensation for the strain readings on the reinforcement.

The strain gages on the bars are SR-4, type AB-7. There are eight gages at the induced crack (Nos. 5 through 12) placed diametrically opposite each other (to compensate for the effects of bending) on four bars equally spaced across the lane width. Gages on the underside of the bar are located at 6, 12, 24, and 48 in. from the induced crack.

The temperature measuring coils are located in the concrete slab near the middle of the lane and 3 to 4 ft from the induced crack. In each panel, there are 3 temperature measuring coils located 1 in. below the pavement surface, at pavement middepth, and 1 in. above the bottom of the slab.

The electrical leads from the strain gages are carried through a conduit beneath the shoulder to a terminal box containing resistance coils for balancing the electric circuits, and a plug-jack board to which connections are made with the strain indicator.

The brass plugs for the Whittemore gage lines were placed in the fresh concrete immediately following the finishing operation. No. 1 is 30 in. from the induced crack. Gage lines 2 and 3 span the induced crack. The average of readings on gage lines 2 and 3 yields the average crack opening.

The object of the strain readings is to determine the reinforcement behavior in the vicinity of a natural crack. To induce a crack as nearly natural as possible, a 2-in. deep transverse saw cut was made over the center of the instrumented mat 6 to 8 hr after placing of the concrete. In all six cases the cut was made without incident or damage to the concrete surface. After the concrete had cured and dried, the saw cut was sealed with a bituminous compound.

Observation Procedure

The zero readings were taken after the mat had been placed in the concrete and the mechanical finishing operations had passed over and beyond its length. Throughout the summer of 1959, while construction was occurring, measurements were taken over 24-hr periods at weekly or more frequent intervals. The weekly readings were continued until January 1960, at which time biweekly readings were taken. Between April 1960 and August 1961, readings were taken monthly. After August 1961, readings were taken every six months during the winter, in January or February, and during the summer, in August, to provide the minimum data necessary to study the pavement behavior.

At each date, four separate readings for each panel were taken over a 24-hr period. These four readings make up the daily cycle. The first was usually taken in the afternoon, when the pavement temperatures were at their maximum; the second, around midnight, when the pavement temperatures had started to drop; the third, early in the morning, when pavement temperatures were at a minimum; and the fourth, during the afternoon of the second day.

Of the original 226 gages installed, after 4½ yr only 25 are either completely inoperable or yield unusable readings.

INDUCED CRACK OPENING, STEEL STRAIN AT CRACK AND SLAB TEMPERATURE OBSERVATIONS

Variables Affecting Behavior

The behavior of continuously-reinforced pavement is affected by several natural variables including: (a) temperature in the concrete; (b) average transverse crack spacing; and (c) changes occurring with age (i.e., creep, changing concrete properties, and effects of traffic loadings).

The effects of these variables on the crack opening and on the reinforcement strains are examined in the data from the field observations. These variables are, of course, uncontrollable in a field investigation such as this. Furthermore, the moisture content of the pavement fluctuates (9, 10) and undoubtedly affects the strains, but this cannot

be studied as a variable since there was no provision made for moisture measurement. No data were taken for the stresses induced by wheel loads, but the cumulative effect of traffic loads is inseparable from the other long-range influences.

Line Graphs

Variations of induced crack opening, steel strain at the crack, and slab temperature with pavement age are shown in Figures 3 and 4. Each vertical line is representative of the readings taken over a 24-hr cycle. The extremities of the lines, that is, the upper and lower ends, show the maximum and minimum readings taken during each daily cycle. This difference is the daily range. Throughout this report, the steel strains are compensated for temperature changes and hence represent strain caused by stress alone.

The daily range of both the steel strain and the crack opening, in general, is larger during the winter daily cycles than during the summer daily cycles, even though the slab temperature range is smaller during the winter than during the summer. This may indicate that certain of the variables, probably moisture, have more effect on the pavement during the winter months than during the summer months, since the coefficients of expansion and contraction at 40 F in water are greater than those at 40 F in air (8). The coefficients of expansion and contraction for concrete were slightly higher at the lower temperature range, 0 to 40 F (5). Compression during the summer months may be a contributing factor to this condition. The available expansion space may be used up before the pavement is subjected to the peak daily temperature.

The line graphs are composed of a series of undulations or cyclic variations. Each cycle occurs over a 1-yr period and is defined as a yearly cycle (as opposed to a daily cycle of 24 hr). Both the steel strain at the crack (average of gages 5 through 12) and the induced crack opening (average of Whittemore readings 2 and 3) vary inversely with the average slab temperature. The yearly cycles of the steel strains have shown a tendency to decrease in amplitude; that is, the variation or difference between the summer and winter readings for the steel strains has become less as the pavement age increases. The crack opening variation, however, is either increasing or remaining essentially constant as age increases. In all panels, except panel 1, the maximum crack opening has increased and the minimum crack opening has increased also, causing an upward trend in the crack opening cycles. This will be discussed in more detail as other curves are introduced.

Crack Openings

The graphs for sites 1, 2, and 3 show that the induced crack opening of panels 1 and 3, with No. 5 and No. 6 bars, respectively, has exceeded 0.03 in. over several winter periods. The induced crack opening in panel 2, with No. 4 bars, has been recorded as opening above 0.03 in. only once. Since each of these panels contains 0.5 percent steel, the size of the bar seems to be a significant factor. The average of the maximum crack openings observed during the five winter periods of observation is plotted against bar size in Figure 5a. The indication seems to be that the smaller bar size, with its greater ratio of surface to cross-sectional area and, consequently, relatively greater bond capacity, is effective in keeping the crack opening as small as possible under conditions of constant steel percentage.

However, panel 5, containing 0.5 percent steel composed of No. 5 bars, has only two recorded crack openings greater than 0.025 in. This indicates that variables other than bar size influence crack opening. In this case, the temperature at which the pavement was placed and cured is considered the controlling variable. Panel 5, along with panels 4 and 6, was concreted during the first two weeks in June and cured under nearly ideal conditions. Panels 1, 2, and 3 were concreted during the first two weeks of July and cured during July under hot, dry conditions.

Panels 4 and 6 with 0.6 and 0.7 percent steel, respectively, have the smallest maximum crack openings of the six test panels. The crack openings of panel 4 remained below 0.020 in. while those of panel 6 were not recorded as exceeding 0.013 in. Figure 5b shows the effect of steel percentage on the maximum crack openings. In

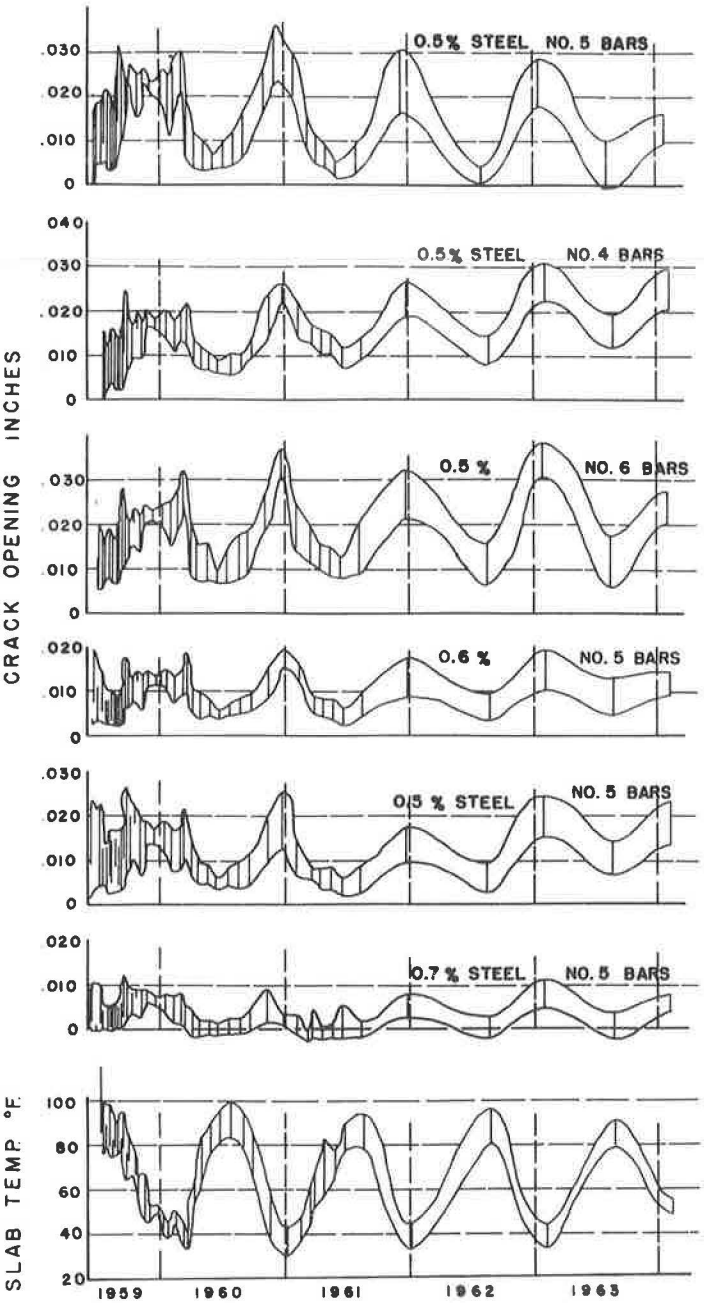

Figure 3. Variation of induced crack opening with pavement age.

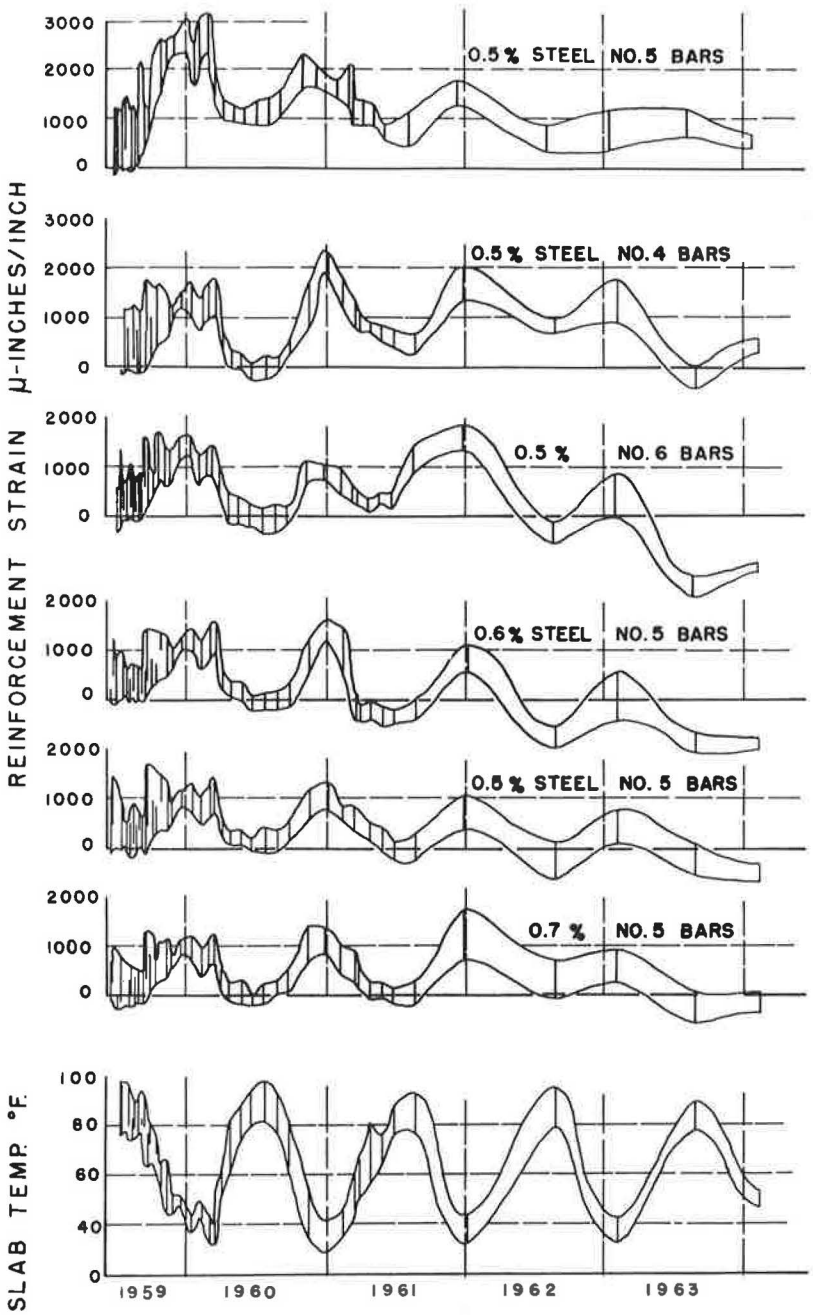

Figure 4. Variation of steel strain at induced crack with pavement age.

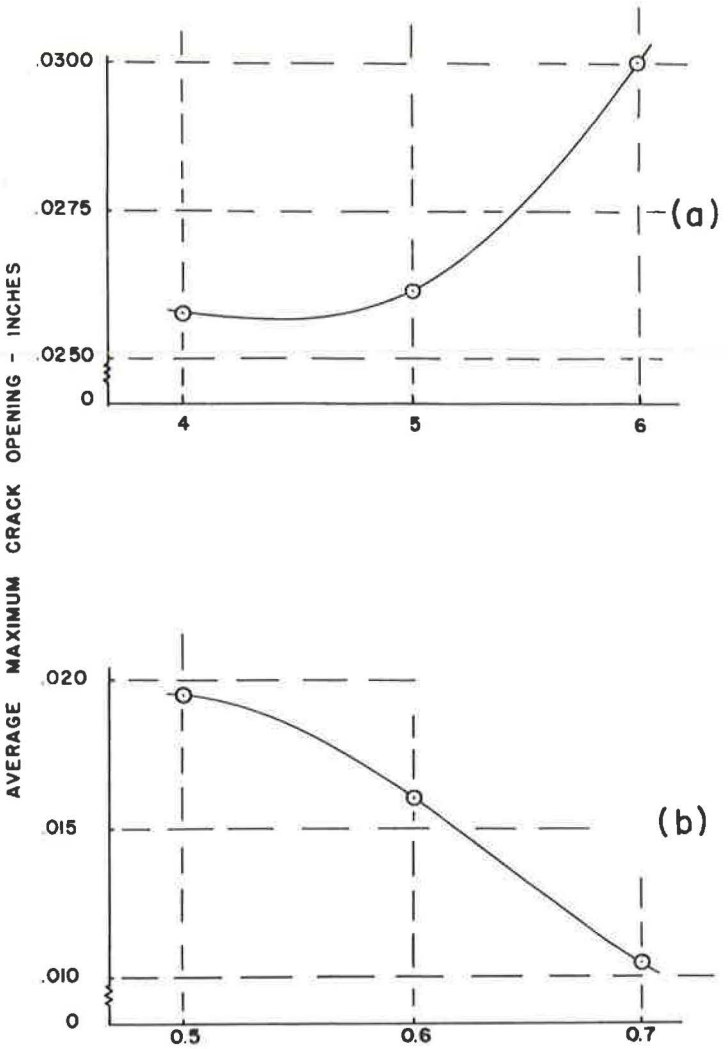

Figure 5. Effect of (a) bar size and (b) steel percent on average maximum crack opening.

addition to bar size and concreting conditions, therefore, the percent of reinforcement is the dominant factor controlling the size of crack opening.

Strains at Induced Crack

The line graphs (Fig. 4) of the steel strains at the induced crack of panels 1, 2 and 3 differ somewhat from the graphs of the crack opening, in that the largest steel strains at the crack do not necessarily coincide with the largest crack opening in any one panel. The steel in panel 1 was strained beyond its yield point during the first winter of exposure—October and November 1959. After the summer of 1960, the seasonal undulations in steel strain at the crack level off, but crack openings have large seasonal changes. The daily range, however, appears unaffected. In panel 2, the yield point of the steel may have been exceeded during the winter of 1960-1961. The steel strains at the crack for the next four readings show signs of leveling off. The steel of panel 3 also shows signs of having been strained beyond its yield point.

The steel strain readings for both summer and winter show a steadily decreasing trend and are going into compression for readings of August 1963 and February 1964.

The pavement temperatures recorded during the winter of 1963-1964 were 10 to 15 deg higher than those of preceding years. These high temperature values together with the high winter moisture content of the pavement may result in the summer-like strains that appear in all the panels.

The steel in panels 4, 5 and 6 has no recorded strains above the yield point and extreme variation in the yearly cycle does not appear. The percentage of steel has very little effect on the maximum strains in these three panels. In each panel the maximum recorded strain is below 2,000 μ-in./in. The temperature and conditions of placing and curing seem to be the factors responsible for the nearly equal strains in these three panels. Each of these panels seems to be following a general trend of decreasing yearly strain variation, with little effect shown on the range of the daily cycle.

In sites 1, 3 and 5 it has been necessary to repair portions of the pavement near the instrumented panels, as described in detail by Lee (4). A failure occurred in site 1 27 ft south of the induced crack during the summer of 1963 at a reinforcement overlap. Extreme cracking was noted in an area 8 ft wide in the shoulder lane of the southbound roadway. Repairs were made in May 1964. Two failures occurred near the induced crack in site 3. One was 39 ft north of the induced crack, the other 60 ft south of the induced crack. Both were noticed during the winter of 1961-1962 and repaired during the fall of 1962. Two failures in site 5 occurred near the induced crack. One was 47 ft south of the induced crack, and 10 ft wide and covered the shoulder lane of the southbound roadway. The other was 70 ft north of the induced crack and extended the entire width of the southbound roadway. Repairs were made in the fall of 1962. The effects of the pavement failures are indicated in the line graphs. In each case, the loss of continuity had a greater effect on the steel strains than on the crack opening widths.

Although these line diagrams show the complete history of crack openings and steel strains at the crack for the 4½-yr observation, they can lead only to general conclusions as to magnitudes of these quantities. In the following sections, an attempt is made to separate some effects to permit better understanding of the behavior shown in these diagrams.

CRACK SPACING

The average crack spacing is equal to a distance divided by the number of cracks contained within this distance. Only the central 500 ft of each test site was studied for crack spacing (3). Records of average crack spacing were started from 1 to 3 mo. after the paving was completed. These records were kept by the Maryland State Roads Commission. The dates of observation of crack spacing do not necessarily coincide with those at which strain and crack opening readings at the induced crack were taken. The average crack spacing decreases as the age of the pavement increases. The curve ranges from the initial crack spacing in August 1959 to an essentially constant value 2 to 3 yr after placing of the concrete. In all the sites, the largest decrease in crack spacing took place during the first year after the pavement was placed. The largest amount of cracking occurred during the time required for the pavement to cure (Fig. 6).

After the first winter, with its low temperatures, the formation of new cracks decreased quite rapidly and the curves began to level off.

The 1963 values indicate that the higher percentages of steel produce the more closely-spaced cracks, and it also appears that the size of the bar contributed to the number of cracks formed (Fig. 7). Site 2 with the smallest bar size, No. 4, for 0.5 percent steel, has the smallest average crack spacing and consequently the largest number of cracks. Site 3 contains No. 6 bars and has the largest average crack spacing. The crack spacing varies directly with the bar size of the reinforcement or inversely with the surface area of the reinforcement. The crack spacing varies inversely with the percentage of reinforcement. The cracks are more evenly distributed throughout the sites containing the higher percentages of steel. The cracks of sites having 0.5 percent reinforcement appear closely spaced in some sections of the sites and widely spaced in others (noted from unpublished crack survey data, similar to those in Figure 11, Ref. 3, taken by Maryland State Roads Commission).

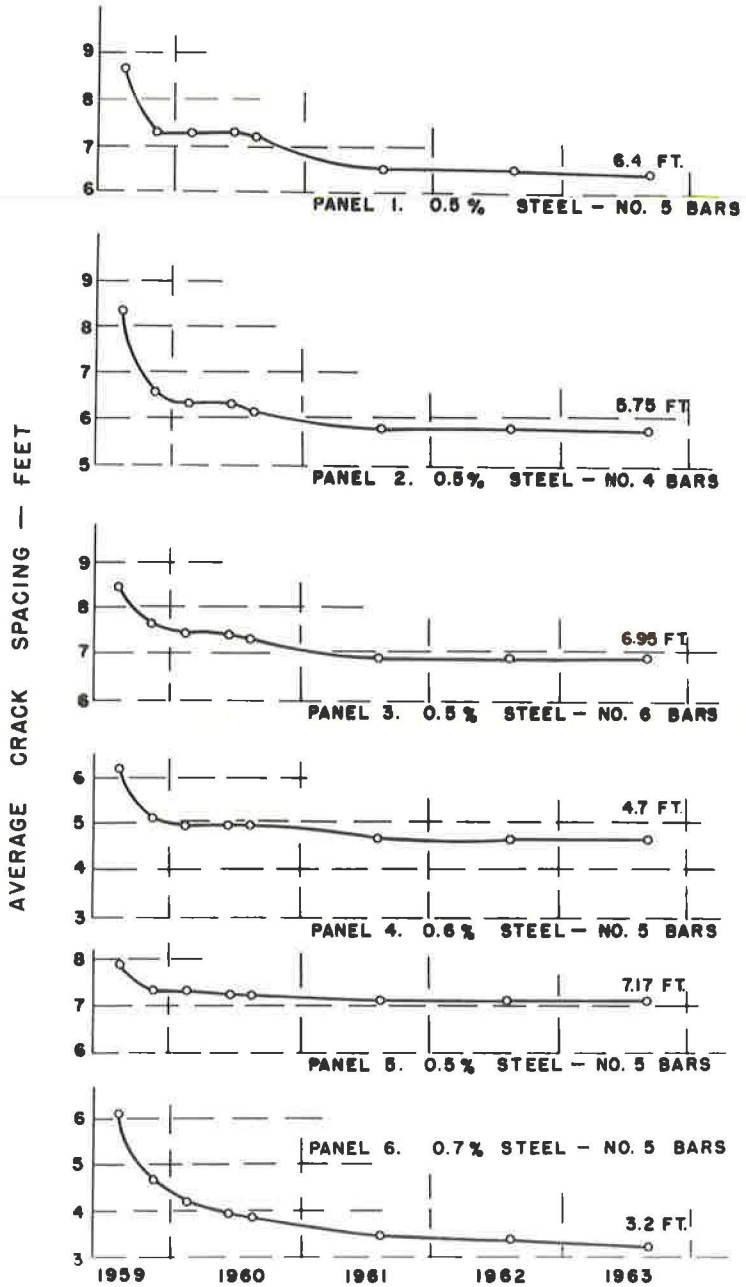

Figure 6. Variation in average crack spacing with pavement age.

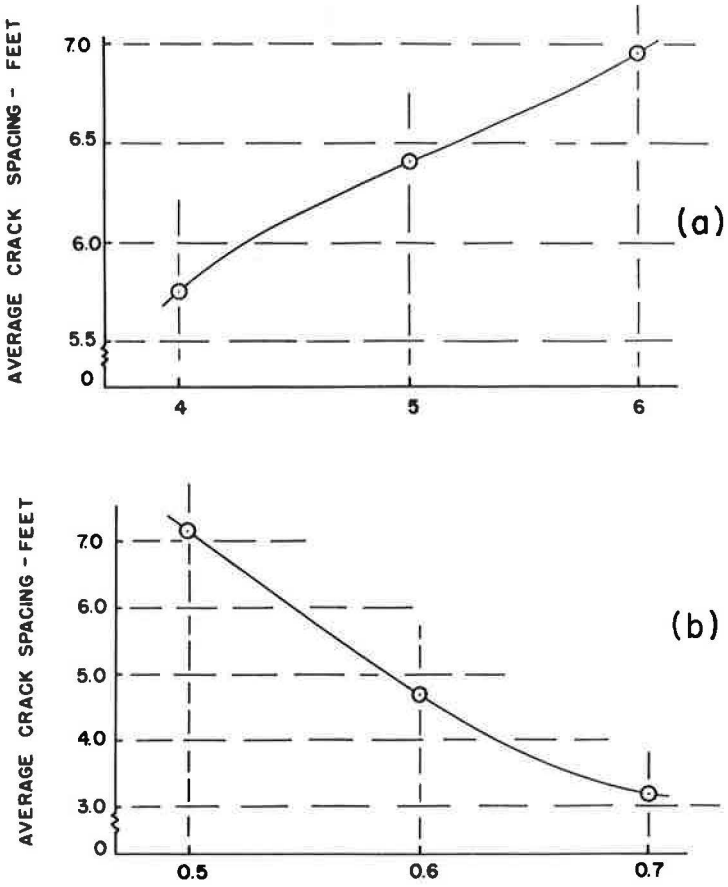

Figure 7. Effect of (a) bar size and (b) percent steel reinforcement on average crack spacing.

DAILY STEEL STRAIN CYCLES

The daily cycles are defined by four readings for each panel taken over a 24-hr period. During this period, it seems logical to assume that the steel strains will be affected only by temperature change since any change in the moisture content of the pavement would be small. Ideally, then, if steel strains were plotted against pavement temperature for a 24-hr period, the points should form a straight line.

Average steel strain (gages 5 through 12) at the induced crack was plotted as a function of average slab temperature (Figs. 8, 9, 10) for panels 4, 5, and 6. These three panels were chosen because of their relatively consistent behavior and their variation in steel content. In most cases the four points observed in the daily cycle fall very close to a straight line, fitted to the points with a small amount of error. In cases where the points were widely scattered, two methods were used. If three points formed a straight line and a fourth fell wide of this, then the line was drawn through these three points, omitting the fourth. If the four points were widely scattered with no apparent order, then a straight line was averaged through the points with a slope that seemed consistent with the slopes of preceding and following daily cycles. The observed points fit well to a straight line in seven of ten cases.

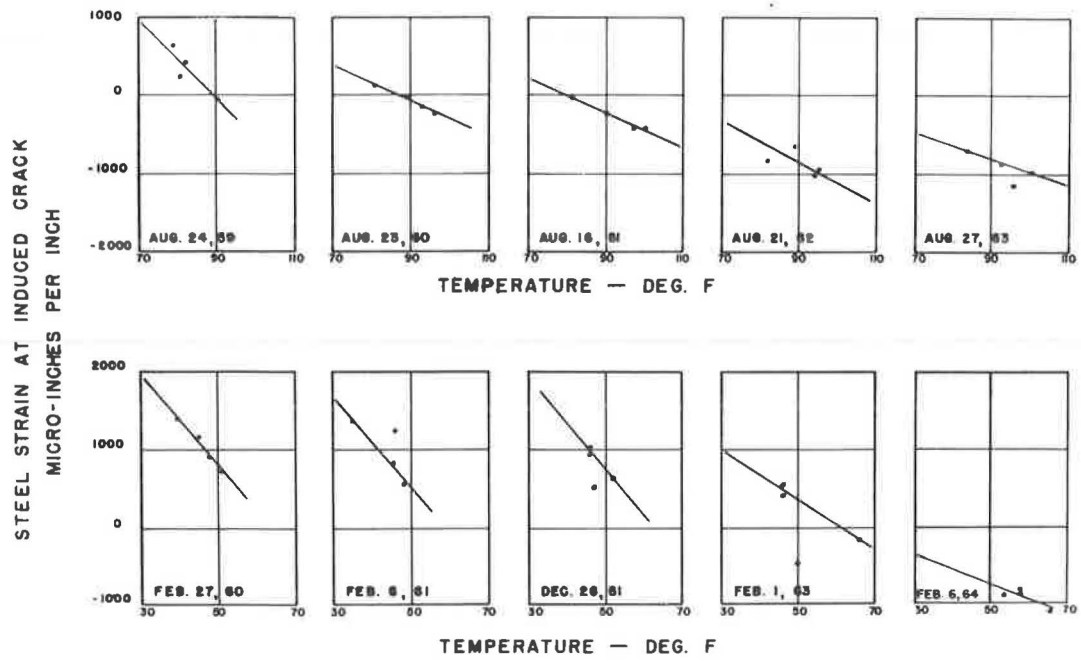

Figure 8. Daily strain-temperature cycle at 6-mo. intervals, panel 4.

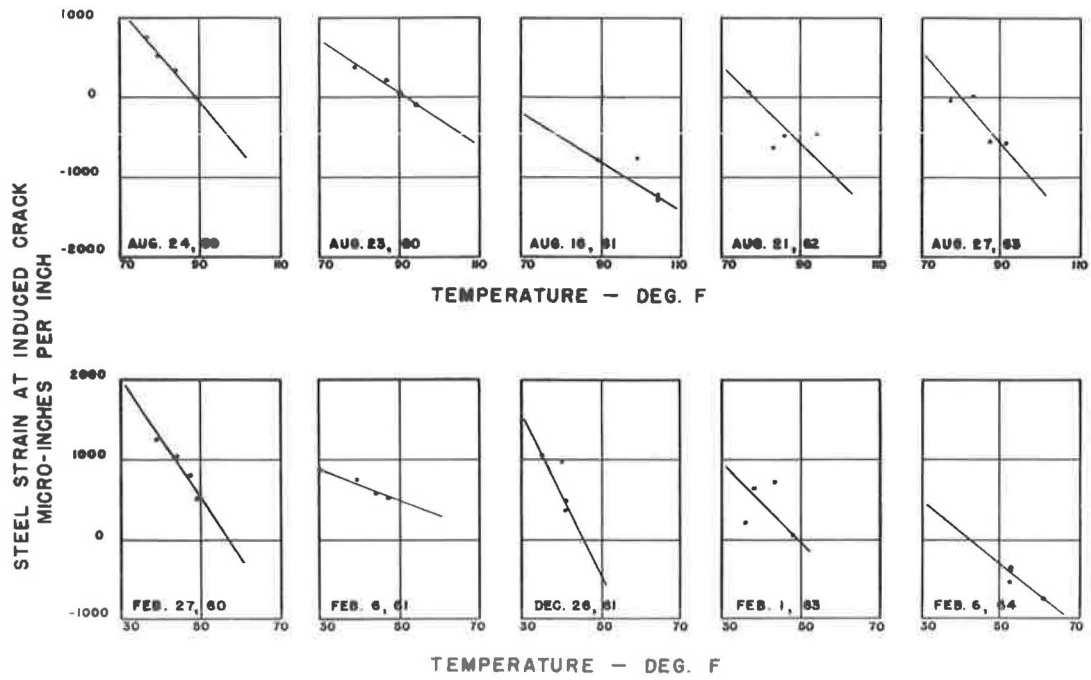

Figure 9. Daily strain-temperature cycle at 6-mo. intervals, panel 5.

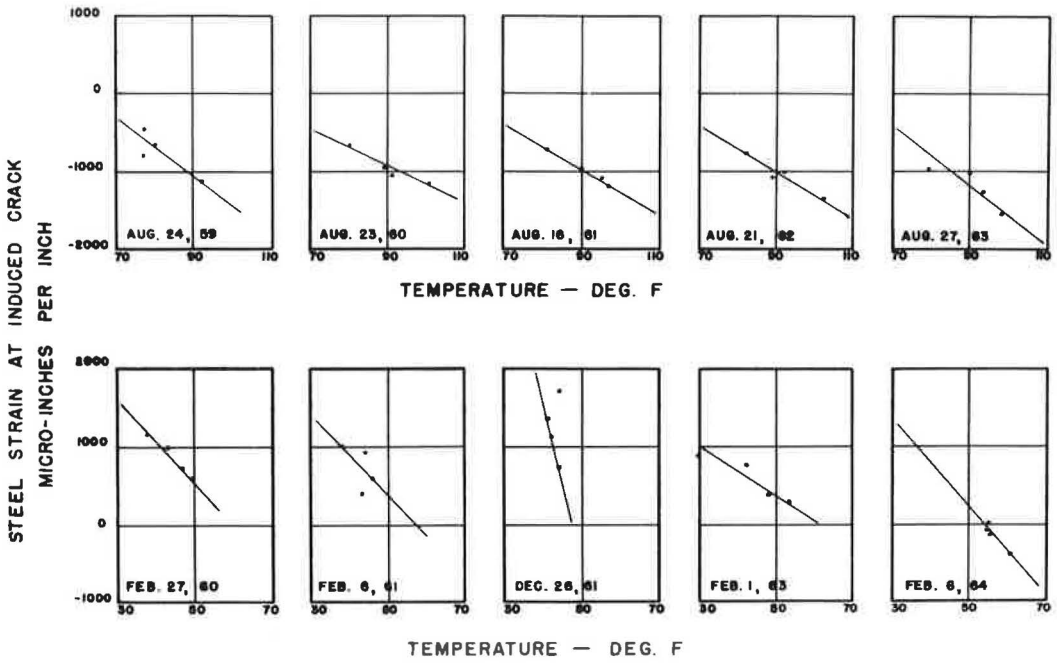

Figure 10. Daily strain-temperature cycle at 6-mo. intervals, panel 6.

Panel 5, with 0.5 percent reinforcement, No. 5 bars, has the largest scattering of points of the three panels (Fig. 9). The steel strain values of the first winter daily cycle, taken February 27 and 28, 1960, fall in a very nearly straight line. The second set of winter readings, taken February 6 and 7, 1961, do not fall on a straight line; however, an average straight line can be drawn through the points without much difficulty. After this time, the points become increasingly widely scattered. In panel 5 the variation of steel strain with temperature goes progressively from a straight-line variation to a four-point variation having no apparent sequential order. These erratic results probably are due to pavement failures that occurred or were in the process of occurring during the winter of 1961-1962.

Panel 4 contains 0.6 percent reinforcement composed of No. 5 bars. The steel strains at the induced crack, when plotted against the pavement temperatures (Fig. 8), fall very close to a straight line, with three exceptions. As in panel 5, the readings of the first winter daily cycle fall very close to a straight line. Three of the readings of the 1961, 1962, and 1963 winters fall on a straight line in each case. One point falls out of line with the others and was not considered when the straight line average was drawn. The slopes of the winter strain-temperature lines (Table 1) do not decrease for the first two winters. Only after the third winter does the slope of the daily cycle begin to decrease. Slopes of the daily cycle graphs became nearly constant for summer readings after 1-yr age.

The winter readings for panel 6, containing 0.7 percent steel, are perhaps the most consistent of the three panels under discussion. As in panels 4 and 5, the February 1960 readings fall on a straight line. The 1961 winter readings are widely scattered. The 1962 and 1963 readings, unlike those of panels 4 and 5, fall quite close to a straight line. The slope of the strain-temperature line decreases from winter 1960 to winter 1961. After this, the slope shows no apparent consistency. The sharp increase in slope of the winter 1961-1962 occurs for no apparent reason, since no breaks or extreme cracking appear in the test section, and this value must be considered as instrumental error.

TABLE 1

OBSERVED VALUES OF STEEL STRAIN AT CRACK PER DEGREE F AND OBSERVED CRACK SPACING

Date	Panel					
	5[a]		4[b]		6[c]	
	μ-in./in./Deg F	Crack Spacing (ft)	μ-in./in./Deg F	Crack Spacing (ft)	μ-in./in./Deg F	Crack Spacing (ft)
Aug. 1959	60	7.94	52	6.25	39	6.10
Feb. 1960	78	7.35	59	5.00	54	4.20
Aug. 1960	33	7.27	23	5.00	24	3.85
Feb. 1961	19	7.20	59	4.92	51	3.60
Aug. 1961	31	7.14	23	4.76	29	3.45
Dec. 1961	104	7.14	59	4.70	200	3.40
Aug. 1962	49	7.14	26	4.70	30	3.35
Feb. 1963	50	7.14	32	4.70	32	3.30
Aug. 1963	58	7.14	17	4.70	39	3.20
Feb. 1964	41	7.14	20	4.70	58	3.15

[a]0.5 percent No. 5 bars.
[b]0.6 percent No. 5 bars.
[c]0.7 percent No. 5 bars.

The observed slopes of the diagrams of steel strain at the crack vs temperature are given in Table 1. These strains, in micro-inches per inch per degree Fahrenheit, are shown, together with average crack spacing in the central 500 ft of each of the three sites. Steel strain at the crack per degree Fahrenheit varies from 17 to 78 μ-in./in./deg F, if the widely inconsistent values for December 1961 are discarded as erroneous readings. Change in stress per degree change in temperature, found by multiplying these strains by modulus of elasticity of the steel, ranges between 510 and 2,340 psi/deg F.

In all three panels, the slopes of the winter strain-temperature lines are greater than the slopes of the summer strain-temperature lines in almost every case. This may indicate that the greater moisture content of the pavement during the winter affects the coefficients of expansion and contraction of the concrete (9).

There does not appear to be any regular change with age in these values of strain per degree temperature change. The irregular data in many instances of daily cycles and the lack of any long-term consistency or trends indicate that many factors affect the forces in the pavement. A simple relation between strain and temperature change does not hold at all times even over the period of a day. Long-term effects such as might be caused by changes in crack spacing, concrete properties and moisture content of the pavement are not great enough to affect the range of values of strain per degree temperature change in the daily cycle.

VARIATION OF CRACK OPENING AND STEEL STRAIN AT CRACK WITH AGE

Trend Lines

Crack openings and strains vary with temperature and with age (Figs. 3 and 4). To study the changes which occur with age, it is necessary to establish comparable strain and crack opening values that are independent of temperature of observation. This was done by fitting straight lines (called trend lines) to plots of strain at crack and crack opening as functions of temperature. The intercepts of these trend lines at 40 and 80 F were the normalized values of the two quantities.

Diagrams were plotted using only the February and August readings because the pavement contains maximum and minimum moisture, respectively, and minimum and maximum temperature, respectively, at these times in the yearly cycle. Although it

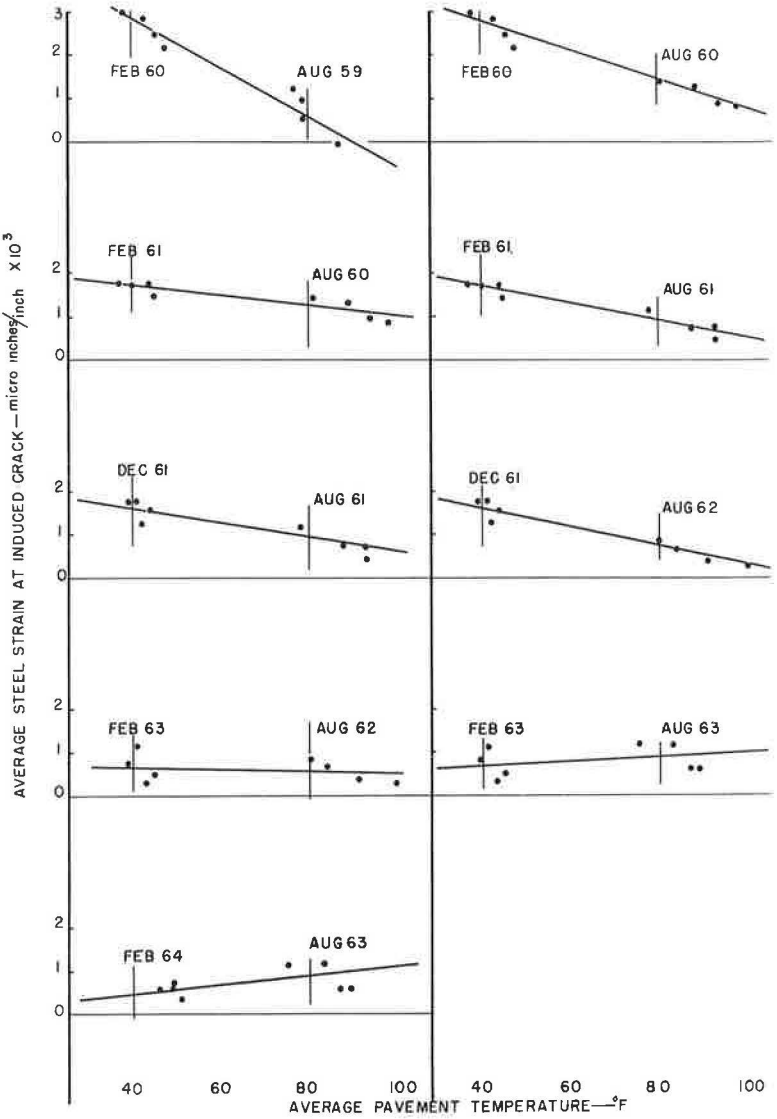

Figure 11. Steel strains at induced crack vs average pavement temperature, panel 1.

was not possible to eliminate the effects of the moisture in the pavement, these times were chosen so that any effects of moisture from one yearly cycle to the next would be approximately the same.

The data were plotted in two sets, from August to February, which will be called warm to cool trends, and from February to August, the cool to warm trends. From the fitted lines steel strain at the induced crack and induced crack opening values were read at slab temperature values of 40 and 80 F, thereby bringing the trend lines to a position where they may be studied for age and crack spacing effects at the same temperature values.

Four readings of induced crack opening or steel strain at the crack were taken over a daily cycle for each August or February. These values were then plotted against the pavement temperature at the time of each reading. One August and one February daily cycle, in each case, make up one trend line. For example, Figure 11 shows the steel

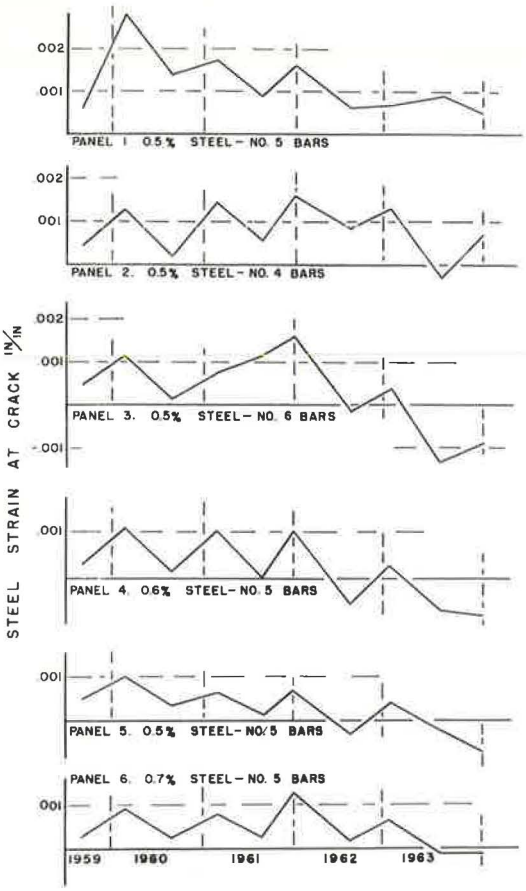

Figure 12. Seasonal variation in average steel strain at crack at 40 and 80 F.

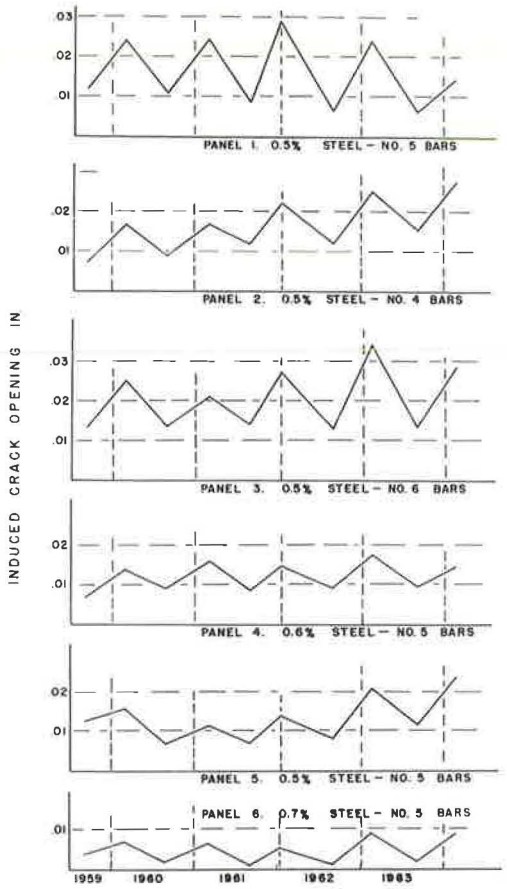

Figure 13. Seasonal variation in average crack opening at 40 and 80 F.

strains at the induced crack plotted as a function of average slab temperature for panel 1. The first plot is composed of August 1959 and February 1960 readings. The trend line is simply a straight line averaged through the eight daily cycle points. The 80 F value for August 1959 is 575 μ-in./in. The 40 F value for February 1960 is 2, 840 μ-in./in. The February 1960 readings and all succeeding readings (except February 1964) are used twice, once for a warm to cool trend and once for a cool to warm trend. In the next plot (February 1960 to August 1960) the 40 F value for February 1960 is 2, 750 μ-in./in. These two 40 F values were averaged to give one February 1960 reading of 2, 795 μ-in./in. The succeeding 40 and 80 F values are all averaged to yield one winter or summer value. This procedure was used for all panels.

Annual Cycles

The steel strain and crack opening values at 40 and 80 F are plotted against pavement age in Figures 12 and 13. The resulting steel strain and crack opening curves are saw-toothed with peaks and valleys at 40 and 80 F, respectively.

The steel in panel 1, Figure 12, was strained beyond the yield point during the first winter. Since then both the summer and winter steel strains at the crack have been decreasing. The difference in strains between the 40 and 80 F values from one February to August or August to February to the next is decreasing. The slightly downward slope of the August 1962 to February 1963 trend line and the upward slope of the February to August 1963 trend line are contrary to what might be expected.

During July 1963, a failure in the pavement at a reinforcement overlap approximately 27 ft south of the induced crack was repaired. There was noted extreme cracking with a hole in the pavement. This shattered area was approximately 1 ft wide and extended about 6 ft in toward the centerline from the shoulder edge of the southbound lane. The depth of the hole extended below the reinforcement so that both ends of the lap were plainly visible. A break of this sort could very well result in loss of continuity in the steel and its strain readings and account for the two odd trend lines. The beginning effects of the break may be noted in the February 1963 strain readings, since it appears that continuity was lost during the autumn of 1962. The strain of about 650 μ-in./in. shown in August 1962 and February 1963 is, most likely, the permanent set remaining in the unstressed steel at this time. This set is consistent with the amount of strain beyond the yield point observed during the 1959-1960 winter.

The break in the pavement of panel 1 did not appear to affect the crack openings as much as it did the steel strain. Its effects, however, may be seen on careful examination of Figure 13. The 40 F crack opening appeared to be on an upward trend until February 1963, at which time it dropped to a value equivalent to earlier values. The 80 F values seemed to be decreasing steadily until August 1963, when the value was equal to the previous summer reading and did not follow the foregoing trend.

Site 2 has no repaired places near the induced crack. The steel strains at the crack at 40 F in this panel remain essentially constant with strain differences, becoming steadily less as the age of the pavement increases (Fig. 12). The August 1963 and February 1964 values, however, show very marked decreases in strain. At this time, these decreases are unexplained; however, they may be the advanced effects of a break near the induced crack that is not yet visible on the surface. Both the 40 and the 80 F crack-opening values are increasing. The result is an upward trend with a slightly increasing seasonal difference in crack opening.

The steel strain in panel 3 is quite erratic, but, in general, is on a downward trend (Fig. 12). There have been two pavement repairs near the induced crack, as described previously. The patches are relatively small and no cracking has occurred in either patch. These breaks and the resulting loss of continuity may explain the upward slope of the February to August 1961 trend and the extreme plunge downward of the succeeding cool to warm trends.

Again, the break has had little effect on the opening of the induced crack (Fig. 13). The 40 F crack opening during the winter of 1960-1961 is much lower than previous and later readings. However, the 40 F crack opening and the crack opening seasonal difference are increasing, resulting in an upward trend.

The steel strains at the crack in panel 4 show a steady downward trend (Fig. 12). Site 4 has no repaired places or wide crack openings near the induced crack. There is, however, a natural crack 4 ft south of the induced crack. This crack occurred during the summer of 1959 and shows its presence in the readings of the two gages located 4 ft from the induced crack.

The crack openings for this panel are steadily increasing with a slightly increasing seasonal difference in the average opening (Fig. 13). The strains at the induced crack seem to be unaffected by the nearby crack.

Site 5 has two patches near the induced crack. These patches in the roadway of site 5 acted as an integral part of the continuously-reinforced pavement, in that transverse cracks have formed in them. The steel strains in panel 5 appear to be leveling off (Fig. 12). The low 40 and 80 F strains during the summer of 1962 and succeeding years may have been caused by the breaks in the pavement and the loss in initial tension. The crack opening values appear to be on an increasing trend with the crack opening seasonal difference increasing also (Fig. 13).

Panel 6, with 0.7 percent steel, is the best performing of the six panels. There are no repaired areas or evidence of breaks. The average crack spacing is quite close, yet the cracks are evenly spaced. The 40 F strains at the crack and the 80 F strains are both decreasing with age (Fig. 12). The seasonal difference in strains at the crack is decreasing also. The crack opening shows an upward trend (Fig. 13), with both 40 and 80 F crack-opening values increasing, but not by an excessive amount.

The steel compression strains and the increase in the crack openings are contrary to expectations. The compression strain readings may be due to creep under tensile stress of the adhesive used to fasten the SR-4 strain gages to the reinforcement. If this stress, which occurs during the summer, were removed, the gages could show compression, while the steel would actually be in tension.

Pavement age and accompanying influences have an effect on the steel strains at the induced crack. The annual cycles have continued but in general show a decreasing trend. This indicates that the longitudinal forces in the pavement are gradually decreasing from their high initial tension. The range, or difference between the summer and winter readings, is decreasing and the 40 F steel strain readings at the induced crack are also decreasing. This would indicate that the behavior of the pavement is becoming less dependent on stresses due to initial shrinkage and crack spacing and is controlled more by concrete moisture content and yearly temperature difference.

The 40 F crack openings in all the panels, except panel 1, are increasing, as indicated by the comparisons in Table 2.

Panels 4 and 6, with their greater amounts of reinforcing steel, are the best performing of the six panels. Panel 5 with 0.5 percent steel, though its crack openings are somewhat wider than those of the other two panels, also appears to be performing well.

As the pavement ages, a loss of bond between the steel and the concrete at the cracks would allow the same amount of deformation to occur in a greater length of steel and thereby resulting in smaller steel strains, while the crack opening remains essentially constant or increases.

STRAIN VARIATION ALONG REINFORCEMENT

In each panel, 24 gages are attached to the reinforcement. Eight of the gages measure the strain at the crack. The steel strains at 6, 12, 24, and 48 in. from the induced crack are measured by four gages at each distance from the crack (Fig. 2).

Figures 14 and 15 show stress variations along the reinforcement over typical daily cycles for summer and winter readings. The strain variation plots are similar in shape. In general, the strains at the induced crack in the daily cycle have maximum values at the early morning readings when pavement temperatures are at a minimum. At colder temperatures early in the pavement life, the entire pavement is in tension with sharp peak values of stress at the crack (Fig. 14a). This peak drops off within 6 to 12 in. from the crack, and stresses in the blocks of pavement between transverse cracks are relatively uniform. Later in the pavement life, the stresses are lower throughout (Fig. 14b), although the same pattern occurs through the daily cycle. The most probable cause of the reduced stresses is the larger number of cracks at the later age. At warmer periods in the daily cycle of temperatures, the peak stress at the crack is blunted, even though stresses in regions away from the crack are reduced very little. Summer temperatures cause stresses away from the crack to be greatly reduced from winter values, even to the extent of becoming compressive at high temperatures and later ages (Fig. 15). A slight tendency for peak stresses at the crack to occur is shown at low temperatures in each daily cycle. There were more irregularities in the data for the small readings in the summer.

The steel strains at the crack and at 6 in. from the crack are plotted in Figure 16. Values for the five winters of observation are shown, since the higher winter stresses are of greatest interest. Pavement temperature range for each date is stated. Despite a few obvious irregularities, these plots are indicative of behavior at the time of high stresses. These curves confirm the comments previously made in discussing the variations of steel strain at the crack with age. Strains at 6 in. from the crack do not, in general, show much change until the fourth or fifth winter, when decreasing values occur.

The pavement temperatures recorded during February 1964 were approximately 10 deg higher in all the panels than those recorded for previous winter readings. These relatively high winter temperatures when coupled with the high moisture content of the pavement, experienced during the winter, may explain the summer-like strain patterns for February 1964.

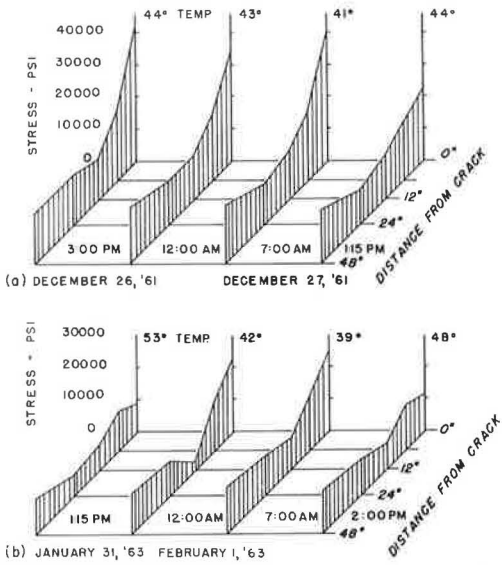

Figure 14. Stress variation along reinforcement over winter daily cycle, panel 6.

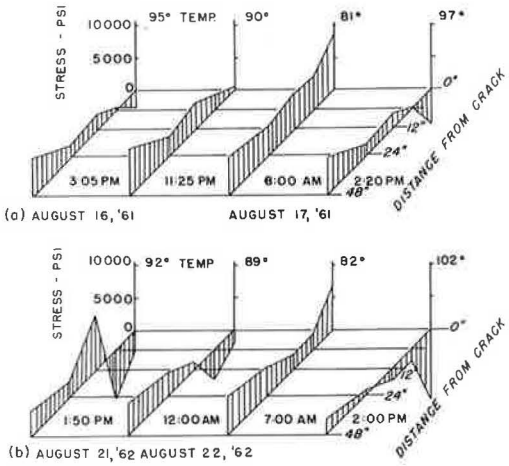

Figure 15. Stress variation along reinforcement over summer daily cycle, panel 6.

A study of the strains along the reinforcement during the winter readings will give some idea of the bond action at and away from the induced crack. During the early life of the pavement, the largest steel strain and consequently the largest stress takes place at the crack. The steel strains decrease for a short distance away from the crack because of the transfer of stress to the concrete by means of bond between the steel and the concrete. Beyond this distance of 6 to 12 in. the steel strains remain essentially constant.

The difference between stress at the crack and stress 6 in. from the crack, times bar area is the difference in force at these sections. Dividing by the surface area of bar in this length gives the average bond stress. Using the greatest strain differences from Figure 16, the highest observed bond stresses are 970 psi in panel 3, Dec. 1961; 860 psi in panel 1, Feb. 1960; around 500 psi in panels 2, 4, and 6; and 390 in panel 5.

Concrete creep may be responsible for the seemingly odd, yet relatively consistent, strain readings along the reinforcement. Some summer readings show a very small

TABLE 2

STEEL STRAINS AT INDUCED CRACK AT 40 F
DURING 5 CONSECUTIVE WINTERS

Panel No.	Strains (μ-in./in.)				
	1959-1960	1960-1961	1961-1962[a]	1962-1963	1963-1964
1	2, 795	1, 700	1, 600	668	470
2	1, 300	1, 450	1, 600	1, 338	750
3	1, 168	720	1, 625	400	-880
4	1, 200	1, 138	1, 010	310	-880
5	1, 005	695	710	425	-750
6	970	800	1, 300	665	-100

[a]The readings taken for the winter of 1961-1962 were consistently high for all panels, possibly due, in part, to having been taken not in February but in December.

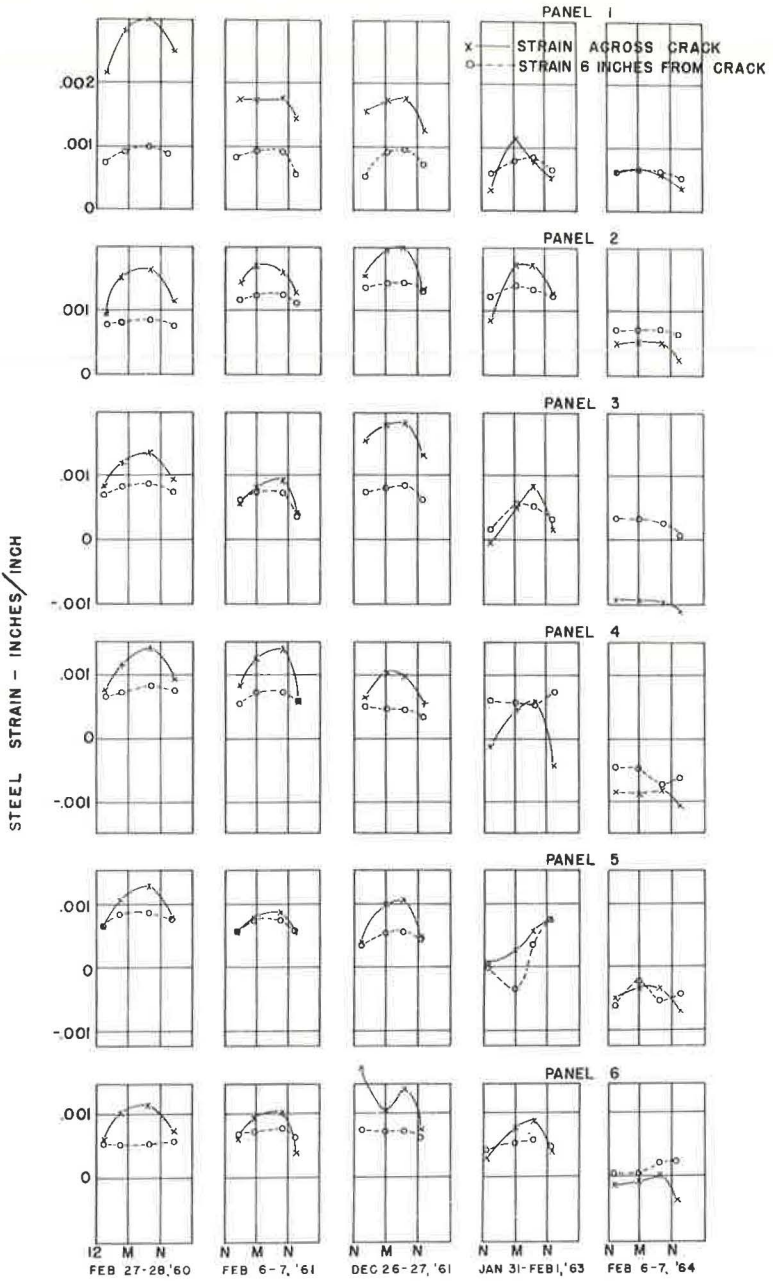

Figure 16. Steel strains at crack and at 6 in. from crack.

tensile strain or a compressive strain at the crack, whereas farther away from the crack the gages show a relatively high tensile strain. A possible explanation of this phenomenon is as follows.

During the winter months, the reinforcing steel and the concrete are subjected to high tensile stresses and would be deformed as shown in Figure 17. The stress values would vary over the daily cycle; however, all the stresses would be tensile. A core of concrete around the reinforcing bar would be subjected to relatively high tensile stresses, whereas farther away from the bar these stresses would be small. Creep in concrete

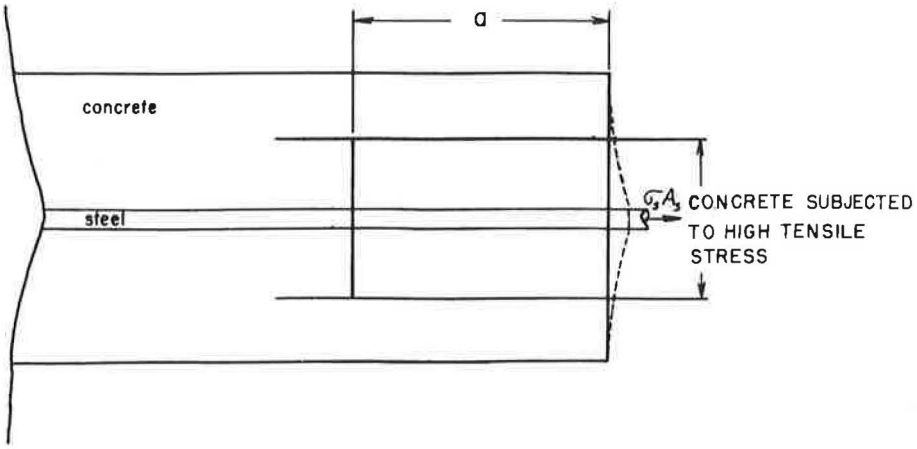

Figure 17. Deformed section.

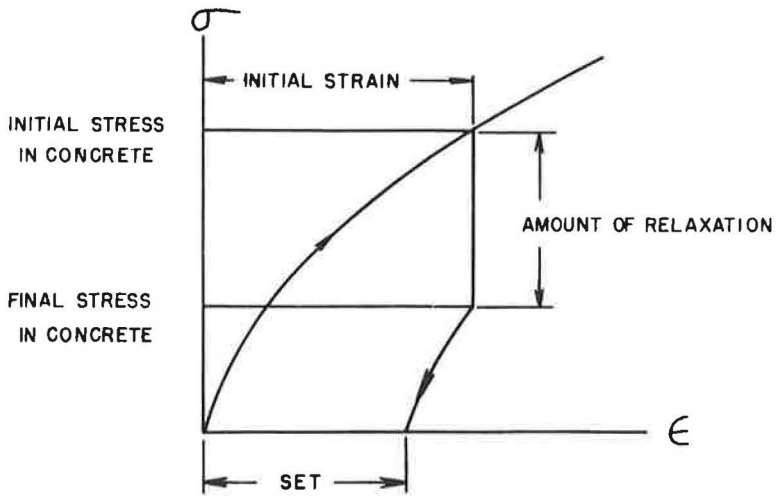

Figure 18. Relaxation of concrete stress.

is a relatively rapid phenomenon, in that approximately one-fourth to three-fourths of the ultimate creep under a load may be expected to take place within 1 to 6 months (2).

During the winter period, creep of the highly strained concrete around the reinforcement would occur, resulting in a permanent set with a corresponding relaxation of stress (Fig. 18).

As the temperature of the pavement increases during the spring and summer, the tensile stresses at the crack would decrease. The creep of the concrete while in tension would cause the concrete to act as a restraining collar on the reinforcing bars. Although the steel stress at the crack may be zero or compressive in nature, the concrete would hold the steel in tension at regions away from the crack. The process of creep would be reversed and the concrete would be in compression. The ultimate amount of creep for concrete in tension or compression is approximately the same. The rate of creep, however, is greater during the early stages if the concrete is in tension (1). If the concrete is considered to be subjected to high tensile stresses for three winter months of the year and to be subjected to relatively high compressive stresses during the three summer months of the year, it becomes evident that the tensile stresses caused by

initial shrinkage of the concrete will eventually be eliminated and the stresses within the pavement will be due to temperature and moisture change only.

SUMMARY AND CONCLUSIONS

The Maryland experimental sections of continuously-reinforced concrete highway pavement have been under observation for 4½ years. Several significant trends have been shown during this time and significant conclusions can be drawn.

The strain at the crack of the reinforcing steel and the opening of the transverse cracks vary inversely with the temperature of the pavement. The amount of steel contained within the continuously-reinforced section has a definite effect on the magnitude of the steel strains and the crack opening. The highest steel strains and the largest crack openings occurred in the sections of pavement containing the smallest amount (0.5 percent) of reinforcement. The size of the reinforcement (No. 4, 5, or 6) does not appear to have any significant effect on the steel strains, since the strains of all the sections containing 0.5 percent steel were quite high, regardless of bar size. The bar size, however, does seem to affect the width of the transverse crack opening. The section containing the smallest diameter bar experienced the smallest crack opening.

The uniformity of crack opening throughout the pavement is dependent on both percentage of reinforcement and reinforcing bar size. The crack openings throughout the central portion of the sections of continuously-reinforced pavement are more uniform in the sites containing 0.6 and 0.7 percent reinforcement. In sections containing the same amount of reinforcing steel, the crack opening throughout the central portion is most uniform in the section containing the smallest bar size, No. 4.

The spacing of transverse cracks affects the steel strains and the width of the crack opening. The smaller steel strains and smaller crack openings occur in the sites with the smaller average crack spacing. Average crack spacing is a function of the two controlled variables. It varies inversely with the percentage of reinforcement and directly with the bar size. The transverse cracks are more evenly distributed throughout the central portion of the pavement in the sections containing the higher percentages of steel. The size of the bar does not appear to affect the uniformity of crack spacing.

In all the sections of experimental pavement, certain trends occur as the age of the pavement increases. After the pavement has been exposed to an extended period of low temperature, the formation of new cracks is reduced quite drastically, and after a 4½-yr period, the formation of new cracks has virtually ceased. The widths of the crack openings increased and the maximum steel strain decreased as the pavement aged. The rate of increase or decrease is greater in sections with the smaller percentages of reinforcement.

The decrease in temperature from the elevated value associated with hydration of the cement and the drying shrinkage attendant on curing cause initial cracking and high initial tensile forces in the pavement. In a climate such as Maryland's, additional cracking and high stresses occur at times of low temperatures. After two or three winters, there is little additional cracking, and stresses are less than they were at earlier ages. Stresses continue to decrease after the crack spacing has become steady. This is evidence of creep in concrete reducing the initial tension. As the tension is lost, compressive stresses at times of warm temperatures may be expected to increase with age.

In general, sites 4 and 6, containing 0.6 and 0.7 percent reinforcement, respectively, are the best performing sections. The steel strains and crack openings of site 5, containing 0.5 percent steel of No. 5 bars, however, were not excessive. This may very well be due to the fact that these three sites were placed and cured under nearly ideal weather conditions.

The experimental aspects of this construction led to the formation of some wide cracks requiring repair early in the pavement life. The need for repairs within the central 500 ft of the sites has been influenced by percent reinforcement and bar size. Three of the four sites reinforced by 0.5 percent steel have undergone some sort of repair work. Of these four sites only site 2, reinforced by No. 4 bars, has experienced no repairs within the central 500 ft of the section. Sites 4 and 6 containing 0.6 and 0.7

percent steel, respectively, have had no areas within the central 500 ft requiring repair. The data for sites 2, 4 and 6 thus indicate behavior of pavement in which continuity has been maintained. The loss in continuity in panels 1, 3 and 5 resulted in loss of the initial tension. Continuity was restored by the repairs, however, and daily and annual cyclic stress fluctuations resumed, but over a different range of stresses.

ACKNOWLEDGMENTS

The Maryland continuously-reinforced concrete pavement investigation is under the direction of Allan Lee, Chief, Bureau of Research, Maryland State Roads Commission. The Chairman of the State Roads Commission is John B. Funk. The investigation is being conducted in cooperation with the U. S. Bureau of Public Roads.

The portions of the investigation concerned with the field measurements of strains are being conducted as part of the work of the Civil Engineering Department of the University of Maryland. An advisory committee for this portion of the investigation consists of the following members: Allan Lee; Harry D. Cashell, Structural Research Division, Bureau of Public Roads; Joseph W. Burdell, Jr., Regional Research Engineer, Region 2, Bureau of Public Roads; Harry L. Hill, Engineering Coordinator, Bureau of Public Roads, Baltimore, Md.; C. T. G. Looney, Head, Civil Engineering Department, University of Maryland; and the authors. The generous cooperation and many thoughtful suggestions and ideas advanced by all who are associated with the project are gratefully acknowledged.

REFERENCES

1. Davis, R. E., Davis, H. E., and Brown, E. H. Plastic Flow and Volume Changes of Concrete. Proc., ASTM, Vol. 37, Pt. 2, p. 317, 1937.
2. Fluck, P. G., and Washa, G. W. Creep of Plain and Reinforced Concrete. Proc., ACI, Vol. 54, p. 882, April 1958.
3. Lee, Allan. Maryland Continuously-Reinforced Concrete Test Pavement. Highway Research Board Proc., Vol. 40, pp. 235-257, 1961.
4. Lee, Allan. Maryland's Two Continuously-Reinforced Concrete Pavements—A Progress Report. Highway Research Record No. 5, pp. 99-119, 1963.
5. Lepper, Henry A., Jr., and Garber, D. L., Jr. Maryland Investigation of Continuously-Reinforced Concrete Pavement. Univ. of Maryland, Sept. 1961.
6. Schiffman, Robert L. Research in Continuously-Reinforced Concrete Pavements. Lehigh Univ. Fritz Lab. Rept. 256.1, July 1957.
7. Shank, J. R. Bond Creep and Shrinkage Effects in Reinforced Concrete. Proc., ACI, Vol. 35, Nov. 1938.
8. Walker, Stanton, Bloem, D. L., and Mullen, W. G. Effects of Temperature Change on Concrete as Influenced by Aggregates. Proc., ACI, Vol. 48, p. 661, April 1952.
9. Saemann, J. C., and Washa, G. W. Variation of Mortar and Concrete Properties with Temperature. Jour., ACI, Vol. 54, p. 385, Nov. 1957.
10. Spencer, R. W. Measurement of the Moisture Content of Concrete. Jour., ACI, Vol. 34, p. 45, Sept., Oct. 1937.

Preliminary Report on Continuously-Reinforced Concrete Pavement in Oregon

F. D. MORGAN, Construction Engineer, Oregon State Highway Department

The experience in Oregon with continuously-reinforced pavements has been rather encouraging, based on present evidence. Of the two pavements of this type constructed during 1962-1963, one has not been subjected to traffic and the other has been open to traffic for only 3 mo at the time of writing.

The design used is probably rather conservative. Two pavement failures have occurred in the major project, but they are apparently unrelated to the type of pavement. There are no further signs of distress.

Although these pavements have been somewhat more expensive on the basis of first costs, the knowledge gained in Oregon is as yet insufficient to warrant any conclusions about the long-term economics of this type of pavement as compared to conventional types.

•THE OREGON State Highway Commission has observed with considerable interest the research by other highway departments on continuously-reinforced concrete pavements.

Oregon has 438 mi (based on 1 mi-24 ft wide) of portland cement concrete pavement in use at the present time and approximately 9 mi scheduled or under construction. Present specifications for standard reinforced concrete are based on wire mesh reinforcement of 0.1 percent of the cross-sectional area, sawed joints at 61½ ft spacing and 1- by 18-in. load transfer dowels spaced at 12-in. centers. Although this concrete is giving good service, it was felt that ever-increasing demands on our pavements would definitely increase maintenance cost, and heavier traffic would increase the difficulty of maintenance work.

For these reasons, Oregon considered it prudent to construct two continuously-reinforced pavements to compare them with the state's standard reinforced concrete. Considering the amount of experimental work done by other departments in recent years, Oregon's continuously-reinforced concrete pavements can hardly be termed experimental projects except in the sense that they permit evaluation of continuously-reinforced concrete against standard reinforced concrete under typical conditions in Oregon.

With this criterion in mind, two projects were planned, both part of Interstate 5. The first project was in the southwesterly portion of the state near Medford; the second was in the Portland metropolitan area.

CLIMATIC AND PHYSICAL CONDITIONS

The Medford project (Fig. 1) is 9.45 mi of four-lane divided highway running southward from the city of Medford. It contains four sections of continuous portland cement concrete pavement with lengths of 6,309.82 ft, 21,064.63 ft, 3,058.42 ft and 19,461.95 ft. The sections are separated by structures.

The climate of the Medford area is essentially continental. The maximum temperature range is approximately 0 to 110 F and the daily minimum-maximum temperature range is 36 to 65 F with an annual mean temperature of 54 F. The average rainfall is 19.7 in. The ADT at this time is 7,600 near Medford, decreasing to 5,900 at the south

Paper sponsored by Committee on Rigid Pavement Design.

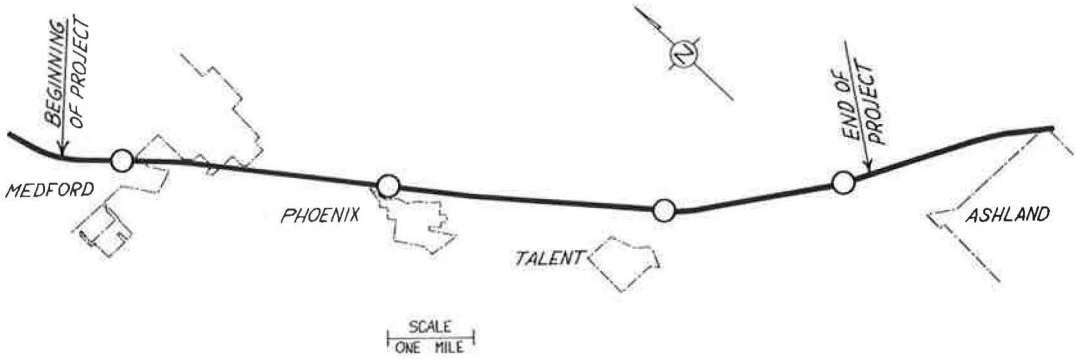

Figure 1. Medford test section.

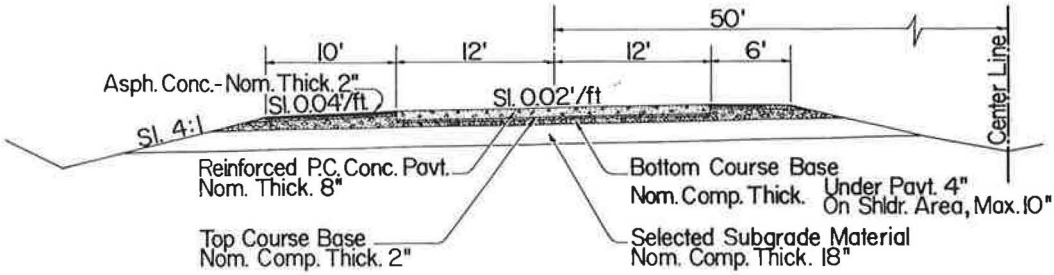

Figure 2. Half-section of test pavement, showing shed roof.

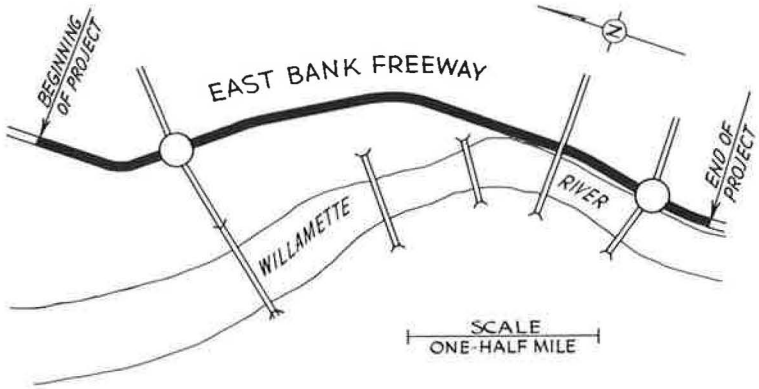

Figure 3. Portland test section.

end of the project near Ashland. The soils were a clayey silt containing 30 to 45 percent small gravels, overlying sandstone, conglomerate and some shales. On projects with large amounts of suitable materials (i.e., rock), an 18-in. lift of selected subgrade material was incorporated into the base design, allowing a reduction in the amount of crushed base rock under conventional pavements, both portland cement concrete and asphaltic-concrete. The selected subgrade was the sandstone and conglomerate from the excavations. This would allow a reduction in crushed rock thickness

to 6 in. under a standard reinforced portland cement concrete pavement; this thickness was retained under the pavement. Figure 2 shows the standard shed roof separated design used in Oregon. The crushed rock under the portland cement concrete is composed of 5 in. of 1½ in.-0 with a 1-in. leveling course of ¾ in.-0 crushed gravel.

The Portland project (Fig. 3), located in the northwesterly portion of the state, has an essentially marine climate. The maximum temperature range is approximately 19 to 97 F and the daily minimum-maximum temperature range is 47 to 62 F with an annual mean temperature of approximately 54.5 F. The annual rainfall averages 42.4 in.

Whereas the Medford project is essentially rural, the Portland project is metropolitan. The estimated ADT varies from 70, 000 with 3 percent heavy vehicles at the north end of the project to 55, 000 with 4 percent heavy vehicles at the south end. This project contains five sections of pavements and varies from 8 lanes to 4 lanes. Construction features are not discussed in this paper.

The two projects cover the relative extremes of conditions existing in Oregon. Both projects have standard reinforced concrete of essentially the same age, traffic, and material sources immediately adjacent.

CONSTRUCTION FEATURES OF MEDFORD PROJECT

Grading and Materials

The Medford project was divided into two contracts, grading and structures being let in the spring of 1961 and paving and signing in the spring of 1962.

The grading project followed standard practice for this region which requires considerable care in handling foundations and subdrainage. Extensive use of foundation excavation was required to remove pockets or small basins of organic and clay deposits caused by irregular formations of the underlying sandstone and conglomerate. Heavy irrigation on adjacent high ground required the use of cutoff ditches and subdrains. Most of these drains carry good flows of water during the summer irrigation season but are dry during the winter months. Of the 1, 900, 000 cu yd of embankment, approximately 1, 000, 000 yd was sandstone and conglomerate. Considerable effort was made to insure densely compacted embankments and AASHO compaction testing method T99 was used wherever practicable. In the embankments composed of solid rock, lift thickness was kept to an absolute minimum and was well worked by a spreadcat and grid roller.

The paving contract was awarded in May 1962, with an early completion date (fall 1962) required on the northern mile of the project.

Both base rock and concrete aggregates came from the same sources as that used in the standard reinforced portland cement concrete pavement to the north, and the same aggregates are now being used on an adjoining standard reinforced portland cement concrete project to the south. This source is an alluvial deposit in the Rogue River Valley. The parent material derives from young volcanic flows from the north and east containing primarily andesite, basalt and rhyolite; however, this material is adulterated by the Bear Creek drainage from the south and west which contains large quantities of sandstone and quartz diorites. The high feldspar content of the quartz diorite has an important effect on concrete strength, which is discussed later.

Base rock was crushed in two sizes. The coarse crushed base was 1½ in.-0, the specifications for which required 20 to 40 percent retained on the ¾-in. screen and 35 to 50 percent passing the ¼-in. screen. A 5 percent oversize tolerance was allowed. The fine crushed base, or leveling course, was ¾ in.-0, the specifications for which required 20 to 40 percent retained on the ⅜-in. screen and 50 to 60 percent passing the ¼-in. screen. A 10 percent oversize tolerance was allowed on the ¾ in.-0.

In addition to gradation, both sizes of base rock were tested for liquid limit, plastic index and sand equivalent essentially according to AASHO testing methods T89, T91 and T176. The sand equivalent value of the basic pit material for base rock was required to be in excess of 35. Considerable washing was required to make the material pass this latter test, and as a result the finished product was delivered to the project with a water content of approximately 10 percent. This latter point is mentioned only because of the effect it had on the compaction of the rock.

When the rock was first placed on the road, it was too wet to work. Only very light processing and laying out could be completed. After approximately 24 hr the contractor found that a few hours of intensive pneumatic and vibratory rolling resulted in an extremely dense base, so well compacted that survey parties had to use a jackhammer to place grade hubs. Oregon requires that all base materials be compacted to 95 percent of maximum density as determined by the Collins Curve (Proctor), an Oregon laboratory test which determines the optimum maximum density in pounds per cubic foot for uniformly graded crushed rock and, in addition, densities in pounds per cubic foot at the extremes of the specified gradation tolerances. The contractor had no difficulty achieving this compaction. At least part of the final smoothness of the completed project can be attributed to this high degree of compaction, since the forms which carried the paving machinery showed no discernible deflection when the equipment passed over them.

Pavement Design

The design of the continuously-reinforced pavement called for a uniform depth of 8 in. and a width of 24 ft. These dimensions are identical to those of conventional portland cement concrete pavements in Oregon. The depth deficiency tolerance was $\frac{1}{8}$ in. without reduction in payment. Subsequent core drilling revealed no portion of the pavement exceeding this tolerance. The design had settled on 0.6 percent longitudinal reinforcing steel, based on cross-sectional area of slab and allowing the contractor the choice between welded wire fabric and bar mats. In this case, the latter was elected. The bar mats used were welded, 12 ft long, and covered one lane (12 ft) width. The governing specifications were AASHO M54. The two mats reinforcing the width of paving were placed with a 2-ft stagger. The longitudinal reinforcement consisted of deformed No. 5 bars at $6\frac{1}{2}$-in. spacing, with a specified overlap of 25 diameters and a $\frac{1}{2}$-in. tolerance. Extra dowels were added at construction joints. The bars were of a hard grade, billet steel with a required yield strength for the longitudinal bars of 60,000 psi and an ultimate strength of 90,000 psi in conformance with AASHO M185 (ASTM A 432). Further details are shown in Figures 4 and 5. Air-entraining cement conforming to the requirements of AASHO M134-60 was used.

The concrete aggregates were produced in three designated sizes: $1\frac{1}{2}$ in.-$\frac{3}{4}$ in. $\frac{3}{4}$ in.-No. 4 and No. 4-0 (sand), the gradation requirements for which were as follows:

1. $1\frac{1}{2}$ In.-$\frac{3}{4}$ In. Aggregate: 2 in.-$1\frac{1}{2}$ in., 0-10 percent; $1\frac{1}{2}$ in.-0, 25-50 percent; $\frac{3}{4}$ in.-0, 0-15 percent.
2. $\frac{3}{4}$ In.-No. 4 Aggregate: 1 in.-$\frac{3}{4}$ in., 0-10 percent; $\frac{3}{4}$ in.-$\frac{3}{8}$ in., 45-65 percent; No. 4-0, 0-5 percent.
3. Sand, Percent Retained: $\frac{3}{8}$ in., 0 percent; No. 4, 0-10 percent; No. 16, 25-55 percent; No. 30, 50-75 percent, No. 50, 70-95 percent; No. 100, 95-100 percent.

A typical design mix of 6.5 sacks of cement per cubic yard contained per $2\frac{1}{2}$-cu yd batch 2,780 lb of $1\frac{1}{2}$ in.-$\frac{3}{4}$ in. material, 2,750 lb of $\frac{3}{4}$ in.-No. 4 material and 2,750 lb of sand. The specified 28-day compressive strength of the concrete was 3,300 psi.

Two-lift construction was specified, with 5- and 3-in. lift depths for the first and second lifts, respectively, to achieve the specified 3-in. steel depth. The specifications emphasized the importance of a minimum time interval between the placing of the two courses. The merits of this method of paving are discussed later.

The ends of the continuously-reinforced slabs were constrained through the use of four lug-type terminal anchors, 4 ft deep by 2 ft wide, extending the width of the pavement. Except at the southern end of the project the continuously-reinforced slabs terminated at bridges. Between the anchored slab end and the bridge were inserted five 40-ft end panels, separated by $\frac{3}{4}$-in. expansion joints of the asphalt mastic filler type, and, adjoining the structure, a 12-in. deep, 20-ft long, heavily reinforced impact panel which is the present design standard for all portland cement concrete pavements of the state. Further details are shown in Figures 6 and 7. The adequacy or conservatism of the terminal features is discussed later, together with two experimental departures from this design.

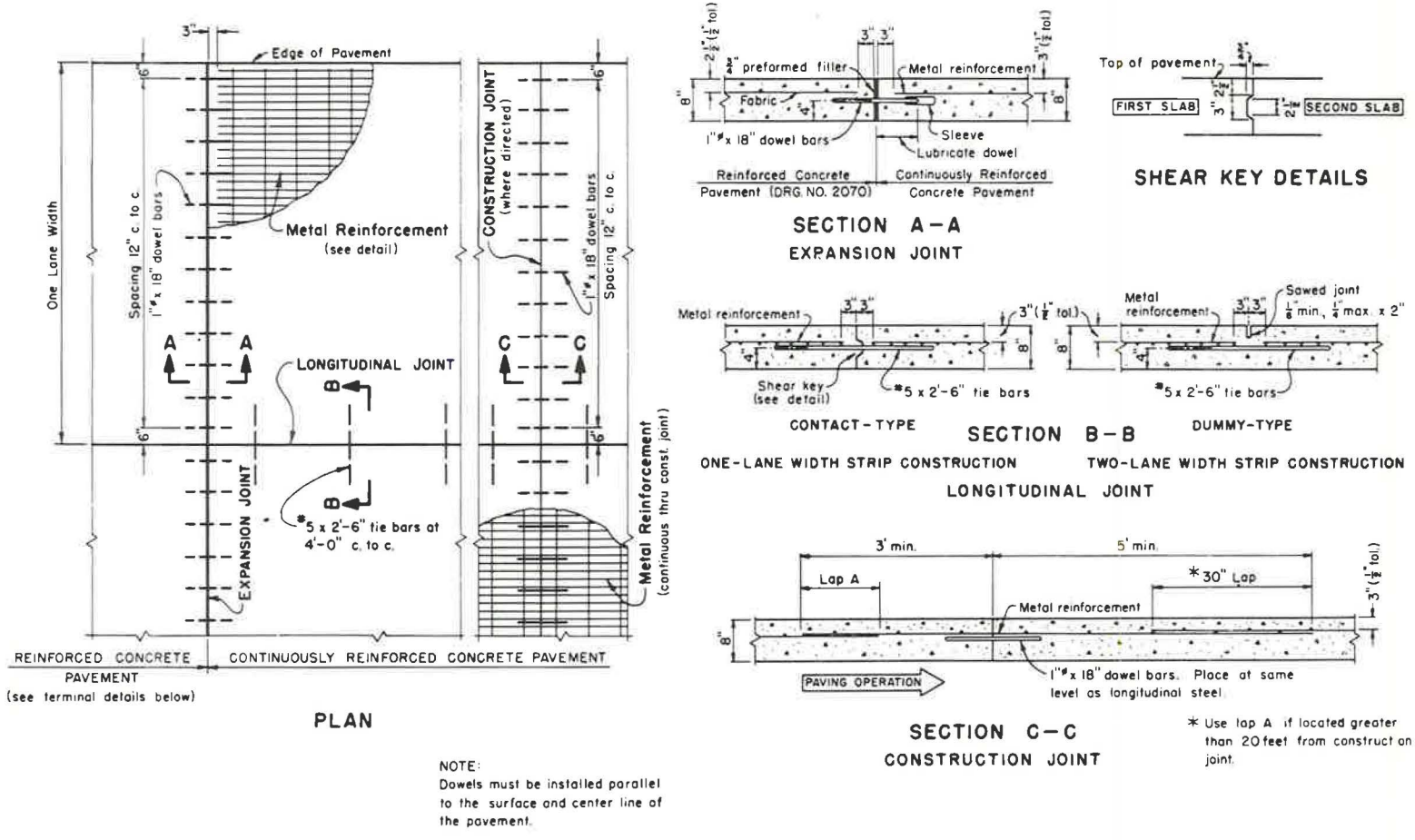

Figure 4. Continuously-reinforced concrete pavement: plan; expansion, longitudinal, and construction joints; and shear key details.

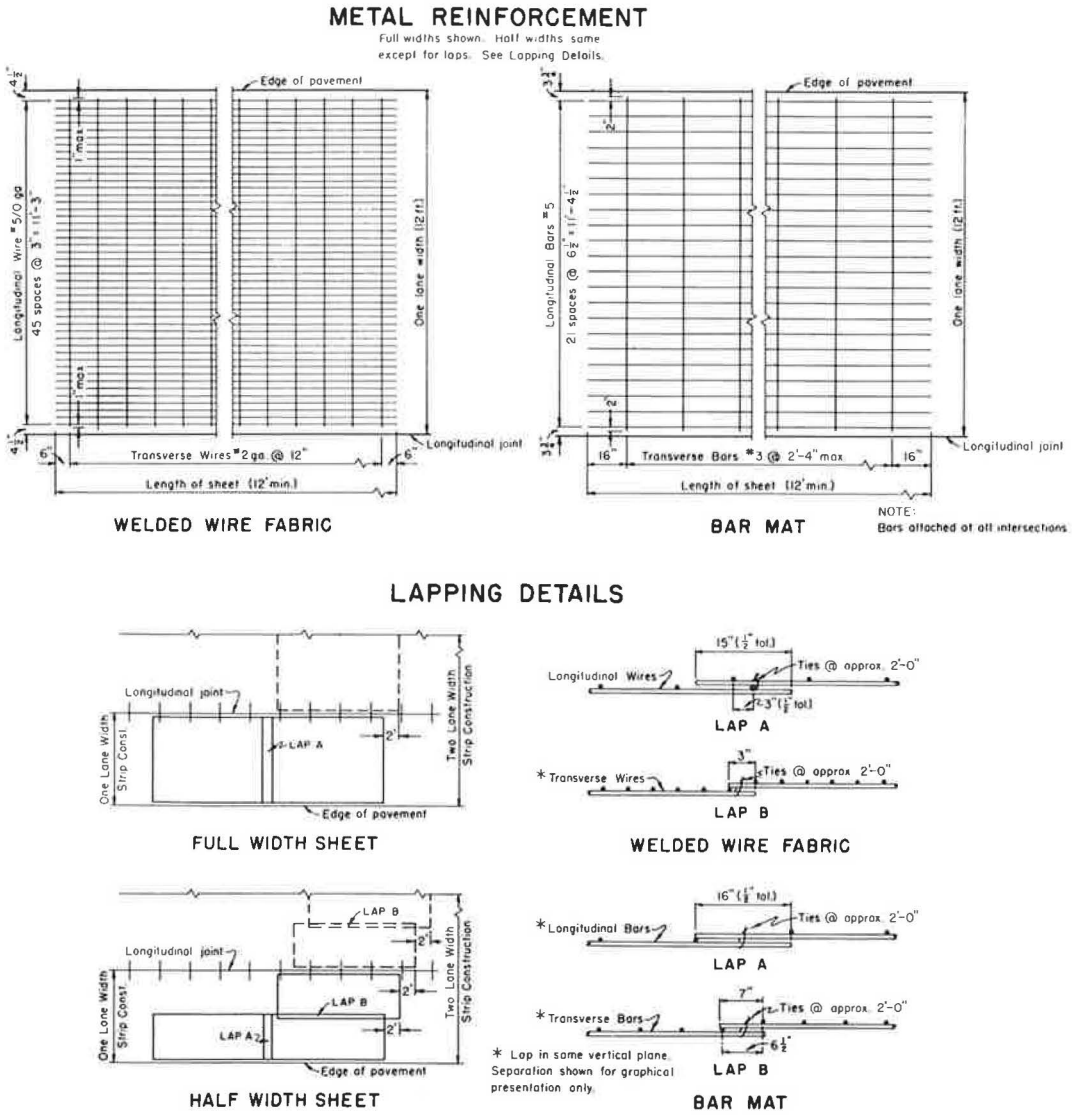

Figure 5. Continuously-reinforced pavement: metal reinforcement lapping details.

Pavement Construction

The paving contractor used 9-in. headers, placed directly on top of 1½ in.-0 crushed rock. One in. of ¾ in.-0 was placed between the headers, giving the 8-in. depth required. A Lewis subgrader was used to fine grade between the forms. It was decided to experiment with a central batch plant and 7½-cu yd tilting Cook-Challenger mobile mixers, each taking three of the 2½-cu yd batches turned out by the plant. All previous portland cement concrete paving in this area had been done with dual-drum Koering mixers. The cement and the mobile mixers were to provide unexpected results as is subsequently shown. The mobile mixers dumped the base lift directly between the headers and the concrete was struck off at approximately 5½ in. of depth by a Blaw-Knox spreader. The concrete slump normally ranged from 1½ in. to 2½ in. A revolving wheel attached to the rear of this machine automatically placed the 30-in. No. 5 tie bars. The bar mats were manually placed immediately behind this operation. Every

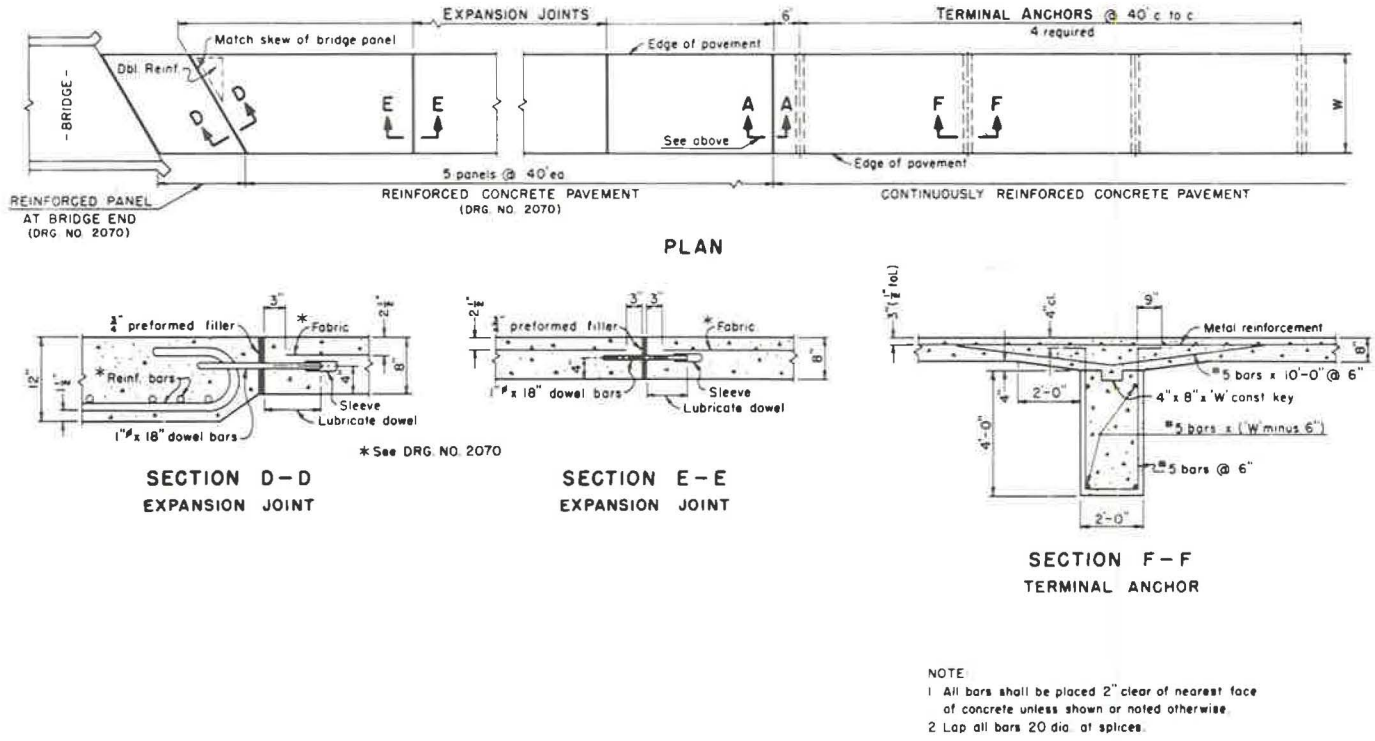

NOTE
1 All bars shall be placed 2" clear of nearest face of concrete unless shown or noted otherwise.
2 Lap all bars 20 dia. at splices.

Figure 6. Continuously-reinforced concrete pavement: details of terminal features.

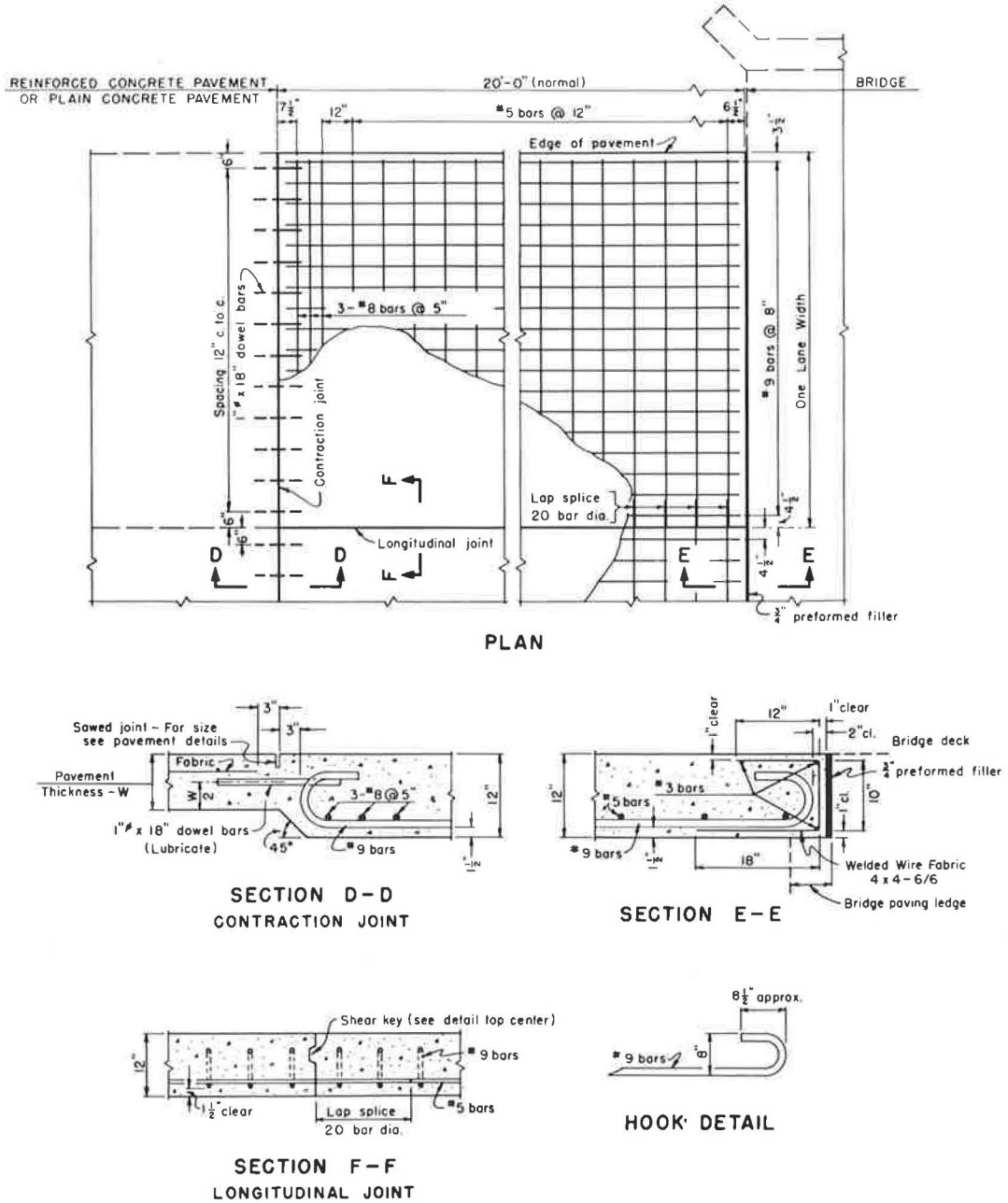

Figure 7. Continuously-reinforced concrete test pavement: reinforced panel at bridge end.

third longitudinal bar at the lap was tied. The concrete for the final lift was dumped from outside the forms onto a dual-belt distributor designed by Vickery and manufactured by Ko Cal. A second Blaw-Knox spreader, which was equipped with two pan vibrators and Dreyer electric vibrators near the forms, completed the placing operations. Every effort was made to keep the placing of the second lift of concrete within 10 or 15 min of the first lift.

Two finishing machines were used, one a Blaw-Knox double-transverse reciprocating screed finisher equipped with a spring-mounted tamping bar, and the other a hybrid,

25-ft wheelbased machine constructed from various pieces of equipment by the contractor. The latter machine was equipped with double-transverse reciprocating screeds centrally mounted, and towed an adaption of a Clary bridge finisher. A highly controversial spray of water was added at the Clary. However, this water contributed materially to the finishing and did no harm as long as the amount was controlled. Final working of the surface consisted of hand drawing a 40-ft, 4-in. diameter aluminum pipe diagonally over the surface, followed by a broom finish and Hunts process-curing compound. Longitudinal centerline sawing followed after the first 24 hr.

Paving started on September 13, 1962, at station 1101+37, northbound, and the operation proceeded from there to the northern end of the project, then reversed and went to the southern end where rains forced the contractor to terminate paving in November. The remainder of the project was paved in April and May 1963.

The northern mile of the project was opened to traffic in December 1962, and the remainder in July 1963.

Construction Features

As previously mentioned, the cement and mobile mixers caused some unexpected results. The aggregate on this project contained approximately 10 percent quartz diorite which in turn had a fairly high feldspar content. The aggregate source also contained a large amount of broken-down sandstone. On previous projects the sandstone particles had been a source of concern. On the Medford project it was decided to include a sand equivalent specification with a minimum value of 75 for the concrete sand. With the type of sand classifier the contractor used, the sandstone particles were almost entirely eliminated and the sand equivalent test ranged in the high eighties. Retesting 30 days later showed failing sand equivalent tests, with retest values ranging from 48 to 65. Rewashing the material again resulted in high sand equivalent; however, a gradual decline of sand equivalent values followed. Obviously, some portion of the sand was breaking down into 100 minus particles. It was decided to produce the sand as the concrete was being placed.

Everything was thought to be under control until the first 7-day compression break test results were received. To achieve the required 3,300 psi in 28 days, approximately 2,150 psi in 7 days would normally be expected. The first 7-day breaks ranged from 1,400 to 1,800 psi. After considering all possible factors it was decided that the cement being used had a much flatter time-strength curve than cement on the previous project, caused in part by the differing relative contents of dicalcium silicate and tricalcium silicate in the two brands of cement. However, the cement content was increased from 6.2 sk/cu yd to 6.8 sk/cu yd until such time as more conclusive information was available.

A second cause was also considered. If handled excessively, the aggregate was known to break down due to the effect of the feldspar in the quartz diorite. For this reason the contractor handled the material as little as possible. This had produced good concrete in the past, even without the specified sand equivalent test minimum of 75. The changed conditions, therefore, were the cement and the mixers. The cement, because of its chemical composition, indicated only that a little longer time was necessary to reach design strength. Therefore, the major difference was in the mixers. Although great care was taken in handling the aggregate, the wet concrete was mixed in the mobile mixers from 5 to 20 min at 6 to 10 rpm. In the past, using dual-drum mixers of the Koehring type, mixing time was 50 sec. Washing fresh concrete through sieve stacks confirmed our suspicions and showed an approximate 10 percent lower aggregate size throughout. The project was completed employing the same methods but using a mix of approximately 6.7 sk. Also, a minimum slump was maintained throughout.

A field experiment was conducted in an attempt to determine compressive strength vs mixing time. The optional mixing time indicated was approximately 15 min (Fig. 8). Only one small series of checks was made in this experiment and results should not be considered valid.

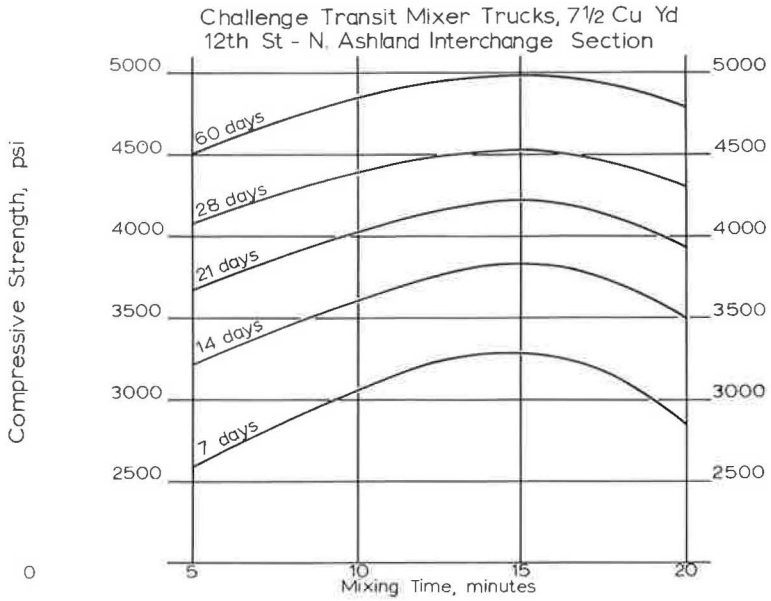

Figure 8. Compressive strength of portland cement concrete related to mixing time.

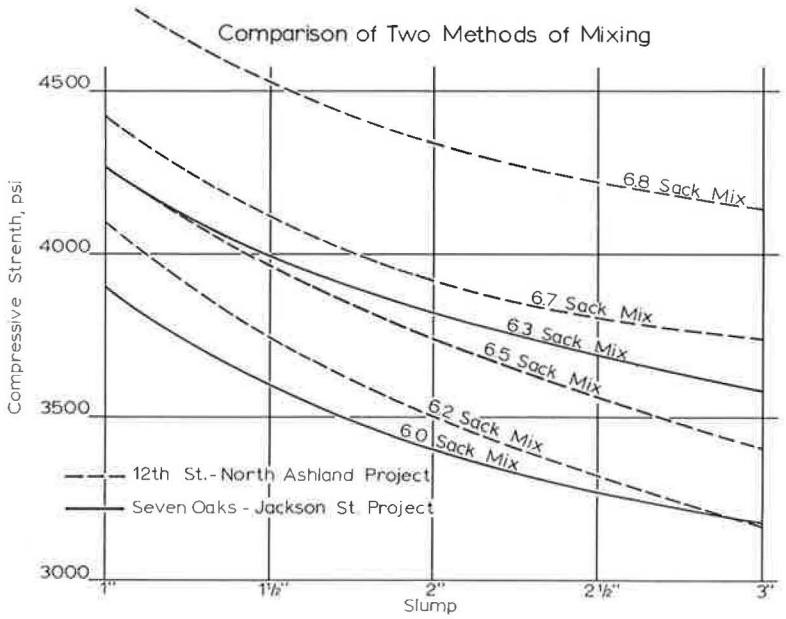

Figure 9. Portland cement concrete 28-day compressive strength vs slump.

To evaluate the mixers used on this project, all the 28-day break strengths were tabulated and analyzed statistically, and the same was done with those of another project in the area paved with Koehring dual-drum mixers and the identical aggregate source but with a lesser cement content. The Koehring mixers seemed to produce somewhat better results, but it must be remembered that a different cement was used (Fig. 9).

The experiences on this project with two-lift paving did not offer convincing evidence of its efficacy. Although the specifications stress that the second lift must be placed as quickly as possible after the first, and every practicable effort is made in this direction, delays longer than desirable will inevitably occur during construction, for a variety of reasons. Some drying out of the contact surface of the lower lift cannot be avoided in practice. Together with the lacking aggregate interlock across the contact surface, undue time lapses, high temperatures, and other factors will result in a weakened plane in the concrete and reduced bond strength. Furthermore, using low slump concrete to promote a number of desirable qualities in the concrete is not conducive to good coherence between the two courses. A substantial consolidation effort on the mix is imperative. Nevertheless, this type of pavement is expected to be particularly vulnerable to a deficient bond at longitudinal lap splices. The two early failures of the pavement give further evidence of the critical quality of bond strength for the design used. It is believed, for example, that single-lift construction with preplaced reinforcement tied in place on bar chairs would give better results than the methods used here, even though the chairs have their built-in difficulties. This would allow a continuous long stagger across the width of pavement instead of the single 2-ft stagger used here. A greater margin of safety would be afforded against the random inferior batch. It is also believed a full-size vibratory mat placement machine would give better results.

The Ko Cal distributor design by Vickery was not very favorably received by state engineers, as a considerable amount of aggregate separation was evident at the discharge end. However, after welding on a baffle plate opposite the discharge flow, the situation was improved materially.

It was decided to allow the steel supplier to weld the bar mats. Considerable difficulty was experienced with loss of ultimate strength at the weld where, after welding, ultimate strengths as low as 72, 000 psi were determined. Various welding procedures were used throughout the Medford project and part of the Portland project. However, steel rejections became so high on the Portland project that the contractor decided to complete it with tied mats. Based on this experience, it seems that high-amperage welding of the mats is not to be recommended.

TESTS AND OBSERVATIONS

As mentioned previously, this project was not considered an experimental one in the conventional sense, and the testing program was aimed more at comparison than research as such. The following tests and observations were made.

1. Air and concrete mix temperatures were continually taken during construction.
2. A crack survey was made on six 500-ft long portions of the pavement in March 1963 after the pavement had experienced one winter. Two of these sections were located in the interior, whereas the other four were at the ends of continuously-reinforced sections.
3. Data on slab end movements were collected by installing gage plugs across expansion joints together with transit reference monuments at the ends of the continuous pavement, three sets of the latter at project ends, and one set elsewhere. (Fig. 10.)
4. A measure of surface roughness was obtained with the California profilograph, a 25-ft wheelbase, rolling, recording straightedge.
5. A traffic count has been prepared, and one permanent traffic counter has been installed.
6. The pavement and the construction procedures have been given extensive photographic coverage.
7. Cores have been taken across several cracks.

EVALUATION

Cracking

The crack development on this project conformed largely to expectations based on previous experience of other states with continuously-reinforced pavements. Except

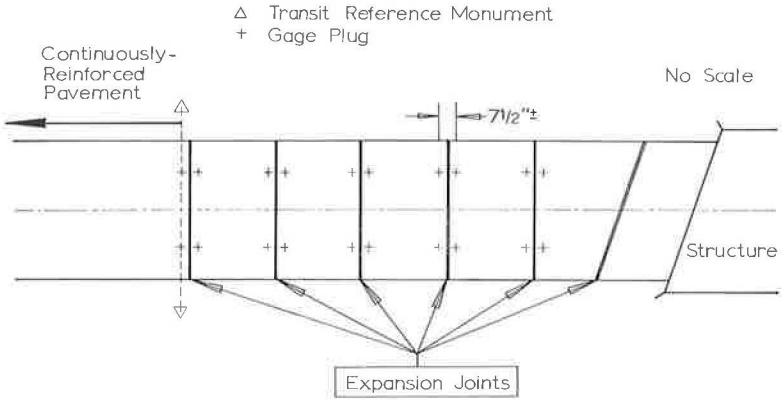

Figure 10. Typical layout of apparatus for recording slab-end movement.

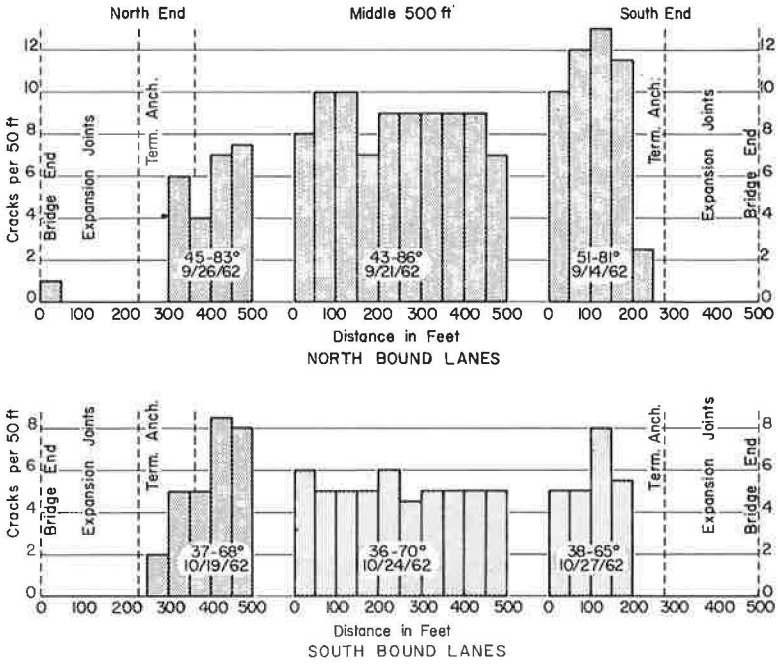

Figure 11. Cracks per foot vs pouring temperatures.

for the failures, all cracks seem tightly closed at present. The shrinkage cracks were so fine initially that only after a considerable amount of construction traffic did a majority of them become clearly visible.

The plotted cracks in the selected interior portions of the pavement showed a shorter average crack interval in the northbound lanes (5.7 ft), than in the southbound lanes, where the interval averaged 9.7 ft. This was expected since the northbound side was poured at a higher temperature than the southbound (Fig. 11).

At the time of writing (October 1963) there has been a slight increase in crack frequency since the time of plotting (March 1963). The increase has not favored any one side, however.

Riding Quality

The surface smoothness of this pavement has generally been recognized as very good. It is, to our knowledge, the smoothest pavement placed in one 24-ft width in the state. The California profilograph reading which was obtained in April 1963 showed an average of 3.6 in./mi. The southbound lanes were decidedly the smoother ones. In the future, new profilograph readings will be made to ascertain the permanence of the present high riding quality and to compare it to that of standard reinforced concrete pavements in the area. Two locations where there appears to be some slight local settlement will be watched.

End Movements

It is yet too early to tabulate all end movements since sufficient data have not been collected at the time of writing. However, the following conclusions can be drawn:

1. The maximum end movement observed till now is 0.29 in.
2. A slight growth of approximately 0.05 to 0.10 in. seems to have occurred in the length of the slabs.
3. Beyond the end panel nearest the continuously-reinforced pavement the only discernible movement has been the thermal expansion and contraction of each individual panel.
4. Two experimental departures were made from the terminal design. In one location all the end panels (except the impact panel) were eliminated, and in another one of the four terminal anchors was eliminated. Present measurements indicate no greater movements at any joint at these locations.

Failures

The first failure, occurring in the fall of 1962 within a short time after paving, started as a bond failure at a bar lap in one of the 12-ft lanes. The bond failure was apparently caused by local, excessive segregation of aggregates in the mix, possibly superimposed on a substandard mixer load. The bond in the other lane was adequate but the severe tensile stresses produced in the remainder of the steel by thermal contraction made it rupture in tension during a cold (0 F) night later in the winter. The resulting crack opened approximately $\frac{3}{8}$ in. After having been tentatively determined through core drilling and other investigation, the cause of the failure was verified when a 9-ft length of concrete was removed to be replaced. The repair, which took place in May 1963, involved the use of extra steel and high-strength concrete, and it appears completely successful.

The second failure differed from the first one in that it took place over a 210-ft long area, in the portion of the pavement placed in the spring of 1963. In this area, nearly all of the lap splices failed owing to lacking bond strength, which in turn was caused by inferior concrete resulting from a temporary malfunctioning of the automatic batch plant. Subsequent investigation showed extremely low cement contents and compressive strengths as low as 875 psi. The shortage of cement was not discovered at the time of paving because it happened at the beginning of the day's operation and was accompanied by an extreme stiffness of the mix. The first test cylinders of the day were taken 80 ft beyond the defective area. Owing to the length of the discontinuity in the slab, the curing shrinkage and thermal movements were distributed over a number of cracks, and, with increasingly warm weather, the result was that no single crack opened up conspicuously at first. In time, five of the cracks became progressively wider and raveled excessively under traffic. This, together with the coincidence of the cracks with lap splices, aroused suspicion. An extensive investigation followed and resulted in the decision to replace a 237-ft long portion of the pavement in which compressive strengths below 3, 300 psi had been found on cores taken from the pavement. For the repair, the typical reinforcement and standard mix concrete were used. The repair took place in October 1963, and at this time it appears successful.

Both repairs were made at the contractor's expense. The project was thoroughly checked in August 1963. No further signs of distress were found but several cracks

appearing larger than the rest and having a stagger at the centerline were plotted for future reference.

Cost Comparison

The continuously-reinforced concrete pavement on the Medford project cost $5.40 per sq yd, the standard reinforced concrete in the end panels cost $4.30 per sq yd, and the terminal anchors cost $264.00 each.

For the standard reinforced concrete project adjoining to the south, the cost was $4.50 per sq yd.

The continuously-reinforced concrete on the Portland project cost $6.50 per sq yd as compared to a standard mesh design price of $5.50 per sq yd in the area.

Although the initial cost of continuously-reinforced concrete is significantly higher than that of conventional pavements, the maintenance expenses will presumably be less. The long-term economics of this type of pavement cannot be predicted on the basis of the limited experience gained in Oregon.

Comments on Design

As mentioned previously, the elimination of one terminal anchor has not thus far led to any greater movements at the pavement end. There has been no evidence of slab end movements being transmitted beyond the first expansion joint, and at the pavement end where all end panels except the standard impact panel were eliminated there is no sign of undue strain on the remaining two joints.

These facts seem to indicate that the terminal design used is rather conservative, at least for the subgrade restraint conditions prevailing on the Medford project.

At this point it appears that the feature most vulnerable to defects in material and workmanship is in the area of the longitudinal bar lap.

CONCLUSIONS

As previously stated, the merits of continuously-reinforced concrete pavement in Oregon must await the test of time. It is believed the two locations chosen will provide satisfactory test sections.

ACKNOWLEDGMENTS

The author gratefully acknowledges the assistance of J. F. Putnam, Assistant Construction Engineer, G. W. Harra, Engineer of Materials, and Don Haller, Resident Engineer in the gathering of data and preparation of the report.

Friction Studies in Bonded Cement Concrete Pavement Slabs

V. VENKATASUBRAMANIAN, Civil Engineering Department, Indian Institute of Technology, Kharagpur (S. E. Rly.), India

A smooth base is desirable for a prestressed concrete pavement so that losses in prestress due to frictional restraint at the interface below can be reduced to minimum. In the case of non-prestressed rigid pavements, opinion is varied regarding the efficacy of a smooth base.

In Indian highway practice, where the stage construction method is common, the concrete slab is bonded to a well consolidated water-bound macadam base below. This bonding increases the effective thickness of the slab. Furthermore, the force of adhesion at the interface is extremely high and in the case of restrained contraction of the slab, the failure takes place well inside the base and the slab simply acts as a bonded surcharge initiating the deformations. In other words, the classical "drag" theory does not seem to be valid for bonded slabs.

•THE GENERALLY accepted "drag" theory based on simple laws of friction developed by Bradbury (1) assumes that the expansion or contraction of a cement concrete pavement due to the variation in its average temperature is resisted by the friction at the interface between the slab and the support below. A value of 1.5 to 2.0 is generally assumed (2) for this coefficient and the slab is supposed to slide freely over the support after failure.

A high friction base is undoubtedly undesirable for a prestressed concrete pavement, and the studies by Timms (3), and Stott (4) were primarily concerned with developing details of construction to reduce the interface friction. In the case of ordinary concrete pavements, plain or reinforced, the role of frictional restraint at the interface is not clearly understood. European highway engineers (5) have expressed doubts about the advocacy of a minimum friction coefficient. They are of opinion that a very high frictional value may serve to distribute stresses caused by expansion and contraction more evenly, and thereby reduce the incidence of cracking. The case histories reported by Walker (6), a British engineer who has had extensive experience in India with thin concrete road slabs bonded to a strong water-bound macadam base, have indicated the advantages of bonding the slab to the base.

BONDING OF SLABS TO BASE

Bonding of the slab to the base is a particular method of increasing the forces of resistance at the interface, and is in principle the same as the American concept (7) of providing terminal lugs or anchors to restrain the movements of the terminal areas in long pavements where the frictional resistance is not fully mobilized. These lugs are analogous to the key trenches used in the construction of rolled-filled earth dams. The success of these lug anchors in restraining the terminal movements greatly depends on the nature of the soil to which it is anchored, especially its shearing strength. While in the case of slabs with terminal lugs, the shearing resistance is highly mobilized in

Paper sponsored by Committee on Rigid Pavement Design.

the immediate neighborhood of the anchors, it is evenly spread throughout the bonded slab.

Stage construction is the common highway practice in India, and the concrete road slab is generally well bonded to a consolidated water-bound macadam base. This is done by thoroughly cleaning the macadam base with wire brushes and removing all the dust and the loose particles. The rugged face of the cleaned surface with small protrusions of the stones provides good bonding to the concrete. The thickness of the slab is much less than that of a slab designed by conventional methods. Their satisfactory performance is due to the bonding of the slab to the water-bound macadam base which is really a sort of prepacked mud concrete. Data presented by Childs (8) have confirmed the beneficial effects of bonding on wheel-load stresses. The Indian experience of bonding the slab to the macadam base has stood the test of time and is favored in Indian highway practice; however, there are practically no experimental data under controlled conditions to help understand rationally the interaction between the base and the bonded slab. This paper attempts to study the resistance offered by the different types of bases to the horizontal movement of the slabs.

GENERAL TEST PROCEDURE

The test procedure adopted was similar to that employed at the Arlington tests (9) in the United States.

CONSTRUCTION DATA

A masonry tank with inside dimensions 4.5 ft long, 2.5 ft wide and 1.0 ft deep was constructed in the basement of the Civil Engineering department where the air temperature variation was negligible. Within this tank, the different types of base courses were constructed and tested. The slabs were either 4 or 6 in. thick and their dimensions were 4- by 2-ft or 3- by 1-ft. The concrete was of 1:1½:3 mix and was hand-rodded and finished. No vibration was done to guard against mortar being forced into the base and thereby vitiating the results. A 4-ft high mass concrete bulkhead of dimensions 3- by 3-ft, constructed on either side of the test tank, and taken 1 ft below the concrete floor level, provided the necessary reactions for the mechanical jacks used in pushing the slabs.

DETAILS OF INSTRUMENTATION

A 3-ton hydraulic load cell, calibrated to 20 kg, was used to measure the total thrusting force. The horizontal movement of the slab was recorded on four dial gages (0.001 in.) set at each corner of the slab; the average of the four values was taken as the displacement of the slab. While testing the 1-ft wide slabs, only two dial gages were used, set at diagonally opposite corners. No attempt was made to measure the vertical displacement of the slab due to the dilatancy of the base, a common phenomenon reported in British tests (10). The dilatancy of the support below caused by the slab movements is not mentioned at all in American literature. The general setup of the test is shown in Figure 1.

The horizontal load was applied in increments corresponding to a displacement of 0.02 in. at a time till a total displacement of about 0.1 in. was reached. The load was then released in steps until completely removed, and was then applied from the opposite direction in a similar manner until 0.10 in. movement was recorded in the reverse direction. This cycle was repeated, and generally it did not exceed 5.

DETAILS OF TEST SLABS AND BASE SUPPORTS

Ten slabs were tested, using different base course conditions. In the first series, brown tar paper 0.006 in. thick was used as an insulating medium on the base before the slab was laid. It actually consisted of two thin papers with a fine layer of hard bitumen between them. Two slabs were laid in the open on the natural subgrade over the paper, the other three slabs were cast over the paper on prepared foundations in the tank mentioned earlier. In the second series, the five slabs were laid directly on the prepared bases inside the tank. The details of the slabs are as follows.

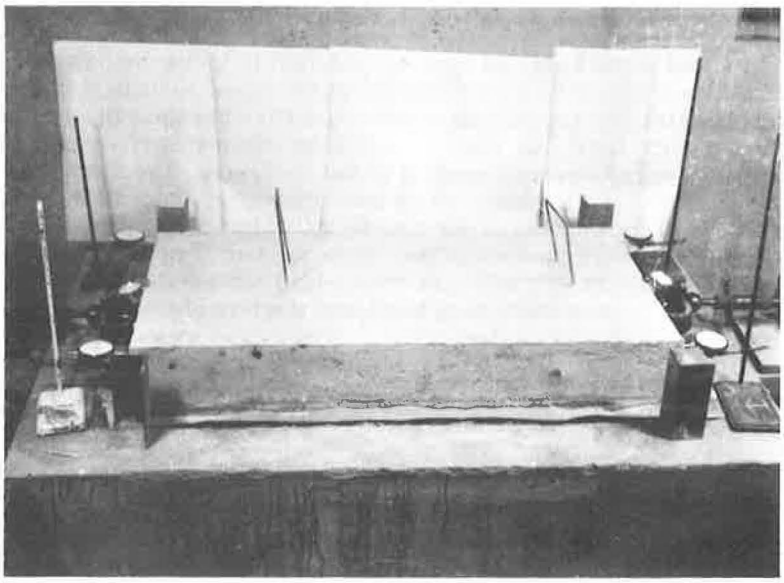

Figure 1. General setup of test to measure resistance of base to horizontal movement of slab, showing 4-ft by 2-ft by 6-in. slab on insulated paper over prepared soil base.

Series 1

1. Slab, 5 ft by 4 ft by 6 in., cast on the natural subgrade with top vegetation removed.
2. Slab, 5 ft by 4 ft by 4 in., cast on the natural subgrade with the top vegetation removed.
3. Slab, 4 ft by 2 ft by 6 in., on prepared soil subgrade.
4. Slab, 4 ft by 2 ft by 6 in., on prepared sand base.
5. Slab, 4 ft by 2 ft by 6 in., on water-bound macadam base.

Series 2

1. Slab, 3 ft by 1 ft by 6 in., on compacted damp sand base.
2. Slab, 4 ft by 2 ft by 4 in., on saturated water-bound macadam base.
3. Slab, 3 ft by 1 ft by 6 in., on saturated water-bound macadam base.
4. Slab, 4 ft by 2 ft by 6 in., on dry water-bound macadam base.
5. Slab, 3 ft by 1 ft by 6 in., on dry water-bound macadam base.

The two field slabs were originally laid for temperature measurement studies previously reported (11). The natural subgrade soil on which these were cast over insulation paper, is a fine silty sand with a classification of A-7-6. A similar procedure was adopted to push these field slabs.

Slab No. 3

The tank was filled with the subgrade soil borrowed from the site near slabs 1 and 2. The soil was compacted in two 6-in. layers at the optimum moisture content. Before casting the 4-ft by 2-ft by 6-in. slab, the insulation paper was spread on this smooth compacted soil.

Compacted Sand Base

Locally available river sand was compacted in layers to the full depth of the tank by tamping, followed by repeated flooding and draining. The surface was smoothed, and

the slab cast over the insulation paper, or directly on the sand base as in the case of slab No. 4 in series No. 1 and No. 6 in series No. 2, respectively.

Water-Bound Macadam Base

The tank was filled with a 2-in. layer of compacted sand, on which a 6-in. thick laterite stone subbase was constructed. The stones were handpacked in the usual manner with smaller pieces wedged in between the larger ones. On this a 4-in. thick water-bound macadam base was constructed using 1½-in. broken stones. Locally available disintegrated gravel, known as "moorum," was used as filler material. Hand-tamping by steel rammers was employed for consolidation. For the subsequent tests the laterite subbase was not disturbed; only the water-bound macadam layer was removed and relaid with fresh materials. The top of the macadam base was cleaned with wire brushes to remove the dust and loose particles before laying the slabs.

To saturate the macadam base in the case of slabs 7 and 8 24 hr after the slabs were cast, the base was flooded with about ½-in. standing water and this condition was maintained for 10 days, after which the slabs were tested. It was presumed that this procedure represented the worst condition that can be expected during the service behavior of the slab. Figure 2 shows the base of the bonded 3-ft by 1-ft by 6-in. slab subjected to flooding by ponding before the test.

To simulate the condition of the dry water-bound macadam base for slabs 9 and 10, apart from the water used in preparing the base and the concrete no extra water was added, and the condition of the base after 10 days of air curing was arbitrarily assumed to represent a reasonably dry condition. The moisture contents of the filler material in the bases varied from 5 to 7 percent immediately after the tests. In actual field conditions in tropical areas having heavy rainfall and high relative humidity, it is reasonable to expect that the base course will always be damp due to subgrade moisture movements.

PRESENTATION OF RESULTS

The relationships between the thrusting force applied in pounds per square foot and the horizontal displacement in inches for slabs laid on the insulation paper are shown in Figures 3 to 7. It is evident that during the first test, much greater force is necessary to produce a given displacement than during the subsequent cycles; and the thrust-displacement relationship becomes stable in about 6 cycles. Such a pattern of behavior appears true even in the case of macadam base when insulation paper is provided. The paper, which adheres to the slab tenaciously (Fig. 8), provides a smooth plane for the slab to slide over the base. However, the conditions appear different when the paper is not provided. The results of the tests without insulation are shown in Figures 9 through 13.

As in the previous cases, for the bonded slabs much larger force is necessary during the first test and the initial curve is parabolic. After about 2 cycles, the force displacement curves do not indicate much variation, and equilibrium conditions appear established. The continuous thrust-displacement curves for the complete cycles in the case of the slabs bonded to saturated macadam base are shown in Figures 14 and 15. After the initial peak curve, the upper right-hand portion and the lower left-hand portion of the subsequent cycles both give forces that do not vary markedly with displacement from each other; hence in the case of bonded slabs, the testing is limited to 5 cycles.

The 4-ft by 2-ft by 6-in. slab (slab No. 9) bonded to the dry macadam base was initially subjected to repeated tests with deformations not exceeding 0.005 in., before pushing it to failure. The results of these tests are shown in Figure 16. For small displacements the macadam base and the slab bonded to it behave as an elastic and composite structure.

After the tests were completed, the slabs were lifted from their beds, and their bottom surfaces examined. Figures 17 through 21 show the bottom surfaces of the bonded slabs after test. Tables 1 and 2 give the values of the coefficients of base resistance computed for the different base course conditions. When the insulating tar paper is provided, the coefficients are considerably lower and are within the generally

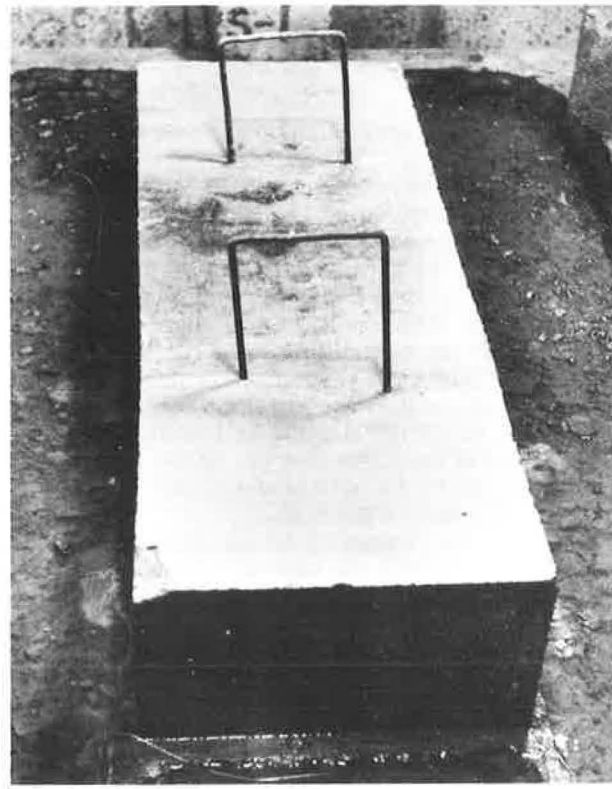

Figure 2. Slab 3 ft by 1 ft by 6 in. bonded to water-bound macadam base, before test, with base saturated by ponding.

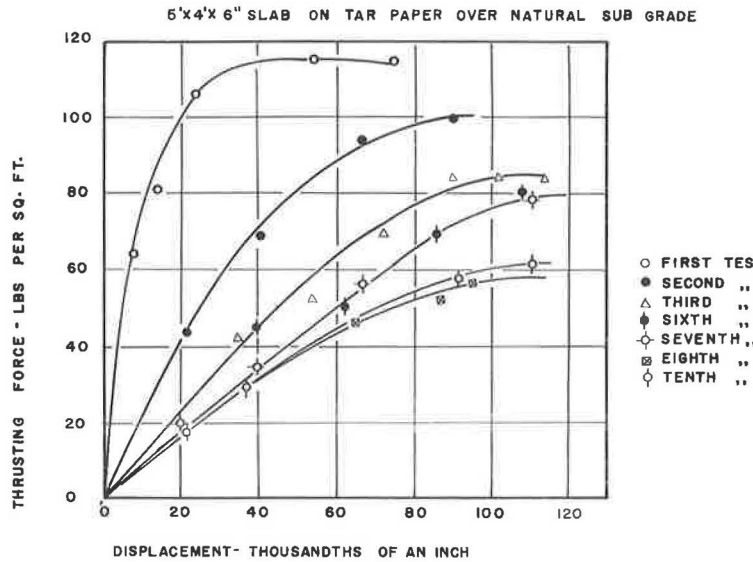

Figure 3. Force-displacement curves for repeated tests on 6-in. field slab.

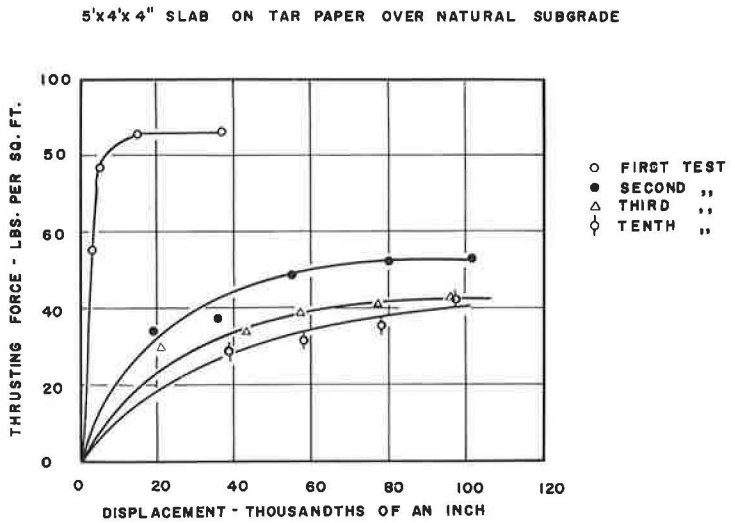

Figure 4. Force-displacement curves for repeated tests on 4-in. field slab.

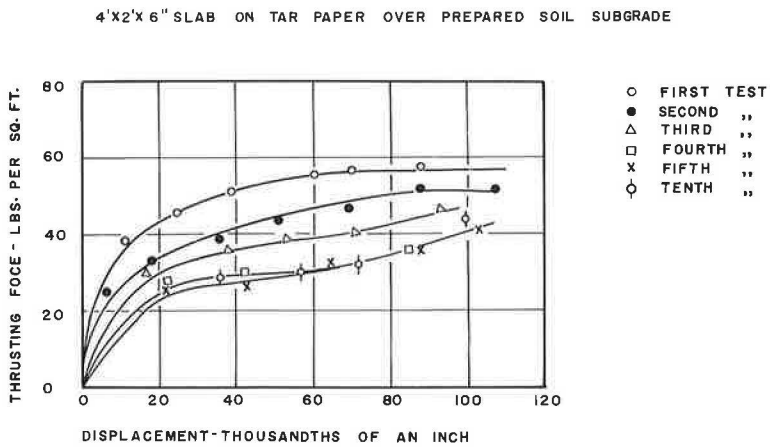

Figure 5. Force-displacement curves for repeated tests on 6-in. slab.

recommended values. In the case of slabs bonded to water-bound macadam bases, they are very much higher than the values reported by Kelly (12). Even after failure, when the slab with a portion of the base adhering to it moves over the remaining part of the base, the coefficient of resistance is greater than 1.5 for displacements larger than 0.06 in.

DISCUSSION

The data presented in this paper indicate that when the tar paper insulation is provided, the coefficients of base resistance are less than 2.0 for displacements less than 0.02 in. for the first cycle, and for the second and subsequent movements this value

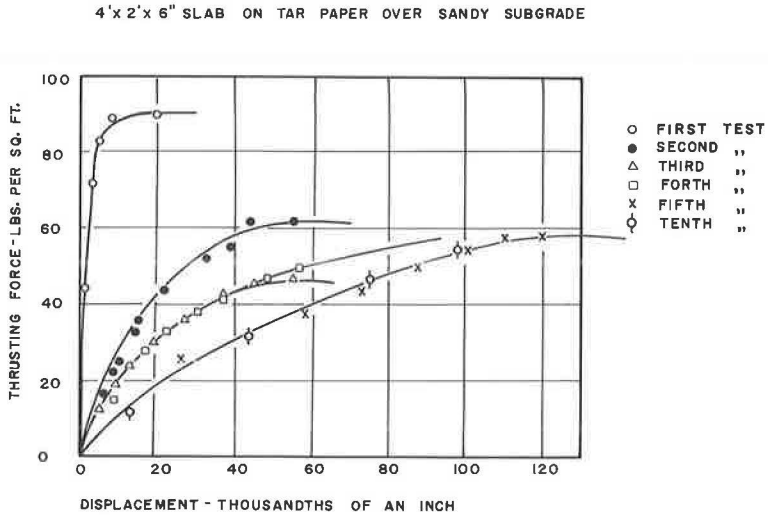

Figure 6. Force-displacement curves for repeated tests on 6-in. slab.

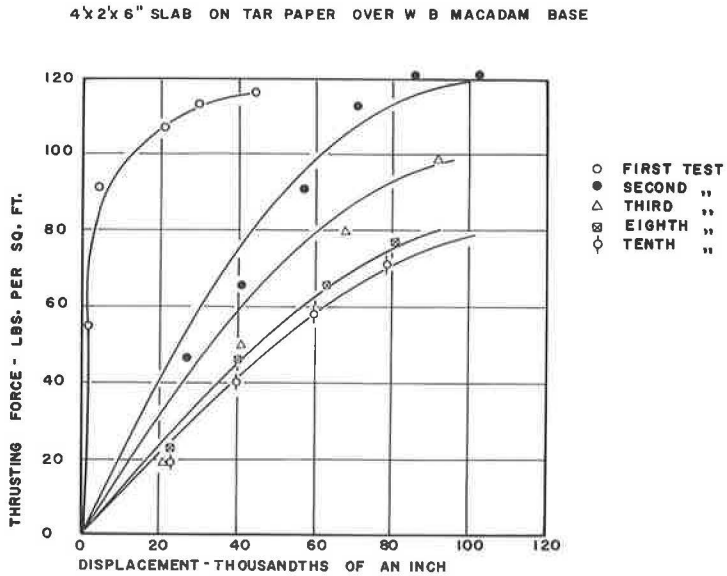

Figure 7. Force-displacement curves for repeated tests on 6-in. slab.

is further reduced and is generally less than 1.0. In the case of the slab in direct contact with the compacted damp sand base, the coefficient does not exceed 1.23 in the first test, and is less than 1.0 for subsequent displacements up to 0.06 in. The low value of the resistance may be because the locally available sand is poorly graded with subrounded particles and a fineness modulus of not more than 1.92.

In the case of bonded slabs on saturated water-bound macadam bases, for 0.05-in. displacements, the coefficients of base resistance are of the order 6.9 and 4.5 for the

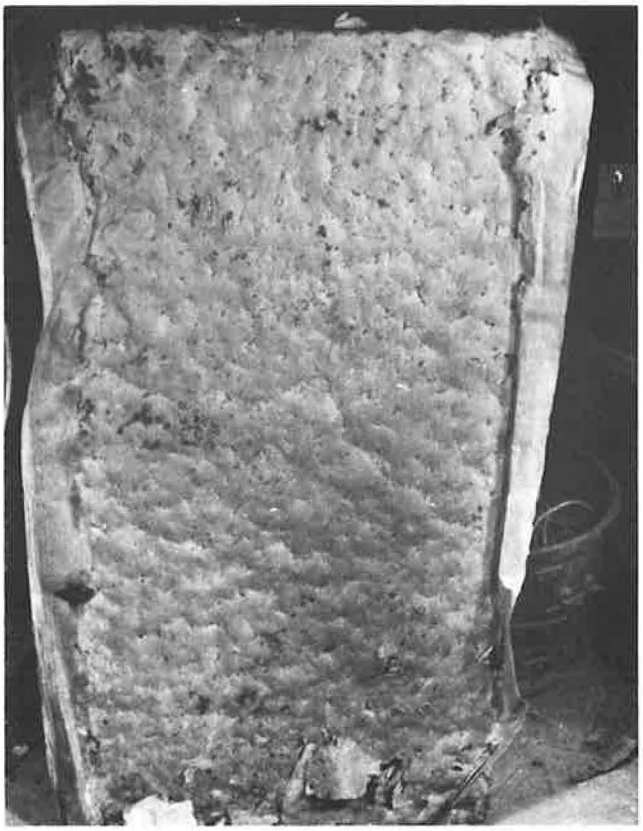

Figure 8. Underside of 4-ft by 2-ft by 6-in. slab on insulation paper over water-bound macadam base, showing scratches on paper due to pushing of slab.

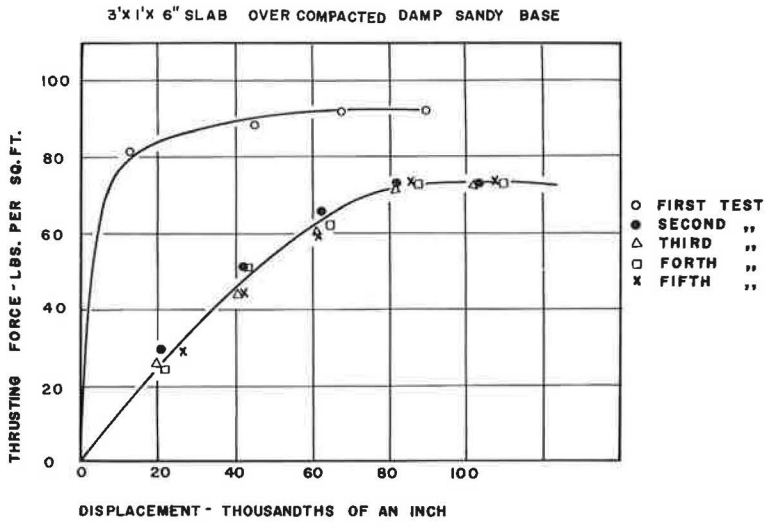

Figure 9. Force-displacement curves for repeated tests on 6-in. slab.

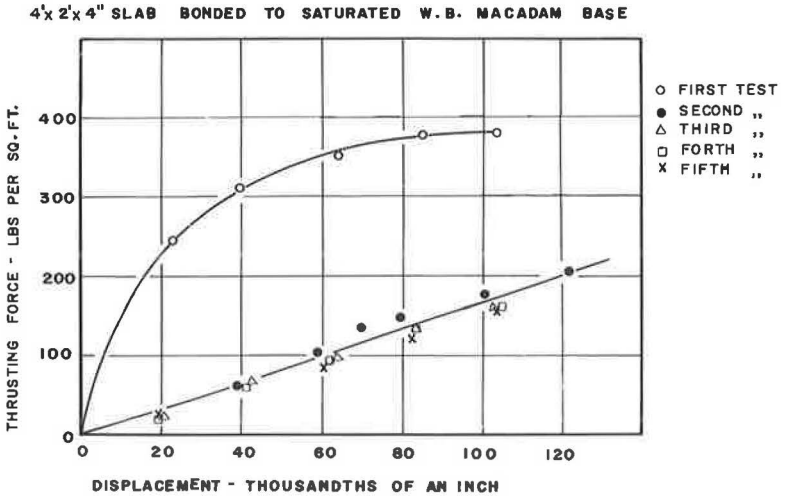

Figure 10. Force-displacement curves for repeated tests on 4-in. slab.

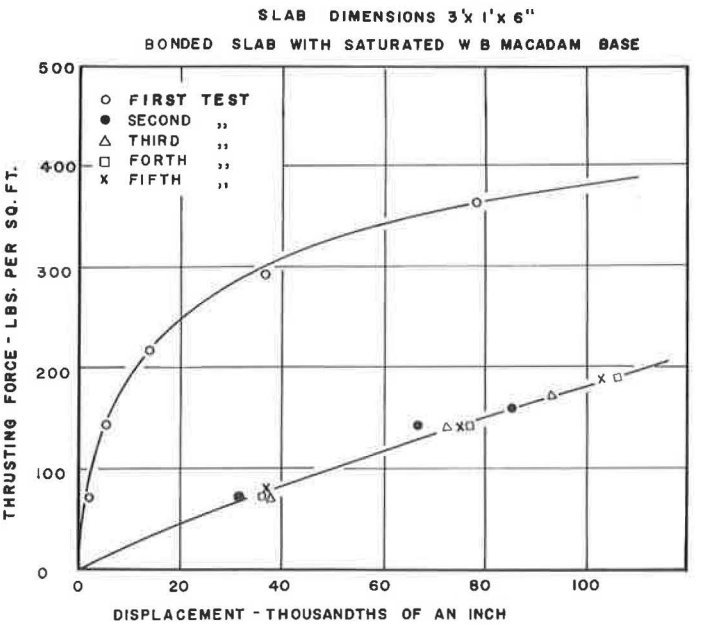

Figure 11. Force-displacement curves for repeated tests on 6-in. slab.

4- and 6-in. slabs, respectively. In other words, the thrusting force on the slabs or the restraint offered by the base for 0.05-in. displacement amounts to 330 and 324 psf, respectively. These values are in close agreement with the British recommendations (13). On dry bases, the thrusting forces vary from 550 to 600 psf. These values are higher than any known recommendations at present. It appears that for slabs laid on water-bound macadam base, the British recommendations represent the minimum values that can be expected under adverse field conditions. In actual practice, where stage construction techniques are adopted as in India, the base will be further consolidated

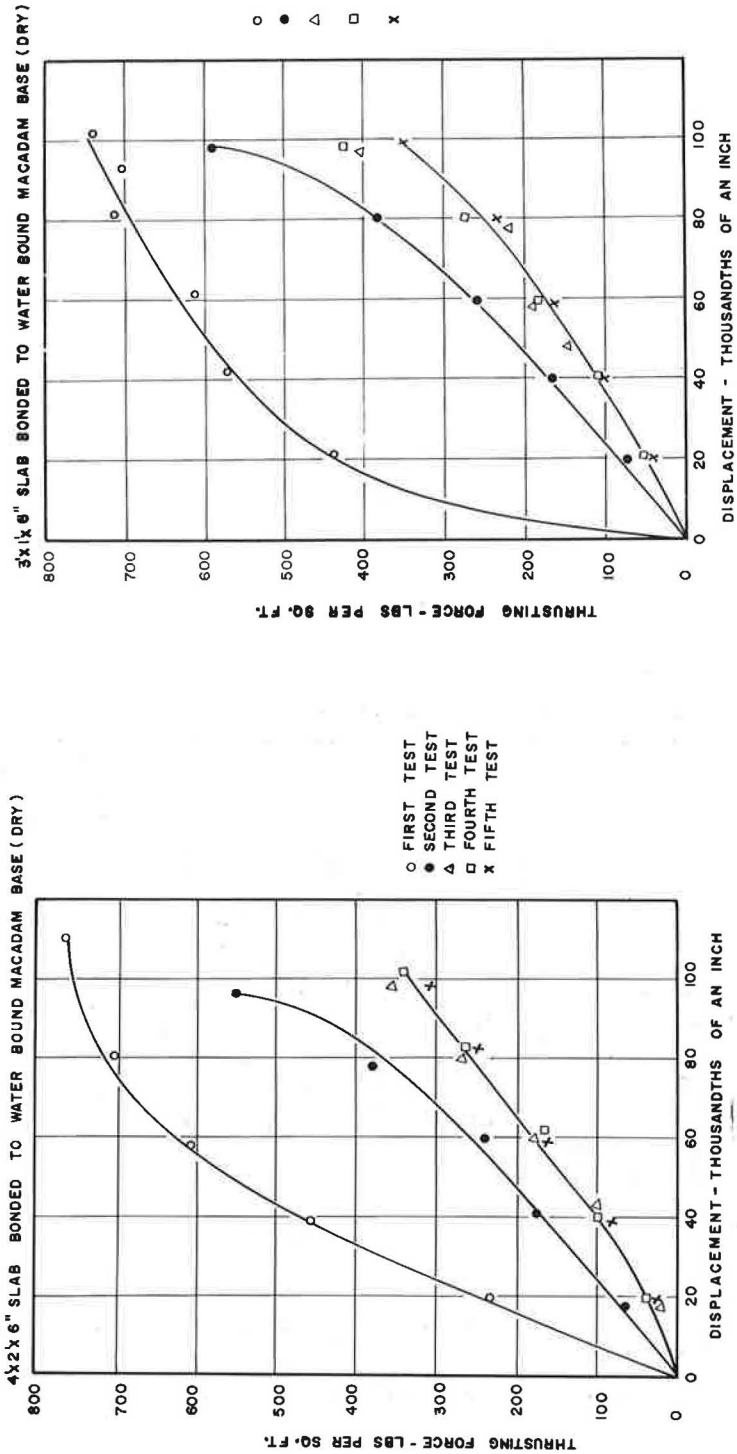

Figure 12. Force-displacement curves for repeated tests on 6-in. slab subjected to repeated tests within elastic range before this series.

Figure 13. Force-displacement curves for repeated tests on 6-in. slab.

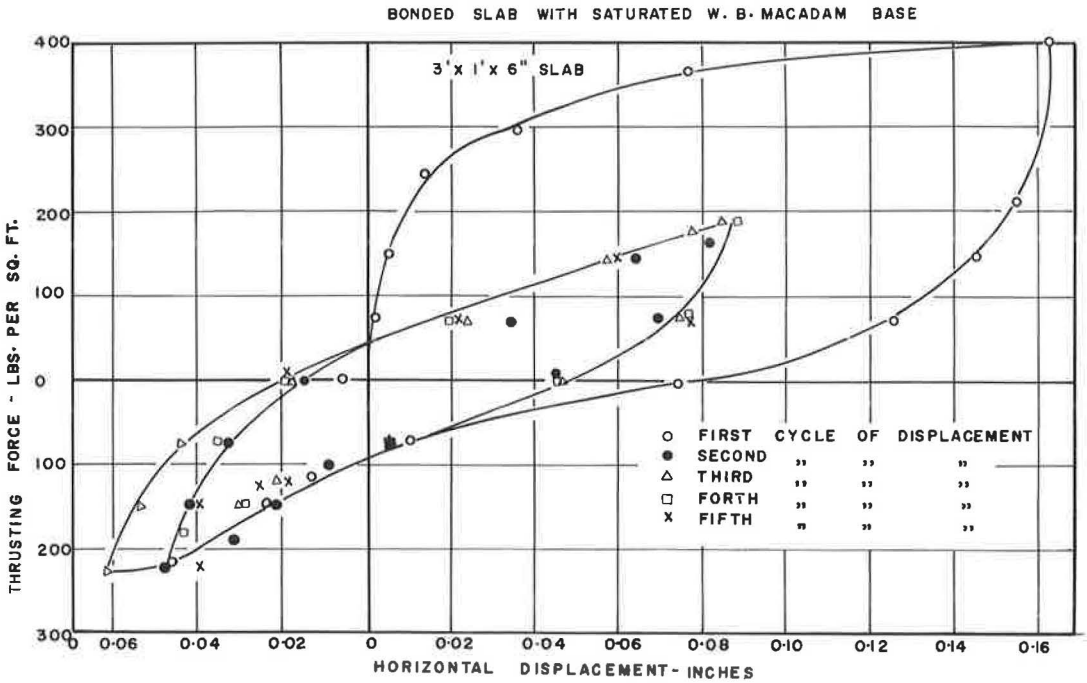

Figure 14. Cycles of force-displacement curves.

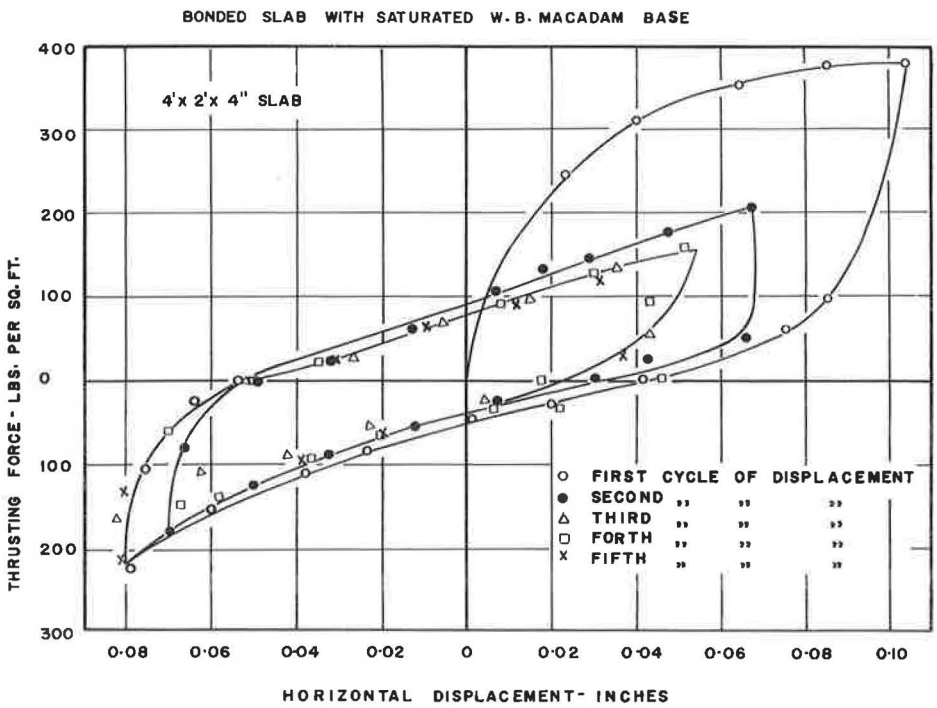

Figure 15. Cycles of force-displacement curves.

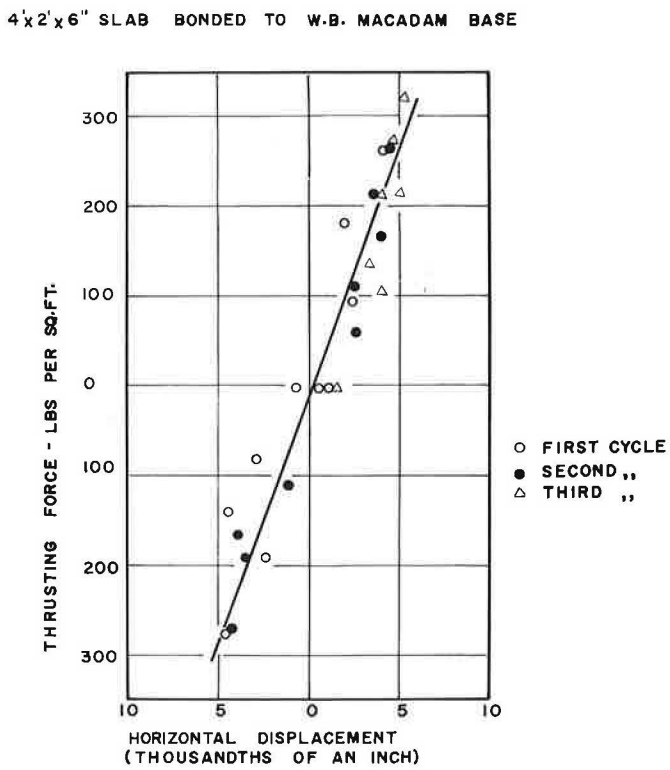

Figure 16. Force-displacement curves for repeated tests on 6-in. slab.

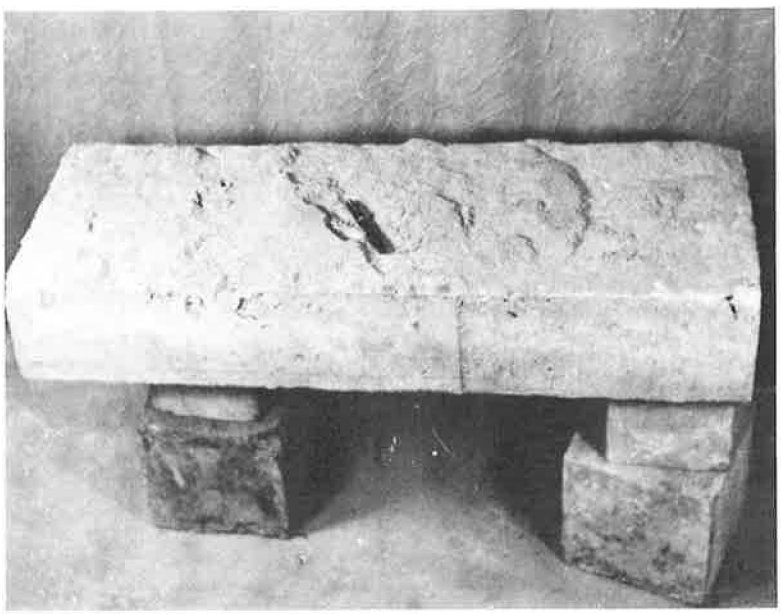

Figure 17. Underside of 3-ft by 1-ft by 6-in. slab bonded to a dense sand base, with masses of sand sticking to surface.

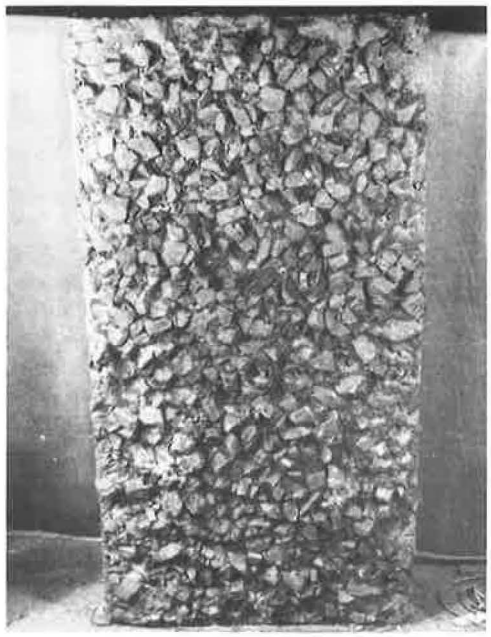

Figure 18. Underside of 4-ft by 2-ft by 4-in. slab bonded to saturated water-bound macadam base after test.

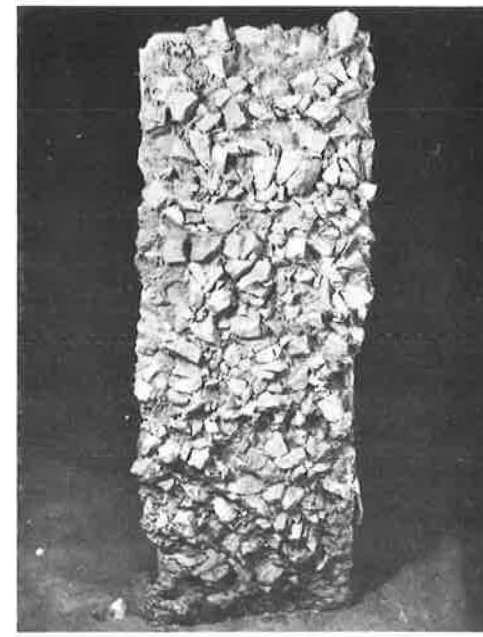

Figure 19. Underside of 3-ft by 1-ft by 6-in. slab bonded to saturated water-bound macadam base after test.

Figure 20. Underside of 4-ft by 2-ft by 6-in. slab bonded to water-bound macadam base (dry) after test.

Figure 21. Underside of 3-ft by 1-ft by 6-in. slab bonded to water-bound macadam base (dry) after test.

TABLE 1

COEFFICIENTS OF BASE RESISTANCE FOR SLABS LAID ON TAR PAPER OVER DIFFERENT BASES

Slab and Base	Coeff. of Resistance for Displacement									
	0.02 In.		0.04 In.		0.06 In.		0.08 In.		0.10 In.	
	1st Test	After Failure	1st Test	After Failure	1st Test	After Failure	1st Test	After Failure	1st Test	After Failure
5-ft by 4-ft by 6-in. field slab	1.39	0.22	2.43	0.44	2.43	0.61	2.43	0.72	2.43	0.80
5-ft by 4-ft by 4-in. field slab	1.76	0.37	1.76	0.58	1.76	0.71	1.76	0.79	1.76	0.83
4-ft by 2-ft by 6-in. slab on prepared subgrade	0.61	0.32	0.72	0.39	0.76	0.41	0.79	0.48	0.79	0.57
4-ft by 2-ft by 6-in. slab on compacted damp sand base	1.25	0.29	1.25	0.43	1.25	0.65	1.25	0.66	1.25	0.73
4-ft by 2-ft by 6-in. slab on water-bound macadam base	1.88	0.28	2.44	0.56	2.44	0.82	2.44	1.00	2.44	1.11

TABLE 2

COEFFICIENTS OF BASE RESISTANCE FOR BONDED SLABS ON VARIOUS BASES

Slab and Base	Coeff. of Resistance for Displacement									
	0.02 In.		0.04 In.		0.06 In.		0.08 In.		0.10 In.	
	1st Test	After Failure	1st Test	After Failure	1st Test	After Failure	1st Test	After Failure	1st Test	After Failure
3-ft by 1-ft by 6-in. slab on compacted damp sand base	1.17	0.34	1.23	0.62	1.26	0.86	1.28	1.00	1.28	1.00
4-ft by 2-ft by 4-in. slab on saturated water-bound macadam base	4.70	0.52	6.46	1.45	7.30	2.10	7.81	2.71	7.81	3.33
3-ft by 1-ft by 6-in. slab on saturated water-bound macadam base	3.47	0.69	4.30	1.17	4.72	1.67	5.14	2.08	5.27	2.50
3-ft by 1-ft by 6-in. slab on dry water-bound macadam base	6.11	0.70	7.64	1.51	8.70	2.43	9.58	3.47	10.14	4.86
4-ft by 2-ft by 6-in. slab on dry water-bound macadam base[a]	3.48	0.55	6.53	1.38	8.68	2.44	10.00	3.61	10.44	4.58

[a]Slab subjected to repeated cycles of initial displacements not exceeding 0.01 in. before test.

by traffic and time, and under reasonably well-drained conditions will offer strong restraint to the failure of the base by shear.

Cracks in Base

During the tests with the bonded slabs, for a displacement of about 0.05 in., a small horizontal crack began to develop in the base course about 1 in. from the edge of the face on which the jack was applied, and it extended to the full width of the tank. The disposition of these surface cracks is shown in Figures 22 and 23. They became wider with further pushing of the slab. A few cracks were also seen along the direction of movement, at an angle of about 45 F and extending away from the longitudinal edges of the slab. When the direction of the thrust was reversed, the cracks in the base previously formed closed themselves, and a fresh set of cracks, similar in pattern, occurred on the pushing side. With repeated tests the cracks at the farther end did not disappear as they did in the initial stages. The result was that at the end of the five cycles cracks approximately $\frac{1}{8}$ in. wide extending to the full width of the base inside the tank near the transverse faces of the slabs could be clearly seen. In other words, the repeated tests revealed that with the bonded slabs, all the distress that occurred took place in the base course, and the slab simply served as a bonded surcharge initiating the movements leading to the final failure by shear inside the base.

DILATANCY OF BASE

Sparkes (10) mentions that the base course below the slab dilates or increases in volume whether the slab expands or contracts. It is well known that in direct shear tests, dense soils expand and loose soils reduce in volume (14), and this dilatancy is maximum for sandy soils and minimum for clays. Concrete roads are rarely laid directly on clayey soils, and since only compacted granular material is commonly used

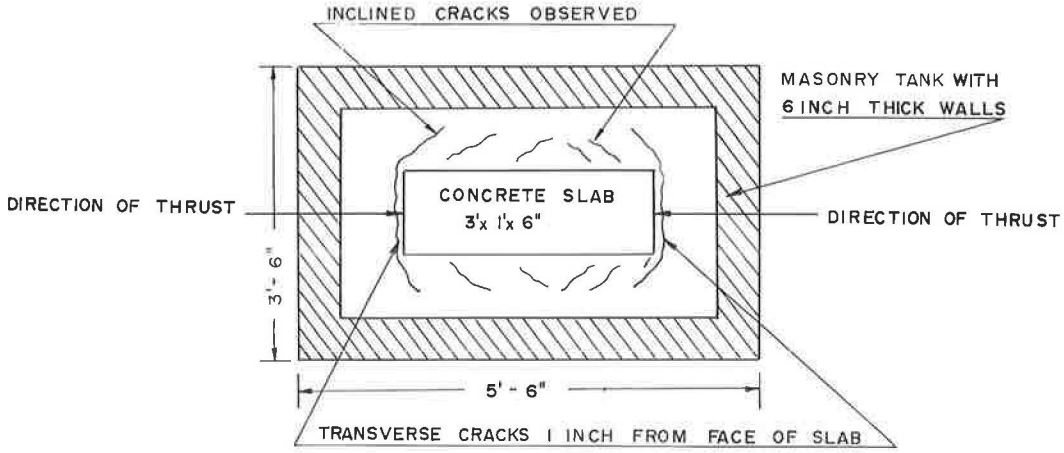

Figure 22. Disposition of surface cracks in the base of bonded slab.

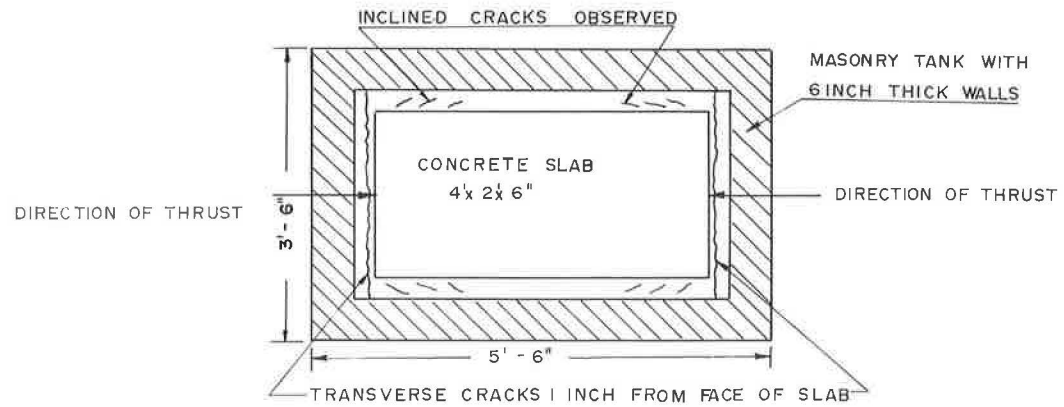

Figure 23. Disposition of surface cracks in the base of bonded slab.

under a concrete pavement, the shear deformation initiated by the expanding or contracting slab causes dilatancy. These observations along with the data presented herein indicate that it is the shear resistance of the soil immediately below the slab that has to be reckoned with in resisting the horizontal strains induced by the slab due to variation in its average moisture and temperature. Contrary to what is generally accepted, the actual plane of failure is inside the base, and not at the interface between the slab and the support below.

ACKNOWLEDGMENT

The writer wishes to record his deep appreciation to Professor B. R. Sen for the many constructive suggestions made in the course of the study on bonded cement concrete road slabs.

REFERENCES

1. Bradbury, R. D. Reinforced Concrete Pavements. Wire Reinforcement Inst., Washington, D. C., 1938.

2. Yoder, E. J. Principles of Pavement Design. New York, John Wiley and Sons, 1959.
3. Timms, A. G. Evaluating Subgrade Friction Reducing Medium for Rigid Pavements. Highway Research Record 60, pp. 28-38, 1964.
4. Stott, J. P. Tests on Materials for Use in Sliding Layers Under Concrete Road Slabs. Civ. Eng. and Pub. Works Rev., Oct., Nov., and Dec., 1961.
5. Sparkes, F. N. The Design of Concrete Roads in Some European Countries. Roads and Road Const., June 1958.
6. Walker, W. F. Evolution of Thin Concrete Road in United Provinces, India. Proc. Fifth Meeting of Indian Roads Cong., Dec. 1939.
7. Mitchell, R. A. End Anchors for Continuously-Reinforced Concrete Pavements. Highway Research Record 5, pp. 50-82, 1963.
8. Childs, L. D. Tests of Concrete Pavement Slabs on Cement Treated Bases. Highway Research Record 60, pp. 39-58, 1964.
9. Teller and Sutherland. The Structural Design of Concrete Pavements. Public Roads. Washington, D. C., Oct. and Nov. 1935.
10. Sparkes, F. N. Stresses in Concrete Road Slabs. Structural Eng., London, Feb. 1939.
11. Venkatasubramanian, V. Temperature Variations in a Cement Concrete Pavement and the Underlying Subgrade. Highway Research Record 60, pp. 15-27, 1964.
12. Kelly, E. F. Applications of the Results of Research to the Structural Design of Concrete Pavements. Public Roads, Washington, D. C., July and Aug. 1939.
13. Concrete Roads, Design and Construction. London, Her Majesty's Stationery Office, 1955.
14. Casagrande, A. Characteristics of Cohesionless Soils Affecting the Stability of Slopes and Earth Fills. Jour. of Boston Soc. of Civ. Eng., Jan. 1936.